

# **Biological Responses to Upwelling and Stratification in the Eastern Arabian Sea**

**Thesis submitted to  
Cochin University of Science and Technology**

**in partial fulfillment of the requirements for the degree of**

**DOCTOR OF PHILOSOPHY  
in  
MARINE BIOLOGY**

**under the  
Faculty of Marine Sciences**

**by  
HABEEBREHMAN, H. M.Sc., B.Ed.  
(Reg. No. 2897)**



**NATIONAL INSTITUTE OF OCEANOGRAPHY  
(Council of Scientific and Industrial Research)**

**Regional Centre, Kochi - 682 018**

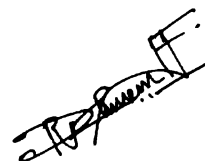
**February 2009**

## ***Declaration***

*I hereby declare that the thesis entitled, **Biological Responses to Upwelling and Stratification in the Eastern Arabian Sea** is an authentic record of research carried out by me under the supervision of Dr. C. Revichandran, Scientist E II, National Institute of Oceanography, Regional Centre, Kochi - 18, in partial fulfillment of the requirement for the Ph D. Degree of Cochin University of Science and Technology under the Faculty of Marine Sciences and that no part of this has been presented before for any other degree, diploma or associateship in any university.*

Kochi

16.02.2009



(Habeebrehman, H.)

## **Certificate**

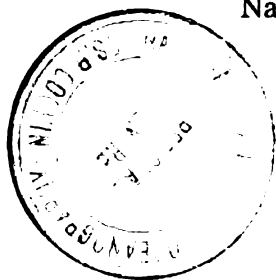
*I hereby certify that the thesis entitled, **Biological Responses to Upwelling and Stratification in the Eastern Arabian Sea** submitted by **Habeebrehman, H.**, Research Scholar (Reg. No. 2897) National Institute of Oceanography, Regional Centre, Kochi -18 is an authentic record of research carried out by him under my supervision, in partial fulfillment of the requirement for the Ph D. Degree of Cochin University of Science and Technology under the Faculty of Marine Sciences and that no part thereof has previously formed the basis for the award of degree, diploma or associateship in any university.*



**Dr. C. Revichandran**  
Supervising Guide  
Scientist EII

**National Institute of Oceanography**  
**Regional Centre, Kochi-18**  
**Kerala, India**

**Kochi**  
**16. 02.2009**



## **Acknowledgement**

*I am deeply indebted to my supervising guide Dr. C. Revichandran, Scientist E II, National Institute of Oceanography (NIO) Regional Centre (RC), Kochi for the guidance and constant encouragement, which enabled me to complete the thesis.*

*I am particularly grateful to Dr. N. Bahulayan, Scientist -in- Charge, NIO RC, Kochi for providing me all facilities with a conducive working environment. I am grateful to Dr. S.R. Shetye, Director NIO, Goa for providing the facilities for completing the thesis.*

*I convey my heartfelt thanks to Dr. K.K.C. Nair, former Scientist-in-Charge of NIO RC, Kochi for providing the facilities, support and scientific advices during the course of this study. I am also grateful to Dr. T.C. Gopalakrishnan, my former supervising guide, for his guidance, support and freedom given to me select the area of research.*

*I would also like to acknowledge with thanks the advices, help and support received from Dr. C.T. Achuthankutty (former Scientist-in-Charge), Research Committee members, scientific and administrative staff of NIO RC Kochi. I thank Dr. N.V. Madhu, Dr. R. Jyothibabu and Dr. P.K. Karuppassamy, Scientists, NIO RC, Kochi for their advices on scientific matters and constructive comments on this thesis.*

*I wish to extend my gratitude to Dr. P.M.A. Bhattathiri, Mr. Kesavadas, Dr. P. Haridas, Dr. Saramma U. Panampunnayil, Dr. Saraladevi, Dr. C.B. Lalithambika Devi, Mr. T. Balasubrahmanyam, Mr. G. Nampoothiri (Late), Mr. P. Venugopal, Mr. O. Raveendran, (Rtd. Scientists of NIO RC, Kochi) for the encouragement and support.*

*I have immense pleasure to express my sincere thanks to Prof. (Dr.) Trevor Platt and Dr. (Mrs.) Shubha Sathyendranath, Bedford Institute of Oceanography, Canada for sharing their knowledge, and valuable lectures during the POGO training programme on 'Calculation of Regional scale Primary Production for Indian Ocean waters and Applications to Ecosystem Dynamics' conducted in NIO, RC Kochi. My special thanks to Dr. Marie Helen Forget, Dalhousie University, Canada and Dr. Vivian Lutz, INIDEP, Argentina, for their lectures and training that helped me in analysis of phytoplankton pigments using HPLC. Thanks are due to Mrs. Linda Payzant and Mr. Peter Payzant, Canada for training in satellite ocean colour image processing.*

*Scientific discussions with Dr. S. Prasannakumar, Dr. Mangesh Gauns and Dr. N. Ramaiah, Scientists, NIO, Goa are also gratefully acknowledged.*

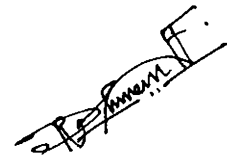
*I express my sincere gratitude to the scientific officials of Centre for Marine Living Resources and Ecology (CMLRE), Kochi for giving me an opportunity to work and avail fellowship under Marine Research on Living Resources Programme and also for utilizing the facilities of the research vessel FORV Sagar Sampada. I sincerely thank the Captains, Officers, Crew and scientific and technical team of various cruises of FORV Sagar Sampda for their skilled co-operation and assistance during the cruises.*

*Assistance and help rendered by all the research fellows of MR-LR programme, and all my friends at NIO, CUSAT and CMFRI are thankfully acknowledged. No words will suffice to thank Dr. M.P. Prabhakaran my dearest friend for his support, suggestions and valuable advices during the course of my study.*

*With love and affection I wish to express my deep sense of gratitude to my brothers and sisters, in-laws, and all my family members for their constant encouragement, prayers and advices, without which I would not have been able to pursue my study. Special interest shown by my wife and her constant encouragement, love and support are highly cherished.*

*My head bows before the God almighty, the cherisher and sustainer of the world, who gave me boundless blessings, rendered through various hands which helped me in completing this work successfully.*

*I dedicate this thesis to the evergreen memories of my beloved parents.*



**Habeebrehman, H.**

## **Preface**

*The Arabian Sea is one of the most productive regions in the world, a highly complex oceanic basin, characterized by eutrophic upwelling and oligotrophic stratified environments. These environments are strongly influenced by biannual monsoon winds. During the summer monsoon, wind-driven upwelling occurs along a broad region parallel to the coast. Upwelling is a process of vertical motion in the sea whereby cool, nutrient rich subsurface water moves upward towards the surface, where it fuels blooming of phytoplankton and enhances primary production. The importance of wind-driven coastal upwelling systems to global primary productivity and fishery production is well known. Upwelling areas on the continental shelf contribute 20% of global fish production while occupying less than 1% of the world oceans' surface area. Primary and secondary productivity in upwelling areas varies from year-to-year and between locations, causing associated fisheries to vary, but the mechanisms underlying this variability are not well understood.*

*Several studies have been carried out in the eastern Arabian Sea for the estimation of plankton productivity in relation to the environmental characteristics. The International Indian Ocean Expedition (IIOE 1962-65), United States Joint Global Ocean Flux Studies (JGOFS, 1994-1995), Indian JGOFS Programme (1994-1996), Marine Research on Living Resources Programme (MR-LR) of CMLRE, Govt. of India (1998- 2007), etc. are major expeditions in the eastern Arabian Sea, which initiated studies on hydrography and productivity characteristics. The present study is a part of the MR-LR Programme (2002-2007) entitled "Environment and Productivity Patterns in the Indian EEZ". This study mainly focused on the biological responses to physical process such as coastal upwelling and stratification in the eastern Arabian Sea (8-21°N, 66- 77°E). Field observations were made at 8 transects (43 stations) during spring intermonsoon (SIM), onset of summer monsoon (OSM), peak summer monsoon (PSM) and late summer monsoon (LSM).*

*The thesis is organized into seven chapters. **Chapter I** deals with the introduction to the thesis, which describes general characteristics of the marine environment, general oceanographic features of the Arabian Sea, and scope and objectives of the study. **Chapter II** outlines the materials and methods used for the study. The complete description of the sampling procedures and methodology are also included in this chapter.*

General hydrographic characteristics of the study area during spring intermonsoon and different phases of summer monsoon are discussed in **chapter III**. The variability of meteorological and hydrographic parameters such as wind speed, temperature, salinity and nutrients in space and time are highlighted in this section. In **chapter IV**, the biological responses to stratified and oligotrophic waters of spring intermonsoon are discussed. Spatial distribution of primary productivity, Chlorophyll a, phytoplankton density, mesozooplankton biomass and composition are highlighted. The biological responses to upwelling during different phases of summer monsoon are discussed in **chapter V**. Satellite derived chlorophyll concentration and annual pelagic fishery landing in the west coast of India during the study period is included in this section to highlight the importance of upwelling events in the pelagic fishery landing in the south west coast of India.

**Chapter VI** deals with the changes in phytoplankton community structure during spring intermonsoon and different phases of summer monsoon. HPLC derived phytoplankton pigment characteristics during onset and peak summer monsoon along the southeastern Arabian Sea are also described in this chapter. The results are summarized in **chapter VII**. The lists of references are given in the end of each chapter.

## ***Acronyms and Abbreviations***

<b>ASHSW</b>	Arabian Sea High saline Water Mass
<b>Chl <i>a</i></b>	Chlorophyll <i>a</i>
<b>CMFRI</b>	Centre Marine fisheries Research Institute
<b>CMLRE</b>	Centre for Marine Living Resources and Ecology
<b>CTD</b>	Conductivity – Temperature –Depth
<b>DCM</b>	Deep Chlorophyll Maximum
<b><i>e.g</i></b>	exempli gratia (latin word meaning for the sake of example)
<b>E</b>	East
<b>EEZ</b>	Exclusive Economic Zone
<b>EICC</b>	East India Coastal Current
<b><i>et al.</i></b>	et alii (Latin word meaning ‘and others’)
<b>FORV</b>	Fisheries and Oceanographic Research Vessel
<b>GF/F</b>	Glass Fibre Filter
<b>IIOE</b>	International Indian Ocean Expedition
<b>JGOFS</b>	Joint Global Ocean Flux Studies
<b>HPLC</b>	High Performance Liquid Chromatography
<b>LH</b>	Lakshadweep High (Laccadive High)
<b>LL</b>	Lakshadweep Low (Laccadive Low)
<b>LSM</b>	Late Summer Monsoon
<b>MLD</b>	Mixed Layer Depth
<b>MoES</b>	Ministry of Earth Sciences
<b>MR-LR</b>	Marine Research- Living Resources
<b>N</b>	North
<b>NASA</b>	National Aeronautics and Space Administration
<b>NE</b>	Northeast
<b>NEC</b>	North Equatorial Current
<b>NIO</b>	National Institute of Oceanography
<b>NOAA</b>	National Oceanic and Atmospheric Administration
<b>ORV</b>	Oceanographic Research Vessel
<b>OSM</b>	Onset of Summer Monsoon
<b>PP</b>	Primary Productivity
<b>PSM</b>	Peak Summer Monsoon
<b>psu</b>	Practical Salinity Unit
<b>RV</b>	Research Vessel
<b>SCM</b>	Sub surface Chlorophyll Maxima
<b>SEAS</b>	Southeastern Arabian Sea
<b>SeaWiFS</b>	Sea-viewing Wide Field of view Sensor
<b>SEC</b>	South Equatorial Current
<b>SIM</b>	Spring Intermonsoon
<b>SM</b>	Summer Monsoon
<b>SSS</b>	Sea Surface Salinity
<b>SST</b>	Sea Surface Temperature
<b>SW</b>	Southwest
<b><i>viz</i></b>	videlicet (Latin word meaning ‘namely’)
<b>WICC</b>	West India Coastal Current

# Contents

<b>Title</b>	<b>Page No.</b>
<b>Chapter I General Introduction</b>	<b>1-27</b>
1.1. Plankton and productivity	
1.2. General hydrography of eastern Arabian Sea	
1.3. Review of literature	
1.4. Scope and objectives of the study	
References	
<b>Chapter II Materials and methods</b>	<b>28-50</b>
2.1. Study Area and sampling stations	
2.2. Sampling seasons	
2.3. Sampling procedure and methods of analysis	
References	
<b>Chapter III Hydrography</b>	<b>51-106</b>
3.1. Introduction	
3.2. Results	
3.2.1. Spring intermonsoon	
3.2.2. Onset of summer monsoon	
3.2.3. Peak summer monsoon	
3.2.4. Late summer monsoon	
3.3. Discussion	
References	
<b>Chapter IV Biological responses during spring intermonsoon</b>	<b>107-135</b>
4.1. Introduction	
4.2. Results	
4.2.1 Primary productivity	
4.2.2 Chlorophyll a	
4.2.3 Phytoplankton abundance	
4.2.4 Mesozooplankton	
4.3 Discussion	
References	
<b>Chapter V Biological responses to upwelling events during different phases of summer monsoon</b>	<b>136-212</b>
5.1. Introduction	
5.2. Results	
5.2.1 Onset of summer monsoon	
5.2.2 Peak of summer monsoon	
5.2.3 Late summer monsoon	
5.2.4 Satellite chlorophyll imagery	
5.2.5 Pelagic fish landings	
5.3. Discussion	
References	
<b>Chapter VI Phytoplankton community structure</b>	<b>213-255</b>
6.1. Introduction	
6.2. Results	
6.2.1. Community structure	
i) Species composition	
ii) Diversity indices	
iii). Similarity indices	
6.2.2 Phytoplankton pigment characteristics	
6.3. Discussion	
References	
<b>Chapter VII Summary and conclusion</b>	<b>256-260</b>

## Chapter I

# General Introduction

---

- 1.1. *Plankton and productivity*
  - 1.2. *General hydrography of eastern Arabian Sea*
  - 1.3. *Review of literature*
  - 1.4. *Scope and objectives of the study*
- References
- 

### **1.1. Plankton and productivity**

The marine environment is known to support vast populations of organisms, which are found distributed in both pelagic and benthic realms. Most of the organisms of the pelagic realm constitute the plankton. Phytoplankton and zooplankton together constitute this community and form the chief primary food source for most of the marine organisms. Their responses to physico-chemical characteristics of the water column determine their distribution, abundance and production. Phytoplankton (*phyton* = plant; *planktos* = wandering) are autotrophic free-floating microscopic plants or microalgae that are mostly unicellular, although colonial or filamentous species also occur. They are a taxonomically diverse group and have a truly global distribution, contributing over 25% of the total vegetation of the planet (Jeffrey and Halegraeff, 1990). This group of organisms consists of approximately 20,000 species distributed among at least eight taxonomic divisions or phyla (Falkowski and Raven, 1997). Unlike terrestrial plants, phytoplankton are species poor but phylogenetically diverse. This deep taxonomic diversity is reflected in

ecological functions (Falkowski and Raven, 1997). Because of their worldwide distribution and their role as primary producers, extensive studies are being conducted and these form an important aspect of biological oceanography.

One of the major themes that needs to be scrutinised is how plankton productivity is influenced by the dynamics of the ocean. This influence operates at many scales, from ocean basin circulation, through localized areas of upwelling, down to small-scale turbulence that affects individual cells. The problems confronting phytoplankton production in the ocean are related to light and nutrients, both for growth and reproduction. But the light comes from above, while the sources of nutrients are located at depth. The sun's energy that reaches the surface water is absorbed as it passes downward, decreasing exponentially with depth. In a finite layer, the euphotic zone, there is enough light for photosynthesis and growth to take place. However in a water column with no turbulence or stratification, the euphotic zone becomes depleted of nutrients as a result of uptake by the phytoplankton. The reserve of nutrients in deeper waters is nevertheless constantly replenished by the decomposition of organisms from the euphotic zone that sink and decay. Consequently, in the situation of zero turbulence, there would be a very low level of nutrients in surface waters, but quite a high level at depths, and the only mechanism for transfer from one to another would be molecular diffusion, which is extremely slow. Generally the ocean water remains turbulent due to wind stress at the surface, internal waves, ocean

currents etc. Phytoplankton production thus depends on the availability of nutrients in the euphotic zone, mainly brought about by turbulence, upwelling etc.

Chlorophyll and its function of converting light energy to chemical energy through the process of photosynthesis possibly began evolving in the ocean about 2,000 million years ago (Callot, 1991; Scheer, 1991). This primary productivity had a dramatic impact on the biogeochemistry of the earth. Phytoplankton productivity in the world oceans is a major concern, because of its role in regulating carbon dioxide in the atmosphere and it plays a vital role in global climate change (Watson, *et al.*, 1991; Hays, *et al.*, 2005) by means of a number of mechanisms. These mechanisms include the utilization of carbon dioxide through photosynthesis, thus affecting the global carbon dioxide budget (Williamson and Gribbin, 1991), contributing to seasonal warming of the surface layers of the ocean, absorbing and scattering light (Sathyendranath, *et al.*, 1991a), and bringing about the production of volatile compounds, which escape into the atmosphere and act as cloud-seeding nuclei (Malin, *et al.*, 1992). Because of the photosynthetic function of chlorophyll, it forms a unique indicator of oceanic plant biomass and productivity; hence it is the most frequently measured biochemical parameter in oceanography. Measurements of chlorophyll distribution in the oceans have revealed areas of contrasting fertility, from the oligotrophic ocean gyres with low concentrations of chlorophyll in surface waters ( $<0.05\mu\text{g L}^{-1}$ ) to chlorophyll rich waters found in upwelling areas, along

continental shelf fronts and coastal seas (1-10 $\mu\text{g L}^{-1}$ ). Chlorophyll measurements have been used to follow diurnal, seasonal and long-term changes in biological productivity in contrasting oceanic regimes.

As an alternative and complement to microscopic examination, photosynthetic and non-photosynthetic pigment distributions can be used to identify the presence of different algal groups (Wright, *et al.*, 1991; Ondrusek, *et al.*, 1991, Jeffrey, *et al.*, 1997; Bidigare and Charles, 2002). Accessory pigments can provide class-specific differentiation, allowing for the recognition of major taxonomic groups of marine phytoplankton (Wright, *et al.*, 1991). Over the last 20 years, the development of High Performance Liquid Chromatography (HPLC) has greatly advanced our understanding of phytoplankton pigment composition and functionality in response to ecosystem changes (Wright, *et al.*, 1991; Barlow, *et al.*, 1999). In the western and central Arabian Sea for example, HPLC-analysed pigments helped provide new information as well as a better understanding of changes in phytoplankton populations associated with the seasonal cycle of the monsoons (Latasa and Bidigare, 1998; Barlow, *et al.*, 1999; Goericke, 2002; Brown, *et al.*, 2002). Disappearance of native pigments and formation of degradation products have also been used to quantify grazing by micro- and macro- zooplankton (Burkill, *et al.*, 1987).

Until recently, chlorophyll was measured on board ships by taking discrete water samples and analysing them. The species composition used to be evaluated by sampling with phytoplankton nets or by harvesting from water samples in a plankton centrifuge,

and counting and identifying the species microscopically. Today, with the advent of remote sensing, ocean temperature and colour can now be monitored on a global scale from space (Aiken, *et al.*, 1992; Sathyendranath, *et al.*, 2005; Chauhan, *et al.*, 2005; Watts, *et al.*, 2005). The full potential of satellite remote sensing technology can be realised only if chlorophyll and accessory pigments are simultaneously measured. Since chlorophyll is the only biological parameter measurable from space; pigments will serve as basic parameters for global mapping of components of oceanic carbon cycle, including total, regenerated and 'new' production (Sathyendrath, *et al.*, 1991b).

Zooplankton are ubiquitous in distribution and encompass an array of macro and microscopic animals and comprise representatives of almost all major taxa, particularly the invertebrates. Classically, phytoplankton forms as the basis of all animal production in the open sea, supporting food webs upon which the world's fisheries are based. They play a vital role in the marine food chain. The herbivorous zooplankton feed on phytoplankton and in turn constitute an important food item to animals in higher trophic level including fish. The pelagic fishes such as sardines, mackerel and silver bellies mostly feed on plankton. The abundance and distribution of the fish population are obviously dependent on the availability of zooplankton, which is in turn dependent on the phytoplankton. The occurrence and abundance of ichthyoplankton (fish eggs and fish larvae) facilitate the location of probable spawning and nursery ground of fishes (Binu,

2003; Dwivedi, *et al.*, 2005). The most characteristic feature is their variability over space and time in any aquatic ecosystem.

There is a sequence of events that occurs in a variety of physical settings and on time scales ranging from a few hours to a year, which enhances phytoplankton production. The essence of it is strong vertical mixing followed by stratification of the water column. Generally, vertical mixing brings nutrients from deeper depths to surface waters and the formation of stratification confines phytoplankton to a well-lit zone where daily photosynthesis exceeds daily respiration. The major driving force for vertical mixing is wind stress at the surface, whereas the chief agent for stratification is solar heating. In areas noted for upwelling, the prevailing winds and upslope of cold nutrient rich water bring nutrient-rich water to the surface. The high productivity is associated with the relaxation of the winds, as the phytoplankton utilize the upwelled nutrients. As the upwelled water streams away from the areas of upwelling, stratification sets in, and there begins to exist a zone in which the zooplankton become more abundant as they feed on phytoplankton.

The alteration of vertical mixing and stratification is surely one of the most important sequences that determine the biological responses in the oceanic realm. Hence, the physical processes appear to set the stage on which a biological play is enacted.

## **1.2. General oceanographic features of eastern Arabian Sea**

The Arabian Sea is unique among low-latitude seas which terminates at latitude of 25°N and is under marked continental

influence. The surface and the sub-surface parameters exhibit significant seasonal variations and eventually these upper ocean physical processes influence the biological productivity considerably. Offshore temperature changes are accompanied by appreciable alteration of mixed-layer depths (MLD), with change in water density or direct wind action. Near the coast, upwelling may further complicate the picture where the physical effects such as warming and cooling of the adjacent land masses are expressed by the prevailing winds, which reverse their directions (Fig. 1.1) seasonally, thereby causing drastic changes in the surface currents.

The Arabian Sea is a highly complex oceanic basin, encompassing eutrophic upwelling, downwelling and oligotrophic stratified environments (Burkill, *et al.*, 1993). The most famous monsoonal upwelling system is located along the North West coast of Arabian Sea (Longhurst, 1998), which supports high plankton production and associated pelagic fishery. Analogous to this, eastern Arabian Sea also forms an important upwelling region, known for high biological production. The SW monsoon winds blow nearly parallel to the Arabian coastline, causing significant coastal upwelling (Fig. 1.2) due to Ekman transport of surface water offshore (Swallow, 1984), but since the offshore boundary current is relatively weak, open-sea upwelling also extends around 400 km seawards in response to positive wind stress curl (Smith and Bottero, 1977). These upwelling processes bring nutrient-rich subsurface water into the euphotic zone (Sastry and D' Souza, 1972; Mantoura, *et al.*, 1993). As a consequence

of this enrichment, high rates of primary and new production occur in the northern Arabian Sea (Owens, *et al.*, 1993).

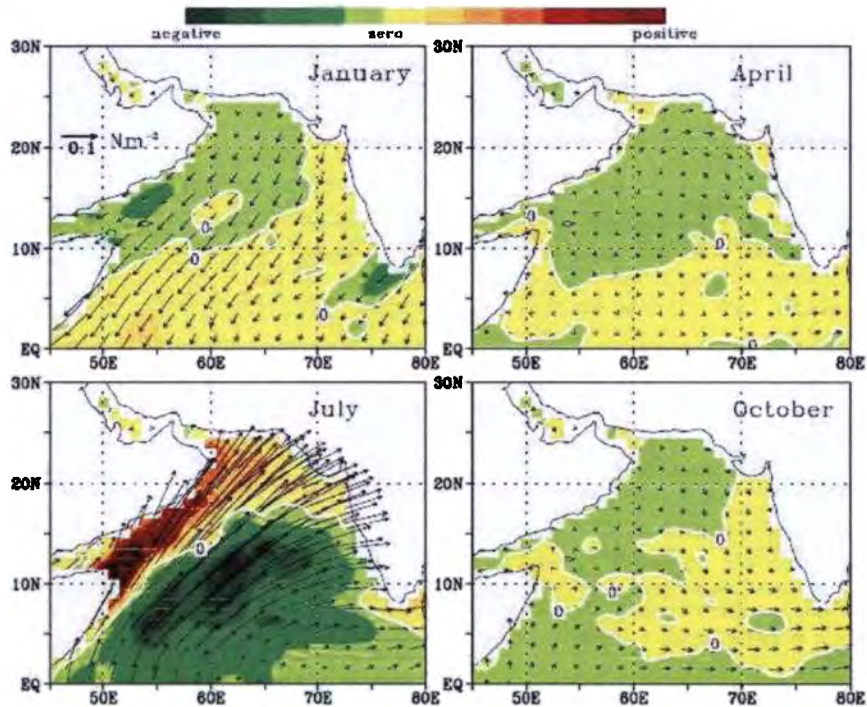


Fig.1.1. Monthly mean wind stress and curl of the wind stress are shaded with zero curl contour for January, July, April and October representing winter, summer, and the two intermonsoon periods. (Adapted from Prasad, 2001)

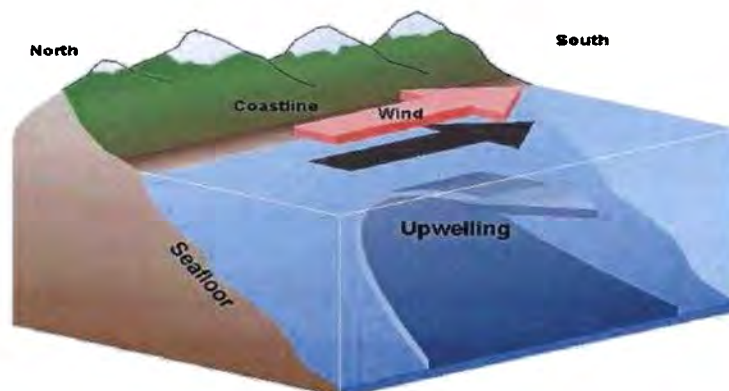


Fig. 1.2. Schematic representation of coastal upwelling process (Courtesy: NOAA)

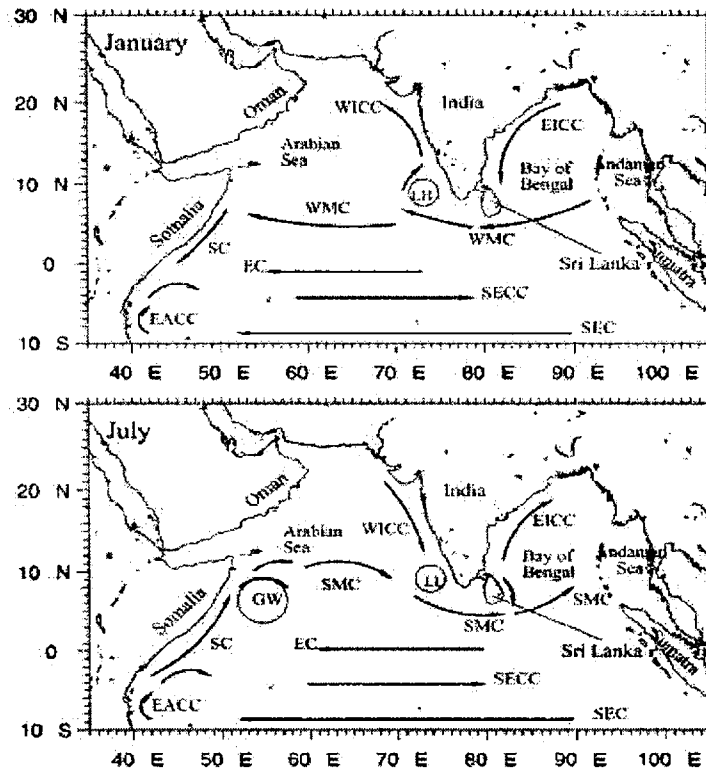


Fig. 1.3. Schematic representation of the circulation in the Indian Ocean during winter monsoon and summer monsoon. (Shankar *et al.*, 2002)

(SC, Somali Current; EC, Equatorial Current; SMC, Summer Monsoon Current; WMC, Winter Monsoon Current; EICC, East India Coastal Current; WICC, West India Coastal Current; SECC, South Equatorial Counter Current; EACC, East African Coastal Current; SEC, South Equatorial Current; LH, Lakshadweep high; LL, Lakshadweep low; and GW, Great Whirl.)

The Arabian Sea normally experiences most dramatic changes in its circulation, concomitant with the evolution of the southwest monsoon. During the southwest monsoon, circulation in the Arabian Sea is clockwise. The Summer Monsoon Current (SMC) is fully developed during July and August (Shanker, *et al.*, 2002). It decreases in its intensity during September and by October, the current direction (Fig.1.3) and intensity become variable over most of the Arabian Sea. From an analysis of ship drift data, Cutler and Swallow (1984) found the presence of SMC flowing towards east in the Arabian Sea. Based on the hydrographic data and ship drift data, Wyrтки

(1973) inferred an overall movement of water in the Arabian Sea from west to east during the southwest monsoon. The surface current in the central Arabian Sea during the southwest monsoon is found to be directed towards northeast with an average strength of about  $0.8 \text{ m s}^{-1}$  (Bauer *et al.*, 1992).

During the late phase of southwest monsoon, the presence of a poleward undercurrent is indicated. Shetye and Shenoi (1988) noticed a shallow equatorward current along the west coast of India. Along the eastern boundary of the Arabian Sea, during the southwest monsoon, the long shore component of the wind stress is generally equatorward and its magnitude is maximum near the southern end. During the northeast monsoon period, over most parts of the Arabian Sea, the currents are directed towards west or northwest. The reversal of currents in the Arabian Sea is observed to be complete by November (Varadachari and Sharma, 1967). In the open Arabian Sea the overall movement of water during this season is from east to west (Wyrtki, 1973). Using hydrography and altimeter data, Bruce *et al.*, (1994) presented the evidence of a large (500-800 km diameter) anti-cyclonic eddy in the upper 300-400 m, namely Laccadive High (LH) in the southeastern Arabian Sea (centered at  $10^{\circ}\text{N}$ ,  $70^{\circ}\text{E}$ ) during early winter. It moves westward across the southern Arabian Sea and dissipates in the mid basin during the inter monsoon period. A cyclonic eddy, Laccadive Low (LL) forms during early summer at the same location and propagates westward across the southern Arabian Sea a few months after genesis. Shankar and Shetye (1997) suggested

that the formation of the LH and LL are a consequence of westward propagating Rossby waves radiated by Kelvin waves propagating poleward along the western margin of the Indian subcontinent.

As indicated, both by its geophysical position and by its large north south extent, this upwelling area bears some resemblance to the 'classical' upwelling region off the west coasts of the continents in low latitudes, i.e., at the eastern sides of the trade wind regions. Off Bombay, from where upwelling is definitely known, the rising of the deep water on the left side of the coastal current may cause similar biological conditions near the sea-bed as noted off Cochin. Upwelling off Cochin and farther south was found by Rama Sastry and Myrland (1959) during their first series of cruises in October 1957. The phenomenon extended to a mean distance of 60 miles from the shore, and it was stated that the upwelled water reaching the surface came from depths between 50 and 75m (Banse, 1959). Off Calicut, upwelling is regularly found during the whole period of southwest monsoon, its effect is felt strongest in July and August and it lasts till October. The near-coast surface region off Trivandrum is marked by upsloping of isotherms and approximately 100 m deep and 150 km wide equatorward flow during June (Shetye, *et al.*, 1990). Below this lies a northward approximately 40 km wide undercurrent with its core (recognised by salinity maximum) at a depth of about 150m. North of 15°N upwelling is hardly visible.

In addition to the strong northward Somali current and upwelling off the coast of Somalia, the southwest monsoon also drives

open ocean Ekman pumping during the boreal summer (Raghu, *et al.*, 1999). During November to January, the general pattern of current in the southern part of the Arabian Sea is westerly (Rao and Jayaraman, 1966). Owing to the coastal conformation, north–northwesterly current develops off the west coast of India. These two currents diverge in the vicinity of Minicoy leading to upwelling in this region. Upwelling appears to be the dominant factor in maintaining the heat balance of the Arabian Sea. Strong upwelling is limited to about one tenth of the total area, and only three months of the year, but the upwelling velocities are of the order of 30 times the required average, which could account for most of the required heat loss (Swallow, 1984).

Bhattathiri, *et al.*, (1996) recorded highest primary production near the southwest coast of India during the summer monsoon. They related this to the upwelling contributing to high nitrate levels in the top layers, which in turn supported high phytoplankton production and chlorophyll. During the summer monsoon, primary production increases in the eastern Arabian Sea as a result of upwelling.

Available information on the upwelling and stratification phenomenon especially its mechanism, intensity, temporal and spatial variability in the eastern Arabian Sea is limited, and needs to be studied through an integrated programme involving *in situ* measurements from ships and data buoys, remote sensing observations and modelling (Rao and Ram, 2005). Observation and understanding of oceanic ecosystems have been limited severely by

our inability to make long-term, continuous, detailed measurements of such basic ecological parameters such as phytoplankton and zooplankton standing stocks and the dynamic oceanic processes which influence them. In the present study, phytoplankton communities, their production rates and chlorophyll levels, together with zooplankton communities and biomass, were studied in relation to the hydrodynamic processes in the eastern Arabian Sea.

### **1.3. Review of literature**

The Arabian Sea used to be largely neglected prior to the 1960s. Most of the studies made were localized and mainly concentrated in the coastal waters (Jayaraman and Gogate, 1957; Jayaraman, *et al.*, 1959; Ramamirtham and Jayaraman, 1960). Apart from the investigations made during the International Indian Ocean Expedition (IIOE, 1962-'65), the information on biological productivity in the eastern Arabian Sea is meagre when compared to other regions of Arabian Sea. IIOE data gave a systematic and comprehensive analysis of physico-chemical and biological productivity status of Arabian Sea (IIOE, 1962-'65). The Indian oceanographic research vessels such as *RV Gaveshani* and *ORV Sagar Kanya* and *FORV Sagar Sampada* played significant roles in data collection under several projects such as the MR-LR programme.

In a majority of studies related to the productivity of the Arabian Sea, it was highlighted that biological processes are strongly influenced by physical processes, while physical processes are largely independent of the biology. Extensive work has been done in the

Arabian Sea (Kabanova, 1968; Radhakrishna, 1969; Qasim, 1977; Bhargava, *et al.*, 1978; Bhattathiri, *et al.*, 1980; Bhattathiri, 1984; Banse and McClain, 1987; Banse, *et al.*, 1996; Unnikrishnan and Antony, 1992; Gunderson *et al.*, 1998; Caron and Dennett, 1999; Nair, *et al.*, 1999., Wiggert, *et al.*, 2000; Dickson, *et al.*, 2001; Barber, *et al.*, 2001; Prasannakumar, *et al.*, 2004; Madhu, 2004; Parab, *et al.*, 2006; Prakash and Ramesh, 2007). Upwelling in the Arabian Sea is a summer phenomenon and is intimately associated with the southwest monsoon circulation (Sharma, 1966; Purushan and Rao, 1974; Shetye, *et al.*, 1990; Stramma, *et al.*, 1996). From SST and MLD distributions along the southern shelf, Muraleedharan and Prasannakumar (1996) inferred the upwelling favourable conditions which were less conspicuous towards north. Stramma, *et al.*, (1996) observed a typical eastern boundary upwelling region along the southwest coast of India during August 1993. A field experiment conducted by Sanilkumar, *et al.*, (2004) during July 2003, off the southwest coast of India indicated intense upwelling within the upper 60 m water column all along the coast, but the width of upwelling zone reduced significantly from south (>200 km) to north (~50 km).

Eastern Arabian Sea showed high surface primary production (Krey and Babenerd, 1976; Devassy, 1983; Sumitra-Vijayaraghavan and Kumari, 1989; Madhupratap, *et al.*, 1990) especially in inshore waters. Bhattathiri, *et al.*, (1996) studied the phytoplankton production and chlorophyll distribution in the eastern and central Arabian Sea during different seasons. Nair, *et al.*, (1999) and

Prasanna Kumar, *et al.*, (2000) reported that the biological productivity of the Arabian Sea tightly coupled with the physical forcing mediated through nutrient availability. Pillai, *et al.*, (2000) studied the seasonal variations in physico-chemical and biological characteristics of the eastern Arabian Sea. High biological productivity reported from the central Arabian Sea during the summer monsoon has been attributed to the open ocean upwelling (Smith, 1995; Prasannakumar, 2001a) driven by Ekman pumping and lateral advection, whereas in northern Arabian Sea winter convective mixing (Banse, *et al.*, 1996; Madhupratap, *et al.*, 1996; Prasannakumar, *et al.*, 2001b). Madhu (2004) has been studied the seasonal patterns of primary production in the EEZ of India. Gauns, *et al.*, (2005) gave a comparative account of the biological productivity characteristics and estimates of carbon fluxes in the Arabian Sea and Bay of Bengal. Vimalkumar, *et al.*, (2008) reported the hydrographic condition of southeast Arabian Sea during summer (SM) and spring inter monsoon (SIM). Variability in biological responses to different phases of summer monsoon was studied by Habeebrehman, *et al.*, (2008).

Several studies on the phytoplankton populations have been done in the coastal waters of India (Hornell and Naidu, 1923; Chacko, 1950; Chidambaram and Menon, 1945; George, 1953; Prasad, 1954 and 1956; Subrahmanyam, 1959; Sawant and Madhuprathap, 1996). Monsoon driven changes in phytoplankton populations in the eastern Arabian Sea were studied based on the microscopic and HPLC pigment analysis (Parab, *et al.*, 2006; Roy, *et al.*, 2006).

Sea truth validation of *SeaWiFS* Ocean Colour Sensor in the coastal waters of the Eastern Arabian Sea was analysed by Desa, *et al.*, 2001; Dwivedi, *et al.*, 2005). The use of remote sensing for ocean colour retrieval of pigment composition was reported by Sathyendranath, *et al.*, (2005). *Trichodesmium* bloom was studied by Desa, *et al.*, (2005), using remote sensing data and *in situ* observations.

The response of micro-zooplankton to coastal upwelling and summer stratification in south-eastern Arabian Sea were analysed by Gauns, *et al.*, (1996) and Jyothibabu, *et al.*, (2008). The relationship between zooplankton biomass and potential fishery resources were observed by Goswami (1996) and Bharagava (1996). Longhurst and Wooster, (1990) made a detailed study on the abundance of oil sardine (*Sardinella longiceps*) and upwelling on the southwest coast of India. The inter relationship between zooplankton and myctophids in deep scattering layer formation was observed by Nair, *et al.*, (1999) Madhupratap, *et al.*, (2001) studied the seasonal and spatial variability of the physics and chemistry of the west coast of India and their relation to potential fisheries.

#### **1.4. Scope and objectives of the study**

Fertility of the sea is determined by its net biological productivity. Phytoplankton being the basic food in the marine food chain, followed by zooplankton play a vital role of significance to our food resources from the sea. The active seasonal upwelling is known to occur annually during summer monsoon (Banse, 1968;

Sankaranarayanan, *et al.*, 1978) in the Arabian Sea but scanty information exists on the physico-chemical interactions and its biological responses. The importance of the upwelling area cannot be underscored considering that about 50% of the world fish catch comes from 0.1% of the upwelling area (Ryther, 1969). This pattern is duplicated along the west coast of India where maximum fish catches are obtained during or immediately after upwelling season, which indicates the importance of monsoon generated upwelling in the Indian economy. Hence, investigations on the distribution, productivity and dynamics of plankton community are necessary to assess the potential fishery resources. The objectives of this investigation include:

- i) To study the seasonal hydrographic characteristics of the eastern Arabian Sea
- ii) To study the biological responses (chlorophyll, primary productivity and zooplankton distribution patterns) in stratification during spring inter monsoon
- iii) To study the biological responses (chlorophyll, primary productivity zooplankton distribution patterns and pelagic fishery resources) of upwelling during different phases of summer monsoon

- iv) To study the phytoplankton community structure during spring inter monsoon and different phases of summer monsoon
- v) To study the composition of accessory pigments of phytoplankton community.

In view of the above, a study of the spatio-temporal variation of sea surface and column parameters (surface winds, SST, SSS, circulation and currents, chlorophyll and primary productivity) and the hydrographic features in the upper 300m has been attempted using the latest available information/data sets and the results are summarized. This study mainly emphasizes the influence of upwelling and stratification on the biological productivity at large.

## References

- Aiken, J., Moore, G.F. and Holligan, P.M., 1992. Remote sensing of oceanic biology in relation to global climate change. *J. Phycol.*, 28: 579-590.
- Banse, K. and McClain, C. R., 1987. Satellite-observed winter blooms of phytoplankton in the Arabian Sea. *Mar. Ecol. Prog. Ser.*, 34: 201-211.
- Banse, K., 1959. On upwelling and bottom trawling off the southwest coast of India. *J. Mar. Biol. Ass. India*, 1: 33-49.
- Banse, K., 1968. Hydrography of the Arabian Sea shelf of India and Pakistan and effects on demersal fishes. *Deep Sea Res.*, 15: 45-79.
- Banse, K., Sumitra-Vijayaraghavan and Madhupratap, M., 1996. On the possible causes of the seasonal phytoplankton blooms along the south-west coast of India. *Indian J. Mar. Sci.*, 25: 283-289.

- Barber, R.T., Marra, J., Bidigare, R.C., Codispoti, L.A., Halpern, D., Johnson, Z., Latasa, M., Goericke, R. and Smith, S.L., 2001. Primary productivity and its regulation in the Arabian Sea during 1995. *Deep Sea Res. II*, 48: 1127–1172.
- Barlow, R.G., Mantoura, R.F.C. and Cummings, D.G., 1999. Monsoonal influence on the distribution of phytoplankton pigments in the Arabian Sea. *Deep-Sea Res. II*, 46: 677– 699.
- Bauer, S., Hitchcock, G.L. and Olson, D.B., 1992. Response of the Arabian Sea surface layer to monsoon forcing. In Desai, B.N., (Ed.), *Oceanography of the Indian Ocean* New Delhi, Oxford & IBH. pp: 659–672.
- Bhargava, R.M.S., 1996. Some aspects of biological production and fishery resources of the EEZ of India. In: *India's Exclusive Economic Zone* (. Qasim, S.Z. and G.S. Roonwal, Eds.). *Omega Scientific Publishers*, pp: 122-131.
- Bhargava, R.M.S., Bhattathiri, P.M.A., Devassy, V.P. and Radhakrishna, K., 1978. Primary productivity studies in the southeastern Arabian Sea. *Indian J. Mar. Sci.*, 7: 267–270.
- Bhattathiri, P.M.A., 1984. Primary production and some physical and chemical parameters of Laccadive and Andaman Sea. *PhD Thesis*. University of Bombay.
- Bhattathiri, P.M.A., Devassy, V.P. and Radhakrishna, K., 1980. Primary production in the Bay of Bengal during southwest monsoon of 1978. *Mahasagar, Bull. Natl. Inst. Oceanogr.*, 13(4): 315-323.
- Bhattathiri, P.M.A., Pant, A., Sawant, S., Gauns, M., Matondkar, S.G.P. and Mohanraju, R., 1996. Phytoplankton production and chlorophyll distribution in the eastern and central Arabian Sea in 1994-95. *Curr. Sci.*, 71: 857-862.
- Bidigare, R.G. and Charles, C.T., 2002. HPLC phytoplankton pigments: sampling, laboratory methods and quality assurance procedures. In: Fargion, G.S. and Mueller, J.L. (Eds.). *Protocols for Satellite Ocean Colour Validation Revision 2*. NASA, Goddard Space Flight Centre, Greenbelt, MD, pp: 154–160.
- Binu, M.S., 2003. Studies on the fish larvae of the Arabian Sea with special reference to clupeiforms. *PhD. Thesis, Cochin University of Science and Technology*, 350p.
- Brown, S.L., Landry, M.R., Christensen, S., Garrison, D., Gowing, M.M., Bidigare, R.R. and Campbell, L., 2002. Microbial community dynamics and taxon-specific phytoplankton production in the Arabian Sea during the 1995 monsoon seasons. *Deep-Sea Research II* 49: 2345–2376.

- Bruce, J.G., Johnson, D.R. and Kindle, J.C., 1994. Evidence of eddy formation in the eastern Arabian Sea during north east monsoon. *J. Geophys. Res.* 99(C4): 7651-7664.
- Burkill, P.H., Mantoura, R.F.C. and Owens, N.J.P., 1993. Biogeochemical cycling in the northwestern Indian Ocean: a brief overview. *Deep Sea Res. II*, 40: 643-649.
- Burkill, P.H., Mantoura, R.F.C., Llewellyn, C.A. and Owens, N.J.P. 1987. Microzooplankton grazing and selectivity of phytoplankton in coastal waters. *Mar. Biol.*, 93: 581-590.
- Callot, H.J., 1991. Geochemistry of chlorophylls. In: Scheer, H. (Ed.) *Chlorophylls. CRC Press. Ann Arbor*, pp: 340-364.
- Caron, D.A. and Dennett, M.R., 1999. Phytoplankton growth and mortality during the 1995 Northeast monsoon and spring intermonsoon in the Arabian Sea. *Deep- Sea Res. II*, 46: 1665-1690.
- Chacko, P.I., 1950. Marine plankton from waters around the Krusadi Island. *Proc. Indian Acad. Sci.*, 31B: 162-174.
- Chauhan, P., Nagamani, P.V. and Nayak, S., 2005. Artificial neural networks (ANN) based algorithms for chlorophyll estimation in the Arabian Sea. *Indian J. Mar. Sci.*, 34(4): 368-373.
- Chidambaram, K. and Menon, M.D., 1945. The correlation of the west coast (Malabar and south Kanara) fisheries with plankton and certain oceanographic factors. *Proc. Indian. Acad. Sci.*, 22B: 355-367.
- Cutler, A.N. and Swallow, J.C., 1984. Surface currents of the Indian Ocean: Compiled from historical data archived by the meteorological office, Bracknell, U.K. *Institute of Oceanographic Sciences, Report No. 187*, 88p. and 36 charts.
- Desa, E., Suresh, T., Matondkar, S.G.P. and Desa, E., 2001. Sea truth validation of SeaWiFS Ocean Colour Sensor in the coastal waters of the Arabian Sea. *Curr. Sci.*, 80(7): 854-860.
- Desa, E., Suresh, T., Matondkar, S.G.P., Desa, E., Goes, J., Mascarenhas, A., Parab, S.G., Shaikh, N. and Fernandes, C.E.G., 2005. Detection of *Trichodesmium* bloom patches along the eastern Arabian Sea by IRS-P4/OCM ocean colour sensor and by *in situ* measurements. *Indian J. Mar. Sci.*, 34(4): 374-386.
- Devassy, V.P., Bhattathiri, P.M.A. and Radhakrishna, K., 1983. Primary production in the Bay of Bengal during August, 1977. *Mahasagar, Bull. Natl. Inst. Oceanogr.*, 16: 443-447.
- Dickson, M.L., Orchardo, G., Barber, R.T., Marra, J., McCrathy, J.J. and Sambrotto, R.N., 2001. Production and respiratory rates in the Arabian Sea during the 1995 northeast and southwest monsoon. *Deep Sea Res. II*, 48: 1199-1230.

- Dwivedi, R.M., Solanki, H.U., Nayak, S.R., Gulati, D. and Somvanshi, V.S., 2005. Exploration of fishery resources through integration of ocean colour with sea surface temperature: Indian experience. *Indian J. Mar. Sci.*, 34(4): 430-440.
- Falkowski, P.G. and Raven, J.A., 1997. *Aquatic photosynthesis*. Blackwell Science Inc., Boston, 375pp.
- Gauns, M., Madhupratap, M., Ramaiah, N., Jyothibabu, R., Fernandes, V., Paul, J.T. and Prasannakumar, S., 2005. Comparative accounts of biological productivity characteristics and estimates of carbon fluxes in the Arabian Sea and the Bay of Bengal. *Deep Sea Res. II*, 52(14-15): 2003-2017.
- Gauns, M., Mohanraju, R. and Madhupratap, M., 1996. Studies on the micro-zooplankton from the central and eastern Arabian Sea. *Curr. Sci.*, 71(11): 874-877.
- George, P.C., 1953. The marine plankton of the coastal waters of Calicut with observations on the hydrological conditions. *J. Zool. Soc. India*, 5: 76-107.
- Goericke, R., 2002. Top-down control of phytoplankton biomass and community structure in the monsoonal Arabian Sea. *Limnol. Oceanogr.*, 47: 1307-1323.
- Goswami, S.C., 1996. Zooplankton biomass and potential fishery resources. In: *India's Exclusive Economic Zone* (Eds. Qasim, S.Z. and Roonwal, G.S.), Omega Scientific Publishers. pp: 94-104.
- Gunderson, J., Gardner, W.D., Richardson, M.J. and Walsh, I.D., 1998. Effects of monsoon on the seasonal and spatial distribution of POC and chlorophyll in the Arabian Sea. *Deep Sea Res. II*, 45: 2103-2132.
- Habeebrehman, H., Prabhakaran, M.P., Jacob, J., Sabu, P., Jayalakshmi, K.J., Achuthankutty, C.T. and Revichandran, 2008. Variability in biological responses influenced by upwelling events in the eastern Arabian Sea. *J. Mar. Syst.*, 74: 545-560.
- Hays, G.C., Richardson, A.J. and Robinson, C., 2005. Climate change and marine plankton. *Trends in Ecology and Evolution*, 20 (6): 337-344.
- Hornell, J. and Naidu, M.R., 1923. A contribution of the life history of the Indian oil sardine with notes on the plankton of the Malabar coast. *Madras. Fish. Bull.*, 17:129-197.
- IIOE (1962-65). International Indian Ocean Expedition. 1965-72. *Collected Reprints*. Vol. 1-8.
- Jayaraman, R. and Gogate, S.S., 1957. Salinity and temperature variations in the surface waters of the Arabian Sea off the Bombay and Saurashtra Coasts. *Proc. Ind. Acad. Sci.*, 45: 151-164.

- Jayaraman, R., Ramamritham, C.P. and Sundara Raman, 1959. The vertical distribution of dissolved oxygen in the deeper waters of the Arabian Sea in the neighbourhood of the Laccadives during the summer of 1959. *J. Mar. Biol. Ass. India*, 1(2): 206-211.
- Jeffrey, S.W. and Hallegraff, G.M., 1990. Phytoplankton ecology in Australian waters. In: Clayton, M.N. and King, R.J. (Eds.). *Biology of Marine Plants, Longman – Cheshire, Melbourne*. pp: 310-348.
- Jeffrey, S.W., Mantoura, R.F.C. and Wright, S.W., 1997. *Phytoplankton Pigments in Oceanography: Guidelines to Modern Methods*. UNESCO Publishing, Paris. 661p.
- Jyothibabu, R., Ashadevi, C.R., Madhu, N.V., Sabu, P., Jayalakshmi, K.V., Josia, J., Habeebrehman, H., Prabhakaran, M.P., Balasubrahmanian, T. and Nair, K.K.C. 2008. The response of microzooplankton (20-200µm) to coastal upwelling and summer stratification in the south-eastern Arabian Sea. *Conti. Shelf Sci.*, 28: 653-671.
- Kabanova, Yu. G., 1968. Primary production of the northern part of the Indian Ocean. *Oceanology*, 8: 214 – 225.
- Krey, J. and Babenerd, B., 1976. Phytoplankton production. *Atlas of the Indian Ocean Expedition. Inst. F. Meereskunde, Uni. Kiel*, 70pp.
- Latasa, M. and Bidigare, R., 1998. A comparison of phytoplankton populations of the Arabian Sea during the Spring Intermonsoon and Southwest Monsoon of 1995 as described by HPLC-analyzed pigments. *Deep-Sea Research II*, 45: 2133– 2170.
- Longhurst, A., 1998. *Ecological geography of the sea. Academic Press*, 398p.
- Longhurst, A.R. and Wooster, W.S., 1990. Abundance of oil sardine (*Sardinella longiceps*) and upwelling on the southwest coast of India. *Can. J. Fish. Aquat. Sci.*, 47: 2407-2419.
- Madhu, N.V., 2004. Seasonal studies on primary production and associated environmental parameters in the Indian EEZ. *PhD. Thesis, Cochin University of Science and Technology*, 234p.
- Madhupratap, M. and Haridas, P., 1990. Zooplankton especially, calanoid copepods in the upper 1000m of the south east Arabian sea. *J. Plankton Res.*, 12: 305-321.
- Madhupratap, M., Gopalakrishnan, T.C., Haridas, P., Nair, K.K.C., Aravindakshan, P.N., Padmavati, G. and Paul, S., 1996. Lack of seasonal and geographical variation in mesozooplankton biomass in the Arabian Sea and its structure in the mixed layer. *Curr. Sci.*, 71: 863-868.
- Madhupratap, M., Nair, K.N.V., Gopalakrishnan, T.C., Haridas, P., Nair, K.K.C., Venugopal, P. and Mangesh, G., 2001. Arabian Sea oceanography and fisheries of the west coast of India. *Curr. Sci.*, 81(4): 355-361.

- Malin, G., Turner, S.M. and Liss, P.S., 1992. Sulfur: The planktonic/climate connection. *J. Phycol.*, 28: 590-597.
- Mantoura, R.F.C., Law, C.S., Owens, N.J.P., Burkill, P.H., Woodward, E.M.S., Howland, R.J.M. and Llewellyn, C.A., 1993. Nitrogen biochemical cycling in the north-western Indian Ocean. *Deep Sea Res. II.*, 40: 651-671.
- Muraleedharan, P.M. and Prasanna Kumar, S., 1996. Arabian Sea upwelling - A comparison between coastal and open ocean regions. *Curr. Sci.*, 71: 842-846.
- Nair, K.K.C., Madhuprathap, M., Gopalakrishnan, T.C. and Haridas, P., 1999. The Arabian Sea: Physical Environment, Zooplankton and Myctophid abundance. *Indian J. Mar. Sci.*, 28: 138-145.
- Ondrusek, M.E., Bidigare, R.R., Sweet, S.T., Defreitas, D.A. and Brooks, J.M., 1991. Distribution of phytoplankton pigments in the North Pacific Ocean in relation to physical and ocean variability. *Deep Sea Res. II*, 38: 243-266.
- Owens, N.J.P., Burkill, P.H., Mantoura, R.F.C., Woodward, E.M.S., Bellan, I.E., Aiken, J., Howland, R.J.M. and Llewellyn, C.A., 1993. Size fractionated primary production and nitrogen assimilation in the north western Indian Ocean. *Deep Sea Res. II*, 40: 697-709.
- Parab, S.G., Matondkar, S.G.P., Gomes, H. and Goes, J.I., 2006. Monsoon driven changes in phytoplankton populations in the eastern Arabian Sea as revealed by microscopy and HPLC pigment analysis. *Conti. Shelf Res.*, 26(20): 2538-3558.
- Pillai, V.N., Pillai, V.K., Gopinathan, C.P. and Nandakumar, A., 2000. Seasonal variations in the physico-chemical and biological characteristics of the eastern Arabian Sea. *J. Mar. Biol. Ass. India*, 42(1& 2): 1-11
- Prakash, S. and Ramesh, R., 2007. Is Arabian Sea getting more productive? *Curr. Sci.*, 92(5): 667-671.
- Prasad, R. R., 1956. Further studies on the plankton of the near shore waters off Mandapam. *Indian J. Fish.*, 3: 1-42.
- Prasad, R.R., 1954. The characteristics of marine plankton at an inshore station in the Gulf of Mannar near Mandapam. *Indian. J. Fish.*, 1: 1-36.
- Prasad, T.G., 2001. Formation of seasonal spreading of water masses in the Arabian sea based on data analysis and modeling. *Ph.D Thesis, Hokkaido University, Japan.*
- Prasanna Kumar, S., Madhupratap, M., Dileepkumar, M., Gauns, M., Muraleedharan, P.M., Sarma, V.V.S.S. and D'Souza, S.N., 2000. Physical control of primary productivity on a seasonal scale in central

- and eastern Arabian Sea. *Proc. Indian Acad. Sci. (Earth Planet. Sci.)* 109(4): 433-441.
- Prasanna Kumar, S., Madhupratap, M., Kumar, M.D., Muraleedharan, P.M., D'Souza, S.N., Gauns, M. and Sarma, V.V.S.S., 2001a. High biological productivity in the central Arabian Sea during the summer monsoon driven by Ekman pumping and lateral advection. *Curr. Sci.*, 81: 1633-1638.
- Prasanna Kumar, S., Narvekar, J., Ajoy Kumar, Shaji, C., Anand, P., Sabu, P., Rejomon, G., Jossia, J., Jayaraj, K. A., Radhika, R. and Nair, K. K. C., 2004. Intrusion of the Bay of Bengal water into the Arabian Sea during winter monsoon and associated chemical and biological response. *Geoph. Res. Lett.*, 31: 5304.
- Prasanna Kumar, S., Ramaiah, N., Gauns, M., Sarma, V.V.S.S., Muraleedharan, P.M., Reghukumar, S., Dileepkumar, M. and Madhupratap, M., 2001b. Physical forcing of biological productivity in the northern Arabian Sea during the north-east monsoon. *Deep Sea Res. II*, 48: 1115-1126.
- Purushan, K.S. and Rao, T.S.S., 1974. Studies on the upwelling off the south west coast of India. *Indian J. Mar. Sci.*, 3: 81-82.
- Qasim, S.Z., 1977. Biological productivity of the Indian Ocean. *Indian J. Mar. Sci.*, 6: 122-137.
- Radhakrishna, K., 1969. Primary productivity studies in the shelf waters off Alleppey, southwest India during the post monsoon 1967. *Mar. Biol.*, 4: 174-181.
- Raghu, G.M., Sergio, S.R., Signorini, R. Christian, J.R., Busalacchi, A.J., McClain, C.R. and Picaut, J., 1999. Ocean colour variability of the tropical Indo-Pacific basin observed by *SeaWiFS* during 1997-1998. *J. Geophys. Res.*, 104: 18351-18366.
- Ramamritham, C.P. and Jayaraman, R., 1960. Hydrological features of the continental shelf waters off Cochin during the years 1958 and 1959. *J. Mar. Biol. Ass. India*, 2(2): 199-207.
- Ramasastri, A.A. and Myrland, P., 1959. Distribution of temperature, salinity and density in the Arabian Sea along the South Malabar Coast (South India) during the post monsoon season. *Indian J. Fish.*, 6(2): 223-255.
- Rao, L.V.G. and Jayaraman, R., 1966. Upwelling in the Minicoy region of the Arabian Sea. *Curr. Sci.*, 35: 378-380.
- Rao, L.V.G. and Ram, P.S., 2005. Upper ocean physical processes in the tropical Indian Ocean. *Monograph, Council for Scientific and Industrial Research, New Delhi*, 68p.

- Roy, R., Pratihary, A., Gauns, M. and Naqwi, S.W.A., 2006. Spatial variation of phytoplankton pigments along southwest coast of India. *Estuar. Coast. Shelf Sci.*, 69: 189-195.
- Ryther, J.H., 1969. Photosynthesis and fish production in the sea. *Science*, 166: 72-80.
- Sanilkumar, K.V., Unni, V.K. and James, V.V., 2004. Upwelling characteristics off the southwest coast of India during 2003. *METOC, Proceedings of National symposium on emerging trends in the fields of Meteorology and Oceanography*, pp: 137-143.
- Sankaranarayanan, V.N., Rao, D.P. and Antony, M.K., 1978. Studies on some hydrographic characteristics of estuarine and inshore waters of Goa during the southwest monsoon 1972. *Mahasagar, Bull. Natl. Inst. Oceanogr.*, 11: 125-136.
- Sastry, J.S. and D'Souza, R.S., 1972. Upwelling and upward mixing in the Arabian Sea. *Indian J. Mar. Sci.*, 1: 17-27.
- Sathyendranath, S., Gouveia, A.D., Shetye, S.R., Ravindram, P. and Platt, T., 1991a. Biological control of surface temperature in the Arabian Sea. *Nature*, 349: 54-56.
- Sathyendranath, S., Platt, T., Horne, E.P.W., Harrison, W.G., Ullno, O., Outerbridge, R. and Hoepffner, N., 1991b. Estimation of new production in the ocean by compound remote sensing. *Nature*, 353: 129-133.
- Sathyendranath, S., Stuart, V., Platt, T., Bouman, H., Ulloa, O. and Maass, H., 2005. Remote sensing of ocean colour: Towards algorithms for retrieval of pigment composition. *Indian J. Mar. Sci.*, 34(4): 333-340.
- Sawant, S. and Madhupratap, M., 1996. Seasonality and composition of phytoplankton in the Arabian Sea. *Curr. Sci.*, 71: 869-873.
- Scheer, H., (Ed.) 1991. *Chlorophylls*. CRC Press, Boca Raton, Florida, 1257pp.
- Shankar, D. and Shetye, S.R., 1997. On the dynamics of the Lakshadweep High and Low in the southeastern Arabian Sea. *J. Geophys. Res.*, 102 (C6): 12551-12562.
- Shankar, D., Vinayachandran, P.N. and Unnikrishnan, A.S., 2002. The monsoon currents in the Indian Ocean. *Progr. Oceanogr.*, 52: 63-120.
- Sharma, G.S., 1966. Thermocline as an indicator of upwelling, *J. Mar. Biol. Ass. India*. 8: 8-19.
- Shetye, S.R., Gouveia, A.D., Shenoi, S.S.C., Sunbar, D., Michael, G.S., Almeida, A.M. and Santanam, K., 1990. Hydrography and circulation off the west coast of India during the southwest monsoon 1987. *J. Mar. Res.*, 48: 359-378.

- Smith, R.L., and Bottero, J.S., 1977. On upwelling in the Arabian Sea, pp. 291-304 in Angel, M. (Ed.), *A Voyage of Discovery, Pergamon, New York*.
- Smith, S.L., 1995. The Arabian Sea: mesozooplankton response to seasonal climate in a tropical ocean. *ICES J. Mar. Sci.*, 52: 427-438.
- Stramma, L., Fischer, J. and Schott, F., 1996. The flow field off southwest India at 8°N during the southwest monsoon of August 1993. *J. Mar. Res.*, 54: 55-72.
- Subrahmanyam, R., 1959. Studies on the phytoplankton of the west coast of India – I and II, *Proc. Indian Acad. Sci.*, 50(B):113-252.
- Sumitra-Vijayaraghavan and Kumari, L.K., 1989. Primary productivity in the southeastern Arabian Sea during southwest monsoon. *Indian J. Mar. Sci.*, 18: 30-32.
- Swallow, J.C., 1984. Some aspects of the physical oceanography of the Indian Ocean. *Deep Sea Res. I*, 31: 639-650.
- Unnikrishnan, A.S. and Antony, M.K., 1992. On an upwelling front along the west coast of India during later part of southwest monsoon: In: Physical process in the Indian seas. *Proc. First. Convention, ISPO (1990)*: 131-135.
- Varadachari, V.V.R. and Sharma, G.S., 1967. Circulation of the surface waters in the North Indian Ocean. *J. Indian Geophys. Uni.*, 4(2): 61-73.
- Vimal Kumar, K.G., Dineshkumar, P.K., Smitha, B.R., Habeebrehman, H., Josia J., Muraleedharan, K.R., Sanjeevan, V.N. and Achuthankutty, C.T., 2008. Hydrographic characterization of southeast Arabian Sea during the wane of southwest monsoon and spring inter monsoon. *Environ. Monit. Assess.*, 140: 231-247.
- Watson, A.J., Robinson, C., Robertson, J.E., Williams, P.J. Le B. and Fasham, M.J.R., 1991. Spatial variability in the sink for atmospheric carbon dioxide in the North Atlantic. *Nature*, 350: 50-53.
- Watts, L.J., Kumari, B. and Maass, H., 2005. Applications of remotely sensed ocean colour data in the Arabian Sea: A review. *Indian J. Mar. Sci.*, 34(4): 396-407.
- Wiggert, J.D., Jones, B.H., Dickey, T.D., Brink, K.H., Weller, R.A., Mara, J., Codispoti, L.A., 2000. The Northeast monsoon's impact on mixing, phytoplankton biomass and nutrient cycling in the Arabian Sea. *Deep Sea Res. II*, 47: 1353-1386.
- Williamson, P. and Gribbin, J., 1991. How plankton changes the climate. *New Scientist*, 129: 44-48.
- Wright, S.W., Jeffrey, S.W., Mantoura, R.G.C., Llewellyn, C.A., Bjornland, D.R., Welschmeyer, N., 1991. Improved HPLC method for the analysis

of chlorophylls and carotenoids from marine phytoplankton. *Mar. Ecol. Prog. Ser.*, 77: 183–196.

Wyrтки, K. 1973. Physical Oceanography of the Indian Ocean. In: *The Biology of the Indian Ocean-Ecological studies – Analyses and Synthesis*, (Eds.) Zeitzschel, B. and Gerlach, S.A. (Springer-Verlag, Berlin), vol. 3: 18-36.

## Chapter II

# Materials and methods

---

- 2.1. *Study area and sampling stations*
  - 2.2. *Sampling seasons*
  - 2.3. *Sampling procedure and methods of analysis*
    - 2.3.1. *Physical parameters*
    - 2.3.2. *Chemical parameters*
      - 2.3.2.1. *Dissolved oxygen*
      - 2.3.2.2. *Nutrients*
    - 2.3.3. *Biological parameters*
      - 2.3.3.1. *Primary productivity*
      - 2.3.3.2. *Chlorophyll a*
      - 2.3.3.3. *Phytoplankton cell counts*
      - 2.3.3.4. *Phytoplankton pigments*
      - 2.3.3.5. *Satellite chlorophyll imagery*
      - 2.3.3.6. *Secondary productivity*
      - 2.3.3.7. *Fish landing data*
    - 2.3.4. *Statistical analysis*
  - References*
- 

The data used for this study are from four cruises carried out in the eastern Arabian Sea (Indian EEZ) by the research vessel, **FORV Sagar Sampada** (Plate 2.1) as a part of the multidisciplinary project entitled **Environment and productivity patterns of the Indian EEZ** (MR-LR) funded by Ministry of Earth Sciences (MoES), New Delhi. The second phase of the programme initiated during 2003, designed to assess and evaluate the environmental parameters and the marine living resources of the Indian Exclusive Economic Zone (EEZ) by the simultaneous collection of physical, chemical and biological oceanographic parameters from the eastern Arabian Sea.

### **2.1. Study area and sampling stations**

Eastern part of the Arabian Sea (Indian EEZ) was selected as the area of study, (8°N-21°N) which would be considered as a tropical

oceanic system (Fig. 2.1). Forty two stations were sampled along eight transects at 8°N, 10°N, 11.5°N, 13°N, 15°N, 17°N, 19°N, and 21°N; and for physico-chemical parameters, namely temperature, dissolved oxygen and macronutrients (nitrate, phosphate and silicate). Along each transect, water samples for the measurement of biological parameters, such as phytoplankton composition, chlorophyll-*a*, and primary productivity, were collected from two locations: one near to the coast (inshore) and another in the oceanic region (offshore). Mesozooplankton samples were collected from all hydrographic stations.

**2.2. Sampling seasons**

The sampling seasons selected for these studies were spring intermonsoon (SIM) and summer monsoon (SM). Summer monsoon further categorized in to three phases – onset of summer monsoon (OSM), peak summer monsoon (PSM) and late summer monsoon (LSM) based on the hydrographic characteristics. The details of the study periods are given in the Table 2.1.

**Table 2.1. Classification of seasons and cruises under taken in the study area**

<b>Seasons</b>	<b>Cruises</b>
Spring Intermonsoon (SIM)	Cruise 223 &224 (March – April 2004)
Onset of Summer Monsoon (OSM)	Cruise 235 (May – June 2005)
Peak Summer Monsoon (PSM)	Cruise 237 (August 2005)
Late Summer Monsoon (LSM)	Cruise 217 (September – October 2003)

## **2.3. Sampling procedure and methods of analysis**

### **2.3.1. Physical parameters**

Meteorological parameters were recorded continuously throughout the cruise using ship borne weather station. The sea surface temperature (SST) was measured using bucket thermometer. A Sea Bird CTD (*Model: SBE-911 USA*) (Plate 2.2) was used to measure temperature – salinity profiles at 1m intervals and water samples were collected from the standard depths. Salinity values from CTD were corrected against the values obtained from Autosal (*Model 8400A*) onboard. The processed 1-m bin averaged temperature and salinity values were used to construct T and S profiles at each station and examined for spikes and spurious data. The data corresponding to spikes were deleted and only quality data on temperature and salinity were used in the present study. Mixed layer depth (MLD) was computed as the depth at which density rises by 0.2 units from the surface. This density difference is equivalent to a 1.0°C change in temperature, if salinity is constant.

### **2.3.2. Chemical parameters**

Collection of water samples were made from standard depths using 1.8 litres *Niskin* bottles attached to the CTD with remotely operated closing mechanism. The samples were sub-sampled immediately and analyzed for dissolved oxygen, nitrate, phosphate and silicate. Standard methods followed for the estimation of these parameters are given below in detail.

### 2.3.2.1. Dissolved Oxygen

Dissolved Oxygen (DO) was determined by Winkler's method as described in Grasshoff (1976). Water samples were carefully collected in glass bottles (125ml) without trapping air bubbles. Samples were immediately fixed by adding 0.5ml of Winkler A ( $MnCl_2$ ) and 0.5ml of Winkler B (alkaline KI) solution and mixed well for precipitation. The dissolved oxygen was later analyzed after acidification by titration against standard sodium thiosulphate ( $Na_2S_2O_3$ ) using starch as indicator. The concentration of oxygen in the sample was calculated as,

$$\text{Dissolved Oxygen (ml/litre)} = 5.6 * N * (S - B_m) * V / (V - 1) * 1000 / A$$

where,

N = Normality of the thio sulphate

S = Titre value for sample

$B_m$  = Mean titre value for blank

V = Volume of the sample bottle (125ml)

A = Volume of sample titrated (50ml)

### 2.3.2.2. Nutrients

The major nutrients analysed were Nitrate - Nitrogen ( $NO_3-N$ ), Phosphate - Phosphorous ( $PO_4-P$ ) and Silicate - Silicon ( $SiO_4-Si$ ). Samples for nutrients were collected in clean glass bottles and analyses were carried out by autoanalyser *SKALAR (Model - SA 1050)* onboard.

Nitrate in the sample was first reduced to nitrite using a reductor column filled with amalgamated cadmium granules and the nitrite ( $NO_2$ ) was reacted with sulphanilamide in an acid solution. The

resulting diazonium compound was coupled with N - (1- Naphthyl) - ethylenediamine dihydrochloride to form a coloured azo dye and the absorbance was measured spectrophotometrically at 543nm.

Dissolved inorganic reactive phosphate was estimated by the formation of a reduced phosphomolybdenum blue complex in an acid solution containing molybdic acid, ascorbic acid and trivalent antimony, adopted by the method of Grasshoff, *et al.*, (1983). The absorbance of the colour complex was made at 882nm.

The determination of dissolved silicate in seawater was based on the formation of molybdenum blue complex when the acid sample is treated with a molybdic solution the absorbance of which was made at 810nm (Grasshoff, *et al.*, 1983).

### **2.3.3. Biological parameters**

#### *2.3.3.1. Primary productivity*

Primary productivity measurements were made according to Indian JGOFS protocol (UNESCO, 1994) using <sup>14</sup>C - technique introduced by Steeman Nielsen (1952). Polycarbonate (*Nalgene, USA*) bottles used for primary productivity incubations were soaked for 72 hours in a 5% solution of detergent, rinsed thoroughly with deionised water and subsequently soaked for 72 hours in 0.5N HCl solution. Bottles were then rinsed with distilled water and kept filled with Milli-Q water for 48 hours.

For measuring *in-situ* primary productivity, water samples were taken from seven depths (0, 10, 20, 50, 75, 100 & 120 metres) one hour before the sunrise. Samples were immediately sieved through a

200 $\mu$ m mesh to remove large zooplankton and transferred to five clean Nalgene PC bottles of 300ml capacity for each depth. Before addition of radioactive carbonate, none of the samples were exposed to light (as either light can enhance productivity or degrade/reduce the photosynthetic efficiency due to light shock in samples from deeper depths). To each PC bottle containing seawater sample, 1ml solution of 5 $\mu$ Ci (185 kbq) radioactive carbon (*BRIT, DAE, Mumbai*) was added. From one bottle, 100ml sample was filtered on to 47mm GF/F (nominal pore size 0.7 $\mu$ m) filter paper for determining the initial adsorption of the  $^{14}$ C by the particles in the bottle. From the remaining bottles at each depth, one was covered with aluminium foil and transferred to a black bag to determine the production in the dark. Thus, one dark and three light bottles were used at each depth for *in-situ* incubation for 12 hours from sunrise to sunset.

The bottles were deployed *in-situ* (Plates 2.3 & 2.4) to suspend them at the appropriate depths of their origin using polypropylene line attached to a buoy. The 'mooring' system was thus deployed approximately one hour before sunrise, and allowed to drift freely for 12 hours during fair weather seasons. During monsoon however, due to inclement weather, primary productivity mooring buoy was tied to the ship and let to drift freely in such a way that the rope was not taut. The ship was occasionally maneuvered to keep the mooring ~ 150 - 200m away from it. The system was then retrieved ~30 minutes after sunset.

Immediately after retrieval, samples in each light and dark bottles were filtered on to GF/F filter and the filters were transferred to scintillation vials. A drop of 0.5N HCl was added to each vial and capped it overnight. All vials were held at room temperature until the radioactivity was counted. Before counting, all vials were uncapped and left open overnight. Five ml of liquid scintillation cocktail (SISCO-Bombay) was added and the radioactivity was counted in a liquid scintillation system (*Wallac 1409, DSA- Perkin Elmer- USA*) (Plate 2.5).

The count (disintegration per minute - DPM) rates were converted to daily production rates ( $\text{mgC m}^{-3} \text{d}^{-1}$ ), which were obtained from the triplicates that generally agreed within  $\pm 10\%$  of covariance and were averaged to obtain mean values for a given depth. Production rate in the dark bottle was subtracted from the mean value of light bottle to correct for non-photoautotrophic carbon fixation or adsorption. Similarly, to determine the initial activity added (Time zero  $T_0$ ) in the bottles, 0.2ml of sample was transferred to a scintillation vial and 0.2ml of ethanolamine was added to it (ethanolamine prevents the radiolabelled inorganic  $\text{CO}_2$  from escaping to the atmosphere). The daily production rate of various depths was used to calculate integrated production of the water column ( $\text{mgC m}^{-2} \text{d}^{-1}$ ).

**Calculation:**

$$\text{Primary productivity (mg C m}^{-3} \text{ day}^{-1}) = 1.05 \times S_{\text{DPM}} \times W / S_A \times T$$

$$\text{Sample Activity (SA)} = V \times T_{\text{DPM}} / A_{\text{vol}}$$

Where,

DPM = Disintegration Per Minute

$S_{DPM}$  = DPM s in filtered sample

$T_{DPM}$  = Total  $^{14}C$  DPMs (in 0.25ml)

$A_{vol}$  = Volume taken to measure sample activity

$V$  = Volume of filtered sample (litres)

$T$  = Time (days)

1.05 = correction for the lower uptake of  $^{14}C$  compared to  $^{12}C$

$W$  = Dissolved Inorganic Carbon (DIC) concentration in sample  
(~25000 mg C m<sup>-3</sup>)

The depth wise production was integrated to obtain the production for the entire euphotic zone (Dyson *et al.*, 1965).

Column production (mg C m<sup>-2</sup>day<sup>-1</sup>)

$$= [(d_1-d_0) (a_0+a_1)/2 + (d_2-d_1) (a_1+a_2)/2 + \dots\dots\dots]$$

Where,  $d_0$ ,  $d_1$ ,  $d_2$  are the depths sampled;  $a_0$ ,  $a_1$ ,  $a_2$  are the respective production rates.

### 2.3.3.2. Chlorophyll *a*

For the estimation of chlorophyll *a*, one litre of water from each standard depth was filtered under low vacuum through GF/F (nominal pore size 0.7 $\mu$ m) filters, added one or two drops of magnesium carbonate solution and kept in refrigerator (Strickland and Parsons, 1972). The filter papers were extracted in 90% acetone, centrifuged and made up to 10ml using 90% acetone and the absorbance was measured using a spectrophotometer (Shimadzu UV/Vis) (Plate 2.6) using 1cm cuvette against 90% acetone as blank at different wavelengths of 750, 664, 647 & 630 nm. The amount of the

plant pigment in the original seawater sample was calculated using the equation (SCOR/UNESCO).

$$\text{Chlorophyll } a = 11.85 E 665 - 1.54 E 645 - 0.08 E 630$$

$$\text{mg Chlorophyll/m}^3 = C/V \times 10$$

Where,

C = value obtained from the formula given above

V = volume of water filtered in litres

10 = volume of 90% acetone

Chlorophyll *a* calculated for each depth was integrated to obtain the column values using the relation given earlier in calculating column primary production.

#### *2.3.3.3. Phytoplankton cell counts*

For enumerating and speciating phytoplankton cells, all samples in duplicate (250ml) were fixed in 1% Lugol's iodine and preserved in 3% formaldehyde solution. The samples were stored in dark at low temperature (5°C) until enumeration, which was performed usually one month after collection. A settling and siphoning procedure was followed to obtain 20-25ml phytoplankton concentrate. Two replicates of one ml each of those concentrates were examined under an inverted stereoscopic binocular microscope (*OLYMPUS CK-30*) (Plate 2.7) at a magnification of 100X in a *Sedgewick-Rafter* plankton counting cell for phytoplankton size >5µm. The total number of cells per litre is expressed as density of phytoplankton in the study area. Species identification is done according to Subrahmanyam (1959) Wimpenny (1966) and Tomas, (1997). Chain forming cells were

counted on a per cell basis where empty cells were excluded. Phytoplankton not identified to species was placed under generic listings.

#### *2.3.3.4. Phytoplankton pigments (HPLC Method)*

For the pigment analysis, samples were immediately filtered on a GF/F filter (pore size 0.7 mm) avoiding exposure of the filter paper to direct light and high temperature. The filter paper was stored in liquid nitrogen until analyzed in the shore laboratory as follows. The frozen filters were immersed in 3 ml of 95% acetone (v/v in deionised water) for extraction using a sonicator probe (5 s, 25 kHz) under low light and temperature (4°C) followed by storage at -20 °C for 4 h. The extract was passed through a Teflon syringe cartridge (Millipore) having a glass fibre pre acrodisc filter (pore size 0.45 mm, diameter 25 mm) to remove the cellular debris. The clarified extract was collected in a 5 ml amber colour glass vial and placed directly into the temperature controlled (5°C) autosampler tray for the (HPLC) analysis.

Pigments were separated following a slight modification of the procedure of Van Heukelem (2002), which provides quantitative analysis of 20 pigments and qualitative analysis of several others. The HPLC system was equipped with an *Agilent 1100* pump together with online degasser, an *Agilent* diode array detector connected via guard column to an Eclipse XDB C8 HPLC column (4.6-150 mm) manufactured by *Agilent Technologies* (Plate 2.8). The column was maintained at 60°C. Elution at a rate of 1.1 ml/minute was performed using a linear gradient program over 22 min with 5/95% and 95/5%

of solvents B/A being the initial and final compositions of the eluant, where solvent B was methanol and solvent A was (70:30) methanol and 1 M ammonium acetate (pH 7.2) instead of 28 mM solution as recommended in the protocol. An isocratic hold on 95% B was necessary from 22 to 27 minutes for the elution of the last pigment (*a*- or *b*-carotene) at approximately 27 min. After returning to the initial condition (5% solvent B) by 31 min, the column was equilibrated for 5 minutes prior to next analysis. The eluting pigments were detected at 450 and 665 nm (excitation and emission) by the diode array detector. All chemicals used were of HPLC-grade, procured from *E. Merck (Germany)*.

Commercially available standards obtained from *DHI Inc (Denmark)*, were used for the identification and quantification of pigments. Solutions of *chlorophyll a*, *chlorophyll b*, *chlorophyll c2*, *chlorophyll c3*, *fucoxanthin*, *peridinin*, *neoxanthin*, *diadinoxanthin*, *diatoxanthin*, *alloxanthin*, *violaxanthin*, *canthaxanthin*, *divinyl chlorophyll a*,  *$\alpha$ -carotene*,  *$\beta$ -carotene* and *zeaxanthin* were run in order to obtain calibration curves and absorption spectra and to determine detection limits. Identification was based on the retention time and peak shape, i.e., through finger print matching with known peak shape from the diode array spectra library created by running pure standard of individual pigments. The concentrations of the pigments were computed from the peak areas.

#### 2.3.3.5. Satellite chlorophyll imagery

To see the variation in the chlorophyll concentrations during the study period, monthly composites of Level-3 Version 9 km resolution mapped *SeaWiFS* chlorophyll images generated by NASA's Giovanni (*Giovanni.gsfc.nasa.gov*.) were used.

#### 2.3.3.6. Secondary productivity

The mesozooplankton samples were collected using Multiple Plankton Net (*HYDRO-BIOS*) with area of 0.25 m<sup>2</sup> and mesh size of 200 µM (Plate 2.9). This sampler is based on the principle of opening and closing of a series of individual plankton nets in succession at desired depth ranges by pressure triggering. The system consists of a main powered Deck Command Unit and square shaped stainless steel frame (0.25m<sup>2</sup>) with canvas part to which five net bags are attached (mesh size – 200 µm). The net bags are opened and closed by means of an arrangement of levers, which are triggered by a battery powered Motor Unit. The towing was vertical from bottom of thermocline layer to surface and hauling speed was 1 m/s. samples were collected from depth strata of thermocline layer and mixed layer.

The term biomass denotes the amount of living matter present in the zooplankton, and is used to evaluate the standing stock. The fixation and preservation of the sample was followed by the standard protocols (Steedman, 1976; Postel, *et al.*, 2000) Prior to estimation of biomass, larger zooplankters such as medusae, ctenophores, salps, siphonophores and fish larvae were separated from the sample and their biomass taken separately and added to the biomass of the rest of

the zooplankton. Biomass was estimated by displacement volume method. For this, the zooplankton sample is filtered through a piece of clean, dried netting material (200 µm mesh size). The interstitial water was removed with the blotting paper. The filtered zooplankton is then transferred with a spatula to a measuring cylinder with a known volume of 4% formalin – seawater solution. The displacement volume was obtained by recording the volume of fixative in the measuring jar displaced by the zooplankton. The formula used for the biomass calculation is as follows:

$$\text{Biomass} = \text{DV}/\text{VWF}$$

$$\text{VWF} = \text{DH} \cdot \text{A}$$

Where,

DV = displacement volume

VWF = volume of water filtered

DH = Difference in depth of haul

A= Mouth area of the net (0.25m<sup>2</sup>)

#### *2.3.3.7. Fish landing Data*

Data of fish landing from the west coast of India, during the years 2003-2005 were obtained from CMFRI special publication No.89 (Srinath, *et al.*, 2006).

#### **2.3.4. Statistical analysis**

Two way analysis of variance (ANOVA) was used to study the significance of variability of phytoplankton cell density, chlorophyll a and primary productivity. The software programmes *viz.*, SPSS (*Statistical Programme for Social Sciences version 14.0*) and PRIMER *v*

5 (*Plymouth Routines in Multivariate Ecological Research*, version 5), were used for univariate and multivariate analyses of data. Statistical analysis for 2 Way ANOVA and standard deviation was done based on SPSS 14.0 software packages for Windows for testing the presence of significant differences among the parameters between stations and between seasons. Correlation results were used to correlate the environmental parameters with the biological parameter.

**Community structure:** *PRIMER v5 for windows* was used for the analysis of community structure.

**(a) Diversity indices**

**1) Shannon - Wiener index (H')**

In the present study, the data were analysed for diversity index (H') using the following Shannon - Wiener's formula (1949):

$$H' = -\sum_{i=1}^S P_i \log_2 P_i \dots$$

which can be rewritten as,

$$H = \frac{3.3219 (N \log N - \sum ni - \log ni)}{N}$$

where, H' = species diversity in bits of information per individual

ni = proportion of the samples belonging to the *i*<sup>th</sup> species (number of individuals of the *i*<sup>th</sup> species)

N = total number of individuals in the collection and

∑ = sum.

**ii) Margalef richness index (d)**

$$d = (S-1)/\log N$$

**iii) Pielou's evenness index (J')**

The equitability (J') was computed using the following formula of Pielou (1966):

$$J' = \frac{H'}{\log_2 S} \text{ or } \frac{H'}{\ln S}$$

where, J' = evenness,

H' = species diversity in bits of information per individual and S

= total number of species

**(b) Similarity indices****i) Cluster analysis**

Cluster analysis was done to find out the similarities between groups. The most commonly used clustering technique is the hierarchical agglomerative method. The results of this are represented by a dendrogram with the x- axis representing the full set of samples and the y-axis defining the similarity level at which the samples or groups are fused. *Bray - Curtis* coefficient (Bray and Curtis, 1957) was used to produce the dendrogram. The coefficient was calculated by the following formula:

$$S_{jk} = 100 \left\{ 1 - \frac{\sum_{i=1}^p |y_{ij} - y_{ik}|}{\sum_{i=1}^p (y_{ij} + y_{ik})} \right\}$$

$$= 100 \frac{\sum_{i=1}^p 2 \min(y_{ij}, y_{ik})}{\sum_{i=1}^p (y_{ij} + y_{ik})}$$

where,  $y_{ij}$  represents the entry in the  $i^{\text{th}}$  row and  $j^{\text{th}}$  column of the data matrix, *i.e.*, the abundance or biomass for the  $i^{\text{th}}$  species in the  $j^{\text{th}}$  sample;

$y_{ik}$  is the count for the  $i^{\text{th}}$  species in the  $k^{\text{th}}$  sample;

$| \dots |$  represents the absolute value of the difference;

'min' stands for, the minimum of the two counts

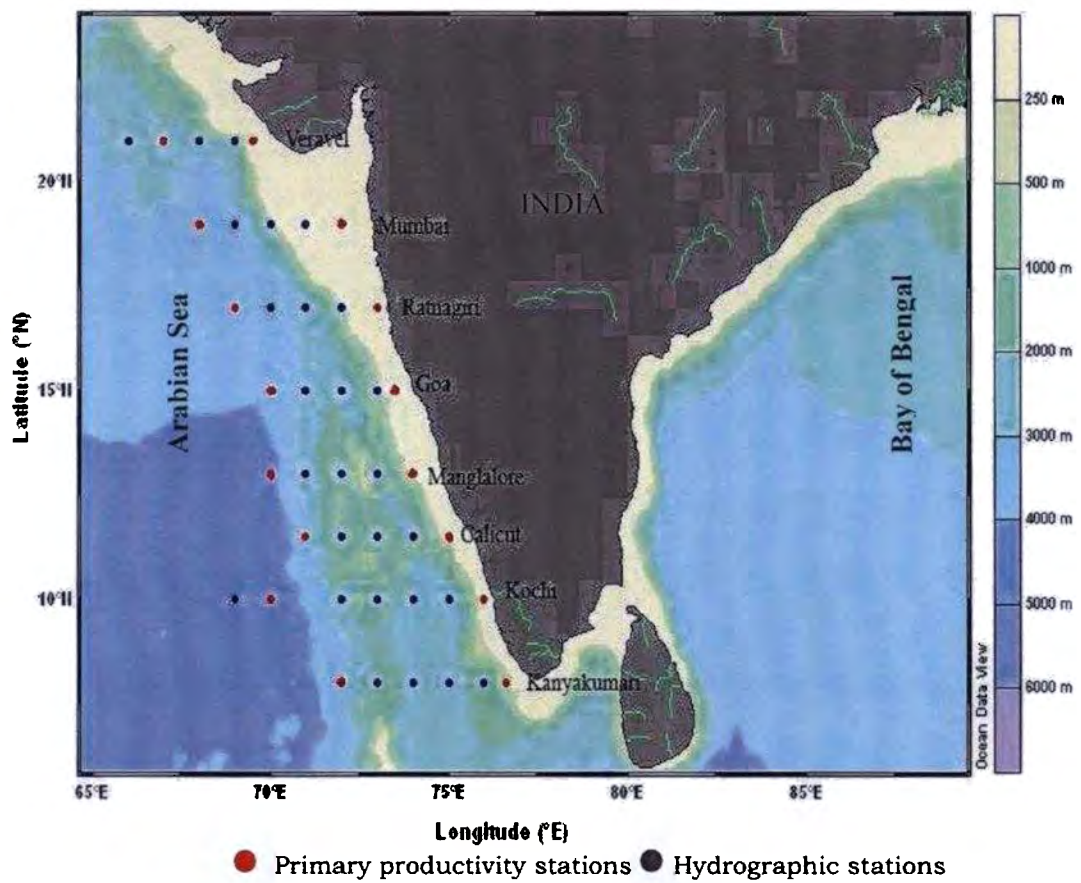


Fig. 2.1. Study area and Sampling stations



Plate 2.1. *FORV Sagar Sampada*



Plate 2.2. CTD rosette with Niskin bottles



Plate 2.3. Deployment of mooring buoy for *in-situ* incubation



Plate 2.4. Schematic diagram of mooring system(Light and dark bottles suspended from the buoy)



Plate 2.5. Liquid Scintillation Counter

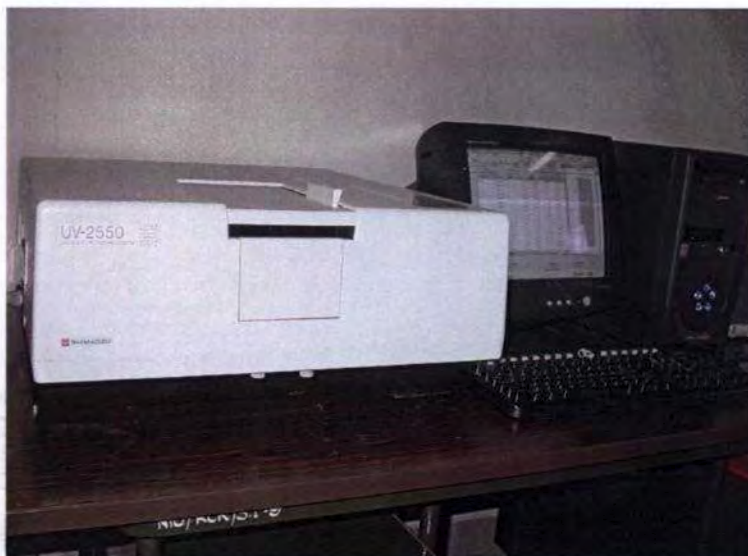


Plate 2.6. Spectrophotometer

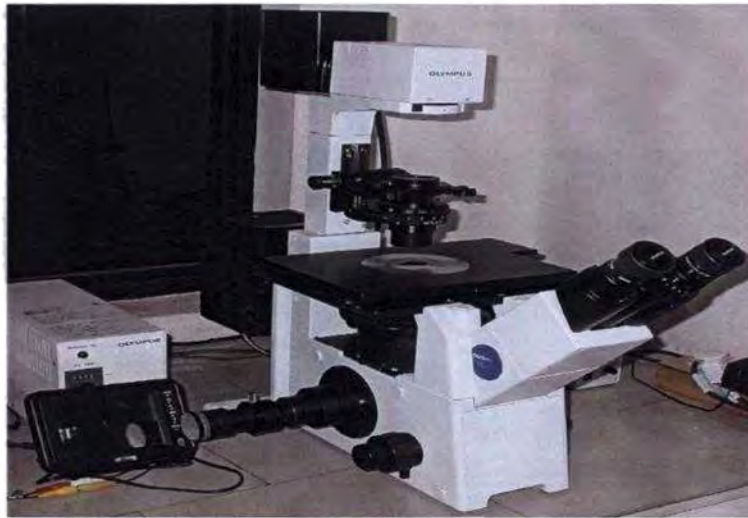


Plate 2.7. Inverted Microscope



Plate 2.8. High Performance Liquid Chromatography (HPLC)



Plate 2.9. Multiple Plankton Net (MPN)

## References

- Bray J.R. and Curtis, 1957. An ordination of the upland forest communities of Southern Wisconsin. *Ecol. Monogr.*, 27: 325-349.
- Dyson, N., Jitts, H.R. and Scott, B.D., 1965. Techniques for measuring oceanic primary production using radioactive carbon. CSIRO Tech. Paper 18: 1-12.
- Grasshoff, K., 1976. Methods of seawater analysis, Verlag Chemie, Weinheim, Germany. 260p.
- Grasshoff, K., Ehrhardt, M., Kremling, K., 1983. Methods of Seawater Analysis. Verlag Chemie, Weinheim, Germany. pp: 89-224.
- Pielou, E.C., 1966. The measurement of diversity of different types of biological collections. *J. Theor. Biol.*, 13: 131-144.
- Postel, L., Fock, H. and Hagen, W., 2000. In: *ICES Zooplankton Methodology Manual*, Harris, R., Weibe, P., Lenz, J. and Huntley, M., (Eds.), Academic Press. USA.
- Shannon, C.E. and Weaver, W., 1949. The mathematical theory of communication. University of Illinois Press, Urbana, 117pp.
- Srinath, M., Somy Kuriakose, P.L. Ammini, C.J., Prasad, Ramani, K and Beena, M.R., 2006. *Marine Fish Landings in India, 1985-2004. Estimates and Trends. CMFRI Spl. Publ.*, No. 89:161p.
- Steedman, H.F., 1976. Zooplankton fixation and preservation. UNESCO Press, Paris, 350p.
- Steeman Nielsen, E., 1952. The use of radio active carbon ( $^{14}\text{C}$ ) for measuring organic production in the sea. *J. Cons. Int. Explor. Mer.*, 18(2).
- Strickland, J.D H. and Parsons, T. R., 1972. In *A practical handbook of sea water analysis*, 2<sup>nd</sup> ed. *Bull. Fish. Res. Board, Can.*, 167, 310p.
- Subrahmanyam, R., 1959. Studies on the phytoplankton of the west coast of India – I and II, *Proc. Ind. Acad. Sci.*, 50 B: 113-252.
- Tomas, C.R., 1997. *Identifying Marine Phytoplankton*. Academic Press, USA, 858p.
- UNESCO, 1994. *Protocols for the Joint Global Ocean Flux Study (JGOFS), Core Measurements IOC Manuals and Guides*, 29, UNESCO, Paris, 170p.
- Van Heukelem., 2002. HPLC phytoplankton pigments: Sampling, Laboratory methods, and Quality assurance Procedures. In: Mueller, J. and Fargion, G., (Eds.), *Ocean Optics Protocols for Satellite Ocean Color Sensor, Revision: 3(2)*. NASA Technical Memorandum 2002-2004 (Chapter 16), pp: 258-268.
- Wimpenny, R.S., 1966. *The plankton of the Sea*. Faber Ltd., London, pp: 330-349.

**Chapter III**  
**Hydrography**

---

**3.1. Introduction**  
**3.2. Results**  
**3.2.1. Spring intermonsoon**  
**3.2.2. Onset of summer monsoon**  
**3.2.3. Peak summer monsoon**  
**3.2.4. Late summer monsoon**  
**3.3. Discussion**  
**References**

---

### **3.1. Introduction**

Hydrographic conditions determine the existence of communities in an aquatic ecosystem and the knowledge about these parameters is important in understanding the dynamics of the ecosystem. The regulatory influence of the environment over the living community which it supports is the result of the independent and interrelated actions of the non-living elements, which are variable in space and time. The interaction of an organism with the environment determines the size of its population and distribution.

The Arabian Sea experiences extremes in atmospheric forcing which leads to one of the largest intra-annual variability in hydrographic conditions (Prasanna Kumar, *et al.*, 2000) compared to other ocean basins of the world. The seasonally occurring upwelling and stratification along with the current patterns determine the physico-chemical characteristics of the Arabian Sea. The strength of

these physical forcings induces the variability in nutrient status and in turn, the biological responses.

In this chapter temporal and spatial variability of physical parameters such as Sea Surface Temperature (SST), Sea surface Salinity (SSS), Sigma-*t*, Mixed Layer Depth (MLD); and the chemical variables such as dissolved oxygen and nutrients (phosphate, nitrate and silicate) are discussed.

## **3.2. Results**

### **3.2.1. Spring Intermonsoon (SIM)**

#### ***a) Physical parameters***

The meteorological factors characterised by uneven and weak (av.  $3\text{ms}^{-1}$ ) winds (Fig. 3.1), without any specific pattern in wind direction was noticed during this season. High solar radiation and clear sky were favourable for the development of a stratified and warm ( $> 30\text{ }^{\circ}\text{C}$ ) waters in the shelf region between  $10^{\circ}\text{N}$  and  $15^{\circ}\text{N}$  (Fig. 3.2a). The surface salinities (Fig. 3.2b) were in the range of 34 – 36psu. The warmer and low saline surface waters in the south east Arabian Sea (SEAS) could be due to the mixing of the north Arabian Sea High Saline water mass (ASHSW) with the low saline waters of the Bay of Bengal. The MLD was low (av. 30m) over the study area (Fig. 3.2c).

Vertical section of physical parameters at  $8^{\circ}\text{N}$  transect (Fig. 3.3a), showed an isohaline layer of  $\sim 25\text{m}$  thick which was embedded in a 50m isothermal layer. The thermocline generally ranged from 180 to 200m below which, the gradient was minimum. A low saline surface water ( $< 34.5$ ) was observed in this transect. The ASHSW ( $> 36$ ) was

present at a depth of 80 – 90m between 72 - 75°E. The pycnocline followed a same trend of halocline, below which, the density variations are quite low. At 10°N transect (Fig. 3.3b), normal isothermal layer (50m) and a thick (200 m) thermocline layer were co-existent with a relatively thin isohaline layer (20 - 30 m), which extended up to 50 m along the coastal stations exhibiting salinity < 35 psu. At 11.5°N and 13°N transects (Fig. 3.3c and 3.3d); the presence of ASHSW (> 36 psu) is peculiar at sub-surface. It was present at depths of 80 – 100m between 70° and 74°E with core intensity (36.4 psu) at 71°E. The pycnocline depth ranged from 30 - 50 m). At 15°N transects (Fig. 3.4a); the isothermal layer (40 m) and thermocline (200m) remained more or less same as observed along 10°N, while the isohaline layer ranged from 20 - 40m. The coastal waters were fresher (< 35psu) up to 40m, but the ASHSW (>36) was raised to a depth of 50 – 100m between 70° and 73°E with core intensity (36.6 psu) at 72°E. The pycnocline was observed between 20– 50m.

The gradient between the isothermal layer (30 m) and thermocline depth (300 m) was found to increase at the 17°N and 19°N transect (Fig. 3.4b and 3.4c). In contrast to the southern transects, the isothermal layer of this transect was characterized by high saline waters (> 36 psu). This ASHSW (>36 psu) waters were seen extending from 80 m in the coastal to 150 m in the offshore between 69° and 71°E with a core intensity of 36.6 at 69°E, where the pycnocline was 40m deep. The thickness of the isothermal layer and thermocline depth along the 21°N transects (Fig. 3.4d) were 40m and

300m respectively. Isohaline layer thickness was about 30m at coastal and 50m at oceanic stations. Surface layer was high saline ( $> 36$  psu) and extended up to 220m depth at oceanic stations and 150 m at coastal stations. An intrusion of ASHSW ( $> 36$  psu) was observed at a depth of 250 – 300m between  $66^\circ$  and  $68^\circ\text{E}$  stations with a core intensity of  $> 36$  psu. Pycnocline was observed between 30m (coastal) – 50m (oceanic) depth range.

**(b) Chemical parameters**

During SIM, the near shore waters of the SW coast of India was saturated with oxygen. Dissolved oxygen concentration was high ( $> 205\mu\text{M}$ ) in the surface waters (Fig. 3.5a). In the shelf waters the nutrients (Fig. 3.5b and 3.5c) were depleted ( $\text{NO}_3 < 1\mu\text{M}$  and  $\text{PO}_4 < 0.6\mu\text{M}$ ) with a moderate value of  $1.5 \mu\text{M}$  of silicate (Fig. 3.5d). In the offshore waters of the northern transects, the nutrient status was moderate.

From the vertical profile of DO and nutrients along  $8^\circ\text{N}$  transect (Fig. 3.6a), the mixed layer remained well-oxygenated and nutrient-depleted, except for silicate, which was moderate ( $2\mu\text{M}$ ) towards the coast. At  $10^\circ\text{N}$  (Fig. 3.6b), it was noted that the oxygen minimum zone (OMZ), which was below 150m depth at  $8^\circ\text{N}$  was vertically lifted up to 150m. Same pattern in the distribution of DO and nutrients were observed at  $11.5^\circ\text{N}$  (Fig. 3.6c) and  $13^\circ\text{N}$  (Fig. 3.6d) transects.

The OMZ was suppressed below 150m, at  $15^\circ\text{N}$  (Fig. 3.7a). Nitrate ( $1\mu\text{M}$ ) remained enriched along the coastal waters. At  $17^\circ\text{N}$  (Fig. 3.7b) and  $19^\circ\text{N}$  (Fig. 3.7c) transects, in association with the deep

thermocline, the OMZ remained well below 180 m. At 21°N transect (Fig. 3.7d), DO and nutrients concentration were same as that of previous transect. Vertical distribution of DO, NO<sub>3</sub>, PO<sub>4</sub> and SiO<sub>3</sub> in the inshore and offshore waters are given in the Fig. 3.8.

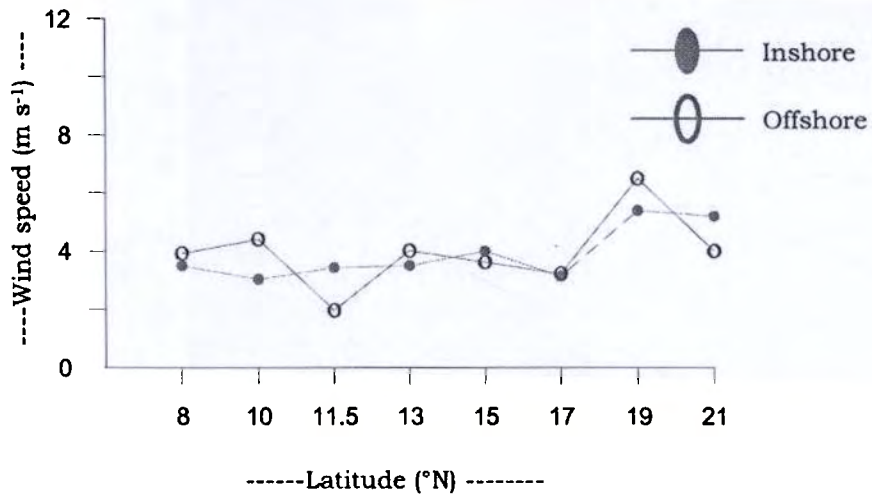


Fig. 3.1. Wind speed during SIM in the EAS

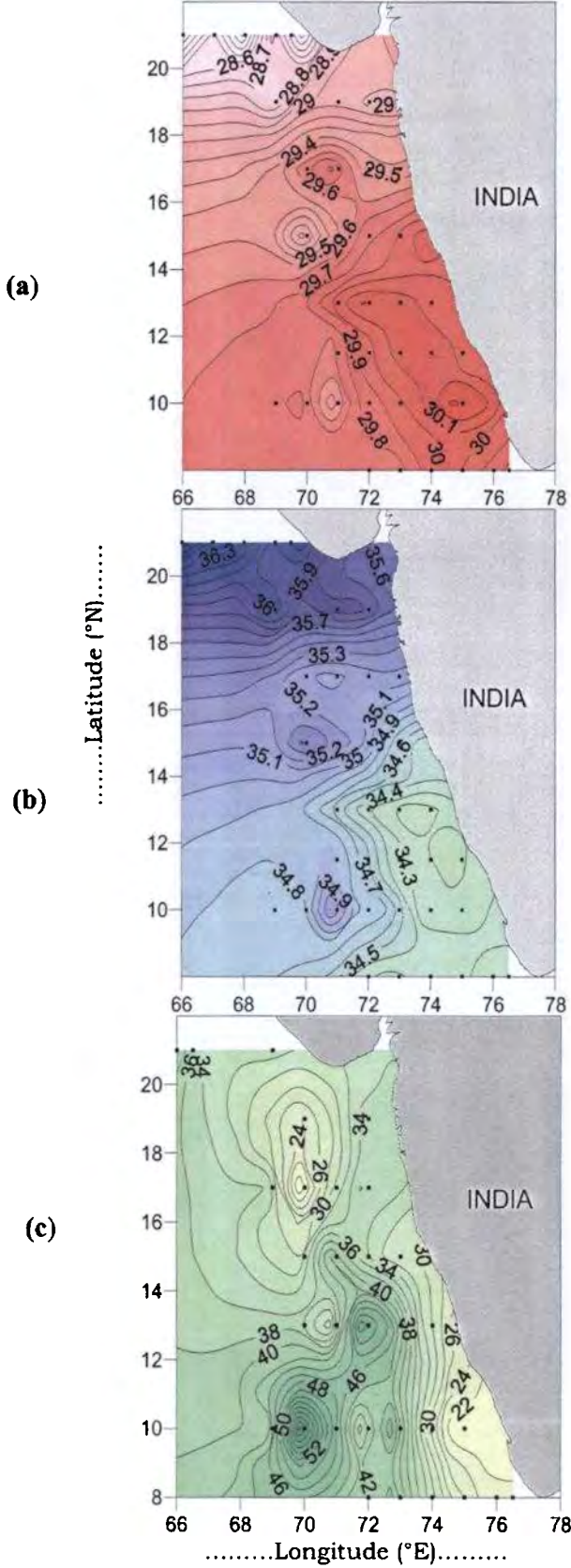


Fig. 3.2. Distribution of (a) SST (b) SSS and (c) MLD during SIM in the EAS

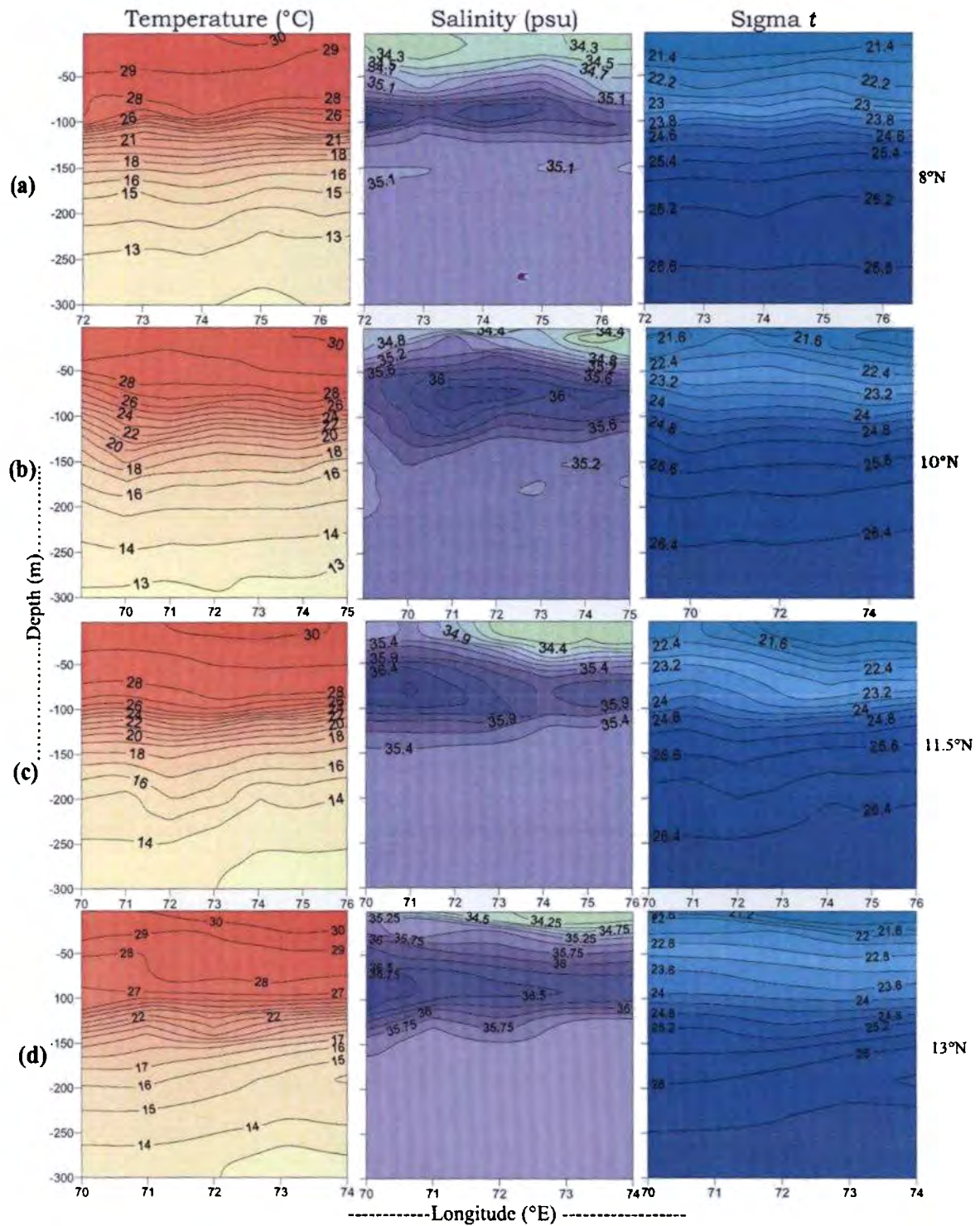


Fig. 3.3. Vertical distribution of temperature, salinity and sigma t along (a) 8°N (b) 10°N (c) 11.5°N and (d) 13°N transects during SIM in the EAS

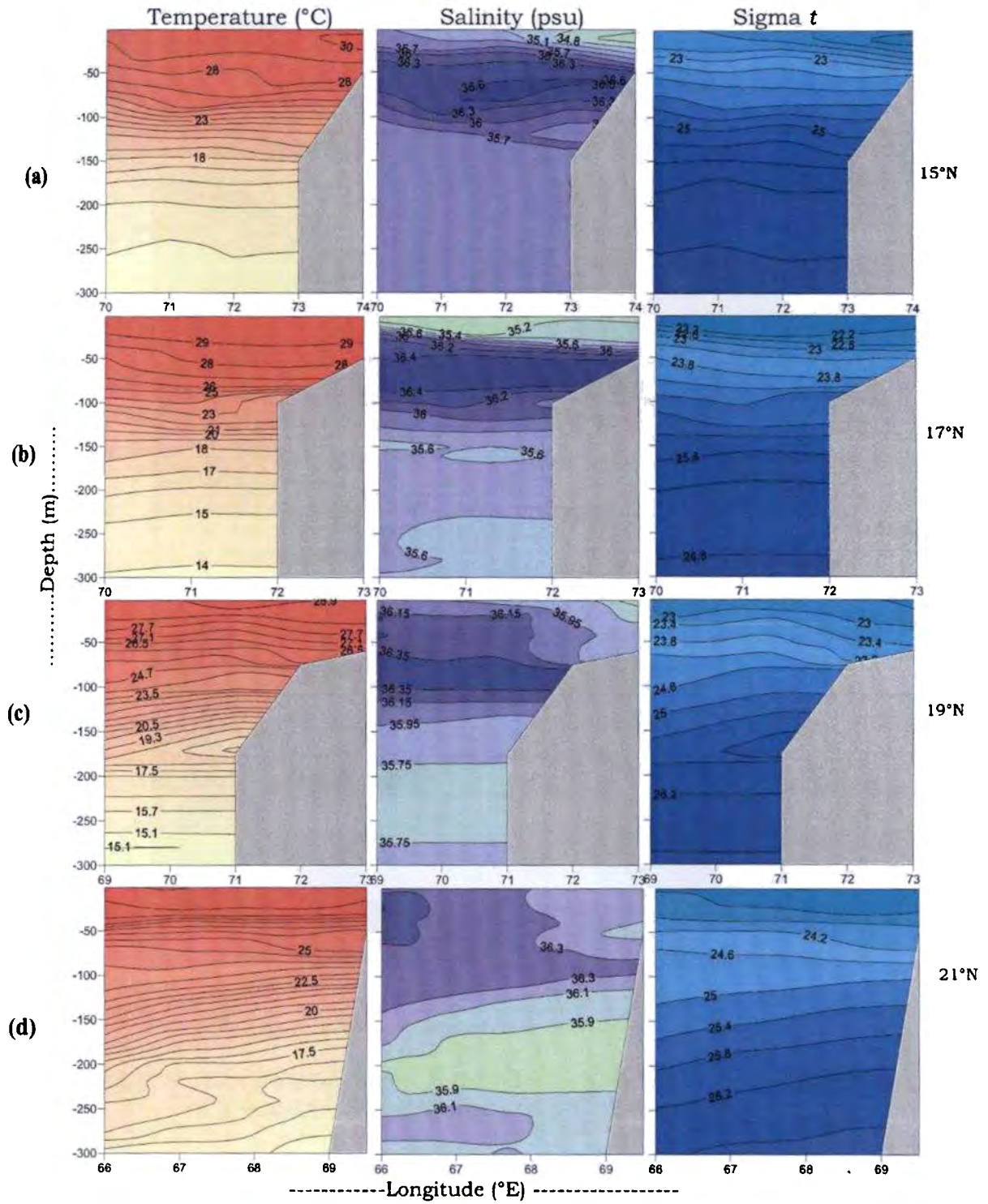


Fig. 3.4. Vertical distribution of temperature, salinity and sigma  $t$  along (a) 15°N (b) 17°N (c) 19°N and (d) 21°N transects during SIM in the EAS

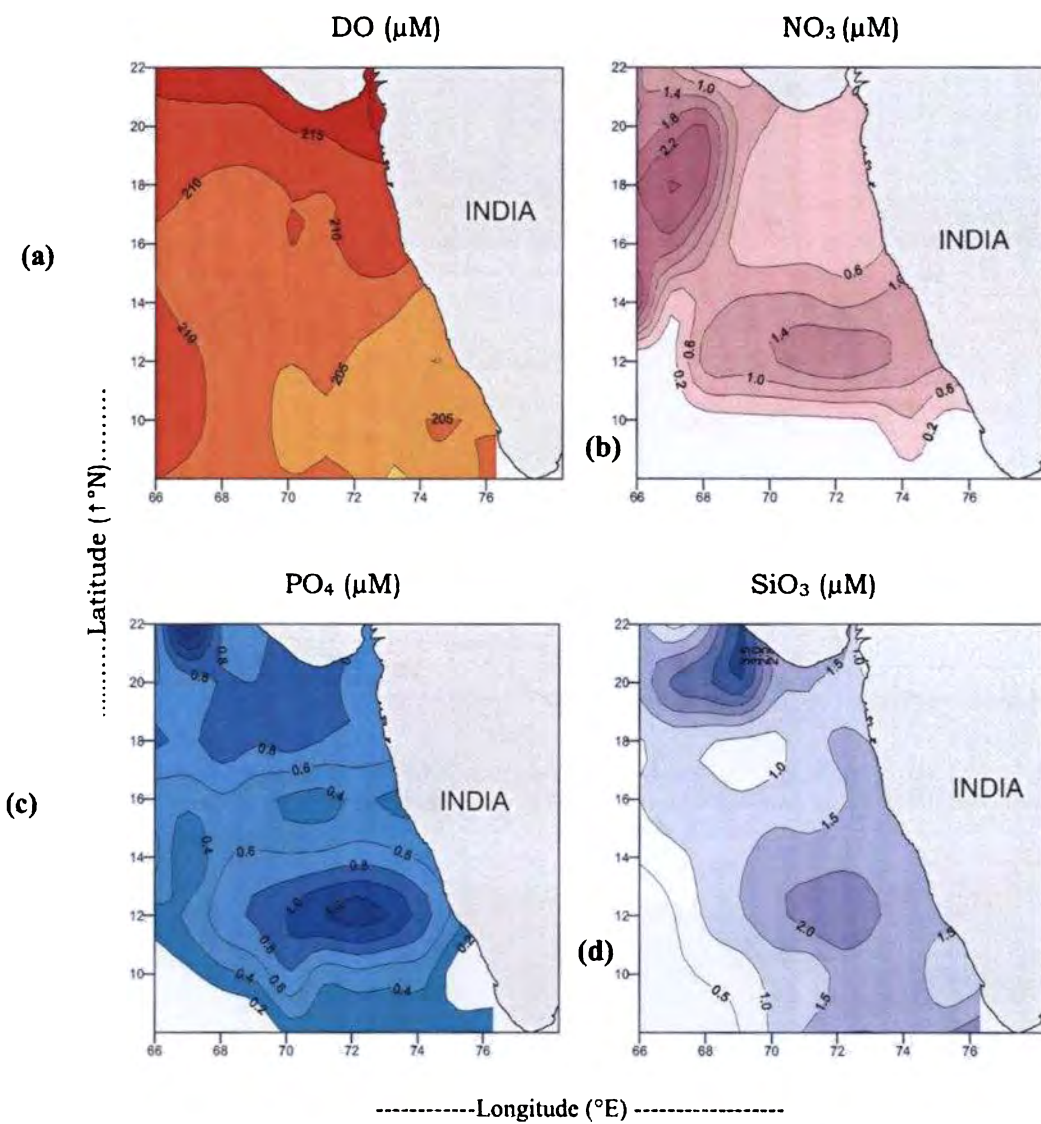


Fig.3.5. Surface distribution of (a) DO ( $\mu\text{M}$ ) (b) Nitrate ( $\mu\text{M}$ ) (c) Phosphate ( $\mu\text{M}$ ) and (d) Silicate ( $\mu\text{M}$ ) during SIM in the EAS

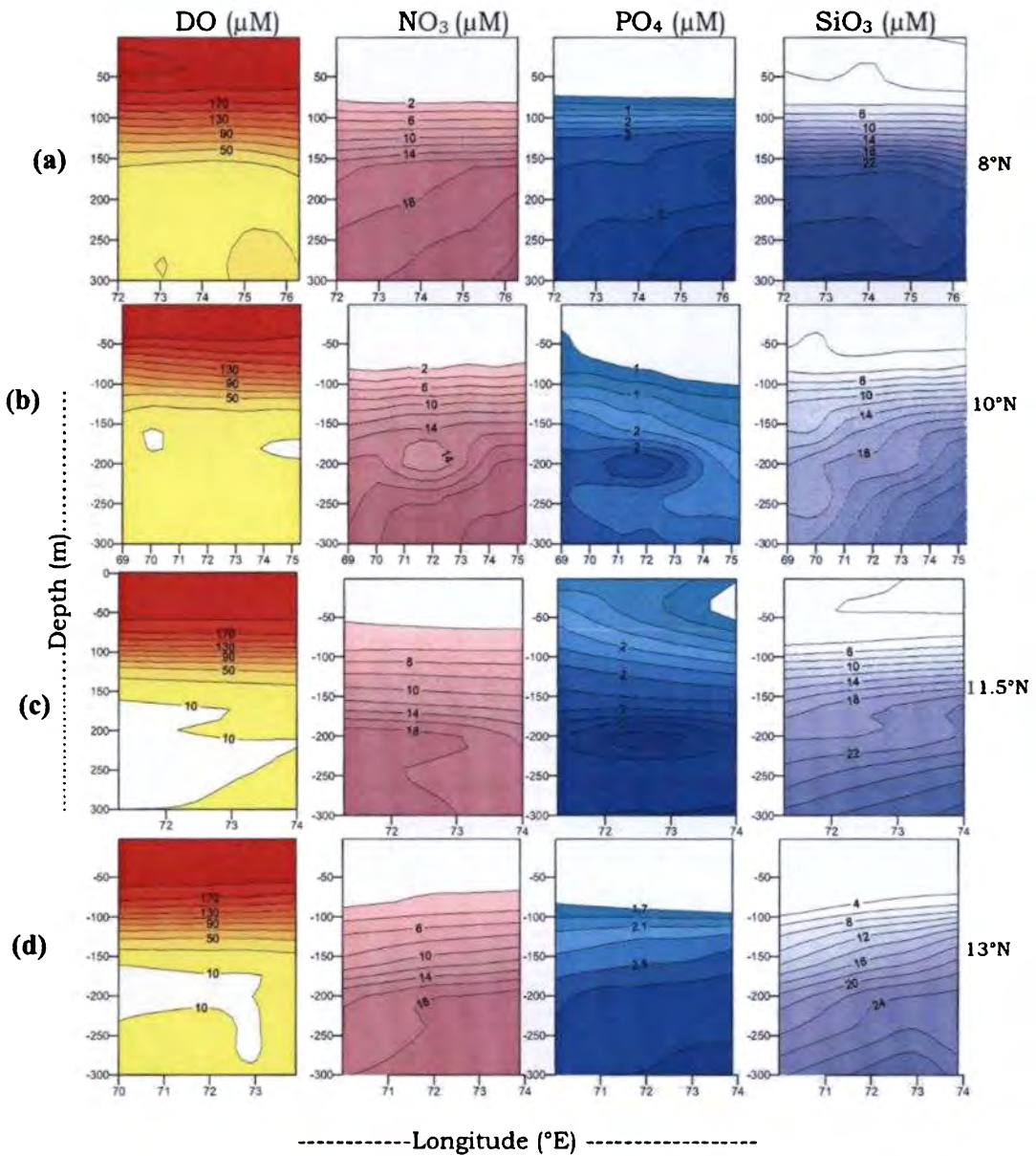


Fig. 3.6. Vertical distribution of DO ( $\mu\text{M}$ ), Nitrate ( $\mu\text{M}$ ), Phosphate ( $\mu\text{M}$ ) and Silicate ( $\mu\text{M}$ ) along (a) 8°N (b) 10°N (c) 11.5°N and (d) 13°N transects during SIM in the EAS

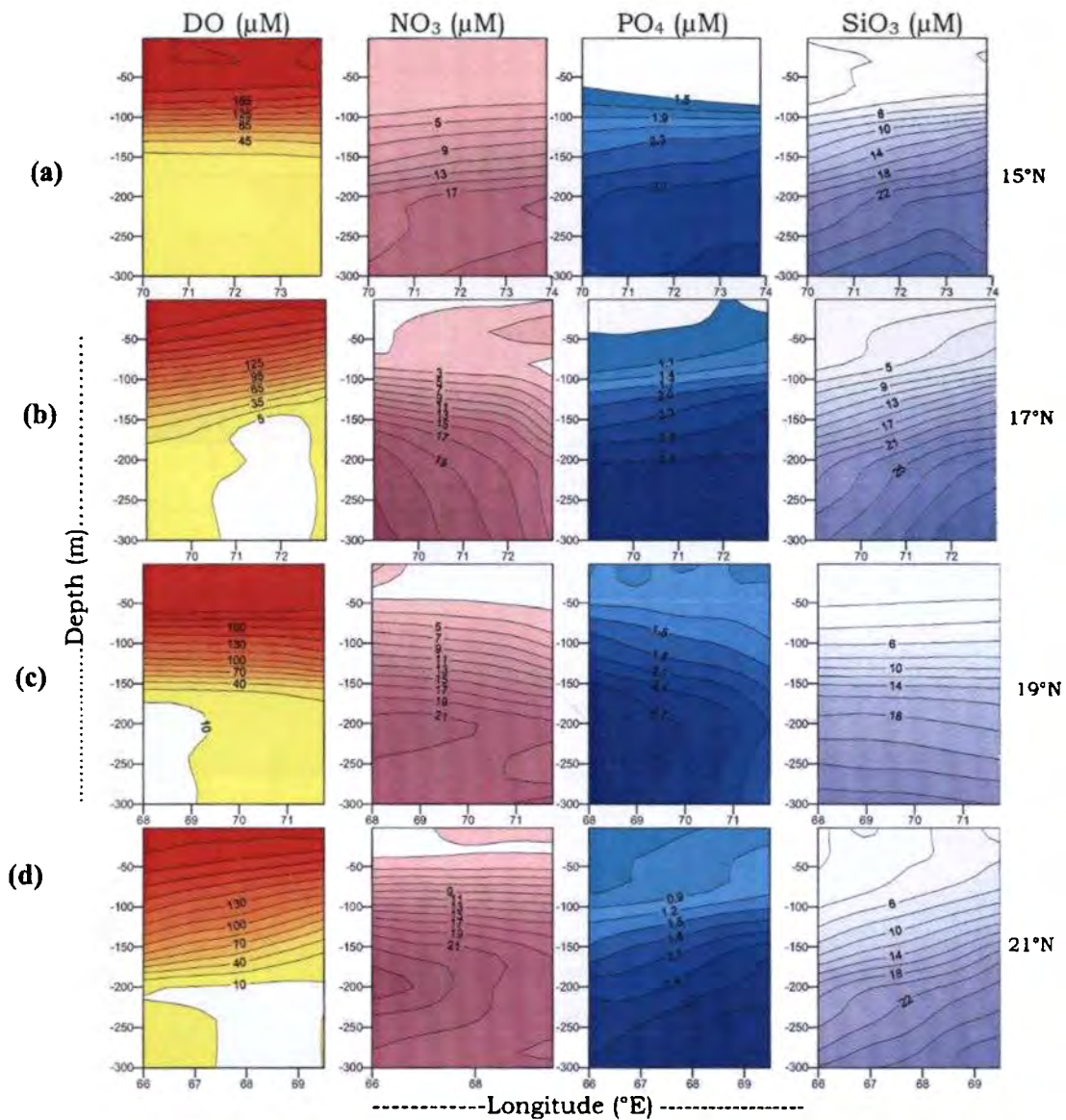


Fig. 3.7. Vertical distribution of DO ( $\mu\text{M}$ ), Nitrate ( $\mu\text{M}$ ), Phosphate ( $\mu\text{M}$ ), and Silicate ( $\mu\text{M}$ ) along (a) 15°N, (b) 17°N, (c) 19°N and (d) 21°N transects during SIM in the EAS

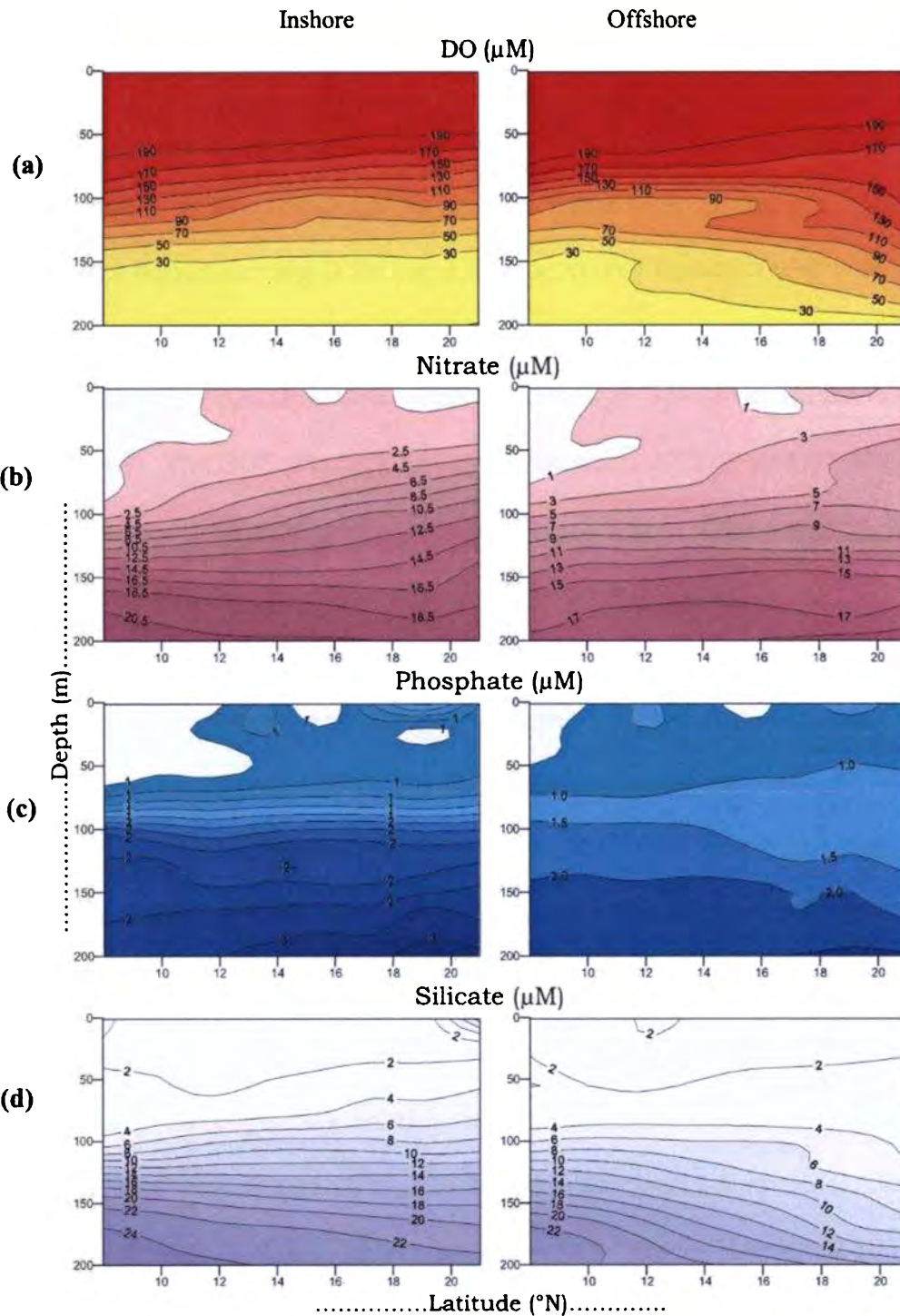


Fig.3.8. Vertical distribution of (a) DO ( $\mu\text{M}$ ), (b) Nitrate ( $\mu\text{M}$ ), (c) Phosphate ( $\mu\text{M}$ ) and (d) Silicate ( $\mu\text{M}$ ) along the inshore and offshore stations during SIM in the EAS

### **3.2.2. Onset of Summer Monsoon (OSM)**

#### ***(a) Physical parameters***

The onset of summer monsoon (May-June) marks the beginning of upwelling phenomenon along the southwest coast of India. The surface winds during OSM were characterized by southwesterly in the open ocean region and northwesterly in the shelf regions of the southeastern Arabian Sea, with an average speed of about  $4.9\text{ms}^{-1}$  (Fig. 3.9). The SST (Fig. 3.10a) varied between  $30.2^{\circ}\text{C}$  and  $31.4^{\circ}\text{C}$ , with meridionally aligned isotherms having higher temperatures in the north. Distribution of SSS (Fig. 3.10b) showed the presence of ASHSW ( $\sim 36.4$  psu) in the upper waters of the northern Arabian Sea, while low saline water (34.6 psu) prevailed in the surface waters of the southwest coast of India. The surface salinity exhibited zonally aligned isohalines in the south and relatively high saline waters in the north. Shallow MLD (Fig. 3.10c) was also observed at inshore stations of  $8^{\circ}\text{N}$  and  $10^{\circ}\text{N}$  transects, which showed the signals of coastal upwelling.

Along the shelf, the thermal structure north of  $10^{\circ}\text{N}$  was vertically homogenous in the top 25m, where the temperature was  $30^{\circ}\text{C}$ ; and at  $8^{\circ}\text{N}$  and  $10^{\circ}\text{N}$ , the temperature was below  $30^{\circ}\text{C}$ . South of  $10^{\circ}\text{N}$ , a region of low saline plume was observed between  $72^{\circ}\text{E}$  and  $76^{\circ}\text{E}$ . A high saline water mass ( $<36.2^{\circ}\text{C}$ ) was also observed below the surface stratified layer. The vertical section of temperature along  $8^{\circ}\text{N}$  and  $10^{\circ}\text{N}$  exhibited gentle upsloping of isotherms towards the coast resulting colder surface waters. However, down sloping of isotherms towards the coast were observed below 100m. At  $11.5^{\circ}\text{N}$  upsloping of

isotherms was found below the subsurface depth. At 13°N transects, gentle upsloping of isotherms were found below the 100 m depth, a high saline water mass below the surface layers was also present in these transects (Fig. 3.11a, b, c and d). Vertical section to north of the 15°N, isolines generally showed a down sloping trend towards the coast (Fig. 3.12a, b and c).

***(b) Chemical parameters***

Subsurface waters (~ 50m) with very low oxygen and high nutrient content was observed along the shelf waters from 8– 13° N transects (Fig. 3. 13a, b, c and d). Along the 8° N transect (Fig. 3.14a) the isolines are found to upslope from the open ocean areas to the subsurface waters of the shelf. Clear signatures of upwelling were observed along the 10°N transects (Fig. 3.14b). The 2  $\mu\text{M}$  contour of  $\text{NO}_3$ , which is found at a depth of 90m along 70°E longitude, can be traced up to the surface waters along 75° E longitude. Similar upsloping was observed for the isolines of the 190 $\mu\text{M}$  contour of DO and 0.8 $\mu\text{M}$  contour of phosphate. Along the 11.5° N (Fig. 3.14c) and 13° N (Fig. 3.14d) transects, the low oxygenated - high nutrient upwelled waters were found to reach only upto the subsurface waters (~ 50m). From 15°N transect onwards the surface waters (Fig. 3.15a, b and c) were found to be nutrient depleted ( $\text{NO}_3 < 0.1\mu\text{M}$ ). DO along the coastal stations showed a concentration of >200  $\mu\text{M}$  in the upper 10m (Fig. 16a) and higher values the southern transects. During this period, the  $\text{NO}_3$  value was 2  $\mu\text{M}$  was above 20m depth in these transects.  $\text{NO}_3$  concentration showed peculiar features which were

typical during the onset of upwelling process (Fig.3.16b). At 8°N and 10°N transects 2  $\mu\text{M}$   $\text{NO}_3$  contour was at 10m depth and in the other transects, it was around 25m depth. Phosphate and silicate distribution was similar to that of nitrate (Fig. 3.16c and 3.16d). Distribution of phosphate showed < 1  $\mu\text{M}$  concentration in the upper 20m depth in 8°N and 10°N, which deepened at the northern transects. Along the offshore stations upper 30m was almost uniformly saturated (>210 $\mu\text{M}$ ) and downsloping of isolines were observed towards northern transects. Nitrate concentration was below the detection level. Distribution of phosphate and silicate was similar to the nitrate in the upper layers.

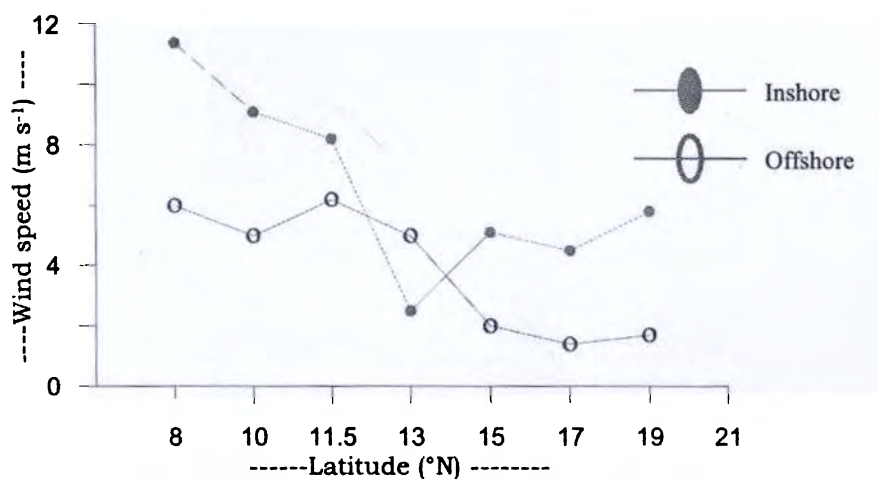


Fig. 3.9. Wind speed during OSM

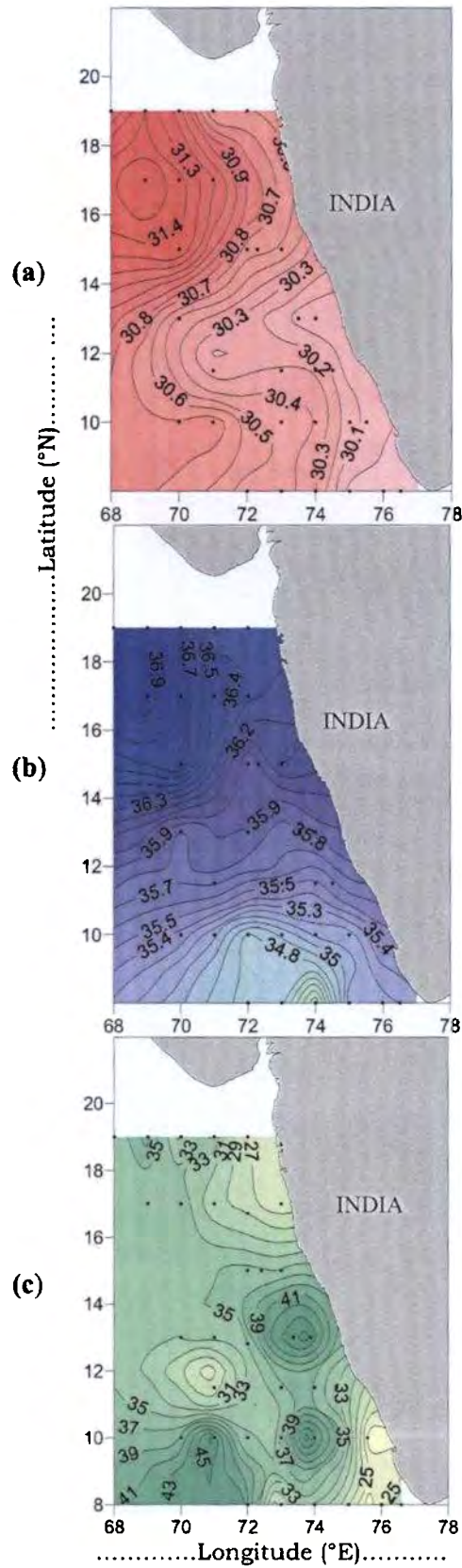


Fig. 3.10. Distribution of (b) SST, (c) SSS and (d) MLD during OSM in the EAS

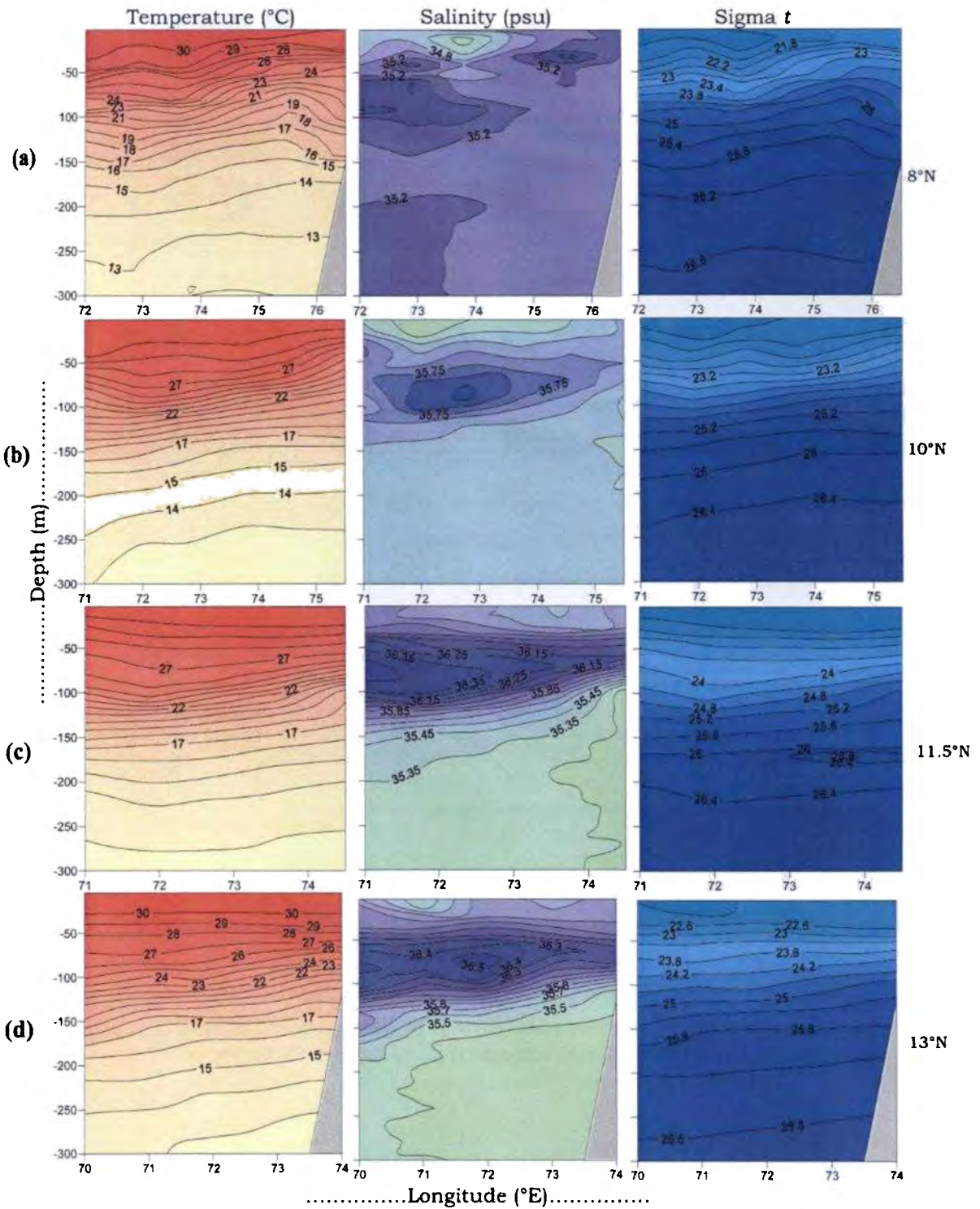


Fig. 3.11. Vertical distribution of Temperature, salinity and sigma along (a) 8°N, (b) 10°N, (c) 11.5°N, and (d) 13°N transects during OSM in the EAS

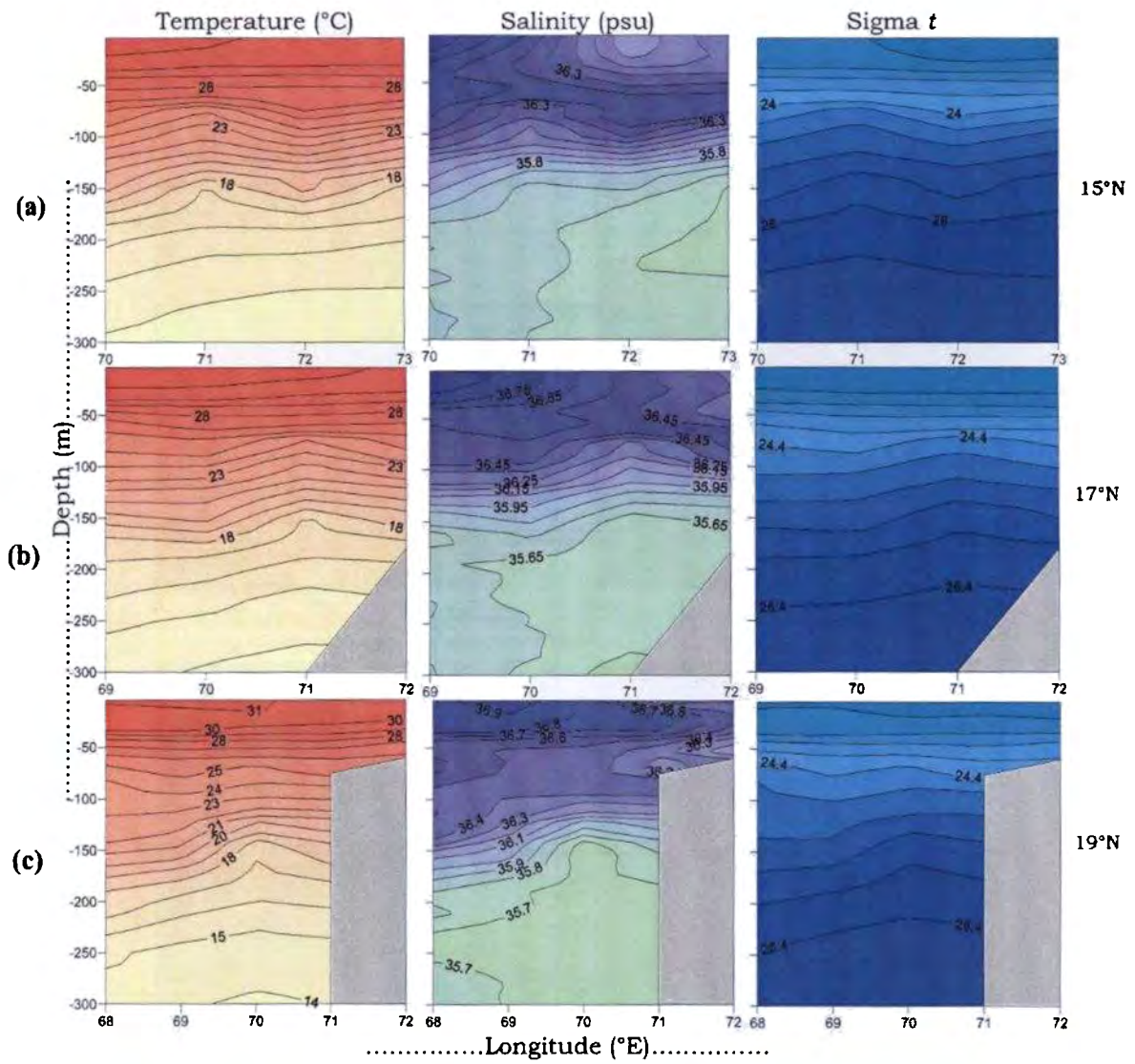


Fig. 3.12. Vertical distribution of temperature, salinity and sigma t along (a) 15°N, (b) 17°N and (c) 19°N transects during OSM in the EAS

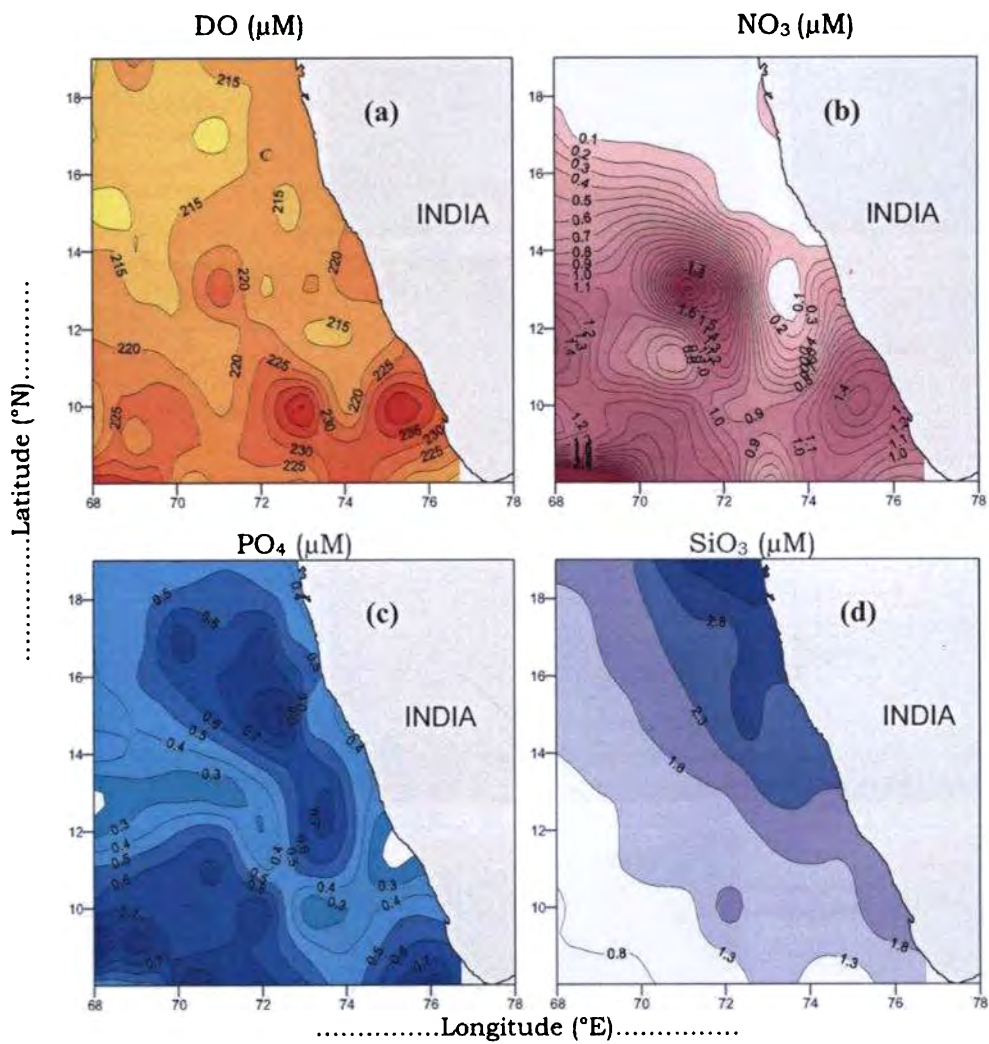


Fig.3.13. Surface distribution of (a) DO ( $\mu\text{M}$ ), (b) Nitrate ( $\mu\text{M}$ ), (c) Phosphate ( $\mu\text{M}$ ) and (d) Silicate ( $\mu\text{M}$ ) during OSM at 10m depth in the EAS

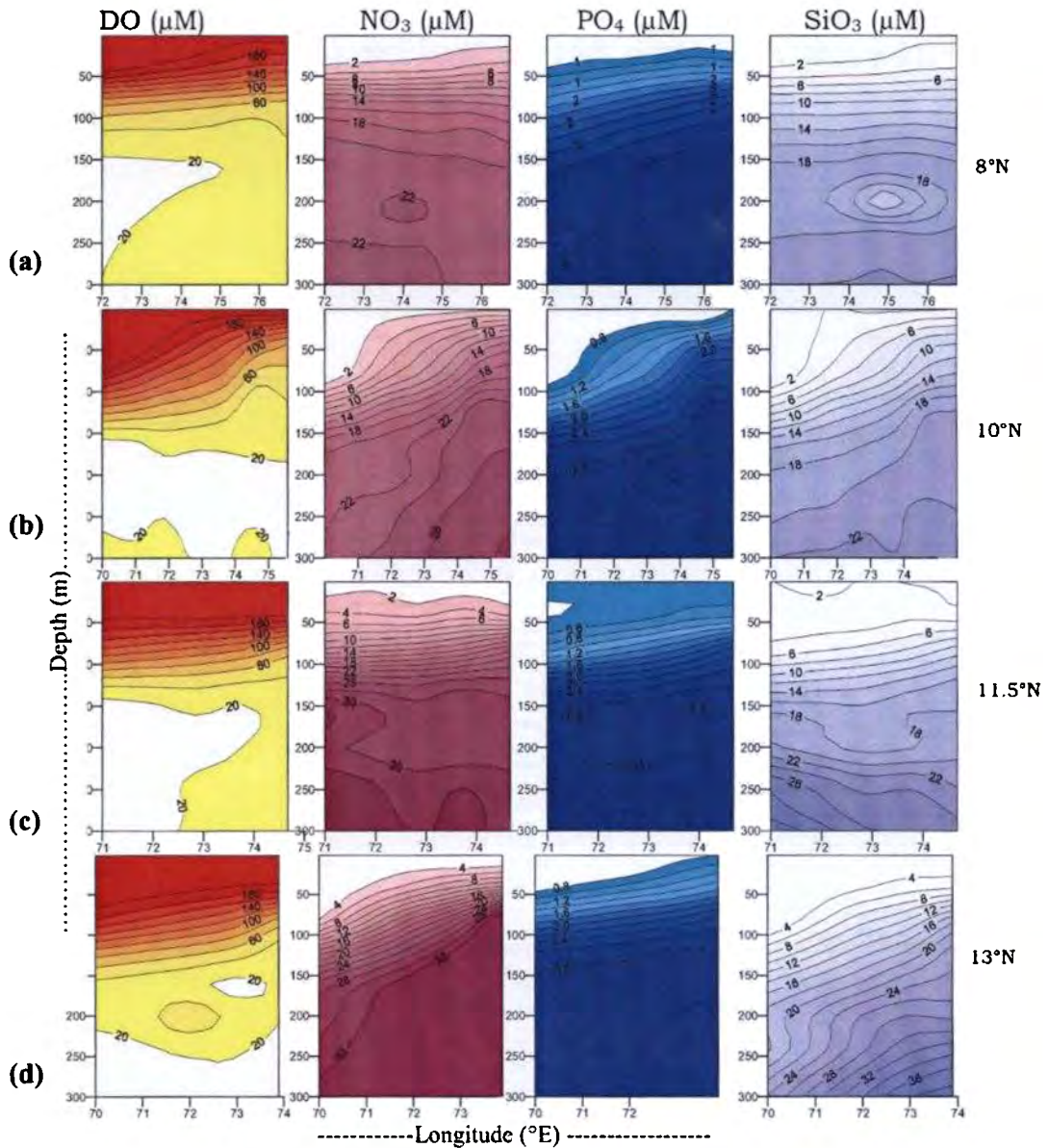


Fig. 3.14. Vertical distribution of dissolved oxygen, Nitrate ( $\mu\text{M}$ ), Phosphate ( $\mu\text{M}$ ), and Silicate ( $\mu\text{M}$ ) along (a)  $8^\circ\text{N}$ , (b)  $10^\circ\text{N}$ , (c)  $11.5^\circ\text{N}$  and (d)  $13^\circ\text{N}$  transects during OSM in the EAS

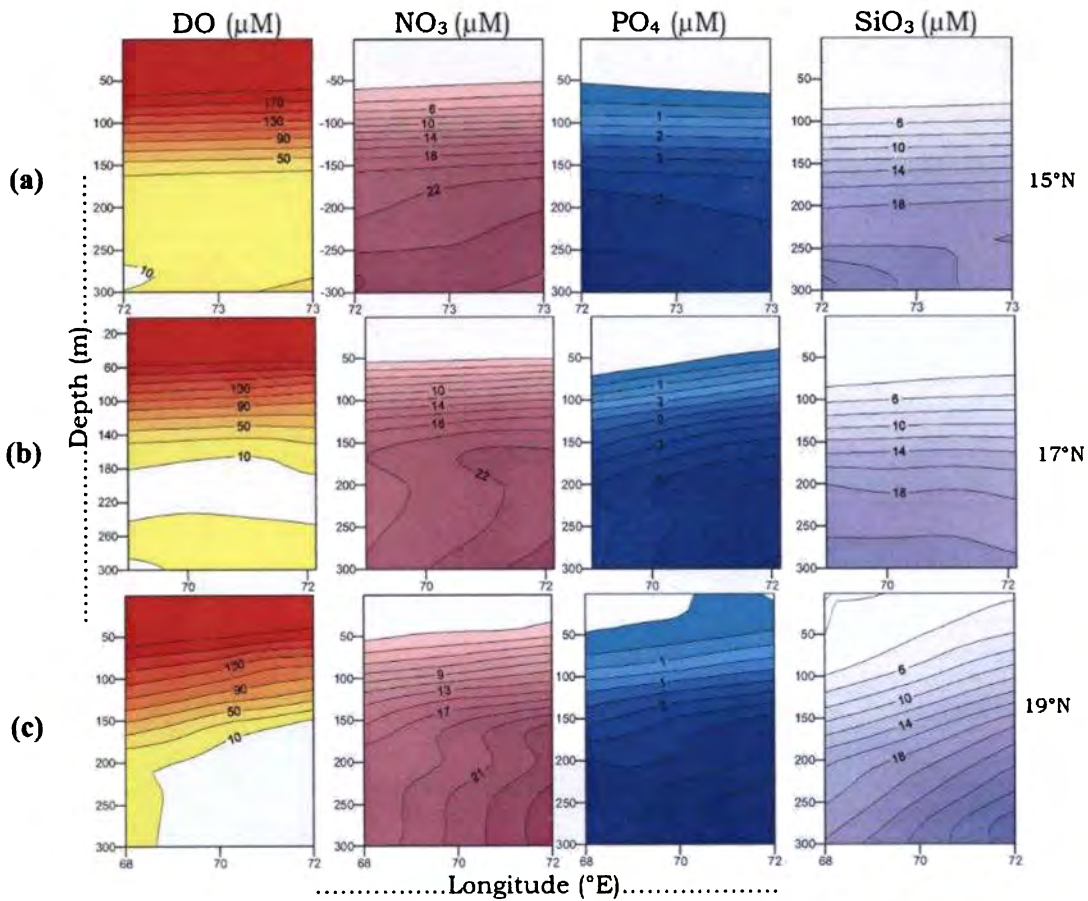


Fig.3.15. Vertical distribution of Dissolved Oxygen, Nitrate ( $\mu\text{M}$ ), Phosphate ( $\mu\text{M}$ ), and Silicate ( $\mu\text{M}$ ) along (a)  $15^\circ\text{N}$ , (b)  $17^\circ\text{N}$  and (c)  $19^\circ\text{N}$  transects during OSM in the EAS



### **3.2.3. Peak Summer Monsoon (PSM)**

#### ***(a) Physical parameters***

Strong, westerly ( $10 \text{ ms}^{-1}$ ), northwesterly winds ( $13 \text{ ms}^{-1}$ ) were recorded in the northern transects and open ocean stations of southern transects respectively (Fig. 3.17), while off Goa and coastal stations of southern transects were weak ( $<3\text{m/s}$ ) with northerly in direction. The observed wind showed a high magnitude (av.  $11.5 \text{ ms}^{-1}$ ) at  $11.5$  and  $13^\circ \text{ N}$  transects. The central SEAS showed a maximum SST of  $28^\circ\text{C}$ . Northern and southern regions showed low SST of  $27.6$  and  $25.8^\circ\text{C}$  respectively (Fig. 3.18a). High surface salinity (Fig. 3.18b) was observed at northern oceanic regions, while most of the coastal regions ( $8 - 17^\circ\text{N}$ ) showed low comparatively low salinity. High saline waters were observed towards open ocean region and relatively low saline water prevailed in the coastal region. MLD ranged between  $15\text{m} - 85\text{m}$  and was very shallow at  $10^\circ\text{N}$  transect (Fig. 3.18c). In general MLD increased towards offshore. Obviously MLD in the southern transects were shallow ( $< 20\text{m}$ ) due to the low surface salinity.

Vertical thermal structure along  $8^\circ\text{N}$  transect, showed that the isothermal layer (Fig. 3.19a) from  $50 \text{ m}$  at oceanic region was shoaling to  $30\text{m}$  at coastal region. The surface salinity was  $< 35\text{psu}$  at coastal stations, but increased to  $35.8$  along  $74^\circ\text{N}$  at  $70 - 100\text{m}$  in the offshore stations. The shoaling of cold, high saline water mass towards coastal region is a signal of persistent coastal upwelling. However, along the coastal stations, a concomitant down sloping of temperature, salinity and density below the depth of  $70\text{m}$  was observed.

The isothermal layer (Fig. 3.19b) thickness was 60m in the oceanic and 30m in the coastal stations of 10°N transect, while thermocline depth was uniformly 160m. The pycnocline shifted vertically from 80 to 20m. Vertical thermal structure along 11.5°N and 13°N showed a fine upsloping of isotherms towards the coast and relatively cold water at the surface. The isohaline and isopycnals also showed upsloping towards the coast (Fig. 3. 19c and 3.19d).

Isothermal layer thickness along 15°N transect was 70m in the oceanic region, 30m at coastal stations and thermocline depth was 210 m and 190m respectively (Fig. 20a). Surface salinity was about 36.7 psu towards oceanic and 36.2 psu at coastal stations. Upsloping of the saline water from deeper depths of oceanic regions to a depth of 100m of the coastal stations was observed in the vertical section. From the oceanic to the coastal regions, pycnocline showed an upward movement of 10m. At the coastal stations a down sloping of temperature and density contours below a depth of 200m was observed.

At 17°N and 19°N transects (Fig. 3.20b and 3.20c), isothermal layer thickness of 30 m was observed at both oceanic and coastal stations and a deep thermocline of 250m was observed at oceanic stations. Surface salinity was >36.6 psu at all stations, shoaling of high saline water below 300m in the oceanic regions to a depth of 150m of the coastal stations was observed in the vertical section. From the oceanic to the coastal regions, pycnocline showed uniform pattern, parallel to depth axis.

At 21°N (Fig. 3.20d) the isothermal layer (20 m) was thin at both oceanic and coastal stations. The thermocline depth at oceanic station was 150m. Surface salinity of this transect was > 36.6 psu at all stations. In the oceanic and coastal regions, pycnocline showed uniform patterns.

***(b) Chemical parameters***

During this phase of summer monsoon the upwelling signatures along the southwest coast of India was found to be, intense and dominant over the entire southwest coast from 8° to 17°N transects. A patch of low oxygenated high nutrient waters were observed along the shelf waters of these transects. Horizontal distribution of DO and nutrients along 10m depth showed a DO concentrations <170 µM and very high nutrients (NO<sub>3</sub> > 4 µM and PO<sub>4</sub> > 1 µM) along the coastal waters off 8° to 17°N (Fig. 3.21a, b, c & d). Vertical distribution of DO and nutrients along 8°N (Fig. 3.22a) showed the existence of nutrient rich upwelled waters in the surface layers. Upwelled waters might have reached the surface layers during the onset of monsoon and was found during PSM. The OMZ seems to dome to as shallow as 75m, especially towards the coast. The high stratification in the mixed layer and nutrient enrichment (NO<sub>3</sub>, SiO<sub>4</sub> > 2 µM) in the surface waters between 74-76° N are the features of the period.

Clear upsloping of the isolines from the open ocean to the shelf waters was observed from the vertical distribution of the DO and nutrients along 10°, 11.5° and 13°N transects (Fig. 3.22b, 3.22c and 3.22d). Along the 15°N (Fig. 3.23a) transect, it was found that the

upwelled waters has not yet reached the surface layers and was limited to the subsurface waters (~ 15m). The intense upwelling was indicated by the expansion of the OMZ to 100m depth. The injection of nutrients into the euphotic column remained as an evidence for the establishment of coastal upwelling. At 17°N (Fig. 3.23b) 1 $\mu$ M contour of nitrate concentration in 50m offshore station upsloped to the surface layers of the inshore stations. Same pattern was observed for silicate and phosphate. However, upwelling signals were still persistent along the coast. At 19°N (Fig. 3.23c), the presence of moderately high silicate and phosphate (> 1 $\mu$ M) in the surface waters was quite unusual. At 21°N (Fig. 3.23d), as seen in the case of the above latitude, the upwelling was not noticed along this transect. Upwelling signatures in the coastal stations are very clear from the vertical plots of inshore and offshore stations (Fig. 3.24a, b, c & d).

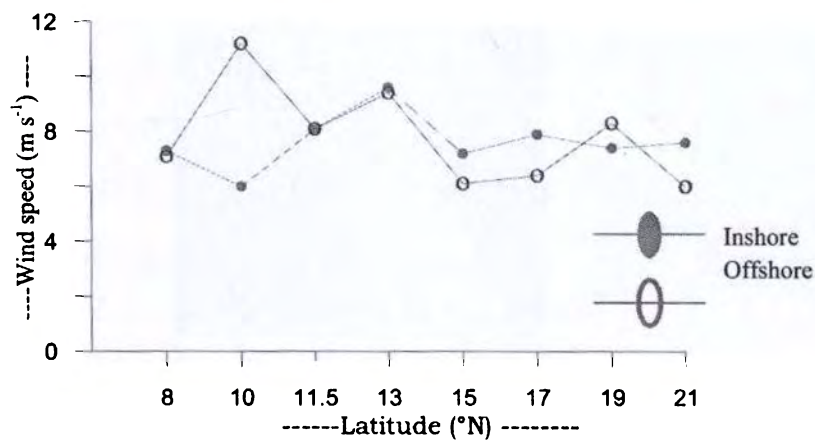


Fig. 3.17. Wind speed during PSM

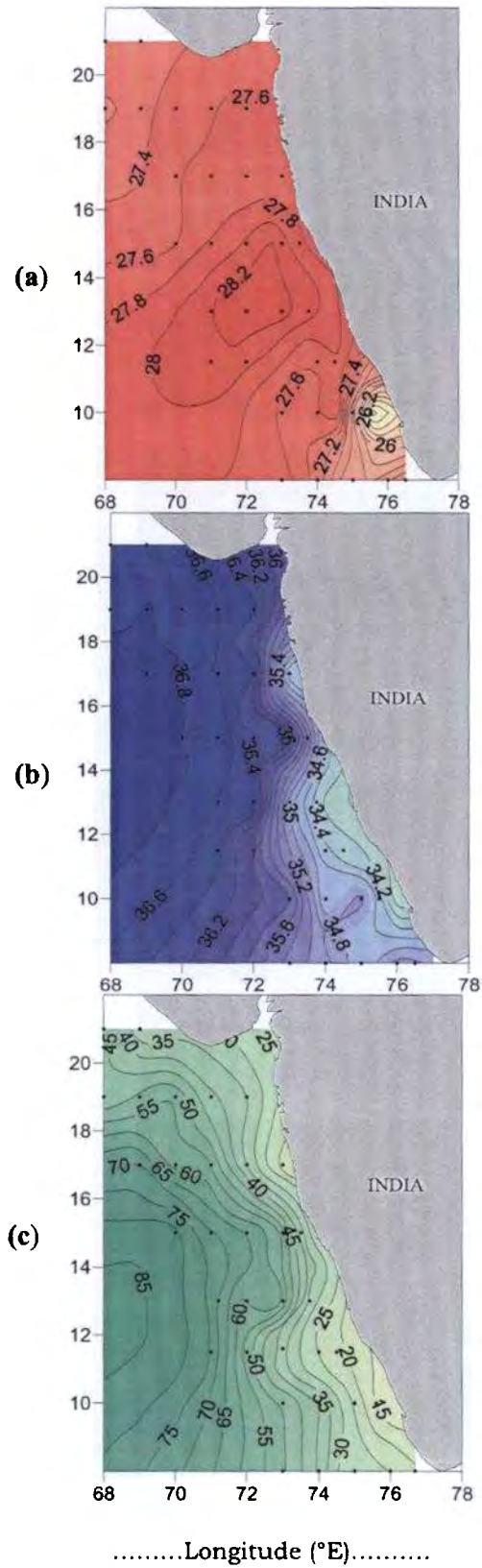


Fig. 3.18. Distribution of (a) SST, (b) SSS and (c) MLD during PSM in the EAS

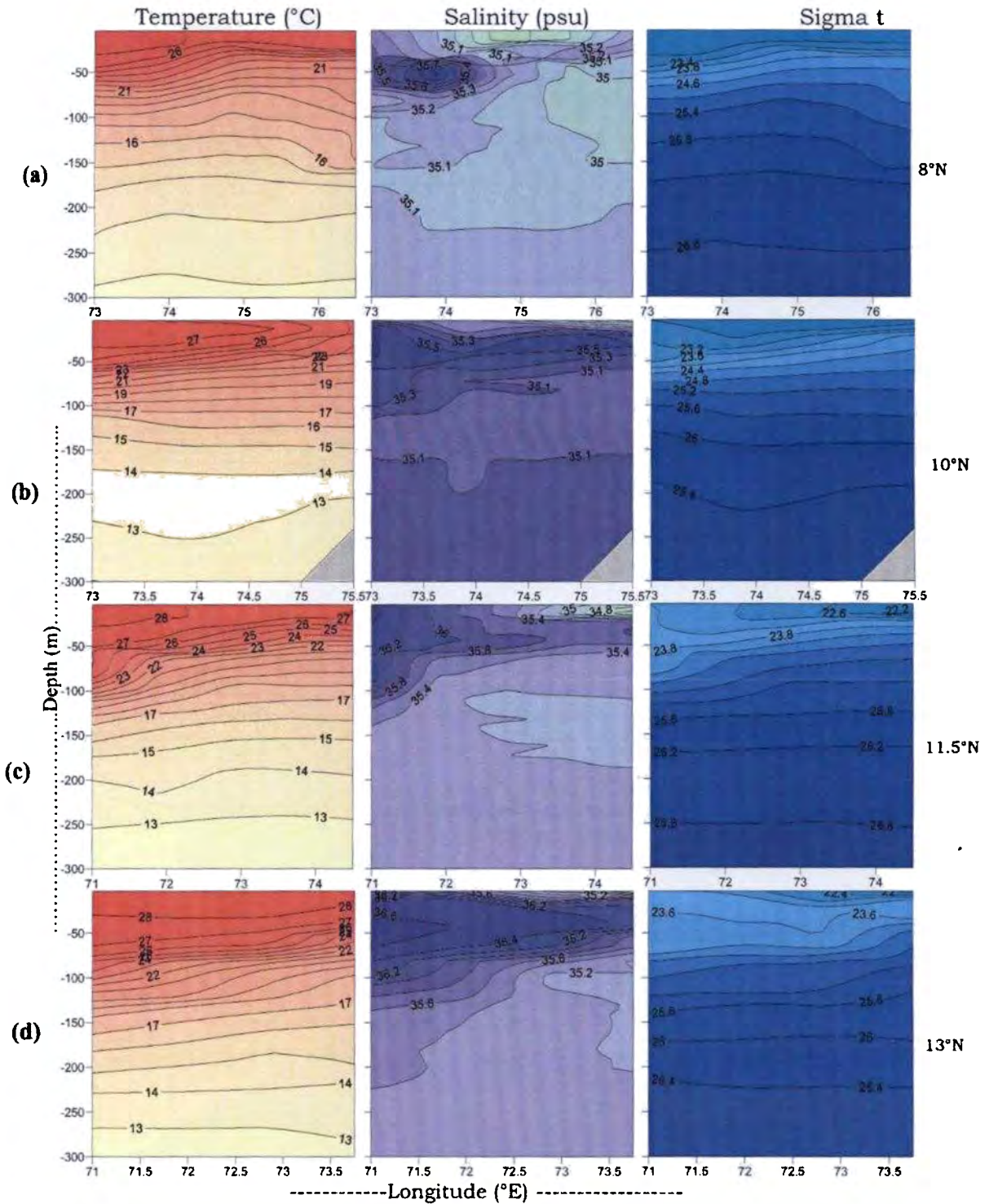


Fig. 3.19. Vertical distribution of temperature, salinity and sigma t along 8°N, 10°N, 11.5°N and 13°N transects during PSM in the EAS

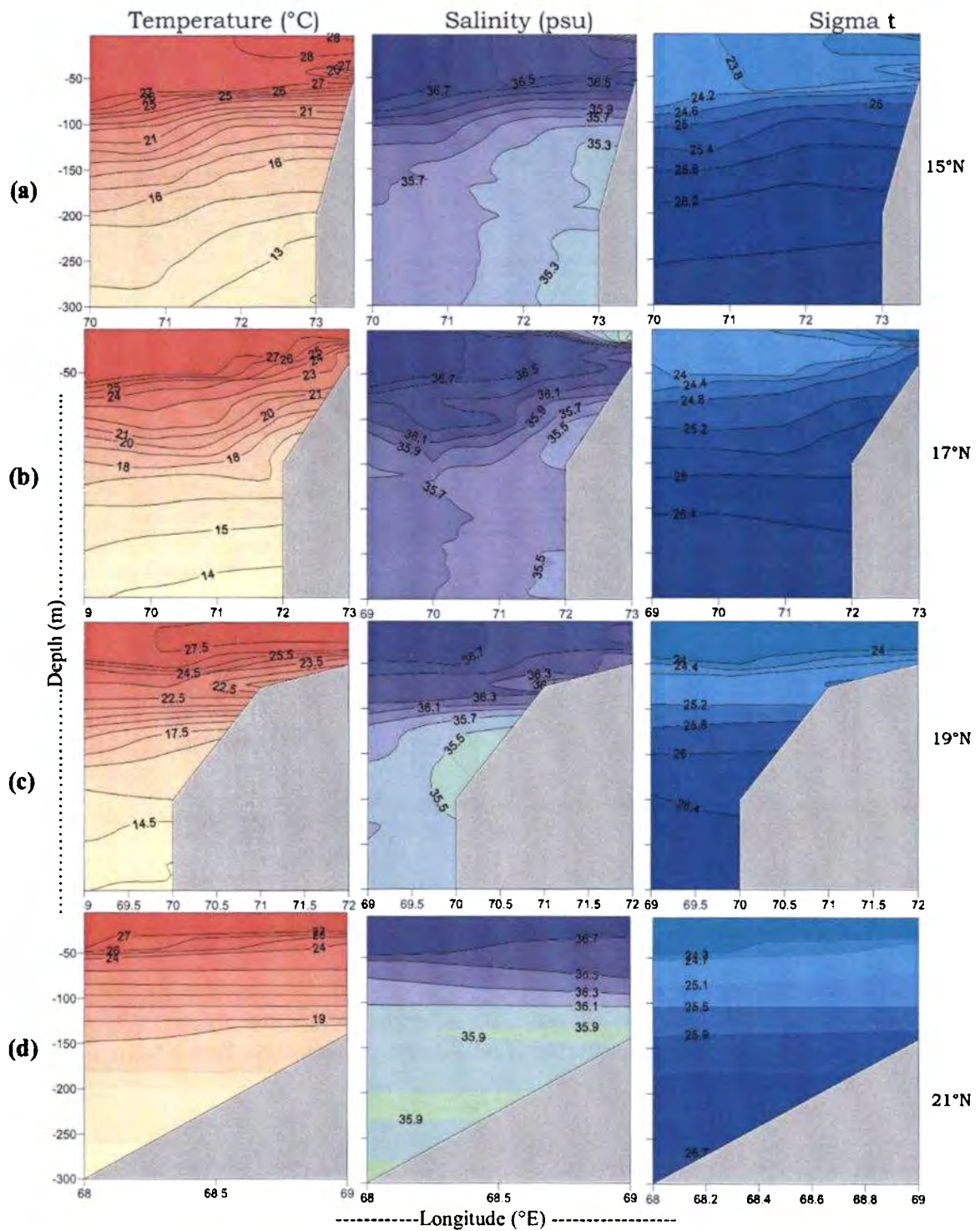


Fig. 3.20. Vertical distribution of temperature, salinity and sigma t along (a) 15°N, (b) 17°N, (c) 19°N and (d) 21°N transects during PSM in the EAS

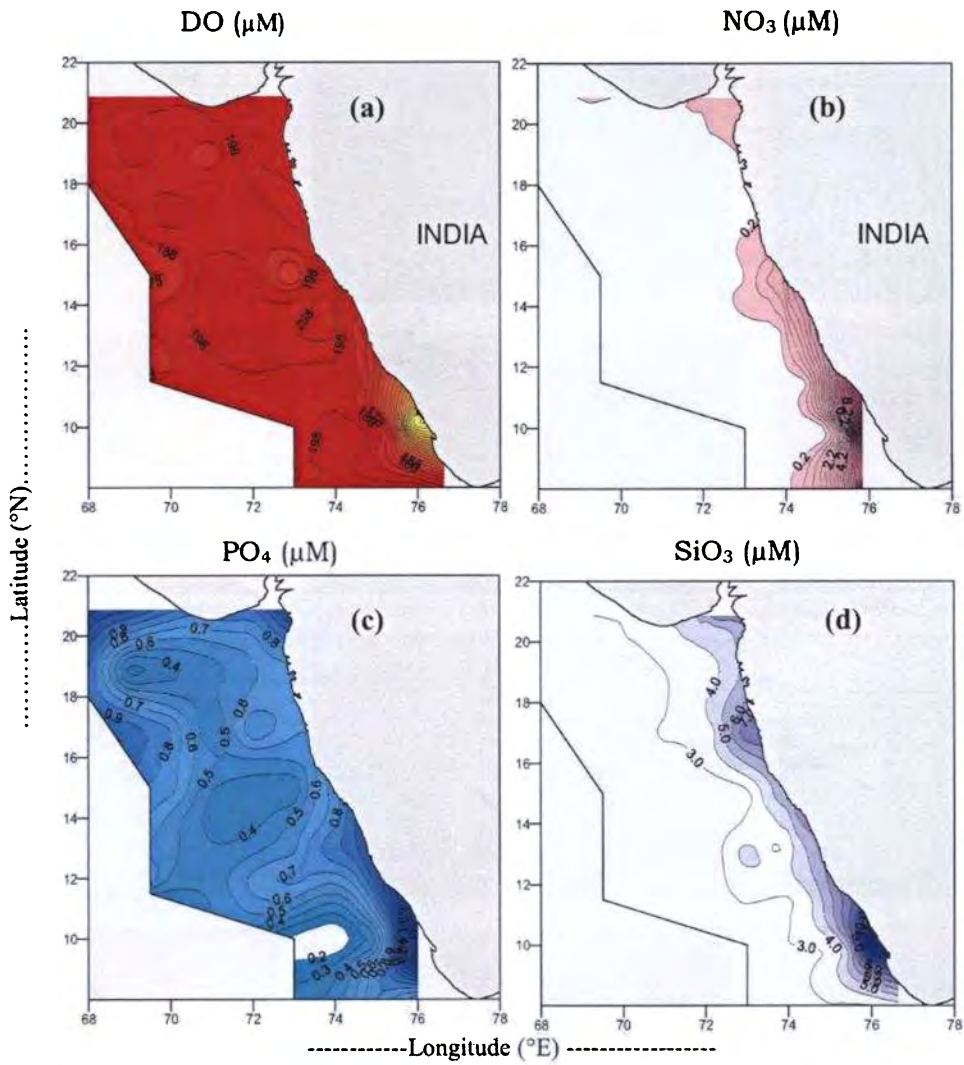


Fig. 3.21. Surface distribution of (a) DO ( $\mu\text{M}$ ), (b) Nitrate ( $\mu\text{M}$ ), (c) Phosphate ( $\mu\text{M}$ ) and (d) Silicate ( $\mu\text{M}$ ) at 10m depth during PSM in the EAS

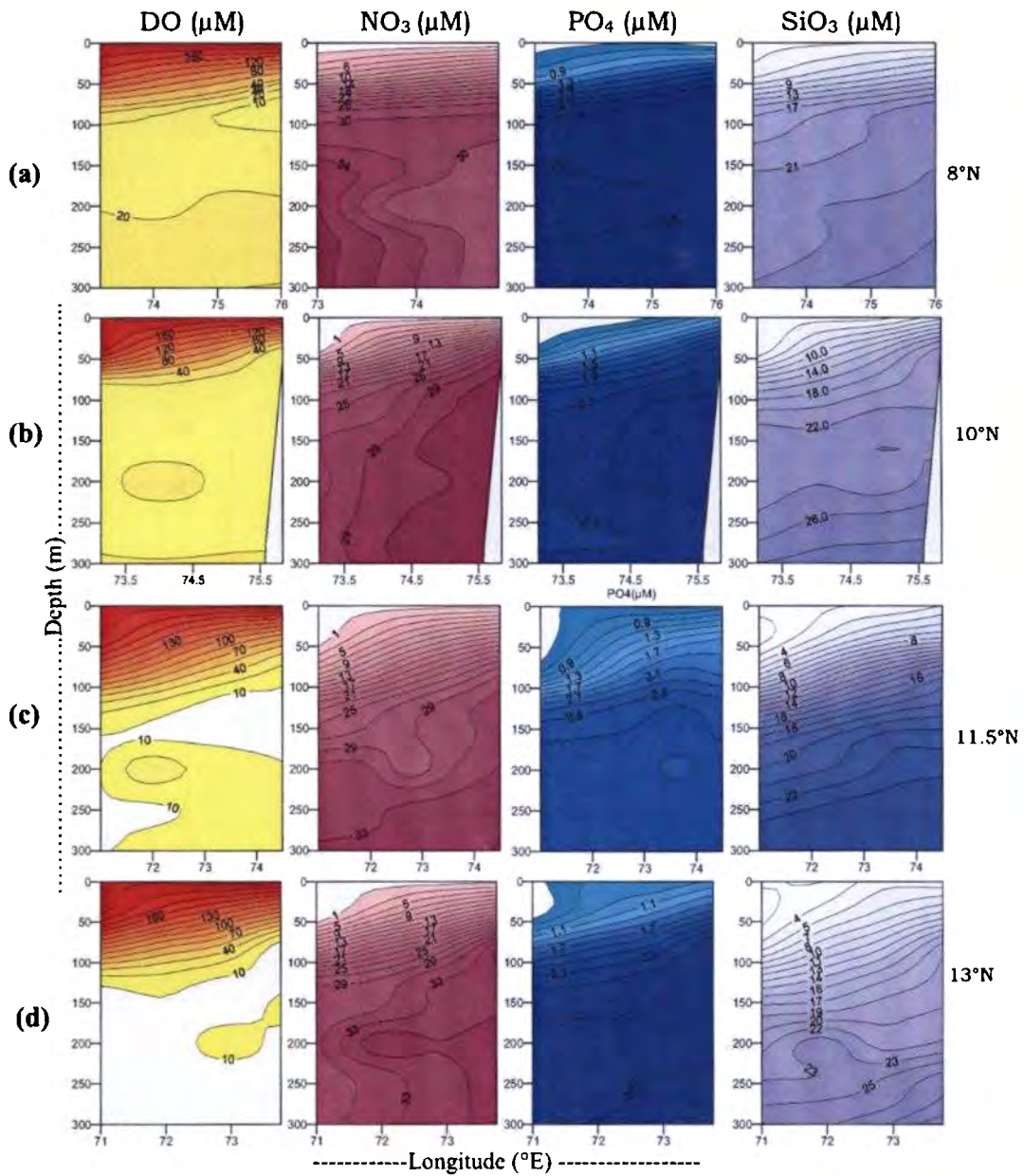


Fig. 3.22. Vertical distribution of DO ( $\mu\text{M}$ ), Nitrate ( $\mu\text{M}$ ), Phosphate ( $\mu\text{M}$ ) and Silicate ( $\mu\text{M}$ ) along (a)  $8^\circ\text{N}$ , (b)  $10^\circ\text{N}$ , (c)  $11.5^\circ\text{N}$  and (d)  $13^\circ\text{N}$  transects during PSM in the EAS

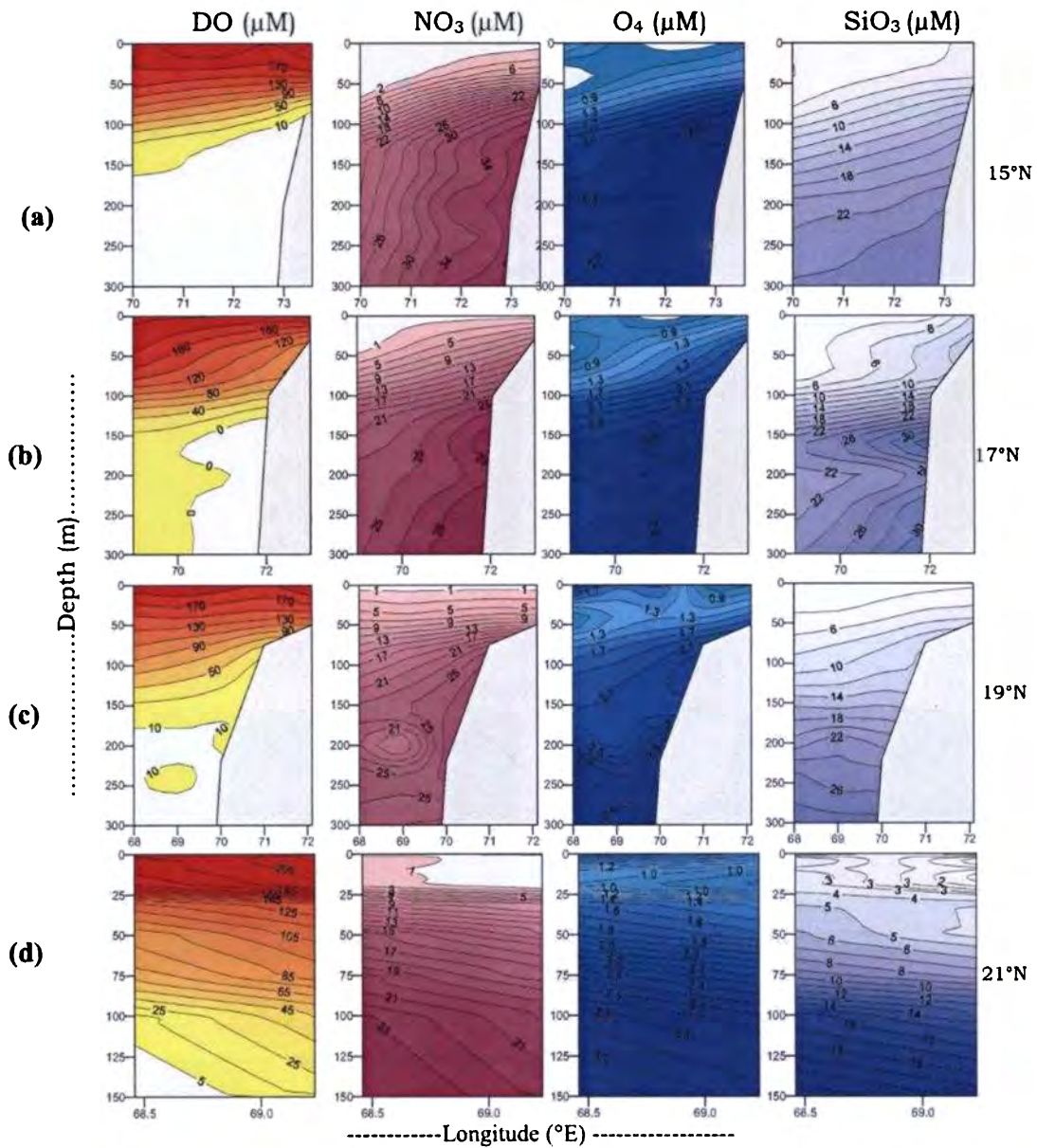


Fig. 3.23. Vertical distribution of DO ( $\mu\text{M}$ ), Nitrate ( $\mu\text{M}$ ), Phosphate ( $\mu\text{M}$ ), and Silicate ( $\mu\text{M}$ ) along (a) 15°N, (b) 17°N, (c) 19°N and (d) 21°N transects during PSM in the EAS

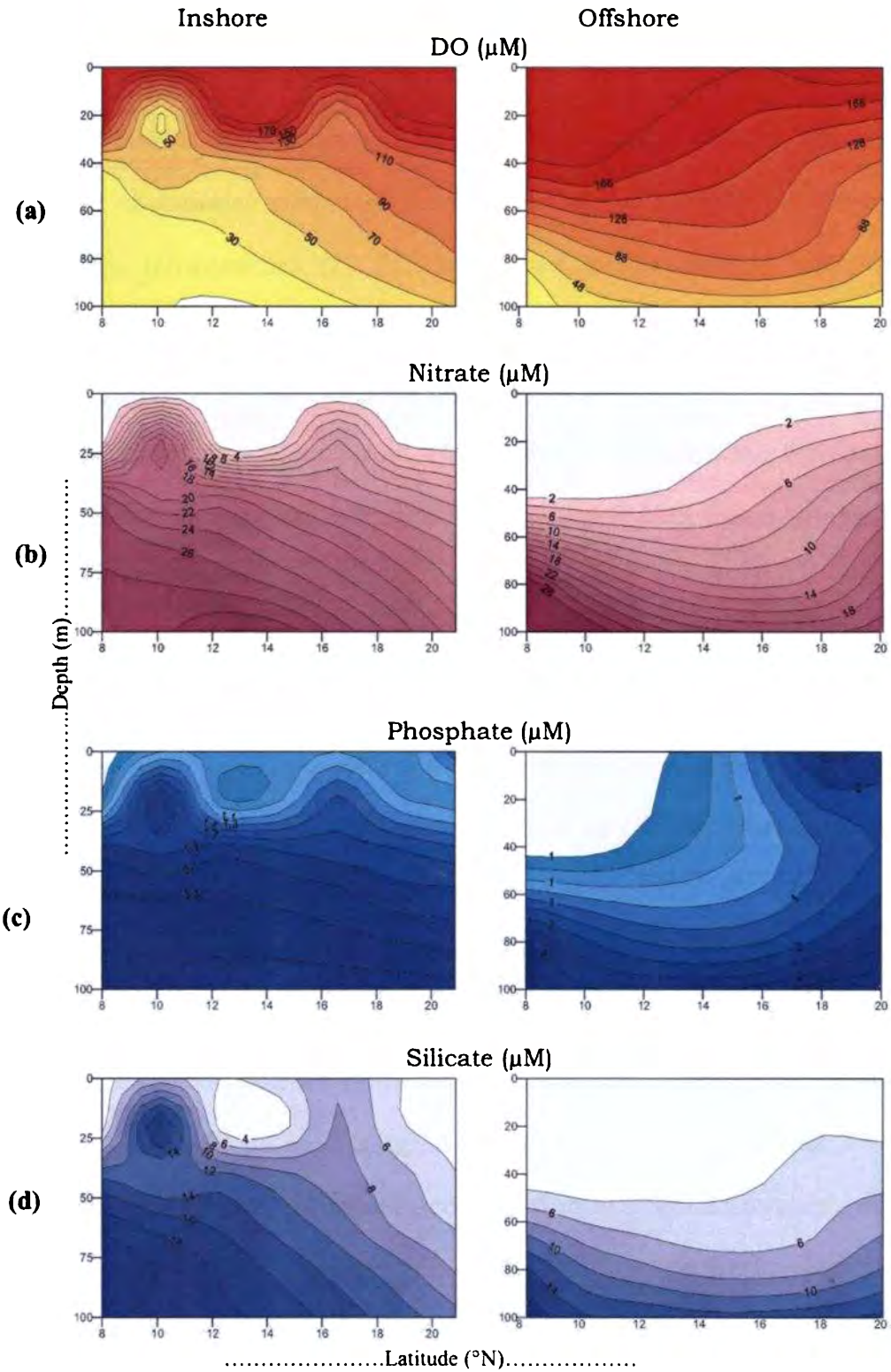


Fig. 3.24. Horizontal distribution of (a) DO ( $\mu\text{M}$ ), (b) Nitrate ( $\mu\text{M}$ ), (c) Phosphate ( $\mu\text{M}$ ) and (d) Silicate ( $\mu\text{M}$ ) along the inshore and offshore stations during PSM in the EAS

### **3.2.4. Late Summer Monsoon (LSM)**

#### ***(a) Physical parameters***

The wind was southwesterly with an average speed of  $6 \text{ ms}^{-1}$  (Fig. 3. 25) with an offshore transport of the surface water. During late phase of summer monsoon, the offshore waters showed maximum sea surface temperature ( $29.5^{\circ}\text{C}$ ) compared to the coastal waters (Fig. 3.26a), which were more or less uniform ( $28.5^{\circ}\text{C}$ ). The minimum SST ( $27^{\circ}\text{C}$ ) was observed at the coastal station of  $15^{\circ}\text{N}$ . Sea surface salinity showed a clear gradient from open ocean to coastal area ranging from 36.6 to 34.8psut (Fig. 3.26b). The MLD (Fig. 3.26c) was in the range of 5m to 75m.

Along  $8^{\circ}\text{N}$  transect (Fig. 3.27a), 70 m thick isothermal layer was observed at oceanic stations, decreasing progressively towards coastal station to a thickness of 25m. Thermocline at a depth of 170m was observed at oceanic stations, while that of coastal stations was still deeper (180m). The ASHSW with a core salinity of  $> 36 \text{ psu}$  was observed at depths of 40 to 90 m between  $72$  to  $74.5^{\circ}\text{E}$ . Upsloping of salinity to the surface along coastal stations indicates upwelling. Pycnocline was almost consistent with the halocline in this transect.

At  $10^{\circ}\text{N}$  transect (Fig. 3. 27b) isothermal layer was 70 m at oceanic stations, but get reduced to 15 m at coastal stations, whereas thermocline depths were 180 and 170m respectively. Uplifting of isotherm from 120m at oceanic stations to 50m depth at coastal water has been observed. Surface salinity of this transect was about 36.7 psu at oceanic and 35 psu at coastal stations. The ASHSW with a core

>36 psu was observed up to 100m depth at 68°E, which shoaled towards coastal station to a range of 60 to 80m at 74°E. A low saline patch of surface waters < 35 psu was observed in the coastal regions of this transect. From the oceanic to the coastal regions, pycnocline showed an upward lift of 40m. At the coastal stations, a down sloping of temperature and density below 90 m was observed. Thickness of isothermal layer in 11.5°N and 13°N transect (Fig. 3.27c and 3.27d) was ~ 60m in the oceanic region and it shoaled into the surface layers of the coastal region. Surface salinity of this transect in the oceanic region was 36.6 psu and 35.2 psu in the coastal region. ASHSW was observed in the subsurface.

Thickness of the isothermal layer in 15°N (Fig. 3.28a) transect was 60m at oceanic and 25m at coastal stations, while thermocline depth was 220 and 230m respectively. Uplifting of isotherms from subsurface in the oceanic stations to surface layers of coastal water was evident. Surface salinity of this transect was about 36.7 psu at oceanic and 35.4 to 36 at coastal stations. The ASHSW with a core salinity of >36.7 psu has now advanced to a depth of 40m between 70°E and 73°E. From the oceanic to the coastal regions, pycnocline showed an upward movement of 20m. Down sloping of temperature and density contours below the depth from 100 to 230m, could be attributed to the pole ward under current in this region. Same trend was observed along 17°N (Fig. 3.28b) transect.

Along 19°N transect (Fig. 3.28c), 40m thick isothermal layer was observed uniformly at both oceanic and coastal stations. Thermocline

depth was 270 m in the oceanic station (68°E) from which it upsloped to 220m at 69°E; then down sloped to 250 m at 70°E station. Upper 100 m of the both oceanic and coastal stations showed a salinity of >36 psu. The core of the ASHSW mass (36.6 psu) was observed at depths of 20m to 60m between 68 and 71°E. Pycnocline was almost at same depth of halocline in this transect. Below 150m depth, density was lowered rapidly to a depth of 200m, due to pole ward under current in this region.

Isothermal layer of 21°N transect (Fig. 3.28d) was 40m at both oceanic and coastal stations. While thermocline depth was uniform (300 m). Surface salinity of this transect was > 36.4 psu at both oceanic and coastal stations. The core of ASHSW mass was observed from surface to 60m. From the oceanic to the coastal regions, pycnocline was uniform.

#### ***(b) Chemical parameters***

During this phase of summer monsoon, it was found that upwelling phenomenon is dominant towards the northern transects and it has started retrieving from the southern transects. Upwelling signatures was found to be still prominent in the coastal waters of 10 – 17°N latitudes even in the late phase of summer monsoon. From the horizontal distribution of DO (Fig. 3.29a) and nutrients (Fig. 3.29b, c and d) along the west coast, it was found that the coastal waters of these transects were characterized by  $DO < 190\mu M$  and nutrient rich waters ( $NO_3 > 2\mu M$  and  $PO_4 > 0.5\mu M$ ). However, the moderate levels of

nitrate ( $> 2\mu\text{M}$ ) in the coastal waters off Cochin and silicate depleted waters along the entire coastal belt are noteworthy.

From the vertical distribution of DO (Fig. 3.30a) and nutrients it was found that the upwelling signatures were not so prominent along  $8^\circ\text{N}$  transect, since the less oxygenated, nutrient rich waters could be traced only up to the near surface layers ( $\sim 20\text{m}$ ) along the coast. The surface layers were saturated but, the sub surface layers showed stratification. The nitracline was shallow ( $\sim 40\text{ m}$ ), but silicate was moderately present ( $> 2\mu\text{M}$ ) in the mixed layer. The OMZ originating from about  $150\text{ m}$  in the offshore region was seen protruding to  $75\text{m}$  as it advanced towards the coast. The upwelling signatures prevalent in the region might have subsided, since this period is the late phase of summer monsoon.

But intense upwelling signatures were still observed along the  $10$ ,  $11.5$ ,  $13$  and  $15^\circ\text{N}$  transects (Fig. 3.30b, c & d) even during the late phase of summer monsoon, which is evident from the upsloping of contours of the different parameters (DO, nitrate and phosphate) to the surface along these latitudes. At  $10^\circ\text{N}$ , nitrate ( $1\mu\text{M}$ ) and silicate ( $> 2\mu\text{M}$ ) were fairly distributed in the mixed layer. The observation of a primary nitrite maxima ( $> 1.4\mu\text{M}$ ) in the subsurface waters along with enrichment of other nutrients should be viewed in relation to its proximity to the coastal input from the adjacent estuarine system.

At  $15^\circ\text{N}$  transect (Fig. 3.31a), the environmental features closely followed the physical properties, as seen from the rising of OMZ above  $100\text{ m}$  towards the coast, rapid increase in nitrate in the mixed layer,

primary nitrite accumulation in the sub surface waters and the coastal enrichment of phosphate and silicate. The 17°N transect (Fig. 3.31b) was also found to be influenced by the prevailing upwelling phenomenon in the region. The 2 $\mu$ M contour of nitrate and the 0.8 $\mu$ M of phosphate found along 75m in the 69°E can be traced immediately below the surface waters (~ 10m) along 75.5° E.

At 19°N transect (Fig. 3.31c), the prominent features were the absence of nitrate, and the presence of surplus amount of phosphate and silicate. The typical oligotrophic conditions prevailed over the region off 21°N transects (Fig. 3.31d), as the mixed layer remained saturated and nutrient-depleted. Vertical distribution of DO, NO<sub>3</sub>, PO<sub>4</sub> and SiO<sub>3</sub> in the inshore and offshore waters were given in the Fig. 32a, b, c & d.

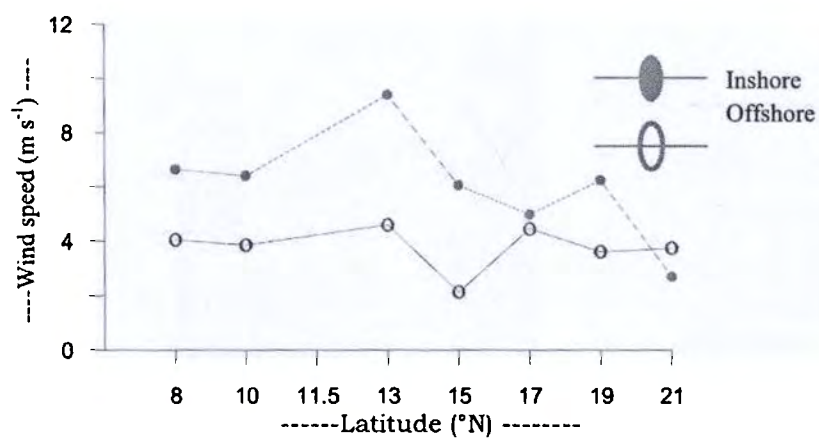


Fig. 3.25. Wind speed during LSM

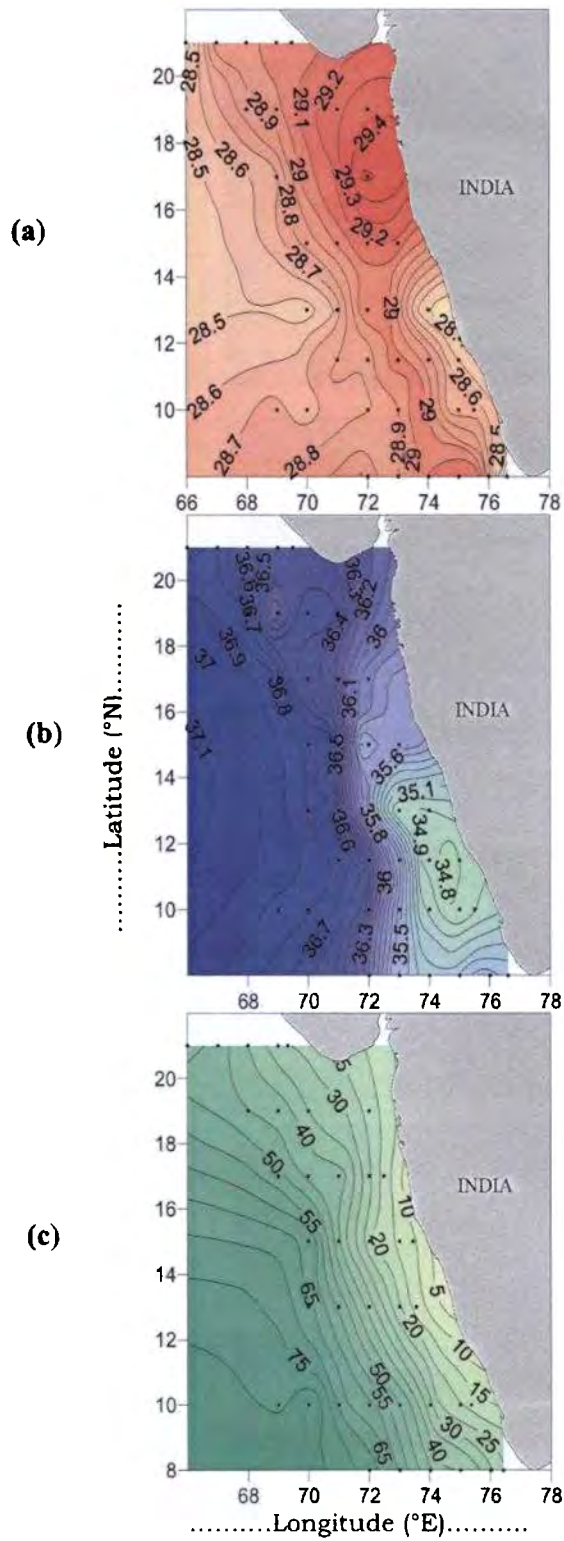


Fig. 3.26. Distribution of (a) SST, (b) SSS and (c) MLD during LSM in the EAS

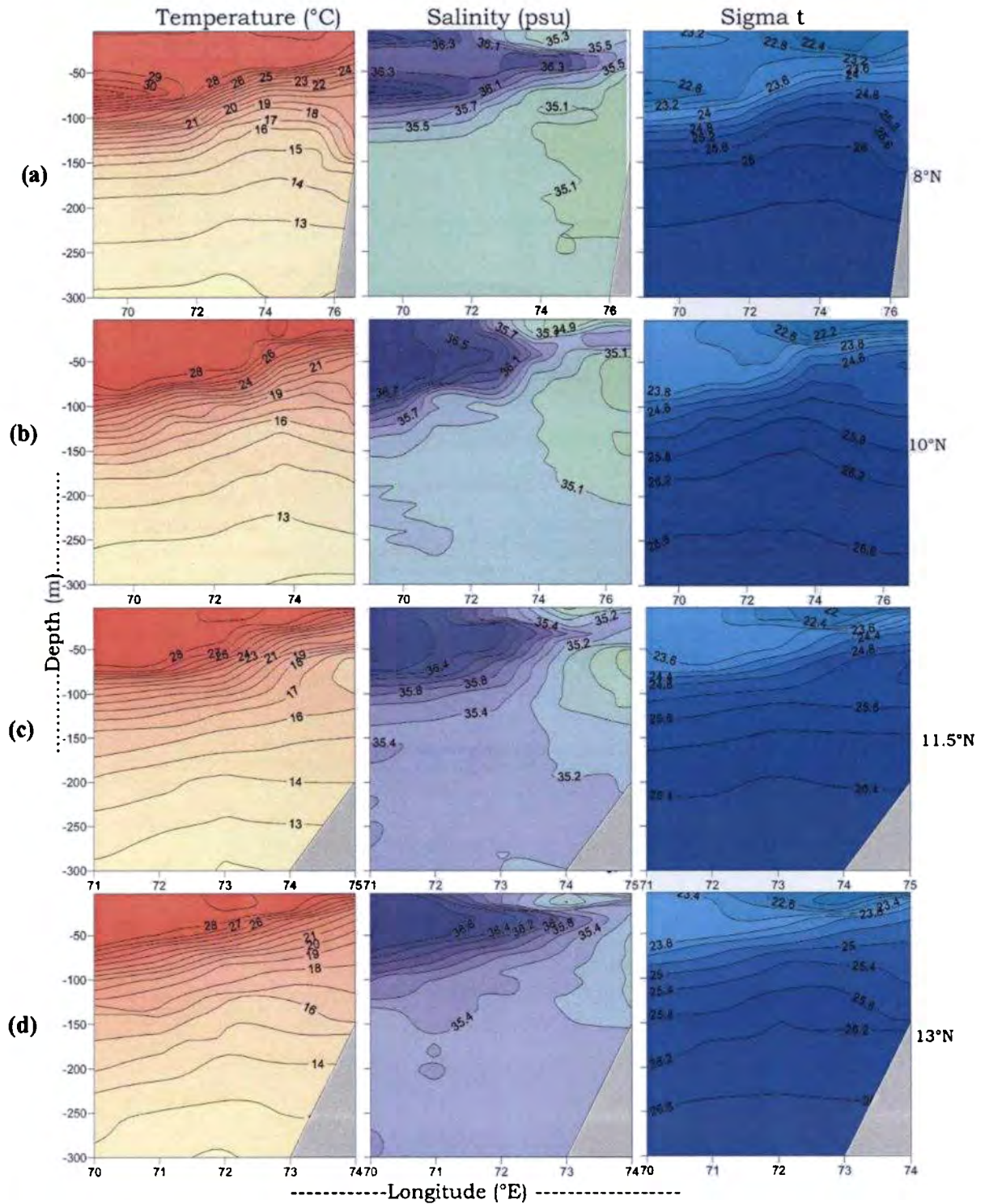


Fig. 3.27. Vertical distribution of temperature, salinity and sigma t along 8°N, 10°N, 11.5°N and 13°N transects during LSM in the EAS

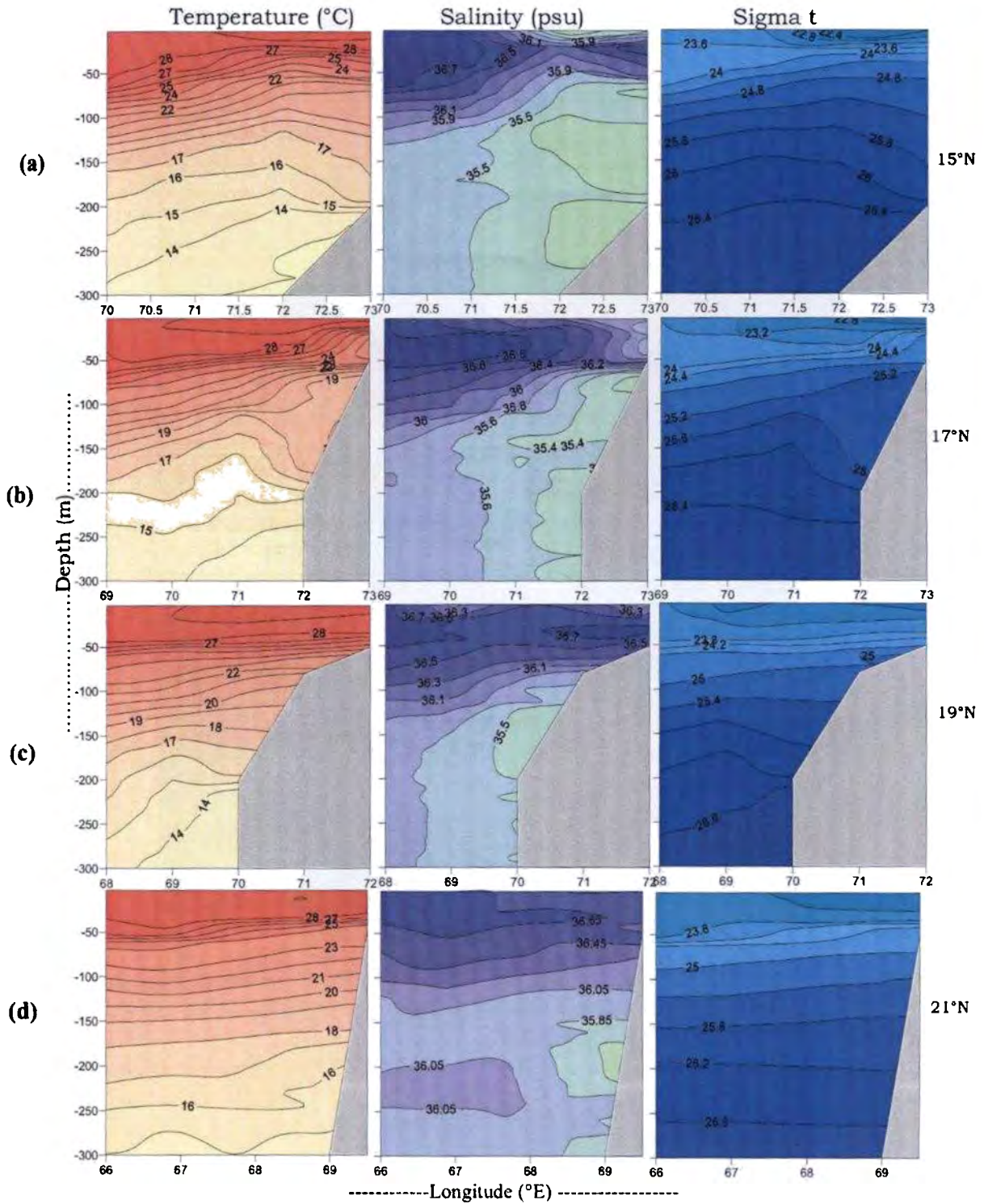


Fig. 3.28. Vertical distribution of temperature, salinity and sigma  $t$  along (a) 15°N, (b) 17°N, (c) 19°N and (d) 21°N transects during LSM in the EAS

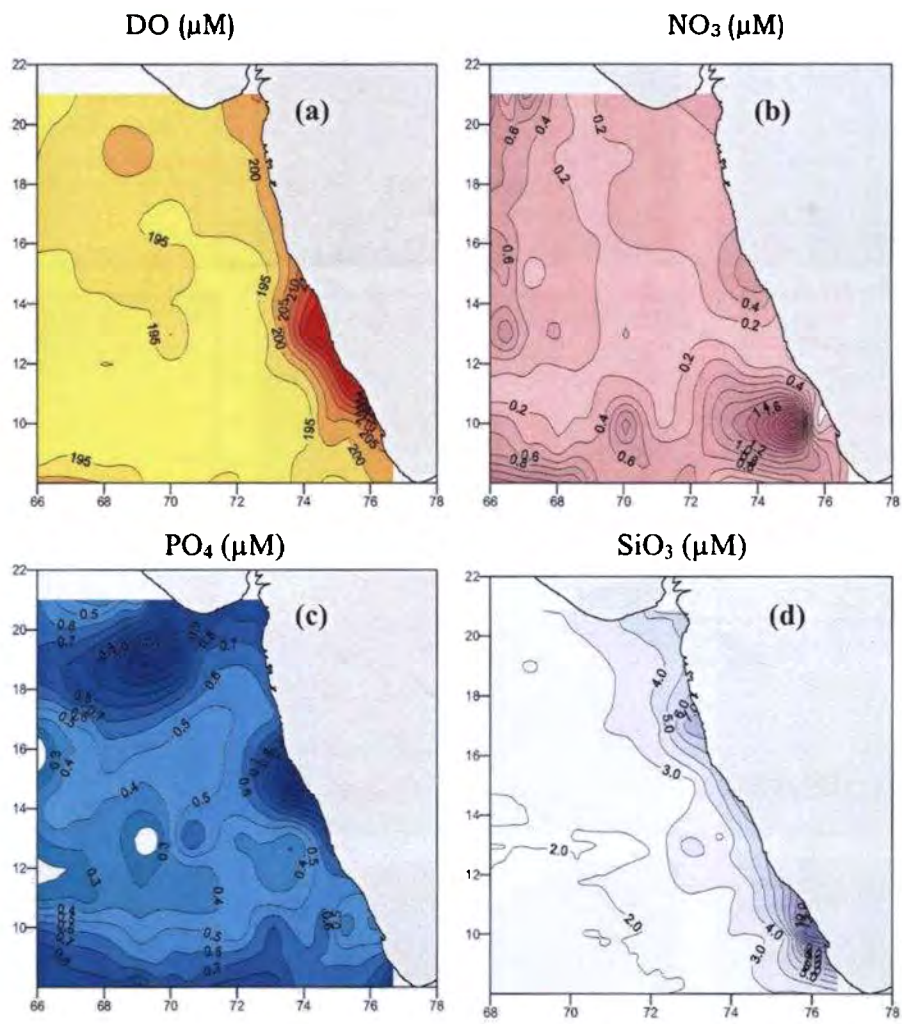


Fig. 3.29. Surface distribution of (a) DO ( $\mu\text{M}$ ) (b) Nitrate ( $\mu\text{M}$ ), (c) Phosphate ( $\mu\text{M}$ ) and (d) Silicate ( $\mu\text{M}$ ) during at 10m depth during LSM in the EAS

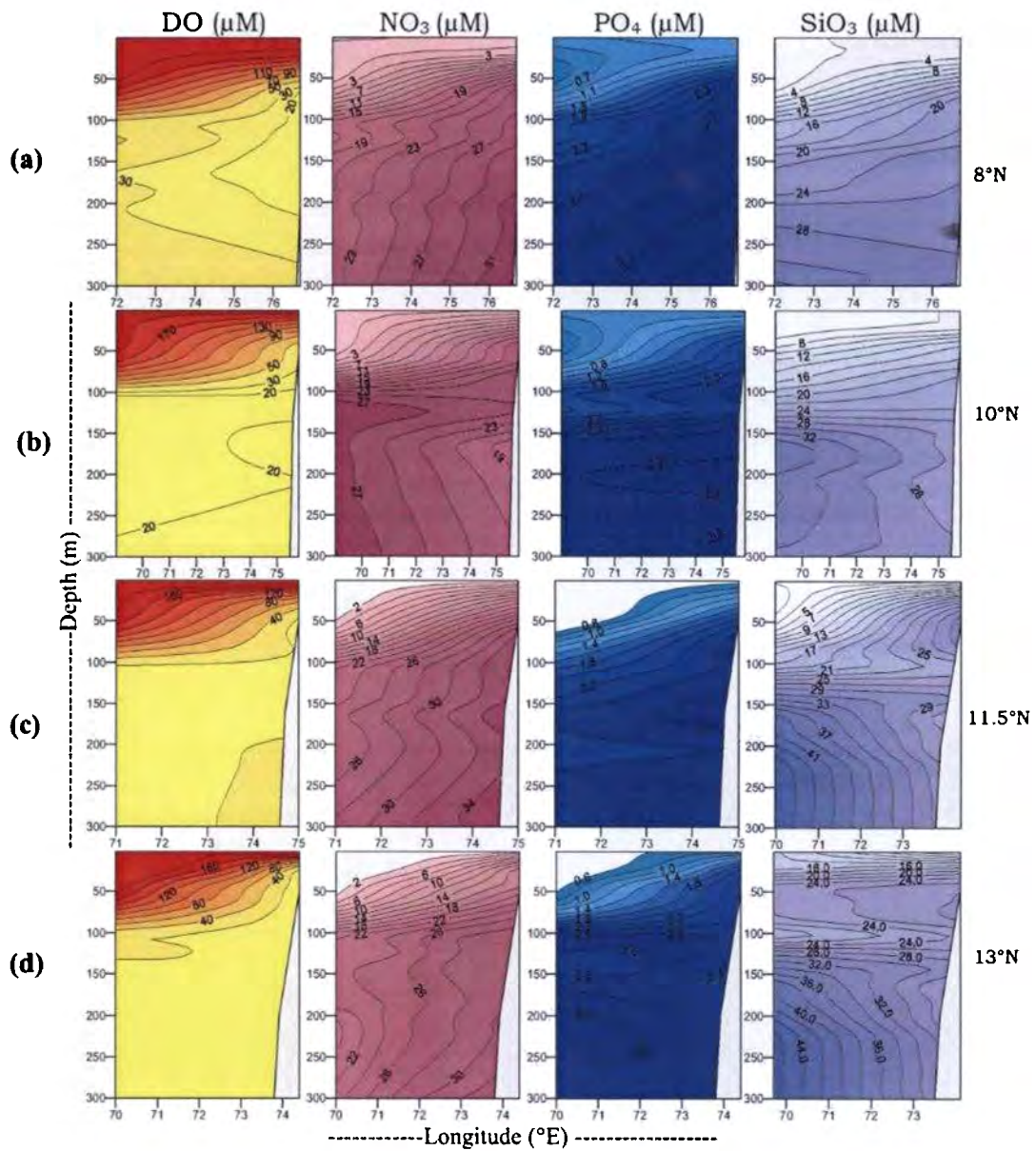


Fig. 3.30. Vertical distribution of dissolved oxygen, Nitrate ( $\mu\text{M}$ ), Phosphate ( $\mu\text{M}$ ) and Silicate ( $\mu\text{M}$ ) along (a)  $8^\circ\text{N}$  (b)  $10^\circ\text{N}$  (c)  $11.5^\circ\text{N}$  and (d)  $13^\circ\text{N}$  transects during LSM in the EAS

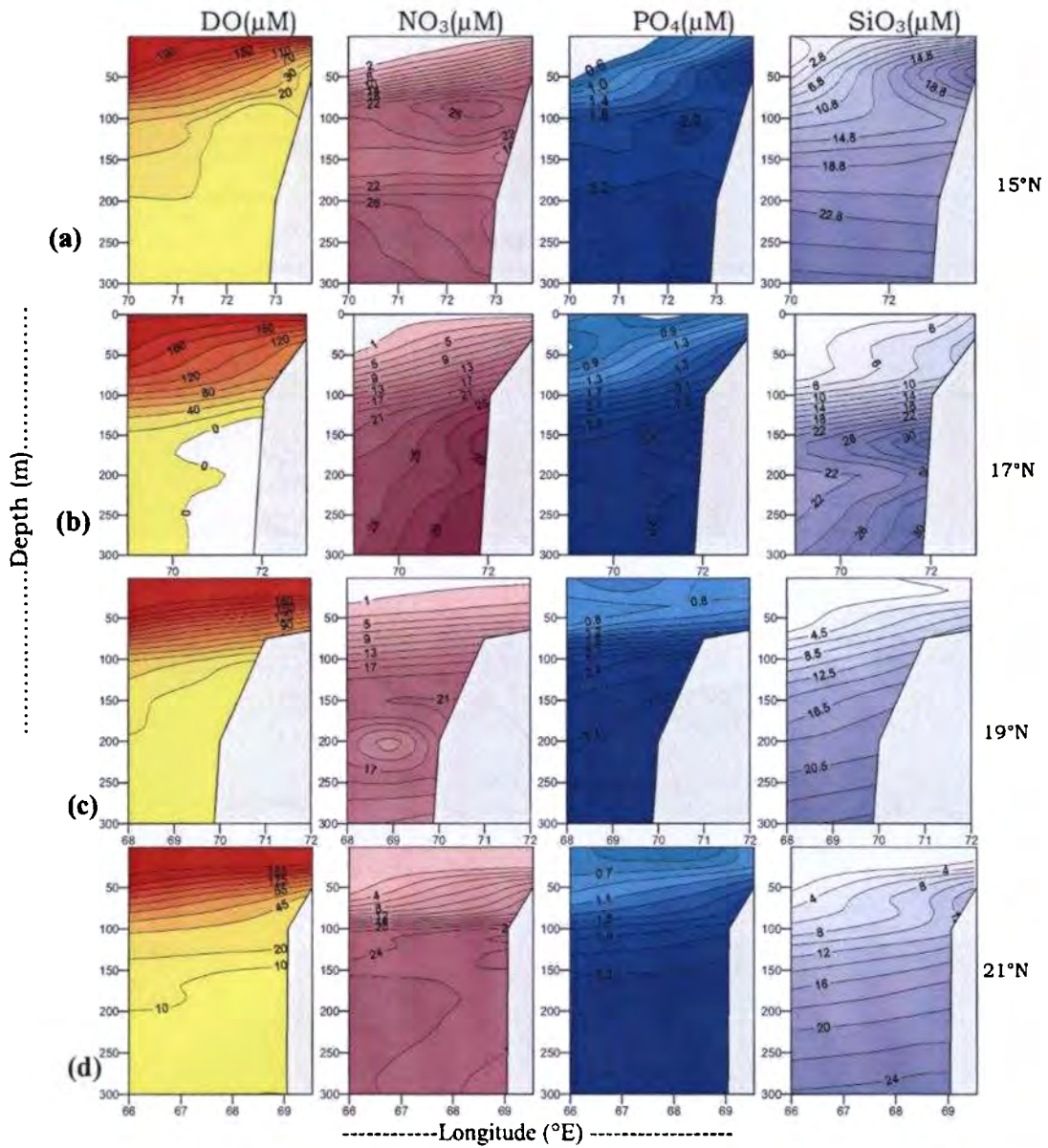


Fig. 3.31. Vertical distribution of DO ( $\mu\text{M}$ ), Nitrate ( $\mu\text{M}$ ), Phosphate ( $\mu\text{M}$ ) and Silicate ( $\mu\text{M}$ ) along (a)15°N (b)17°N (c)19°N and (d) 21°N transects during LSM in the EAS

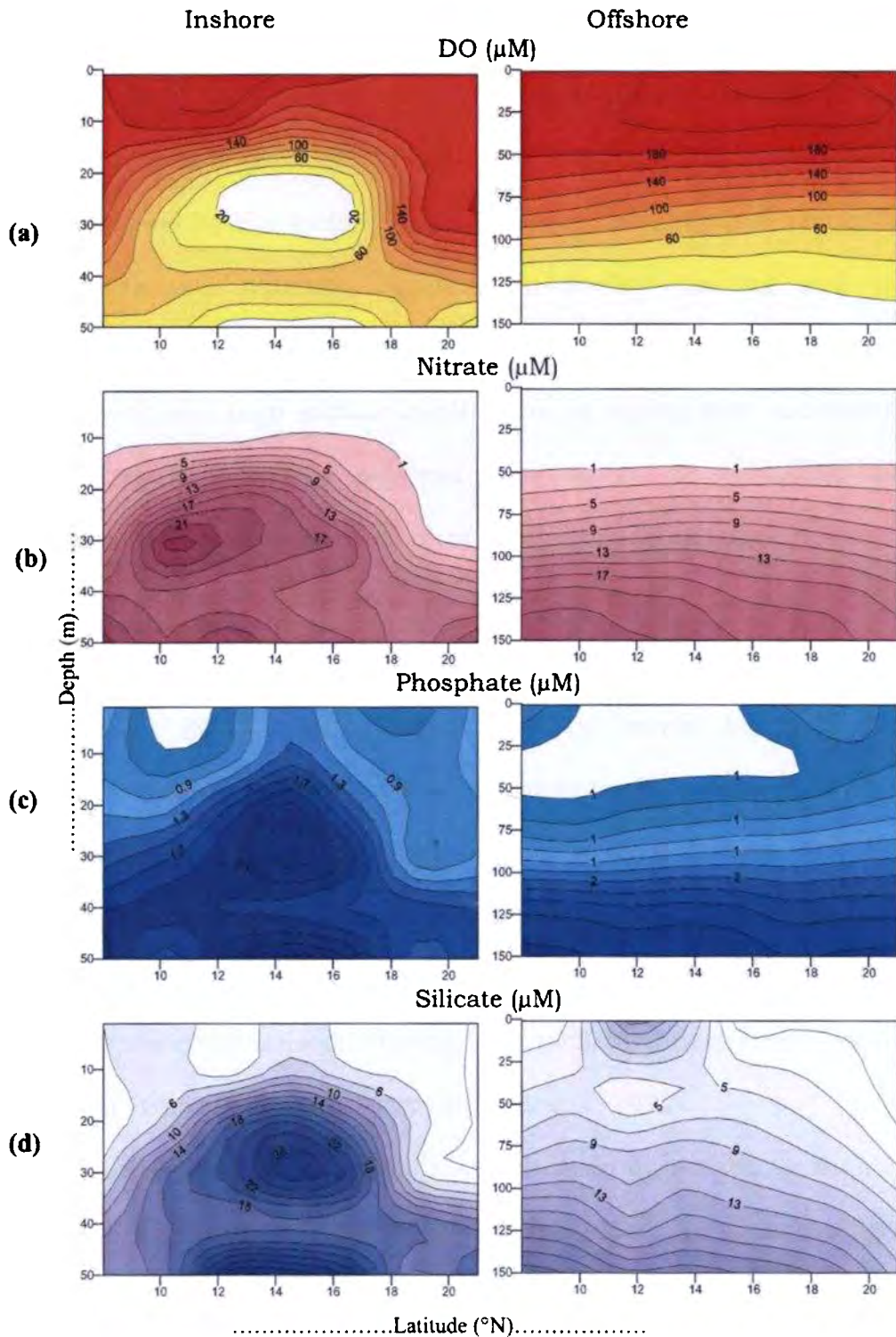


Fig. 3.32. Horizontal distribution of (a) DO ( $\mu\text{M}$ ), (b) Nitrate ( $\mu\text{M}$ ), (c) Phosphate ( $\mu\text{M}$ ) and (d) Silicate ( $\mu\text{M}$ ) along the inshore and offshore stations during LSM in the EAS

### **3.3. Discussion**

The upper layers of the ocean play an important role in the regulation of the ocean–atmosphere as a coupled system (Prasanna Kumar and Narvekar, 2005). The hydrographic conditions are determined by the factors such as seasonality, regional precipitation, currents and radiation resulting in surface heating and cooling (Andrews and Pickard, 1990). The strong winds during south-west monsoon and high surface heating during spring inter-monsoon; and the resultant current patterns have significant influences on the hydrographic characteristics of eastern Arabian Sea. The highly productive periods of Summer Monsoon (SM) and winter monsoon (WM) are interrupted by the Fall Inter Monsoon (FIM) and Spring Inter Monsoon (SIM), during which surface winds become relatively quiescent and the Arabian Sea relaxes towards a more typical tropical oligotrophic character. Variation in the wind pattern results in a complete reversal of atmospheric circulation over the basin, with the NE monsoon winds blowing from December through to February, while the SW monsoon during May to September is associated with much stronger winds (Sastry and D'Souza, 1972).

The SIM period forms the main heating season in the Arabian Sea (Hastenrath and Lamb, 1979). The season experiences light and variable winds, with an av. speed of  $3 \text{ ms}^{-1}$ . The winds were predominantly northerlies with fluctuating patterns. Consistent with the wind reversal, the surface circulation of the basin also undergoes seasonal changes. The hydrography is associated with high SST

(>29°C) and low saline waters (33.9psu). The down welling and low salinity surface waters provided conditions for the formation of high SST during SIM (Shenoi, *et al.*, 1999). The comparatively low salinity (33.9psu) indicated the presence of Bay of Bengal water (Prasanna Kumar, 2004). In the present study, low saline waters were observed up to 15°N. It is noted that when low salinity waters appear in thin surface layers, non-linear combination of salinity and temperature produces more density stratification just below the mixed layer and thereby inhibits mechanical mixing below the stratified layer. Consequently heat accumulates in the thin layer and resulted in high SST. This high SST resulted in the formation of warm pool (Sanilkumar, *et al.*, 2004; Vimalkumar, *et al.*, 2008). The thermal structure during SIM showed a stratified surface layer, extending to 100m depth and the SST (28.0-30.5°C). The low winds and high temperature is not conducive to vertical mixing. In contrast to this, during peak summer monsoon, heavy westerly and northerly winds having an av. speed of 11.5 m/s were predominant. These winds generate localized upwelling as seen in the southern transects, especially in the 10°N. In the upwelling system, there exists a lag period between the onset of favourable wind conditions and the onset of upwelling (Servian, *et al.*, 1982). The prevailing current system in the region is also regarded as the main reason for the upwelling off the southwest coast of India (Gopalakrishna, *et al.*, 2008).

Several studies have been reported in the literature to describe and explain the observed upwelling in the eastern Arabian Sea (Banse,

1958, 1968; Sharma, 1968; Shetye, 1984; McCreary and Chao, 1985; Johannessen *et al.*, 1987; Shetye *et al.*, 1990; Shankar, *et al.*, 2005). All these studies based on relatively sparse and limited hydrographic data sets, reported the onset of upwelling in the deeper depths as early as February/March that gradually reaches the near-surface layers by May and continues until September in association with southward flowing surface coastal current (Sharma, 1968; Shetye, 1984). Cold water is found off the southwest coast of India from June to September and even in October and is extending to about 15°N, south of Goa. The time of commencement of upwelling differs from depth to depth along the west coast of India.

The surface circulation along the west coast between 8° and 15°N closely follows the wind pattern during the summer monsoon and their influence is felt to a depth of 75 m, below which the current reverses, indicating the zone of pole ward undercurrent at depth of 200m (Muraleedharan, *et al.*, 1995). It has been noted that upwelling along the south west coast of India begins sometime in February (Longhurst and Wooster, 1990), well before the onset of the upwelling favourable southwest monsoon winds. The upwelled water reaches the surface in late May and persists up to July/August. The downward movement sets in by the end of August at all depths and earlier in deeper layers (Sharma, 1966). A study of the seasonal variation of oceanographic conditions of the southwest coast of India using the data collected during 1971-'75 under Pelagic Fishery Project (Johannessen, *et al.*, 1987) indicated that an uplift of water onto the

shelf region begins in March or April. Associated with a south-flowing current, this upwelling lasts throughout the southwest monsoon period until September-October.

The along shore wind stress and wind stress curl have been identified as the most important local forcings responsible for the occurrence of upwelling through Ekman dynamics during the SM (Shetye *et al.*, 1985; Shetye and Shenoi, 1988). The upwelling first appears in the southern latitudes along the southwest coast of India and progressively advances in association with the northward propagating coastal Kelvin waves during the pre monsoon season resulting in maximum upwelling off Kochi (McCreary *et al.*, 1993; Shankar and Shetye, 1997). The process of upwelling off Kanyakumari coast (8°N) and the west coast of India are highly localised features with different forcing mechanisms and cannot be treated as a uniform wind driven upwelling system. Off the Kanyakumari coast upwelling is due to the southwest monsoon winds that are tangential to the coast. The area between 8°N and 9°N represents the shadow zone (Smitha *et al.*, 2008) where the influence of the remote forcing on the upwelling process is minimal and the upwelling is forced by the long shore component of the wind stress. From the isolines of DO, nitrate and phosphate it was found that upwelling is only gradually proceeding to the surface during the onset of summer monsoon. Strong and steady south westerly wind during this season cools the northern region by evaporation, while in the southern region, in addition to strong wind, intense coastal upwelling plays a vital role to reduce the SST.

However, along the coastal stations, a concomitant down sloping of temperature, salinity and density below the depth of 70m was observed. The influence of fresh water/estuarine flow and coastal upwelling was evident, as there was a uniform increase in the silicate ( $>3\mu\text{M}$ ) and phosphate concentrations ( $>1\mu\text{M}$ ) through the entire width of the west coast.

During the PSM, the upwelling signatures were dominant and intense between  $8^\circ\text{N}$  and  $17^\circ\text{N}$  of the study region. The observed wind speed showed a high magnitude (av.  $11.5\text{m/s}$ ) at  $11.5$  and  $13^\circ\text{N}$  transects. High cross-shore and along shore component of wind stress was also noticed along these transects. The SST frontal structure clearly showed that Cochin and Calicut was under the grip of strong upwelling. Highest MLD observed at offshore regions were coinciding with high wind stress; and lowest MLD ( $13\text{m}$ ) observed at  $10^\circ\text{N}$  transect was evident for the existence of the intense upwelling in this transect. Upwelled waters might have reached the surface layers during the onset of monsoon and is still found to be prevailing. Clear upsloping of the isolines from the offshore to the shelf waters is observed from the vertical distribution of the  $\text{NO}_3$  along  $10^\circ$ ,  $11.5^\circ$  and  $13^\circ\text{N}$  transects as shown in the Fig. 8a. From a vertical plot of the hydro chemical parameters along the  $15^\circ\text{N}$  transect, it was found that the upwelled waters has not yet reached the surface layers and is limited to the subsurface waters ( $\sim 15\text{m}$ ) during PSM.

The prevalence of upwelling during LSM was evident from the vertical structure of temperature, salinity and nutrients. The

upwelling signatures were less pronounced in the 8°N transect, but still persisting in the 10°N onwards.

The atmospheric forcings would modulate the thickness of the upper ocean by altering the thermal and mechanical inertia of the layer. Several studies in the past attempted to understand the changes in the mixed layer in the Arabian Sea (Rao, 1986; Vimalkumar, *et al.*, 2008). These studies attributed the changes in the mixed layer to the wind-mixing and net heat flux. The mixed layer depth (MLD) remained shallow (av. 40m) during SIM. Increased SST, due to increased insolation, combined with weak winds during this season led to the formation of the observed shallow and uniform mixed layer during SIM. The observed variability of the MLD in the Arabian Sea clearly showed a strong seasonality that could be understood in the context of time varying atmospheric forcing such as incoming solar radiation, wind-stress curl and fresh-water/estuarine flux. The intense solar heating resulted in the highly stratified and shallow mixed layer (30m) observed in April–May. The weak winds (5m/s) prevalent during this time of the year were unable to break the stratification and induce mixing of subsurface waters with surface waters. As a result, the upper layer was devoid of any nutrients as inter monsoon value, which increased the evaporation (E–P 4100 mm/month). The packed isotherms indicated a strong thermocline.

The increased wind speed was along with the low level Findlater Jet (Prasanna Kumar and Narvekar, 2005) that becomes active over the Arabian Sea during the onset of summer monsoon. Thus, both

increased wind speed and reduced solar insolation lead to the observed cold SST (25.8°C). The sea surface cooling is usually associated with upwelling (Shetye *et al.*, 1990). Associated with the shoaling of the mixed layer, the nitracline also shoaled, as is evident from the depth of the >1µM nitrate isopleth. With the onset of summer monsoon, wind speeds are generally high (av. = 15ms<sup>-1</sup>). The OSM was characterized by intense vertical mixing; leading to increased mixed layer thickness (up to 75m) and enrichment of nutrients in the upper layer, which could support higher biological production. The surface circulation along the west coast between 8° and 15°N closely follows the wind pattern during the summer monsoon season and their influence is felt to a depth of 75 m, below which the current reverses. Muraleedharan, *et al.*, (1995) indicated such reversal of currents due to the zone of pole ward under current at depth of 200m.

The comparative study of different phases of the summer monsoon revealed the corresponding spatial variability in upwelling intensities. The upwelling phenomenon is characterized by three sequential phases: (1) the upwelling phase, when the cold nutrient-rich waters well up (Type -1), (2) the productive phase or mature phase, when a superficial heating occurs, accompanied by an increase in biomass and primary production and the simultaneous decrease in nutrient concentrations (Type -2) and (3) the downwelling phase or relaxing phase leading to an oligotrophic situation as a consequence of decrease in phytoplankton biomass due to the dispersion and nutrient depletion (Type -3) (Rodriguez, *et al.*, 1992 and Barlow, 1982). The

cycling of these three phases is strongly influenced by local winds (Banse, 1968; Halpern, 1976; Barton, *et al.*, 1977; Nair, *et al.*, 1989). The wind blowing parallel to the coast generates offshore transport, which causes coastal upwelling between May to September. Within the upwelled area, the uplift of deep water results in colder temperatures, a shallow thermocline and enhanced nutrients in surface waters. The onset of summer monsoon (May-June) marks the beginning of upwelling along the SW coast of India (Unnikrishnan and Antony, 1992). Moderate to relatively high levels of upwelling occur in the (8°N to 13°N) region is due to the combined action of the wind stress, the coastally trapped Kelvin waves and the offshore propagating Rossby waves. North of this area (13°N to 15°N), perhaps up to 17°N, upwelling is weak and closely confined to the coastal belt despite winds favourable for upwelling. This is explained as due to the suppressive effect of the southward flowing ASHSW on the process of upwelling along this stretch. The intensity of upwelling is evident from the LTA indices, which was highest in the 10° N transect during PSM and during LSM it was at 15°N. During the present studies, based on the cruises conducted during the onset, peak and late summer monsoon periods, it is evident that the upwelling takes place sequentially from south to north along and off the south west coast of India with its corresponding influences on hydrography and productivity. It is also noted that the northward propagation of upwelling events during the summer monsoon lasts till October. From

the observations it is clear that intensity of upwelling shows northward propagation.

These interpretations of thermo-haline and density structure gives a general idea of the hydrography of the eastern Arabian Sea during spring inter monsoon and summer monsoon.

## References

- Andrews, J.C. and Pickard, G.L., 1990. The physical oceanography of coral reef systems. In: Ecosystem of the world, 25. *Coral Reefs* (Ed. Dubinsky, Z.) Elsevier, Amsterdam. pp: 11-48.
- Banse, K., 1958. On upwelling and bottom trawling of the southwest coast of India. *J. Mar. Biol Assn. India*. 1: 33-49.
- Banse, K., 1968. Hydrography of the Arabian Sea shelf of India and Pakistan and effects on demersal fishes. *Deep - Sea Res.*, 15: 45-79.
- Barlow, R.G, 1982. Phytoplankton ecology to the Southern Benguela Current. I Biochemical composition. *J. Exp. Mar. Biol. Ecol.*, 63: 209-227.
- Barton, E.D., Huyer, A. and Smith, R.L, 1977. Temporal variations observed in the hydrographic regimes near Cabo Cobeiro in the north west African upwelling region, February to April 1974. *Deep Sea Res.*, 24: 7-24.
- Gopalakrishna, V.V., Rao, R.R., Nisha, K., Girishkumar, M.S., Pankajakshan, T., Ravichandran, M., Johnson, Z., Girish, K., Anishkumar, N., Srinath, M., Rajesh, S. and Rajan, C.K., 2008. Observed anomalous upwelling in the Lakshadweep Sea during summer monsoon season of 2005. *J. Geophys. Res.*, 113: C 05001 doi: 10.1029/2007 JC 004240, 2008.
- Halpern, D., 1976. Structure of coastal upwelling event observed off Goa during July 1973. *Deep Sea Res.*, 23: 495-508.
- Hastenrath, S. and Lamb, P.J., 1979. Climatic Atlas of the Indian Ocean. *University of Wisconsin Press. Madison Wisconsin*, 97p.
- Johannessen, O.M., Subharaju, G. and Blindheim, G., 1987. Seasonal variations of the oceanographic condition off the southwest coast of India during 1971 - 1975. *Fisk Dir. Skr. Ser. Hav. Unders.*, 18: 247-261.

- Longhurst, A.R. and Wooster, W.S., 1990. Abundance of oil sardine (*Sardinella longiceps*) and upwelling on the southwest coast of India. *Can. J. Fish. Aquat. Sci.*, 47: 2407-2419.
- McCreary, J.P. and Chao, S.Y., 1985. Three dimensional shelf circulation along an eastern ocean boundary. *J. Mar. Res.*, 43: 13-36.
- McCreary, J.P., Kundu, P.K. and Molinari, R.L., 1993. A numerical investigation of the dynamics, thermodynamics and mixed layer processes in the Indian Ocean. *Progr. Oceanogr.*, 31: 181-244.
- Muraleedharan, P.M., Ramesh Kumar, M.R., and Rao, L.V.G., 1995. A note on poleward undercurrent along the southwest coast of India. *Cont. Shelf Res.*, 15: 165-184.
- Nair, R.R., Ittekot, V., Manginini, S., Ramaswamy, V., Haake, B., Degens, E., Desai, B. and Honjo, S., 1989. Increased particle flux to the deep ocean related to monsoons. *Nature*, 338: 749-751.
- Prasanna Kumar, S. and Narvekar, J., 2005. Seasonal variability of the mixed layer in the central Arabian Sea and its implication on nutrients and primary productivity. *Deep-Sea Res. II*, 52: 1848-1861.
- Prasanna Kumar, S., Madhupratap, M., Dileep Kumar, M., Gauns, M., Muraleedharan, P.M., Sarma, V.V.S.S. and De Souza, S.N., 2000. Physical control of primary productivity on seasonal scale in central and eastern Arabian Sea. *Proc. Indian Acad. Sci., (Earth Planet. Sci.)*, 109: 433-442.
- Prasanna Kumar, S., Narvekar, J., Ajoy Kumar, Shaji, C., Anand, P., Sabu, P., Rejomon, G., Josia, J., Jayaraj, K.A., Radhika, R. and Nair, K.K. C., 2004. Intrusion of the Bay of Bengal water into the Arabian Sea during winter monsoon and associated chemical and biological response. *Geophys. Res. Lett.*, 31, 5304, doi: 10.1029/2004GL 020247.
- Rao, R.R., 1986. Cooling and deepening of the mixed layer in the central Arabian Sea during Monsoon-77: observations and simulations. *Deep Sea Res.*, 33: 1413-1424.
- Rodriguez, E.G, Valentine, J.L., Andre, D. L. and Jacob, S.A., 1992. Upwelling and down welling at Cabo Frio (Brazil). Comparison of biomass and production responses. *J. Plankton. Res.*, 14(2): 289-306.
- Sanilkumar, K.V., Hareesh Kumar, P.V., Joseph, J., and Panigrahi, J.K., 2004. Arabian Sea mini warm pool during May 2000. *Curr. Sci.* 86(1): 180-184.
- Sastry, J.S. and D'Souza, R.S., 1972. Upwelling and upward mixing in the Arabian Sea. *Indian J. Mar. Sci.*, 1: 17-27.
- Servain, S., Picaut, J. and Merle, J., 1982. Evidence of remote sensing in the equatorial Atlantic Ocean. *J. Phys.Oceanogr.*, 12: 457-463.

- Shankar, D. and Shetye, S.R., 1997. On the dynamics of the Lakshadweep high and low in the southeastern Arabian Sea. *J. Geophys. Res.*, 102(C6): 12551-12562.
- Shankar, D., Shenoi, S.S.C., Nayak, R.K., Vinayachandran, P.N., Nampoothiri, G., Almeida, A.M., Michael, G.S., Rameshkumar, M.R., Sundar, D. and Sreejith, O.P., 2005. Hydrography of the eastern Arabian Sea during summer monsoon 2002. *J. Earth Syst. Sci.*, 114: 475-491.
- Sharma, G.S., 1966. Thermocline as an indicator of upwelling. *J. Mar. Bio. Ass. India*, 8: 8-19.
- Sharma, G.S., 1968. Seasonal variation of some hydrographic properties of the shelf waters off the west coast of India. *Bull. Nat. Inst. Sci. India*, 38: 263-276.
- Shenoi, S.S.C., Shankar, D. and Shetye, S.R., 1999. On the sea surface temperature high in the Lakshadweep Sea before the onset of the southwest monsoon. *J. Geophys. Res.*, 104: 15703-15712, doi: 10.1029/1998JC900080.
- Shetye, S. R., Shenoi, S.S.C., Antony, M.K. and Krishnakumar, V., 1985. Monthly mean wind stress distribution along the coast of the North Indian Ocean. *Proc. Indian Acad. Sci. Earth Planet. Sci.*, 94:129-137.
- Shetye, S.R. and Shenoi, S.S.C., 1988. Seasonal cycle of surface circulation in the coastal North Indian Ocean. *Proc. Indian Acad. Sci. (Earth Planet. Sci.)*, 97: 53-62.
- Shetye, S.R., 1984. Seasonal variability of temperature fields off the southwest coast of India. *Proc. Indian Acad. Sci. Earth Planet. Sci.*, 93: 399-411.
- Shetye, S.R., Gouveia, A.D., Shenoi, S.S.C., Sunbar, D., Michael, G.S., Almeida, A. M. and Santanam, K., 1990. Hydrography and circulation off the west coast of India during the southwest monsoon 1987. *J. Mar. Res.*, 48: 359-378.
- Smitha, B.R., Sanjeevan, V.N., Vimalkumar, K.G. and Revichandran, C., 2008. On the upwelling of the southern tip and along the west coast of India. *J. Coastal Res.*, 24: 95-102.
- Unnikrishnan, A.S. and Antony, M.K., 1992. On the upwelling front on the west coast of India during the later part of southwest monsoon. Physical Processes in the Indian Seas. *Proc. First Convention, ISPSO, 1990*. pp: 131-135.
- Vimalkumar, K.G., Dineshkumar, P.K., Smitha, B.R., Habeebrehman, H. Josia., J., Muraleedharan, K.R., Sanjeevan, V.N. and Achuthankutty, C.T., 2008. Hydrographic characterization of southeast Arabian Sea during the wane of southwest monsoon and spring intermonsoon. *Environ. Monit. Assess.*, 140: 231-247.

## Biological responses during spring intermonsoon

---

4.1. Introduction  
4.2. Results  
4.2.1. Primary productivity  
4.2.2. Chlorophyll *a*  
4.2.3. Phytoplankton abundance  
4.2.4. Mesozooplankton  
4.3. Discussion  
References

---

### 4.1. Introduction

Spring inter monsoon (SIM) season forms the intermediate season between two productive seasons, i.e., winter and summer monsoons. It is characterized by light winds and warm surface oligotrophic waters (Mantoura, *et al.*, 1993; Bhattathiri, *et al.*, 1996). The seasonal wind stress modifies mixed layer depth (Niiler, 1977) and nutrient status, which in turn determines the amount of nutrients available for phytoplankton growth (Longhurst, 1998). Such strong coupling between the prevailing physical conditions and biological processes occurs in the Arabian Sea (Brock and McClain, 1992; Brock, *et al.*, 1994). During summer monsoon, nutrient enrichment due to upwelling promotes phytoplankton production, which often exceeds  $2\text{gmCm}^{-2}\text{d}^{-1}$  (Savidge and Gilpin, 1999) where as in the oligotrophic SIM season, nitrate reaches concentrations as low as  $10\text{nM}$  at surface waters (Woodward, *et al.*, 1999), resulting in low phytoplankton productivity, that is often  $<0.1\text{gC m}^{-2}\text{d}^{-1}$  (Jochem, *et al.*,

1993). Evidences of localized high phytoplankton production were reported by Devassy, *et al.*, (1978) and Capone, *et al.*, (1998) due to the occurrence of *Trichodesmium* bloom as they absorb atmospheric nitrogen.

In this chapter, the spatial variations in biological responses, such as primary productivity (PP), Chl *a*, phytoplankton density, mesozooplankton biomass and composition during SIM are discussed.

## **4.2. Results**

### **4.2.1. Primary productivity**

The EAS was more or less oligotrophic and showed lowest primary productivity during SIM. The distribution of primary productivity in the surface layer and 120 m water column are given in Figs. 4.1a & b. The inshore-offshore and north south variability in primary productivity was minimum during this season. On an average primary productivity found to be less both in surface ( $<7 \text{ mgC m}^{-3}\text{d}^{-1}$ ) and in column ( $<300 \text{ mgC m}^{-2}\text{d}^{-1}$ ). The surface primary productivity in the inshore waters was in the range of 0.8 to 6.7  $\text{mgC m}^{-3} \text{d}^{-1}$  (av.  $3.75 \pm 2.11 \text{ mgC m}^{-3} \text{d}^{-1}$ ) and in the offshore waters the values were 0.9 to 4.6  $\text{mgC m}^{-3}\text{d}^{-1}$  (av.  $2.18 \pm 1.56 \text{ mgC m}^{-3}\text{d}^{-1}$ ) (Table 4.1). The column primary productivity varied from 67 to 296  $\text{mg Cm}^{-2} \text{d}^{-1}$  (av.  $189 \pm 93 \text{ mg Cm}^{-2}\text{d}^{-1}$ ) in the inshore waters and, 61 to 174  $\text{mg Cm}^{-2}\text{d}^{-1}$  (av.  $117 \pm 40 \text{ mgCm}^{-2}\text{d}^{-1}$ ) in the offshore. The maximum surface primary productivity of 6.7  $\text{mg Cm}^{-3}\text{d}^{-1}$  was recorded in the inshore waters of 13°N and the maximum column primary productivity was recorded at

11.5°N inshore waters. Primary productivity maxima were observed at depths below 20m at most of the study area (Fig. 4.2)

#### **4.2.2. Chlorophyll *a***

Chl *a* was found to be low, along the southeastern Arabian Sea during SIM (Fig. 4.1c & d). The surface Chl *a* was in the range of 0.09 to 0.51 (av.  $0.24 \pm 0.17$   $\text{mgm}^{-3}$ ) along the inshore waters and 0.02 to 0.28 (av.  $0.12 \pm 0.08$   $\text{mgm}^{-3}$ ) along the offshore. The corresponding column Chl *a* along the inshore stations were in the range of 4.6 to 29.5  $\text{mgm}^{-3}$  (av.  $18.7 \pm 8.5$   $\text{mgm}^{-2}$ ) and in the offshore stations it varied from 7.5 to 38.8 (av.  $17.3 \pm 10.8$   $\text{mgm}^{-2}$ ) (Table 4.2). Maximum surface and column Chl *a* was recorded at (0.51  $\text{mgm}^{-3}$ ) and 13°N (38.8  $\text{mgm}^{-2}$ ) respectively. The vertical distribution of Chl *a* at different depths at each station is shown in Fig. 4.3. Subsurface Chl *a* maxima was observed below the depth of 20m were observed in most of the stations. The inshore - off shore and north south variability was also minimum as evidenced from the *SeaWiFS* chlorophyll imagery (Fig. 4.4).

#### **4.2.3. Phytoplankton abundance**

The vertical distribution of phytoplankton density in the inshore and offshore waters are shown in Figs. 4.5 & 4.6. The total phytoplankton abundance at the surface waters of inshore and offshore region was in the range of 720 to 15440 cells  $\text{L}^{-1}$  (av. 4350 cells  $\text{L}^{-1}$ ) and 640 to 3440 cells  $\text{L}^{-1}$  (av. 1472 cells  $\text{L}^{-1}$ ) respectively (Table. 4.3). The inshore-offshore variations in phytoplankton

abundance is depicted in the Figs. 4.7 a, b, c & d. The population density of diatoms, dinoflagellates and blue green algae in the surface and column waters are given in Table 4.4 & 4.5. During this season the blue green algae formed the most abundant group (64.5%) the inshore stations, where as in the offshore it was less (30%). Diatom formed an average of 23.6% and 49% in the inshore and offshore waters respectively. The proportion of dinoflagellate to the total population along inshore and offshore stations was 11.9% and 20.7% respectively (Fig. 4.8).

The relationship between Chl *a* and nutrients is shown in the Figs. 4.9a - c. Nutrients showed no significant correlation with Chl *a*. where as significant correlation Chl *a* and primary productivity ( $r = 0.70$ ,  $p < 0.05$ ). Similarly significant linear correlation with total phytoplankton abundance ( $r = 0.63$ ,  $p < 0.05$ ) and diatom abundance ( $r = 0.60$ ,  $p < 0.05$ ) during this season (Fig. 4.10). Primary productivity also showed significant correlation and total phytoplankton density ( $r = 0.60$ ,  $p < 0.01$ ), diatom density ( $r = 0.58$ ,  $p < 0.01$ ) and dinoflagellate density ( $r = 0.53$ ,  $p < 0.05$ ) (Figs. 11 a, b & c).

#### **4.2.4. Mesozooplankton**

The distribution of mesozooplankton biomass in the mixed layer and thermocline layer are shown in Fig. 4.12 a & b. Mesozooplankton biomass in the mixed layer was found to be higher ( $0.62 \text{ ml m}^{-3}$ ) as compared to the offshore ( $0.42 \text{ ml m}^{-3}$ ). Maximum zooplankton biomass ( $1.4 \text{ ml.m}^{-3}$ ) was observed in the mixed layer of  $15^\circ\text{N}$  and  $17^\circ\text{N}$ . In the thermocline layer the average biomass in the

inshore and offshore stations was  $0.27 \text{ mlm}^{-3}$  and  $0.20 \text{ ml m}^{-3}$ , respectively (Table 4.6). During this season the southern region, ( $8\text{--}13^\circ\text{N}$ ) recorded the minimum zooplankton biomass in the mixed layer and thermocline layers. Copepod was the most abundant mesozooplankton group (80%) both mixed layer and thermocline layer. followed by ostracods (8%) and chaetognaths (5%) (Table 4.7).

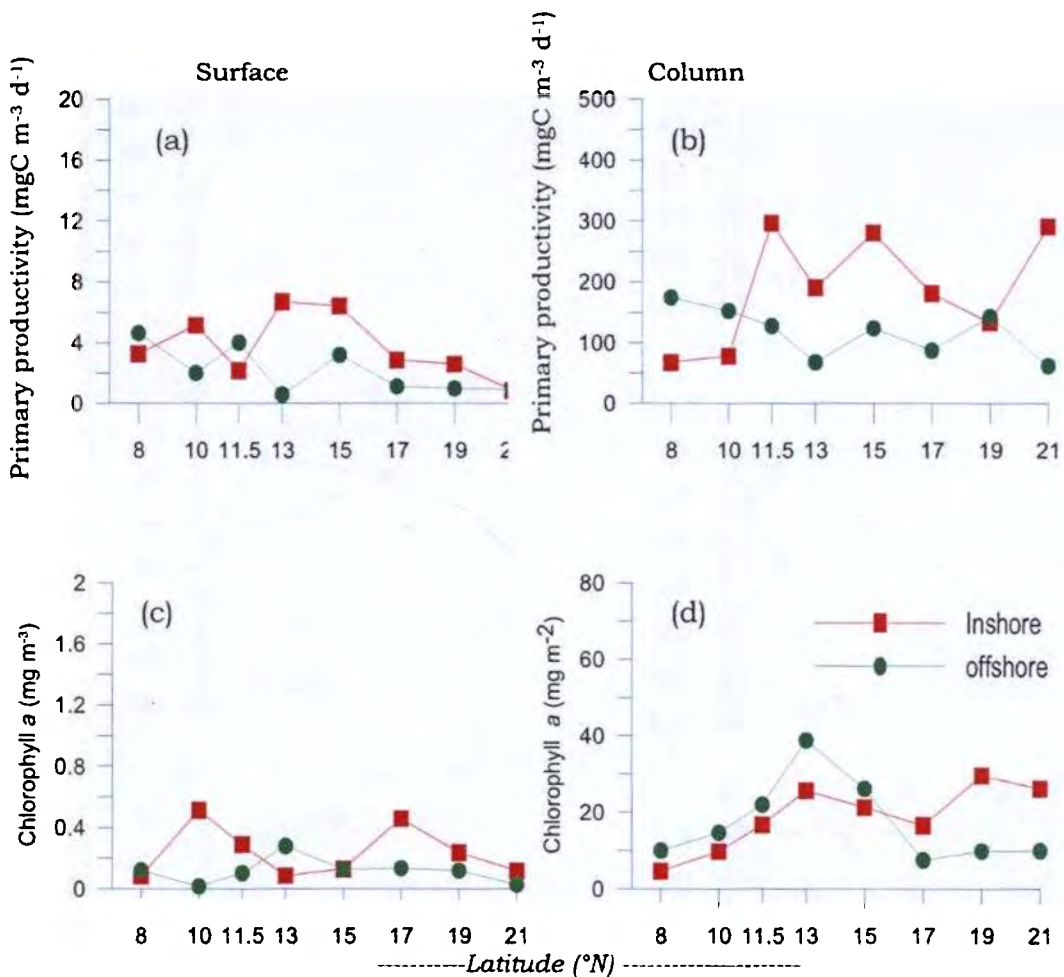


Fig. 4.1. Distribution of primary productivity (a & b) and Chl a (c & d) in the EAS during SIM

Biological responses during spring intermonsoon

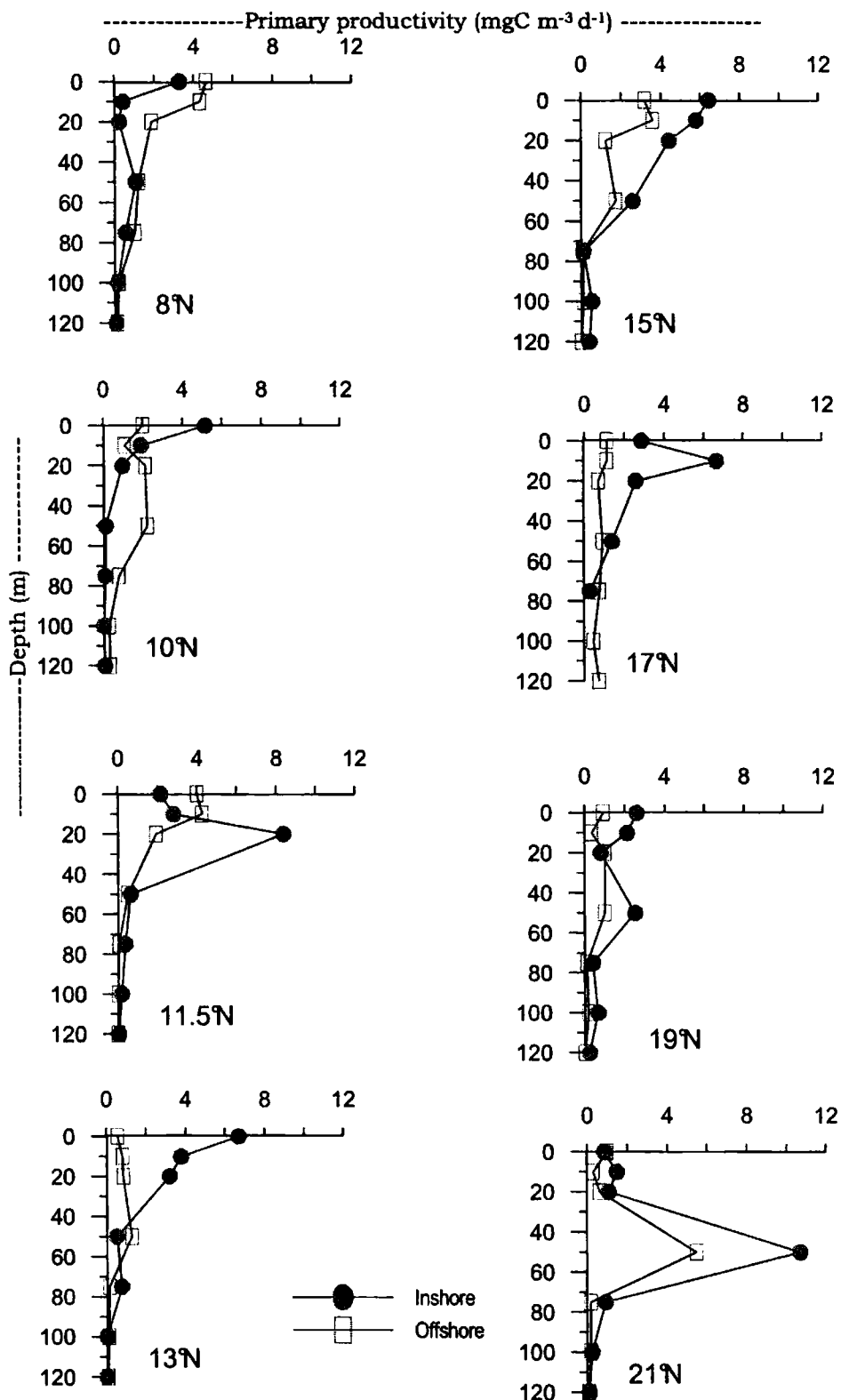


Fig. 4.2. Vertical distribution of primary productivity ( $\text{mgC m}^{-3} \text{d}^{-1}$ ) along the inshore and offshore waters of EAS during SIM

Biological responses during spring intermonsoon

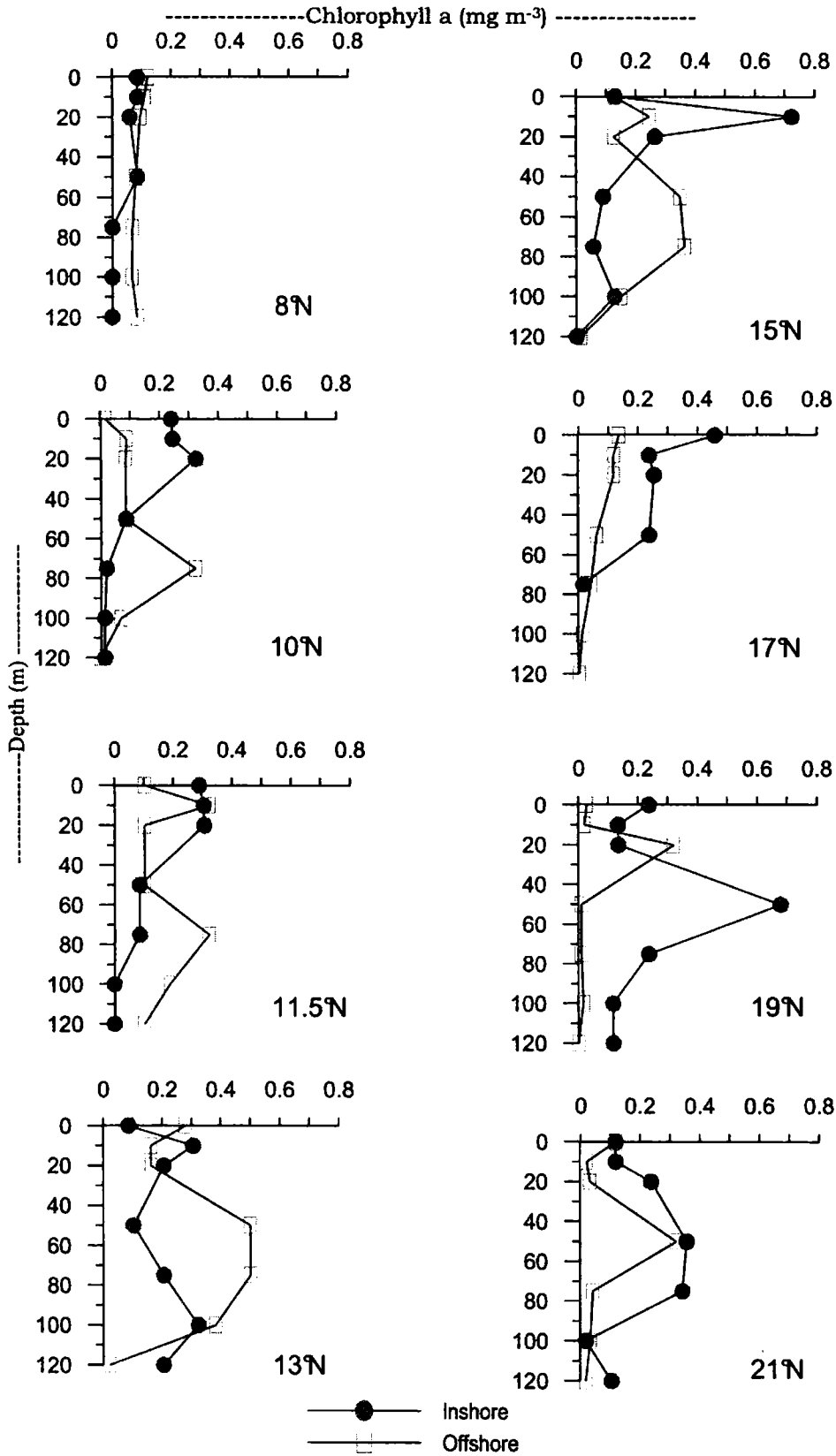


Fig. 4.3. Vertical distribution of Chl a (mgm<sup>-3</sup>) in the inshore and offshore waters of EAS during SIM

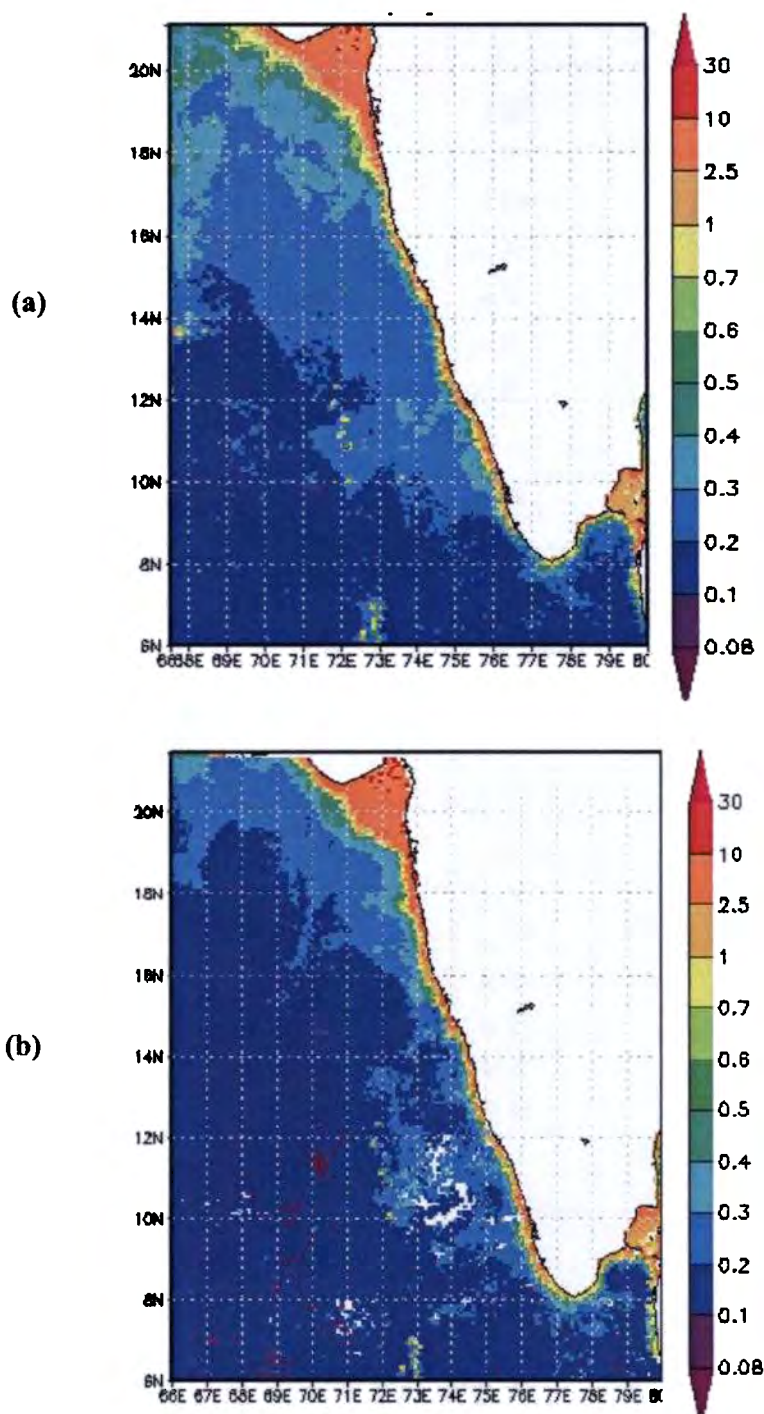


Fig. 4.4. Satellite derived (Monthly average *SeaWiFS*) Chl *a* concentration in the EAS during SIM (a) March and (b) April, 2004

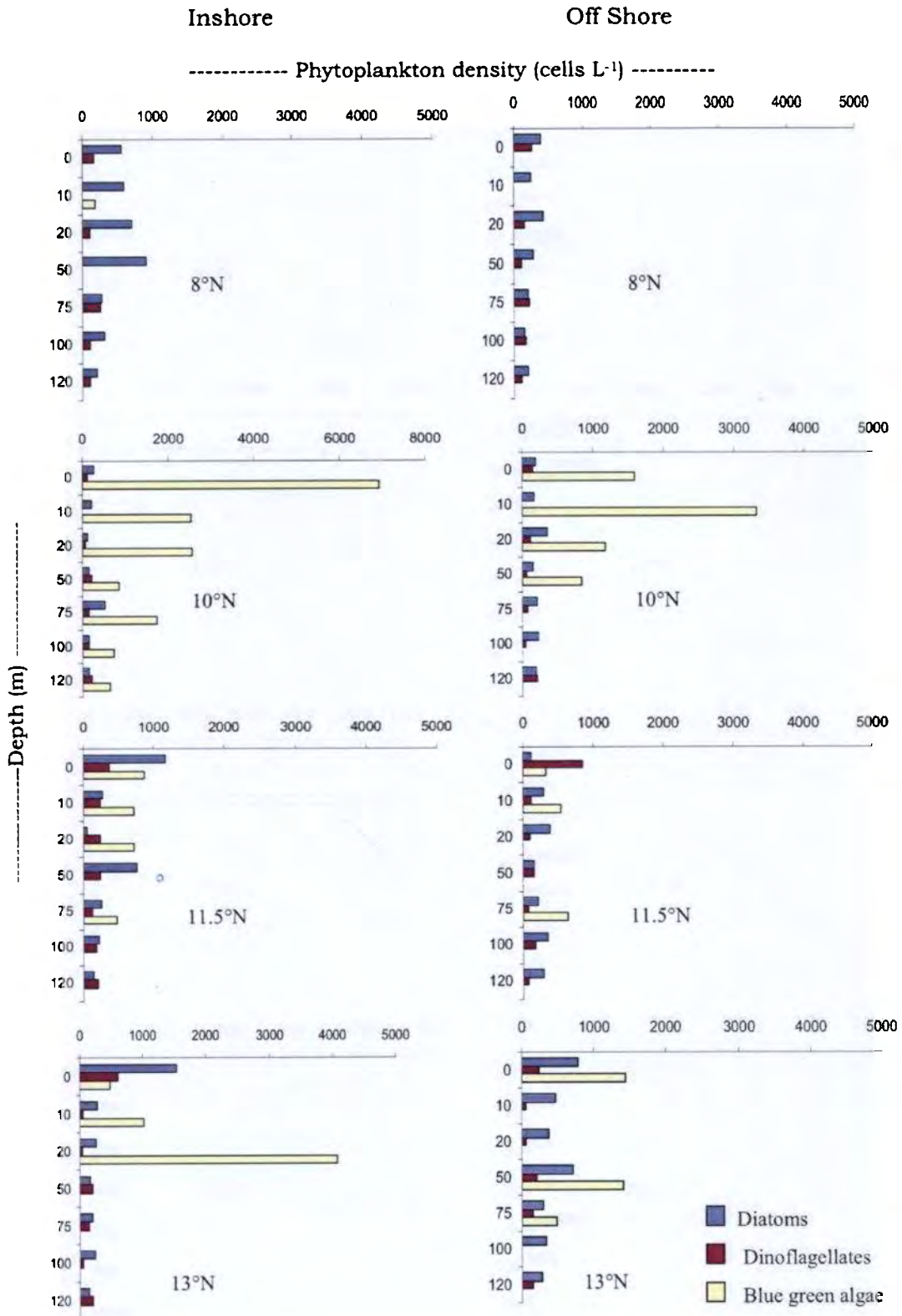


Fig. 4.5. Vertical distribution of phytoplankton density (cells L<sup>-1</sup>) along the inshore and offshore waters of EAS during SIM

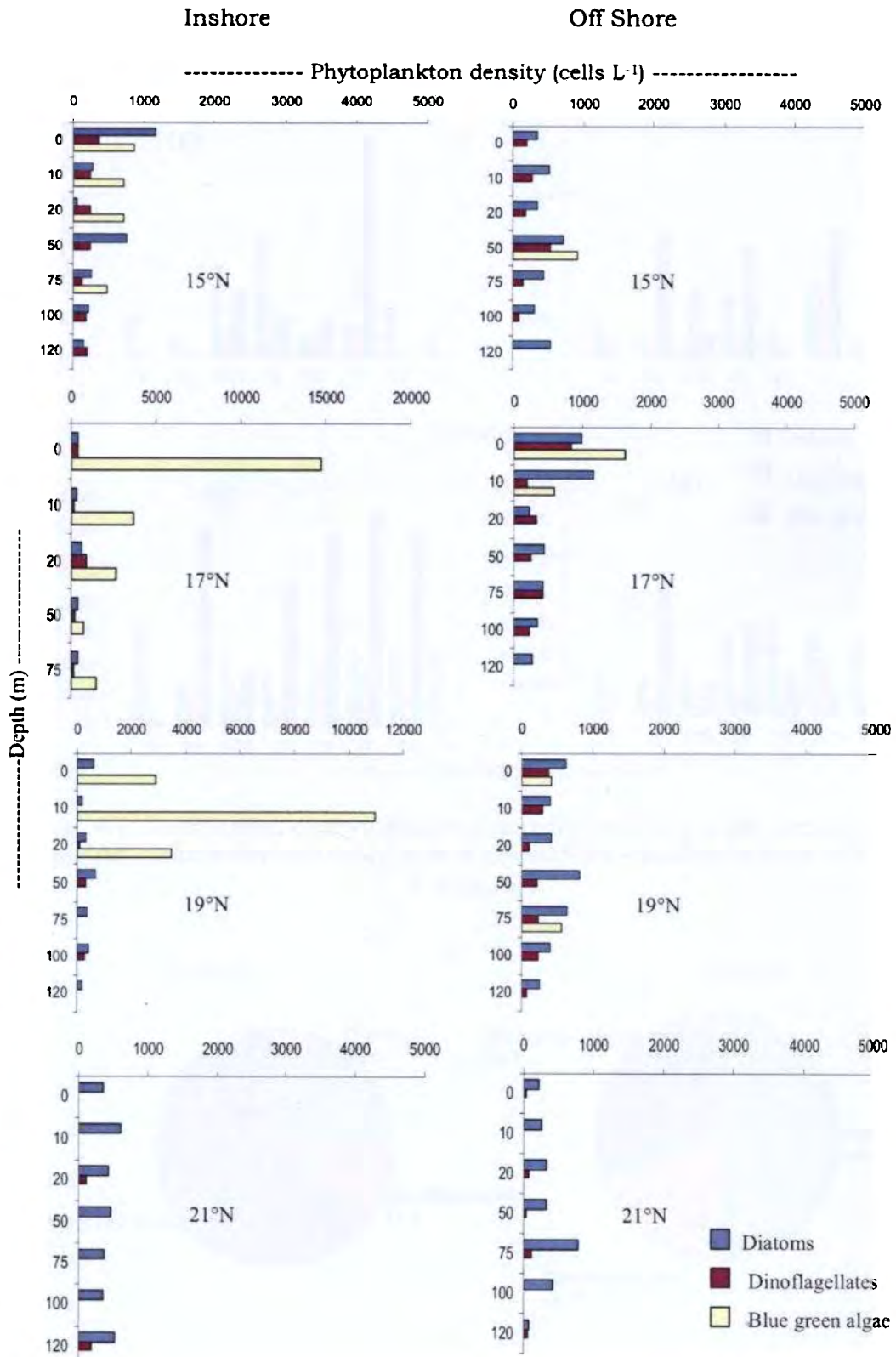


Fig. 4.6. Vertical distribution of phytoplankton density (cells L<sup>-1</sup>) in the EAS during SIM

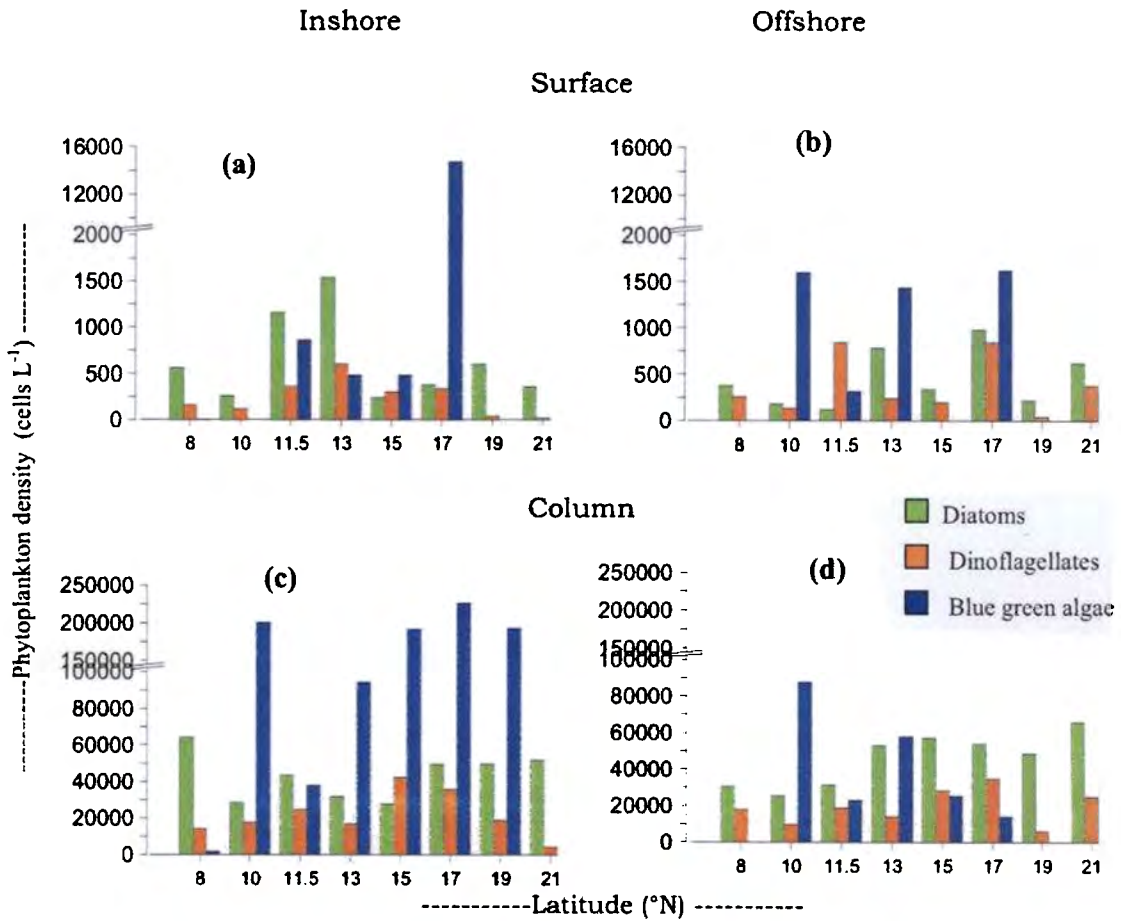


Fig. 4.7. Distribution of phytoplankton density (cells L<sup>-1</sup>) in the surface (a & b) and 120m water column (c & d) of the inshore – offshore waters of EAS during SIM

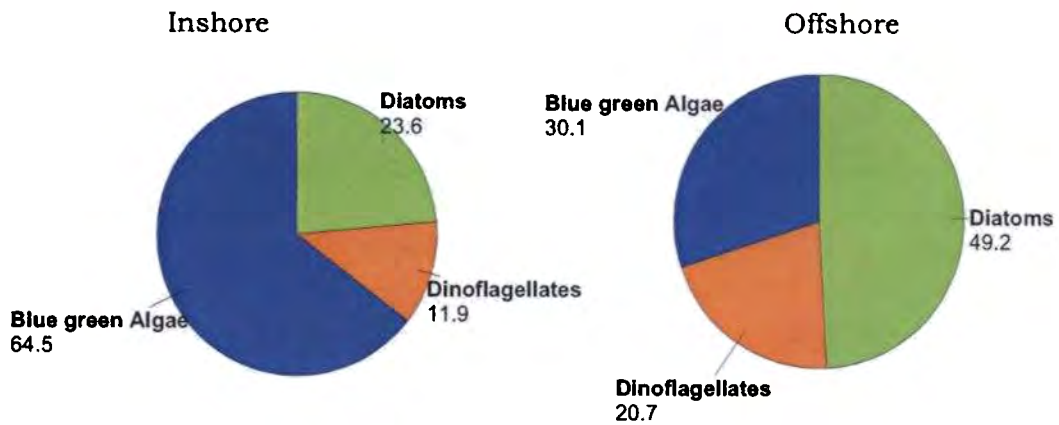


Fig. 4.8. Percentage composition of phytoplankton density in the inshore and off shore waters of EAS during SIM

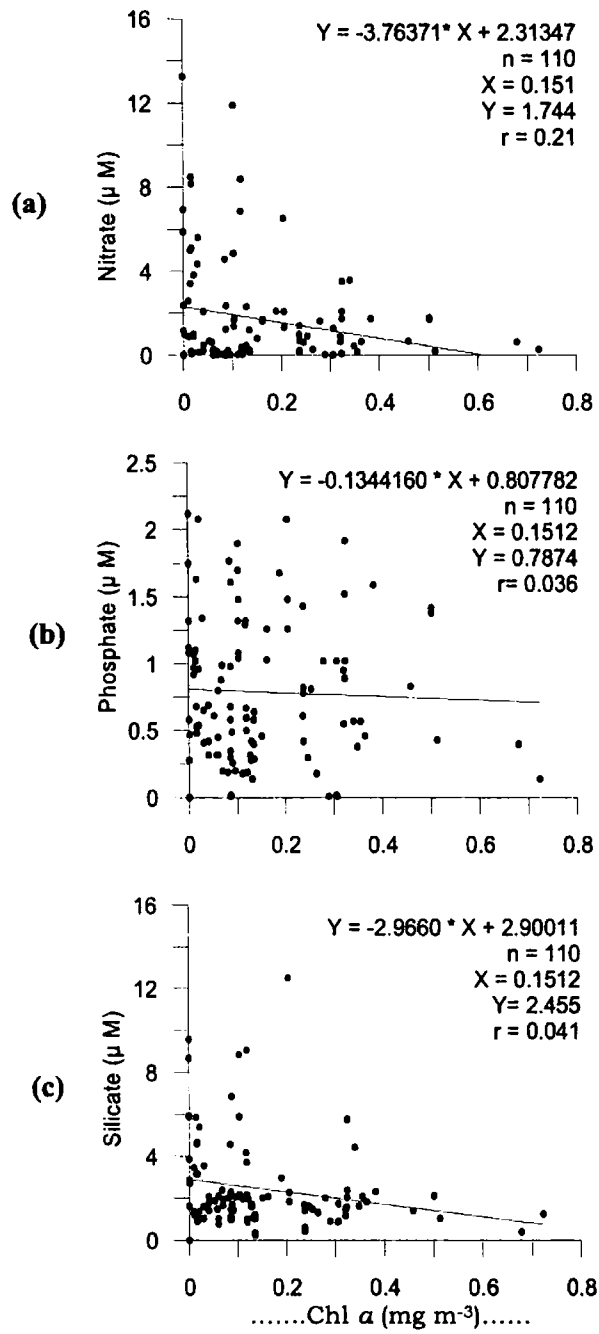


Fig. 4.9. Linear correlation of (a) Chl  $a$  between nitrate (b) phosphate and (c) silicate in the EAS during SIM

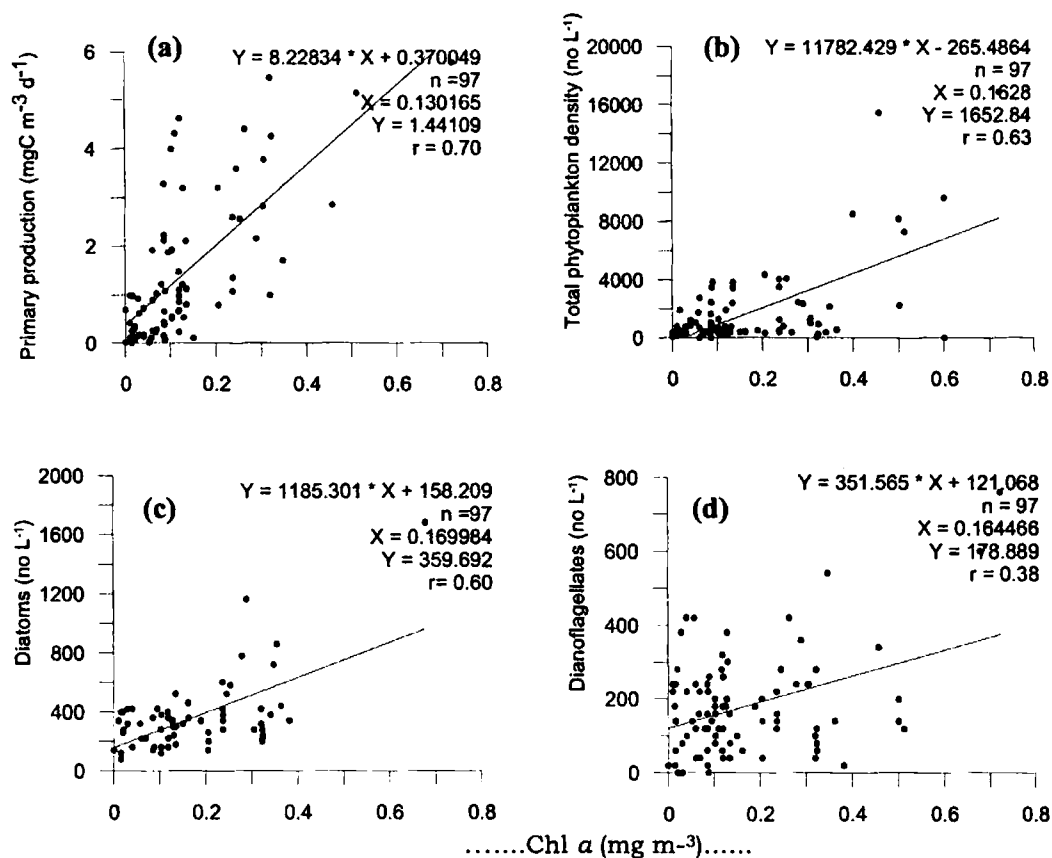


Fig. 4.10. Linear correlation of Chl a between (a) primary productivity (b) total phytoplankton density (c) diatoms and (d) dinoflagellates in the EAS during SIM

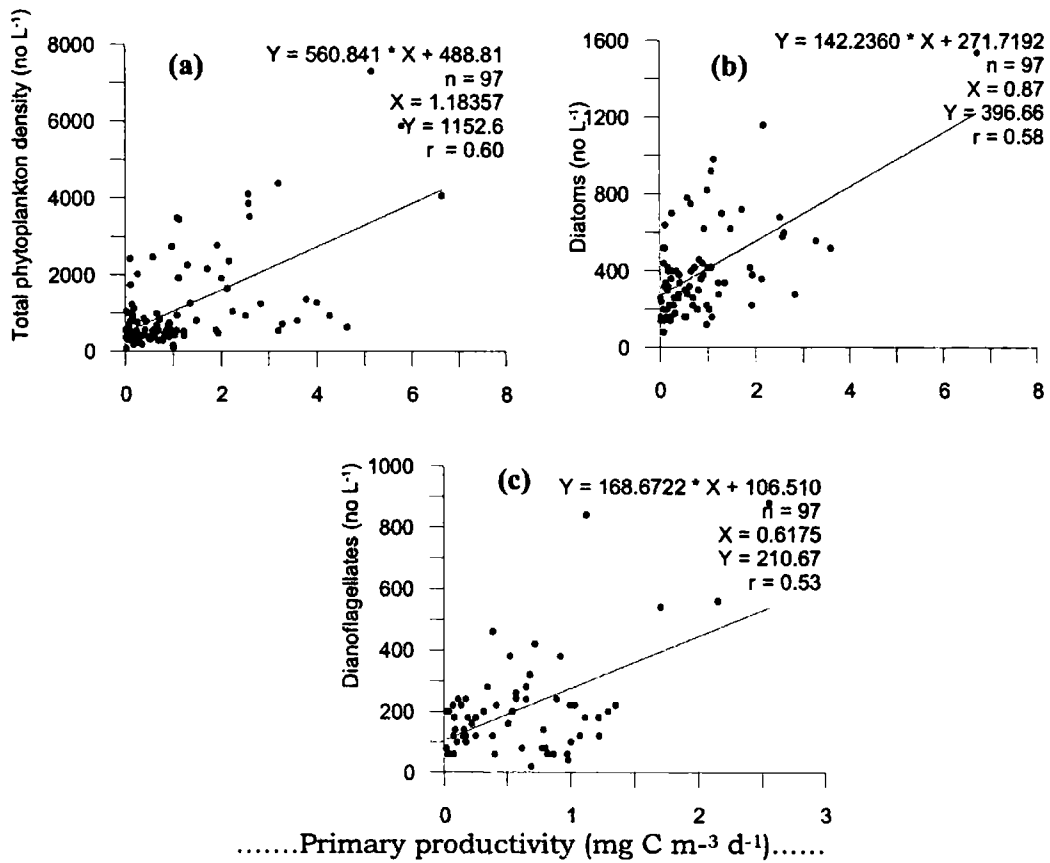


Fig.4.11. Linear correlation of primary productivity between (a) total phytoplankton cell density (b) diatoms and dinoflagellates in the EAS during SIM

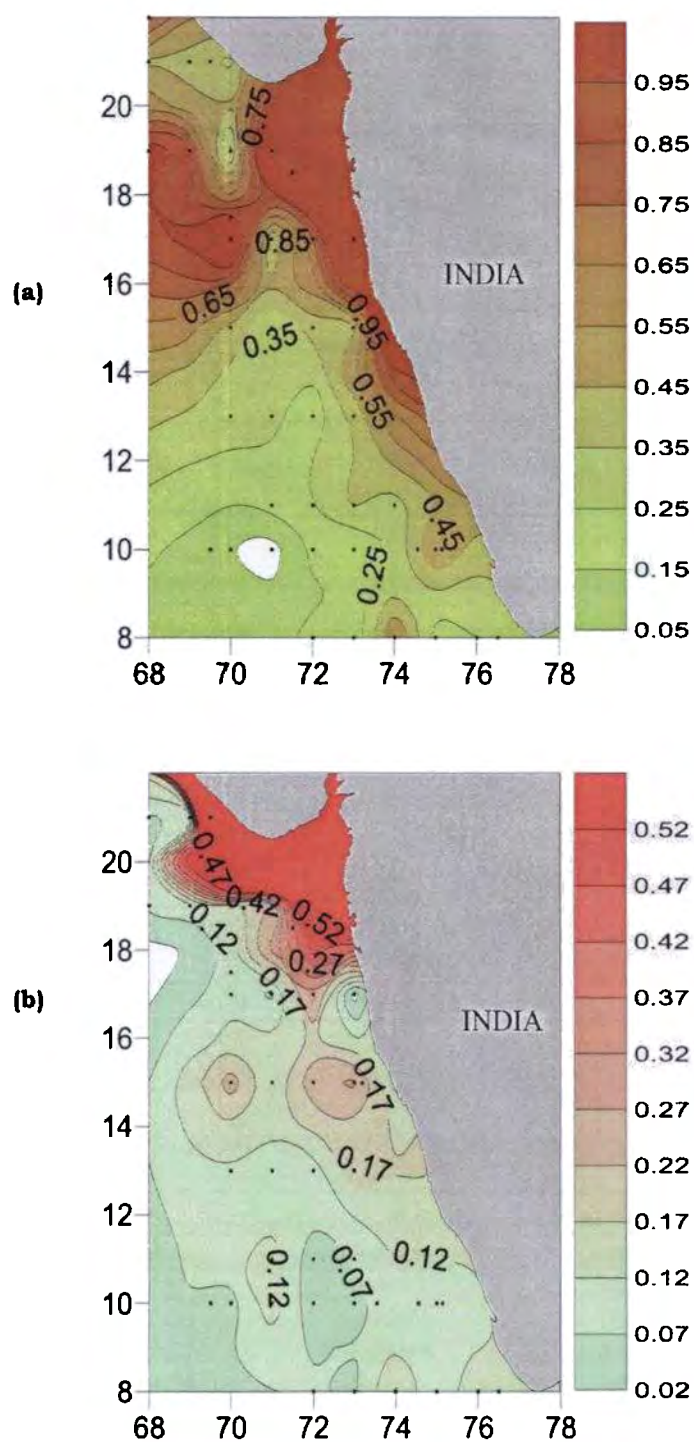


Fig. 4.12. Distribution of Mesozooplankton biomass ( $\text{ml m}^{-3}$ ) in the (a) mixed layer and (b) thermocline layer of EAS during SIM

*Biological responses during spring intermonsoon*

Table 4.1. Primary productivity in the inshore and offshore waters of EAS during SIM

Latitude (°N)	Surface (mg Cm <sup>-3</sup> d <sup>-1</sup> )		Column (mg Cm <sup>-3</sup> d <sup>-1</sup> )	
	Inshore	Offshore	Inshore	Offshore
8	3.3	4.6	68	174
10	5.1	2.0	78	152
11.5	2.2	4.0	296	127
13	6.7	0.6	190	68
15	6.4	3.2	281	124
17	2.9	1.1	181	87
19	2.6	1.0	133	143
21	0.9	0.9	291	62
<b>Average</b>	<b>3.7</b>	<b>2.2</b>	<b>190</b>	<b>117</b>

Table 4.2. Chl *a* in the inshore and offshore waters of EAS during SIM

Latitude (°N)	Surface (mg m <sup>-3</sup> )		Column (mg m <sup>-2</sup> )	
	Inshore	Offshore	Inshore	Offshore
8	0.09	0.12	4.7	10.0
10	0.51	0.02	9.8	14.6
11.5	0.29	0.10	16.8	22.0
13	0.09	0.28	25.7	38.8
15	0.13	0.13	21.3	26.1
17	0.46	0.13	16.5	7.5
19	0.24	0.12	29.5	9.8
21	0.12	0.03	26.1	10.0
<b>Average</b>	<b>0.24</b>	<b>0.12</b>	<b>18.8</b>	<b>17.4</b>

Table 4.3. Total phytoplankton density in the inshore and offshore waters of EAS during SIM

Latitude (°N)	Surface (cells L <sup>-1</sup> )		Column (x 10 <sup>6</sup> cells m <sup>-2</sup> )	
	Inshore	Offshore	Inshore	Offshore
8	770	640	790.5	48.5
10	7300	1920	246.6	122.5
11.5	2360	1280	105.7	73.0
13	2460	2460	141.5	122.3
15	780	540	232.7	110.1
17	15440	3440	309.5	102.3
19	3520	740	260.3	77.7
21	540	540	67.3	36.8
<b>Average</b>	<b>4146</b>	<b>1445</b>	<b>180.3</b>	<b>86.6</b>

*Biological responses during spring intermonsoon*

Table 4.4. Abundance of diatoms, dinoflagellates and blue green algae in the surface water of inshore and offshore waters of EAS during SIM

Latitude (°N)	Inshore (cells l <sup>-1</sup> )			Off shore (cells (cells L <sup>-1</sup> ))		
	Diatoms	Dino	Blue green algae	Diatoms	Dino	Blue green algae
8	560	160	50	380	260	0
10	260	120	6920	180	140	1600
11.5	1160	360	860	120	840	320
13	1540	600	480	780	240	1440
15	240	300	480	340	200	0
17	380	340	14740	980	840	1620
19	600	40	2880	220	40	0
21	360	20	100	620	380	420
<b>Average</b>	<b>638</b>	<b>243</b>	<b>3314</b>	<b>453</b>	<b>368</b>	<b>675</b>

Table 4.5. Abundance of diatoms, dinoflagellates and blue green algae in the upper 120m water column of inshore and offshore waters of EAS during SIM

Latitude (°N)	Inshore (x10 cells <sup>6</sup> m <sup>-2</sup> )			Off shore ( x10 <sup>6</sup> cells m <sup>-2</sup> )		
	Diatoms	Dino	Blue green algae	Diatoms	Dino	Blue green algae
8	64.3	14.2	1.8	30.5	17.9	0
10	28.3	17.6	200.65	25.3	9.7	87.5
11.5	43.3	24.6	37.9	31.5	18.7	23.0
13	31.9	16.8	94.2	52.9	13.85	57.7
15	27.5	42.3	191.6	57.1	28.2	25.3
17	49.5	35.8	226.1	53.8	34.7	13.9
19	49.6	18.9	193.4	48.7	6	0
21	51.9	4.3	2	65.7	24.9	16.1
<b>Average</b>	<b>43.3</b>	<b>21.8</b>	<b>118.5</b>	<b>45.6</b>	<b>19.2</b>	<b>27.9</b>

Table 4.6. Abundance of mesozooplankton in the mixed layer and thermocline layer in the inshore and offshore waters of EAS during SIM

Latitude (°N)	Mixed layer (No m <sup>-3</sup> )		Thermocline layer (No m <sup>-3</sup> )	
	Inshore	Offshore	Inshore	Offshore
8	0.21	0.18	0.14	0.08
10	0.55	0.10	0.11	0.08
11.5	0.31	0.15	0.12	0.08
13	0.39	0.30	0.20	0.11
15	1.29	0.42	0.10	0.24
17	0.76	0.69	0.30	0.15
19	1.62	0.88	0.00	0.10
21	0.11	0.68	1.20	0.11
<b>Average</b>	<b>0.66</b>	<b>0.42</b>	<b>0.27</b>	<b>0.12</b>

Table 4.7. Percentage composition of mesozooplankton in the mixed layer and thermocline layer of EAS during SIM

Mesozooplankton (%)	Depth	
	Mixed Layer	Thermocline layer
Foraminifera	0.11	0.46
Medusa	0.05	0.11
Siphonophore	0.64	0.45
Anthozoa	0.00	0.01
Polychaeta	0.27	0.56
Pteropoda	0.31	0.57
Heteropoda	0.04	0.02
Gatropoda	0.08	0.03
Ostracoda	7.96	7.57
Copepoda	83.83	81.24
Amphipoda	0.26	0.24
Euphausid	0.31	1.24
Decapoda	0.59	0.56
Chaetognatha	4.61	3.77
Copelata	0.01	0.00
Salpa	0.89	2.51
Doliolida	0.06	0.10
Fisheggs	0.09	0.09
Fish larvae	0.08	0.20
Other organisms	0.03	0.03
Mysids	0.02	0.05

### 4.3. Discussion

The spring intermonsoon (SIM) is generally regarded as the oligotrophic season owing to the less phytoplankton production (Jochem, *et al.*, 1993; Mantoura, *et al.*, 1993; Landry, *et al.* 1998; Liu, *et al.*, 1998; Woodward, *et al.*, 1999). SIM, the primary heating season in the Arabian Sea, showed lowest chlorophyll concentration as well

as primary production in the eastern Arabian Sea. This is mainly because, the Arabian Sea being a tropical basin, the biological production is controlled by the availability of nutrients in surface waters when light is not a limiting factor in this season. This was primarily due to the thermal stratification in the upper layer, under the influence of peak insolation together with light winds, which in turn inhibits vertical mixing and upward transport of subsurface nutrients as discussed in the chapter III and there is no source of nutrients from lateral advection (Vimalkumar, *et al.*, 2008). These conditions lead to rapid utilization of available nutrients by phytoplankton in the euphotic zone and eventually which cause the depletion of nutrients in the surface layers.

The physical and chemical data of the present study showed that strong seasonal variability in wind stress determines the dynamics of the upper ocean, which drives the biological responses of the pelagic realm of EAS. The seasonal changes in the wind stress quickly modifies the oceanic circulation, is a unique characteristic of this area. SIM is characterized by weak and variable winds (av.  $\sim 3\text{ m s}^{-1}$ ). Being the primary heating season of the year (Hastenrath and Lamb, 1979), the air temperature increase to more than  $29^{\circ}\text{C}$ . Consequently, during the study period, the SST rose to above  $29^{\circ}\text{C}$ . Joseph (1990) reported this as the Indian Ocean warm pool because it is the warmest area of the world oceans during March-April. During the present study also a warm pool was found in SEAS (between  $8^{\circ}\text{N}$  to  $15^{\circ}\text{N}$ ). In this region, the primary productivity and chlorophyll rates

were low. The MLD remained very shallow (< 30m) in the south. Increased SST, due to increased insolation, combined with weak winds during this season led to the formation of the observed shallow and highly stratified uniform mixed layer. The downwelling and low salinity surface waters provided conditions for the formation of high SST during SIM (Shenoi, *et al.*, 1999). Shenoi, *et al.*, (2005) inferred the circulation pattern based on the spatial patterns of salinity during SIM. Surface circulation revealed the WICC flowing poleward north of 13°N, but equatorward in the south, with a clockwise circulation around Lakshadweep High (Vimalkumar, *et al.*, 2008). The present observations showed that the southeastern Arabian Sea is exhibit different physico-chemical characteristics compared to northeastern region. This is largely due to the formation of warm pool and associated eddies in the Lakshadweep Sea (Bruce, *et al.*, 1994).

The strong stratification acted as a barrier interrupting the input of nutrients to the surface layers during this season. As a result, the surface waters were almost devoid of nutrients (especially nitrate), which makes the area less productive. In the surface waters, nitrate showed the lowest value of 0.01 $\mu$ m in the 8°N and highest (1.24  $\mu$ m) in the 13°N inshore transect. Nitracline was observed at depths greater than 75 m. This condition was earlier reported by Prasanna Kumar, *et al.*, (2000), which is applicable to the entire Arabian Sea, except during summer and winter monsoon. Open ocean circulation at during this period is weak and zonal (Prasanna Kumar, *et al.*, 2000), and there is no source of nutrients from lateral advection was

reported. This nutrient depleted condition ultimately leads to the limiting of phytoplankton production.

There were scanty reports (Bhattathiri, *et al.*, 1996; Vimalkumar, *et al.*, 2008) on biological responses during SIM. In these studies, it was reported that the lowest primary productivity was observed during SIM. Generally, SIM is considered as oligotrophic, evidences of localized high phytoplankton production were reported (Devassy, *et al.*, 1978; Capone, *et al.*, 1998), due to the occurrence of *Trichodesmium* bloom as they absorb atmospheric nitrogen. This phenomenon is evident every year with a marked periodicity from February to April. Bhattathiri, *et al.*, (1996) reported that during SIM the surface primary production varied from 0.7 to 11.9 mgC m<sup>-3</sup>d<sup>-1</sup> in the open ocean stations and from 3.3 to 8.8mgC m<sup>-3</sup>d<sup>-1</sup> in the coastal stations. Column PP was in the range of 193-306 mgC<sup>-2</sup>d<sup>-1</sup>. The results of the IIOE and JGOFS (India) have also showed lowest primary productivity during SIM (Zeitzhel, 1973; Bhattathiri, *et al.*, 1996). The inshore - offshore and north south variation in primary productivity and Chl *a* was minimum during this season except 11.5°N and 13°N. Maximum column productivity during this season (296 mgC m<sup>-2</sup>d<sup>-1</sup>) was recorded in the inshore station of 11.5°N, which was mainly contributed by the *Trichodesmium* abundance. Similarly, 13°N offshore waters showed highest surface productivity (6.73 mgCm<sup>-3</sup>d<sup>-1</sup>). This high primary production is attributed to the ability of *Trichodesmium* to fix atmospheric nitrogen for the abundant growth in the oligotrophic stratified waters. Thus, seasonal variability in primary

productivity of EAS is primarily, driven by variations in water column mixing, as indicated by the depth of the mixed layer (Sathyendranath and Platt, 1994). The relationship between productivity and mixed layer depth, however, is not directly linked each other (McCreary, *et al.*, 1993). Chl *a* values found to be relatively low both in surface (0.18 mg m<sup>-3</sup>) and column (18.0 mgm<sup>-2</sup>) compared to summer monsoon season. The *SeaWiFS* chlorophyll images for the SIM confirmed the prevalence of low concentration of Chl *a* as in the EAS during SIM.

The oligotrophic conditions are a barrier for the abundant growth of phytoplankton, even though localized blooming occurs as a result of the absorption of atmospheric nitrogen by *Trichodesmium*. Abundance of *Trichodesmium erythraeum* is common in this region during SIM (Devassy, *et al.*, 1978; Anoop, *et al.*, 2007). Sawant and Madhupratap (1996) compared the seasonality of phytoplankton in the eastern and central Arabian Sea, and reported the low phytoplankton abundance during SIM season. North eastern Arabian Sea shows different scenario during SIM, higher cell density (15440 cells L<sup>-1</sup>) was recorded in the 17°N transect, where blue green algae dominated in the phytoplankton community. The abundance of phytoplankton in this region is mainly the result of the nutrient replenishment after the winter cooling. The integrated phytoplankton cell density showed an abundance of blue green algae in the inshore stations (65%). The variability in cell density was well correlated with the existence of deep chlorophyll maximum (DCM). Observations demonstrate that the changes in the mixed layer depth significantly

affected the distribution of Chl *a*, and presumably influenced primary productivity by pumping nutrients. Comparatively high Chl *a* values were observed in the specified areas having *Trichodesmium* bloom. It ranged from 0.6 to 0.8 mgm<sup>-3</sup> in the offshore waters of Goa and Mumbai.

Deep chlorophyll maximum (DCM) was common at depths of 50–75 m and it was more prominent in the offshore waters. Savidge and Gilpin (1999) and Gardner, *et al.*, (1999) reported the same condition in the Arabian Sea with >2mgm<sup>-3</sup> below mixed layer depth. Modelling studies by Brock, *et al.*, (1994) suggested that during monsoons, the upper thermocline is extremely light limited, whereas during the inter monsoon periods; the euphotic zone extends well into this region of the water column. This increase in euphotic zone depth is a direct consequence of reduced concentrations of Chl *a* in the mixed layer within waters characterized by near-oligotrophic conditions, and the resulting upper thermocline photosynthesis leads to the development of a deep chlorophyll maximum (DCM). At the end of the SIM, the entire Arabian Sea exhibits such conditions (Brock, *et al.*, 1994). DCM was identified during the SIM of 1987 in the Arabian Sea (Pollehne, *et al.*, 1993). The position of this layer was at the bottom of the euphotic zone but in high nutrients suggested it was a major component of new production and sub-euphotic zone flux. Campbell, *et al.*, (1998) found sub surface maxima in *Prochlorococcus*, *Synechococcus* and Picoeukaryotic algae (green flagellates) during SIM. According to this study, these are most likely the source of the high

Chl *-a* in the formation of DCM. *Prochlorococcus* were probably the largest contributors to the DCM (Veldhuis, *et al.*, 1993) which actually increased with depth in the Arabian Sea (Johnson, *et al.*, 1999). It is noted that in past studies the DCM during SIM was deeper than the detection depth of a satellite sensor (Banse, 1994; Gunderson, *et al.*, 1998) and similar condition existed during the present study, where the DCM is around 50-75 m.

The total mesozooplankton biomass exhibited a significant north-south gradient during SIM. It was high both in mixed layer ( $0.95 \text{ ml m}^{-3}$ ) and thermocline layer ( $0.52 \text{ ml m}^{-3}$ ) in northern region as compared to the southern region ( $0.45 \text{ ml m}^{-3}$  and  $0.12 \text{ ml m}^{-3}$ ) Inshore-offshore gradients in zooplankton distribution was prominent only in the northern region as shown in the Fig. 4.8. It was reported that from February to March, the nutrient availability in the euphotic zone was substantial in the northern region due to winter cooling and convective mixing (de 'Souza, *et al.*, 1996). During SIM, even though the phytoplankton biomass was less, mesozooplankton biomass, consisted mostly of herbivorous copepods (>80%) which sustained its biomass through a partial switch over from feeding on phytoplankton to microbial loop (Madhupratap, *et al.*, 1996). It is now established that these organisms are capable of feeding small organisms such as microzooplankton and bacteria (Christoffersen, *et al.*, 1990; Painting, *et al.*, 1993; Jyothibabu, *et al.*, 2008). Such adaptation in the zooplankton population helps their sustainability during the oligotrophic environment of SIM. The enhanced zooplankton biomass,

higher potential food levels, and possible short food chains suggested active biological modification of the sinking flux in this depth zone.

The correlation between Chl *a* with nutrients, primary productivity and total phytoplankton cell density indicated the influence of the physical processes on biological responses. The correlation between Chl *a* and nutrients (nitrate, phosphate and silicate) was not significant. Significant correlation was obtained between the primary productivity and Chl *a*, and that with total cell density ( $r = 0.70$ ,  $p < 0.01$  and  $r = 0.63$ ,  $p < 0.01$ ). In the group wise correlation, diatoms showed significant correlation with Chl *a* concentration, but the dinoflagellates is not significantly correlated. This difference confirms that the diatoms were the major contributor of Chl *a* during the SIM season. Similar relationship was observed between the primary productivity and phytoplankton groups.

The combination of a wide range of physico-chemical conditions during SIM resulted in variability in biological responses in the EAS. The intense stratification has caused low phytoplankton abundance, standing stock (Chl *a*) and productivity at various trophic levels.

## References

- Anoop, A.K., Krishnakumar, P.K., Rajagopalan, M., 2007. *Trichodesmium erythraeum* (Ehrenberg) bloom along the southwest coast of India (Arabian Sea) and its impact on trace metal concentrations in seawater. *Estuar. Coast. Shelf Sci.*, 71, 641-646.
- Banse, K., 1994. On the coupling of hydrography, phytoplankton, zooplankton and settling organic particles offshore in the Arabian Sea. *Indian Acad. Sci. (Earth Planet. Sci.)*, 103: 125-161.
- Bhattathiri, P.M.A., Pant, A., Sawant, S., Gauns, M., Matondkar, S.G.P. and Mohanraju, R., 1996. Phytoplankton production and chlorophyll distribution in the eastern and central Arabian Sea in 1994-1995. *Curr. Sci.*, Special section: JGOFS (India), 71: 857 - 862.
- Brock, J.C. and McClain, C.R., 1992. Interannual variability in phytoplankton blooms observed in the northwestern Arabian Sea during southwest monsoon. *J. Geophys. Res.*, 97: 733-750.
- Brock, J.C., Sathyendranath, S. and Platt, T., 1994. A Model study of seasonal mixed layer production in the Arabian Sea. *Proc. Indian Acad. Sci. (Earth Planet. Sci.)*, 103: 65-73.
- Bruce, J.G., Johnson, D.R. and Kindle, J.C., 1994. Evidence for eddy formation in the eastern Arabian Sea during the northeast monsoon. *J. Geophys. Res.*, 99: 7651-7664.
- Campbell, L., Landry, M.R., Constatinou, J., Nolla, H.A., Brown, S.L., Liu, H. and Caron, D.A., 1998. Response of microbial community structure to environmental forcing in the Arabian Sea. *Deep Sea Res.* II(45): 2301-2325.
- Capone, D.G., Subramaniam, A., Montoya, J.P., Voss, M., Humborg, C., Johansen, A.M., Seifert, R.L., Carpenter, E.G., 1998. An extensive bloom of the N<sub>2</sub>-fixing cyanobacterium *Trichodesmium Erythraeum* in the central Arabian Sea. *Mar. Ecol. Prog. Ser.*, 172: 281-292.
- Christoffersen, K., Riemann, B., Hansen, L.R., Klysner, A. and Sorensen, H.B., 1990. Qualitative importance of the microbial loop and plankton community structure in a eutrophic lake during a bloom of cyanobacteria. *Microb. Ecol.*, 20: 253-272.
- De Souza, S.N., Dileepkumar, M., Sardesai, S., Sarma, V.V.S.S. and Shirodkar, P.V., 1996. Seasonal variability in oxygen and nutrients in the central and eastern Arabian Sea. *Curr. Sci.*, 71: 847-851.
- Devassy, V.P., Bhattathiri, P.M.A. and Qasim, S.Z., 1978. *Trichodesmium* phenomenon. *Indian J. Mar. Sci.*, 7: 168-186.
- Gardner, W.D., Gundersen, J.S., Richardson, M.J. and Walsh, D.I., 1999. The role of seasonal and diel changes in mixed layer depth on carbon

- and chlorophyll distributions in the Arabian Sea. *Deep Sea Res.* II(46): 1833-1858.
- Gundersen, J.S., Gardiner, W.D., Richardson, M.J. and Walsh, I.D., 1998. Effects of monsoons on the seasonal and spatial distributions of POC and chlorophyll in the Arabian Sea. *Deep Sea Res.* II,45: 2103-2132.
- Hastenrath, S. and Lamb, P.J., 1979. Climatic Atlas of the Indian Ocean. *University of Wisconsin Press. Madison Wisconsin, 97p.*
- Jochem, F.J., Pollehne, F. and Zeitzschel, B., 1993. Productivity regime and phytoplankton size structure in the Arabian Sea. *Deep Sea Res.*, II (40): 711-735.
- Johnson, Z., Landry, M.L., Bidigare, R.R., Brown, S.L., Campbell, L., Gundersen, J., Marra, J. and Trees, C., 1999. Energetics and growth kinetics of a deep *Prochlorococcus* spp. Population in the Arabian Sea. *Deep Sea Res.*, II(46): 1719-1743.
- Joseph, P.V., 1990. Warm pool over the Indian Ocean and monsoon onset. *Tropical Ocean News Letter*, 53: 1-5.
- Jyothibabu, R., Ashadevi, C.R., Madhu, N.V., Sabu, P., Jayalakshmi, K.V., Josia, J., Habeebrehman, H., Prabhakaran, M.P., Balasubrahmanian, T. and Nair, K.K.C. 2008. The response of microzooplankton (20-200µm) to coastal upwelling and summer stratification in the south-eastern Arabian Sea. *Conti. Shelf Sci.*, 28: 653-671.
- Landry, M.R., Brown, S.L., Campbell, S.L., Constantinou, J. and Lui, H., 1998. Spatial patterns in phytoplankton growth and microzooplankton grazing in the Arabian Sea during monsoon forcing. *Deep Sea Res.*, II(45): 2353-2368.
- Liu, H., Campbell, L., Landry, M.R., Nolla, H.A., Brown, S.L. and Constantinou, J., 1998. *Prochlorococcus* and *Synechococcus* growth rates and contributions to production in the Arabian Sea during the 1995 southwest and northeast monsoons. *Deep Sea Res.*, II 45: 2327 - 2352.
- Longhurst, A.R., 1998. Ecological geography of the sea. *Academic Press, New York.* 398p.
- Madhupratap, M., Gopalakrishnan, T.C., Haridas, P., Nair, K.K.C, Aravindakshan, P.N., Padmavati, G. and Shiney Paul, 1996. Lack of seasonal and geographic variation in mesozooplankton biomass in the Arabian Sea and its structure in the mixed layer. *Curr. Sci.*, 71(11): 863-868.
- Mantoura, R.F.C., Law, C.S., Owens, N.J.P., Burkill, P.H., Woodward, E.M.S., Howland, R.J.M. and Llewellyn, C.A., 1993. Nitrogen biogeochemical cycling in the northwestern Indian Ocean. *Deep-Sea Res.* II, 40: 651-671.

- McCreary, J.P., Kundu, P.K. and Molini, R.L., 1993. Numerical investigation of the dynamics, thermodynamics and mixed layer processes in the Indian Ocean. *Prog. Oceanogr.*, 31: 181-244.
- Niiler, P.P., 1977. One dimensional models of the seasonal thermocline. In: *The Sea* (Goldberg, E.D (Ed.), pp: 97-115.
- Painting, S.J., Moloney, C.L. and Lucas, M.I., 1993. Simulation and field measurements of phytoplankton - bacteria-zooplankton interactions in the southern Benguela upwelling region. *Mar. Ecol. Prog. Ser.*, 100: 55-69.
- Pollehne, F., Klein, B. and Zeitschel, B., 1993. Low light adaptation and export production in the deep chlorophyll maximum layer in the northern Indian Ocean. *Deep Sea Res. I*, 40: 737-752.
- Prasanna Kumar, S., Madhupratap, M., Dileep Kumar, M., Gauns, M., Muraleedharan, P.M., Sarma, V.V.S.S. and De Souza, S.N., 2000. Physical control of primary productivity on seasonal scale in central and eastern Arabian Sea. *Proc. Indian Acad. Sci., (Earth Planet. Sci.)*, 109(4): 433-442.
- Sathyendranath, S. and Platt, T., 1994. New production and mixed layer physics. *Proc. Indian Acad. Sci. (Earth Planet. Sci.)*, 103: 177-188.
- Savidge, G. and Gilpin, L., 1999. Seasonal influences on the size - fractionated chlorophyll *a* concentrations and primary production in the north-west Indian Ocean. *Deep Sea Res.*, II (46): 701-724.
- Sawant, S. and Madhupratap, M., 1996. Seasonality of phytoplankton in the Arabian Sea. *Curr. Sci.*, 71(11): 869-873.
- Shenoi, S.S.C., Shankar, D. and Shetye, S.R., 1999. On the sea surface temperature high in the Lakshadweep Sea before the onset of the southwest monsoon. *J. Geophys. Res.*, 104:15703-15712, doi: 0.1029/1998JC900080.
- Shenoi, S.S.C., Shankar, D., Michael, G.S., Kurian, J., Varma, K.K., Ramesh Kumar, M.R., Almeida, A.M., Unnikrishnan, A.S., Fernandes, W., Barreto, N., Gnanaseelan, C., Mathew, R., Praju, K.V. and Mahale, V., 2005. Hydrography and water masses in the Southeastern Arabian Sea during March-June 2003. *J. Earth System Sci.*, 114(5): 475-491.
- Veldhuis, M.J.W., Kray, G.W. and Gieskas, W.W.C., 1993. Growth and fluorescence characteristics of ultraplankton on a north-south transect in the eastern North Atlantic. *Deep Sea Res.*, II(40): 609-626.
- Vimalkumar, K.G., Dineshkumar, P.K., Smitha, B.R., Habeebrehman, H., Josia, J., Muraleedharan, K.R., Sanjeevan, V.N. and Achuthankutty, C.T., 2008. Hydrographic characterization of southeast Arabian Sea during the wane of southwest monsoon and spring inter monsoon. *Environ. Monit. Assess.*, 140: 231-247.

- Wishner, K.F., Marcia, M.G. and Celia, G., 1998. Mesozooplankton biomass in the upper 1000m in the Arabian Sea: Overall seasonal and geographic patterns, and relationship to oxygen gradients. *Deep Sea Res.*, II: 45(10-11): 2405-2432.
- Woodward, E.M.S., Rees, A.P. and Stephens, J.A., 1999. The influence of the south-west monsoon upon the nutrient biogeochemistry of the Arabian Sea. *Deep Sea Res.*, II(46): 571-591.
- Zeitschel, B., (Ed.), 1973. *The Biology of Indian Ocean*. Springer Verlag, 549p.

## Biological responses to upwelling events during different phases of summer monsoon

---

5.1. Introduction  
5.2. Results  
5.2.1. Onset of summer monsoon  
5.2.2. Peak summer monsoon  
5.2.3. Late summer monsoon  
5.2.4. Satellite chlorophyll imagery  
5.2.5. Pelagic fish landings  
5.3. Discussion  
References

---

### 5.1. Introduction

Arabian Sea is an ideal region for studying monsoon driven tropical ocean dynamics, characterized by regular seasonal oscillations in biological activities. During summer monsoon, upwelling along the southwest coast of India results in high biological productivity (Qasim, 1982; Banse, 1987; Prasanna Kumar, *et al.*, 2001; Madhu, 2004), making the Arabian Sea one of the most productive areas in the world (Gardner, *et al.*, 1999; Wiggert, *et al.*, 2005). An upwelling zone exhibits both short-term and long-term temporal changes in nutrient uptake, productivity rates and community structure of phytoplankton in response to the rapid changes in nutrient fields. Such oscillations in biological productivity, influenced by upwelling events are the characteristic feature of these zones. During SIM, the surface layers of the Arabian Sea was nutrient depleted while during summer, phytoplankton growth has been

derived from the upwelling events. The primary forcing mechanism that affects the upwelling along the Arabian Sea during summer is wind stress and its spatial and temporal variability. The upwelling processes bring nutrient rich cold subsurface water into the euphotic zone (Sastry and D'Souza, 1972) and a threefold increase of nitrate in the upwelled waters was reported compared to the surrounding area (Mantora, *et al.*, 1993). As a consequence of this enrichment, high productivity occurs in the Arabian Sea during the season.

The upwelling phenomenon is characterized by three sequential stages: (1) the upwelling phase, when the cold nutrient-rich waters well up (Type-1), (2) the productive phase or mature phase, when a superficial heating occurs, accompanied by an increase in biomass and primary production and the simultaneous decrease in nutrient concentration (Type-2) and (3) the downwelling phase or relaxing phase leading to an oligotrophic situation as a consequence of decrease in phytoplankton biomass due to the dispersion and nutrient depletion (Type-3) (Barlow, 1982; Rodriguez *et al.*, 1992). The cycling of these three phases is strongly influenced by local winds (Banse, 1968; Halpern, 1976; Barton *et al.*, 1977; Nair *et al.*, 1989). Several studies have been carried out on temporal and spatial variations of primary productivity and phytoplankton biomass in the Arabian Sea (Qasim, 1977; Radhakrishna, *et al.*, 1978; Qasim, 1982; Banse, 1987; Bhattathiri, *et al.*, 1996; Prasanna Kumar, *et al.*, 2000, 2001; Madhu, 2004; Roy, *et al.*, 2006). Coastal upwelling in the Arabian Sea is an annual phenomenon occurring during summer monsoon (Banse,

1968; Sankaranarayanan, *et al.*, 1978). However, its propagation and influences on biological responses during different stages remains scanty. Moreover, the importance of the upwelling area cannot be underestimated considering the fact that about 20% of the world fish catch comes from the 0.1% of the upwelling zones (Ryther, 1969). This pattern is duplicated along the west coast of India where the maximum fish catches are obtained during or immediately after the upwelling season, which clearly indicates the significance of monsoon influenced coastal upwelling in the Indian economy.

In this chapter, the changes in Chl *a*, phytoplankton cell density, primary productivity, mesozooplankton standing stock and fish landing status were investigated during different phases of upwelling in relation to the prevailing environmental changes in the eastern Arabian Sea.

## **5.2. Results**

### **5.2.1. Onset of Summer Monsoon (OSM)**

#### ***(a) Primary productivity***

During OSM, the surface primary productivity (Fig. 5.1a & b) varied from 1.9 to 5.5 mgC m<sup>-3</sup>d<sup>-1</sup> (av. 3.8±1.7 mgC m<sup>-3</sup>d<sup>-1</sup>) at the offshore stations and 4.4 to 13.5 mgC m<sup>-3</sup>d<sup>-1</sup> (av. 8.8±3.4 mgC m<sup>-3</sup>d<sup>-1</sup>) along inshore stations. Integrated column production for the euphotic zone varied from 143 to 268 mg C mg<sup>-2</sup>d<sup>-1</sup> (av. 211±42 mgC m<sup>-2</sup>d<sup>-1</sup>) at the offshore stations and from 218 to 452 mgC m<sup>-2</sup>d<sup>-1</sup> (av. 301±96 mgC m<sup>-2</sup>d<sup>-1</sup>) at the inshore stations (Table 5.1). Compared to other

Biological responses to upwelling events in the different phases of summer monsoon

transects, off Kochi (10°N) recorded the maximum primary production (452 mgC m<sup>-2</sup>d<sup>-1</sup>). Vertical distribution of primary production in the inshore- offshore waters is shown in the Fig. 5.2. Most of the inshore waters showed primary productivity maxima at the surface waters but offshore stations and some inshore station (15°N) transects exhibited maximum primary productivity between the depths of 10- 50m.

**(b) Chlorophyll a**

Latitudinal distribution of Chl a (Fig. 5.1c & d) shows that inshore waters off Kochi (10°N) recorded maximum Chl a (24.9 mgm<sup>-2</sup>) compared to other transects. The vertical distribution of Chl a concentration is represented in the Fig. 5.3. and it showed more or less similar trend as of primary productivity. Along the inshore waters subsurface Chl a maximum was observed at a depth of 10-20m depth at 10°N stations. Along the offshore stations SCM was observed slightly deeper depths (20-50m). The concentration of surface Chl a ranged from 0.2 to 0.42 mg m<sup>-3</sup> (av. 0.27 ± 0.08 mgm<sup>-3</sup>) in the inshore and 0.10 to 0.24 mgm<sup>-3</sup> (av. 0.18±0.06 mgm<sup>-3</sup>) in the offshore waters. The variation in the Chl a in the euphotic column was between 15.9 and 24.9 mgm<sup>-2</sup> (av. 19.5±4.3 mgm<sup>-2</sup>) and between 12.9 and 33.3 mgm<sup>-2</sup> (av. 23.0±7.1 mgm<sup>-2</sup>) in the inshore and offshore waters, respectively (Table 5.2).

**(c) Phytoplankton abundance**

The vertical distribution of diatoms, dinoflagellates, blue green algae and green flagellates is depicted in Fig. 5.4a & b. The total

Biological responses to upwelling events in the different phases of summer monsoon

phytoplankton density along the inshore and offshore surface waters was in the range of 900 to 22800 cells L<sup>-1</sup> (av. 7326 cells L<sup>-1</sup>) 5560 to 27520 cells L<sup>-1</sup> (av. 11320 cells L<sup>-1</sup>), respectively. The corresponding integrated total phytoplankton density in the 120m water column were 89.65 x 10<sup>6</sup> to 744.82 x 10<sup>6</sup> cells m<sup>-2</sup> (av. 320.84 x 10<sup>6</sup> cells m<sup>-2</sup>) in the inshore waters and 103.64 to 498.52 cells m<sup>-2</sup> (233.78 x 10<sup>6</sup> cells m<sup>-2</sup>) in the offshore waters, respectively (Table 5.3). Maximum phytoplankton cell density were observed in the (surface 22800 cells L<sup>-1</sup>, column 744.82 x 10<sup>6</sup> cells m<sup>-2</sup>) at the inshore waters off Kochi (10°N) transects (Fig. 5.5). The abundance of diatoms, dinoflagellates and blue green algae in the surface and column were given in the Tables 5.4 & 5.5 respectively.

Along the inshore waters diatoms contributed 38.8% of the total phytoplankton density, followed by dinoflagellates (29.5%) and blue green algae (28.8%). Along the offshore waters, diatoms contributed 38.4%, followed by blue green algae (37.1%) and dinoflagellates (23.4%). The contribution of green flagellates in the inshore and offshore waters was 2.6% and 0.9% respectively (Fig. 5.6). Green flagellates were present only in the inshore stations of southern region. Distribution of diatoms, dinoflagellates, blue green algae and green flagellates in the surface and the 120 m water column along the inshore-offshore stations of each transect is given in the Fig. 5.5. *Trichodesmium erythraeum* (blue green algae) was commonly observed during this season through out the study area with varying densities.

**(d) Mesozooplankton biomass**

During OSM, the mesozooplankton biomass in the mixed layer ranged between 0.12 to 0.74  $\text{mlm}^{-3}$  (av. 0.35  $\text{mlm}^{-3}$ ) in the inshore and 0.11 to 0.21 (av. 0.17  $\text{mlm}^{-3}$ ) in the offshore waters. (Table 5.6). In the thermocline layer, mesozooplankton biomass was found to be less (0.02 to 0.16  $\text{mlm}^{-3}$ ) with an average of 0.06  $\text{mlm}^{-3}$ . Relatively higher mesozooplankton biomass was observed in the southern transects (8-11.5°N) both in mixed layer and thermocline layer (Fig.5.7). Copepod was the dominant zooplankton group (av. 83.8%) both in mixed layer and thermocline layer followed by ostracods (av.7.9%), chaetognaths (av. 4.6%), and siphonophores (av. 0.64%) (Table 5.7). Abundance of zooplankton observed in the newly upwelled waters of 8°N to 10°N transects, where primary productivity, Chl *a* and phytoplankton abundance were relatively higher than other transects. The distribution of fish larvae in the mixed layer and thermocline in the inshore and offshore waters is given in Fig. 5.8. Relatively higher abundance (4.5 ind.  $\text{m}^{-3}$ ) of fish larvae observed in the mixed layer off 10°N transect. In the thermocline layer abundance of fish larvae was in the range 0.05 to 0.55 ind.  $\text{m}^{-3}$ .

Linear correlation of Chl *a* between nutrients such as nitrate, phosphate and silicate is given in the Fig. 5.9. Chl *a* showed significant linear correlation to primary productivity ( $r = 0.74$ ), total phytoplankton cells ( $r = 0.65$ ), diatoms ( $r = 0.69$ ), dinoflagellates ( $r = 0.50$ ), and blue green algae ( $r = 0.18$ ) (Fig. 5.10). Similarly, primary productivity also showed significant linear correlation (Fig. 5.11) with

Biological responses to upwelling events in the different phases of summer monsoon

total phytoplankton density ( $r = 0.65$ ), diatoms ( $r = 0.61$ ) and dinoflagellates ( $r = 0.60$ ).

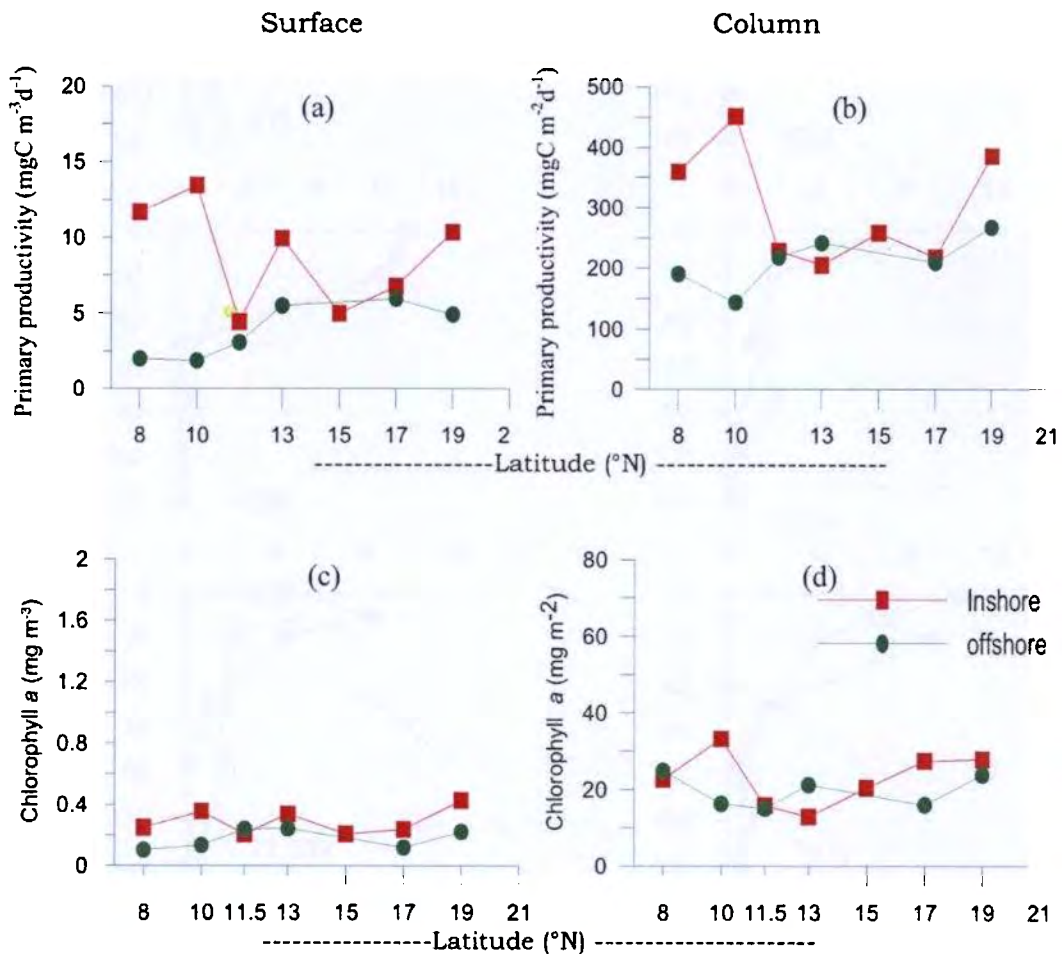


Fig.5.1. Distribution of primary productivity (a & b) and Chl *a* (c & d) in the inshore and offshore waters of EAS during OSM

*Biological responses to upwelling events in the different phases of summer monsoon*

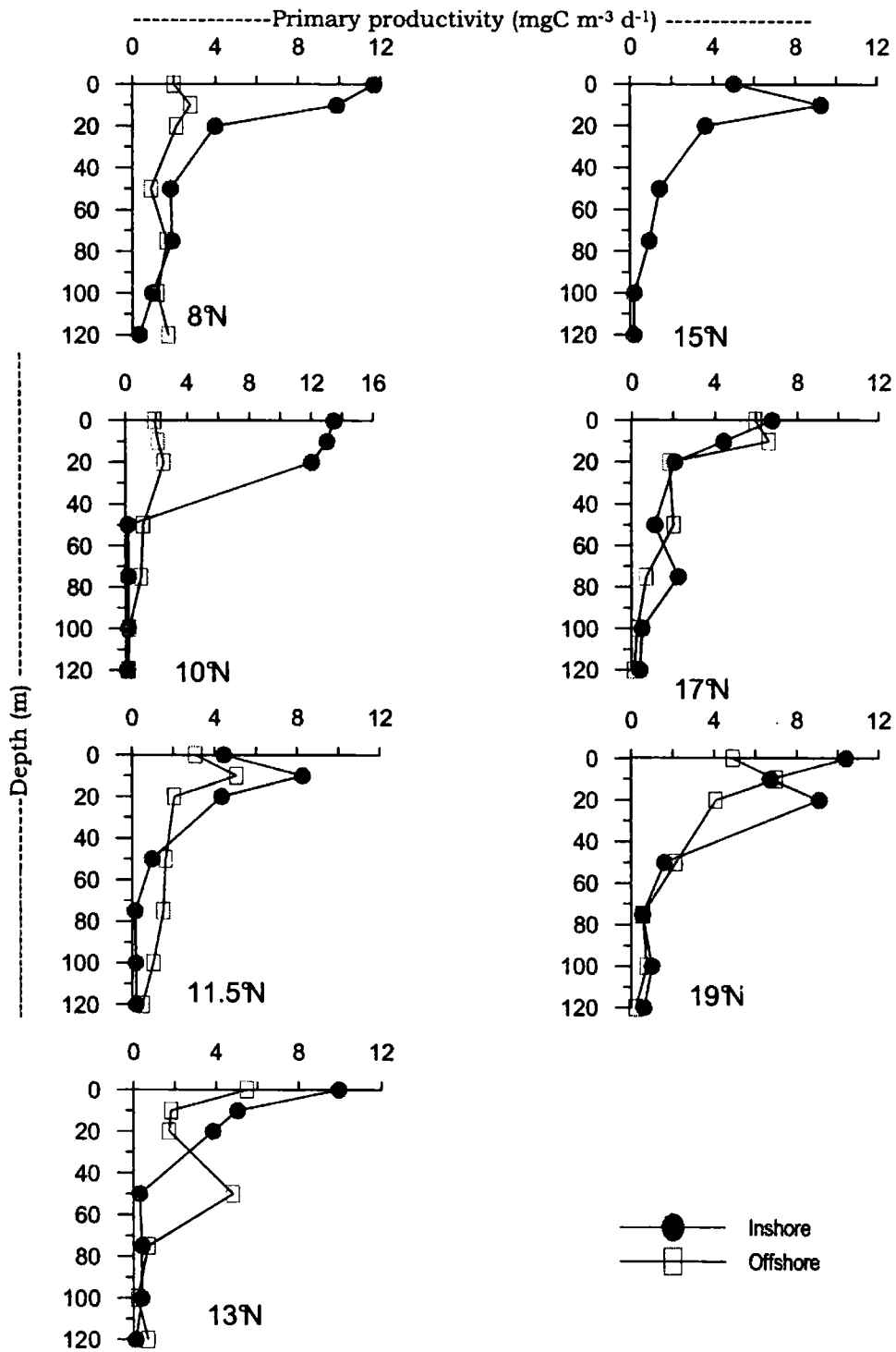


Fig.5.2. Vertical distribution of primary productivity (mgC m<sup>-3</sup>d<sup>-1</sup>) in the inshore and offshore waters of EAS during OSM

*Biological responses to upwelling events in the different phases of summer monsoon*

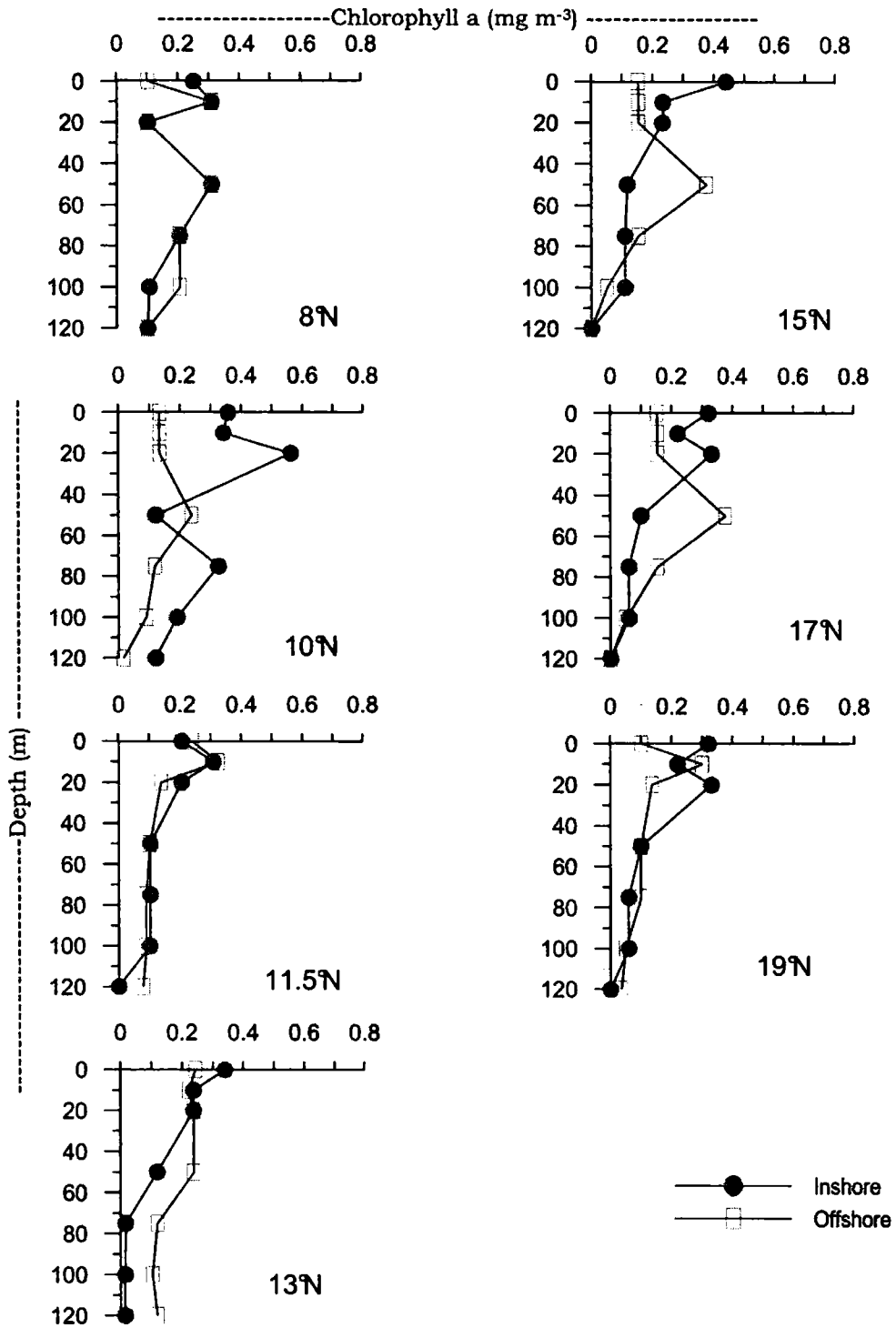


Fig. 5.3. Vertical distribution of Chl *a* (mg m<sup>-3</sup>) in the inshore and offshore waters of EAS during OSM

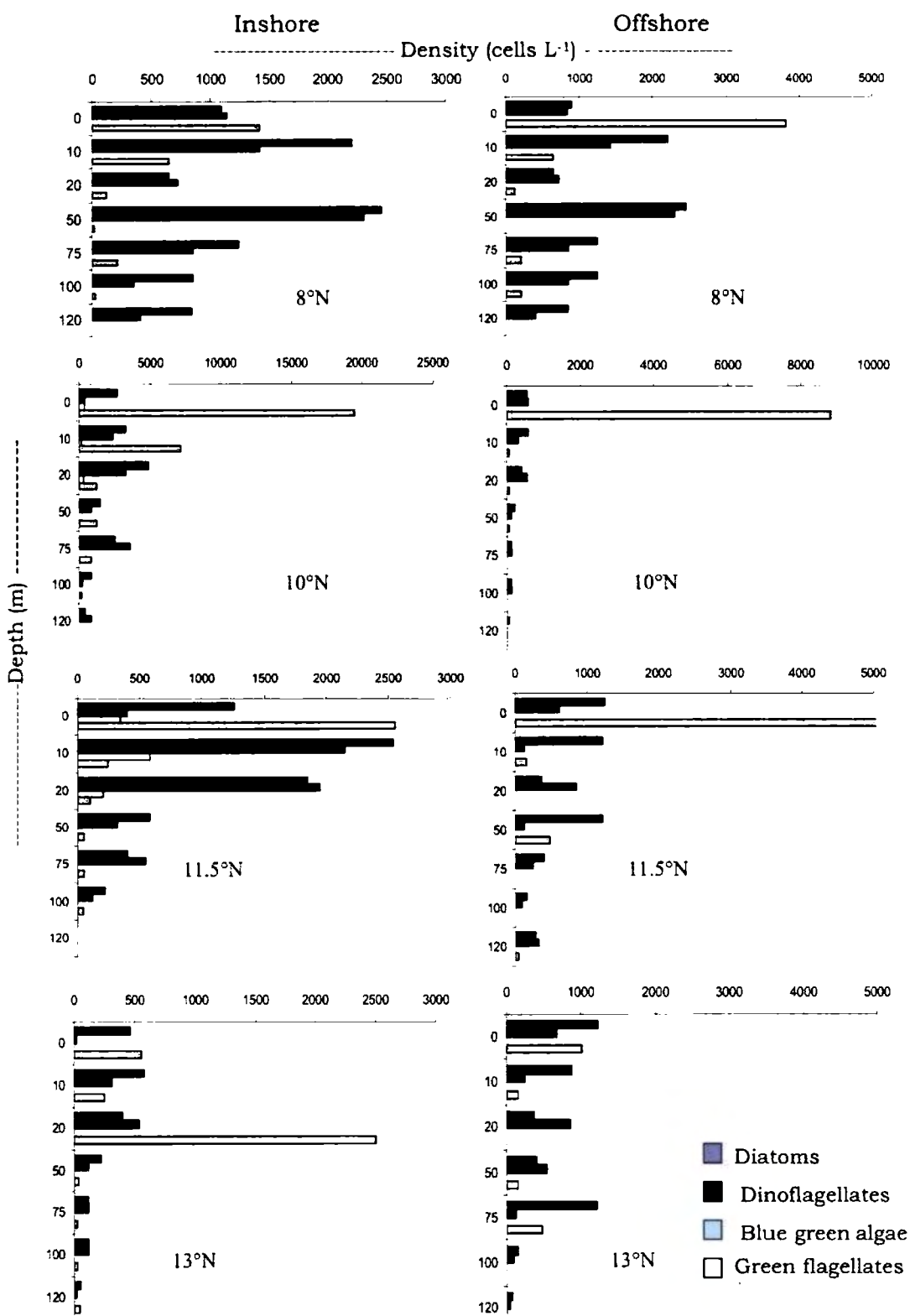


Fig.5.4a. Vertical distribution of phytoplankton density in the inshore and offshore waters of EAS during OSM

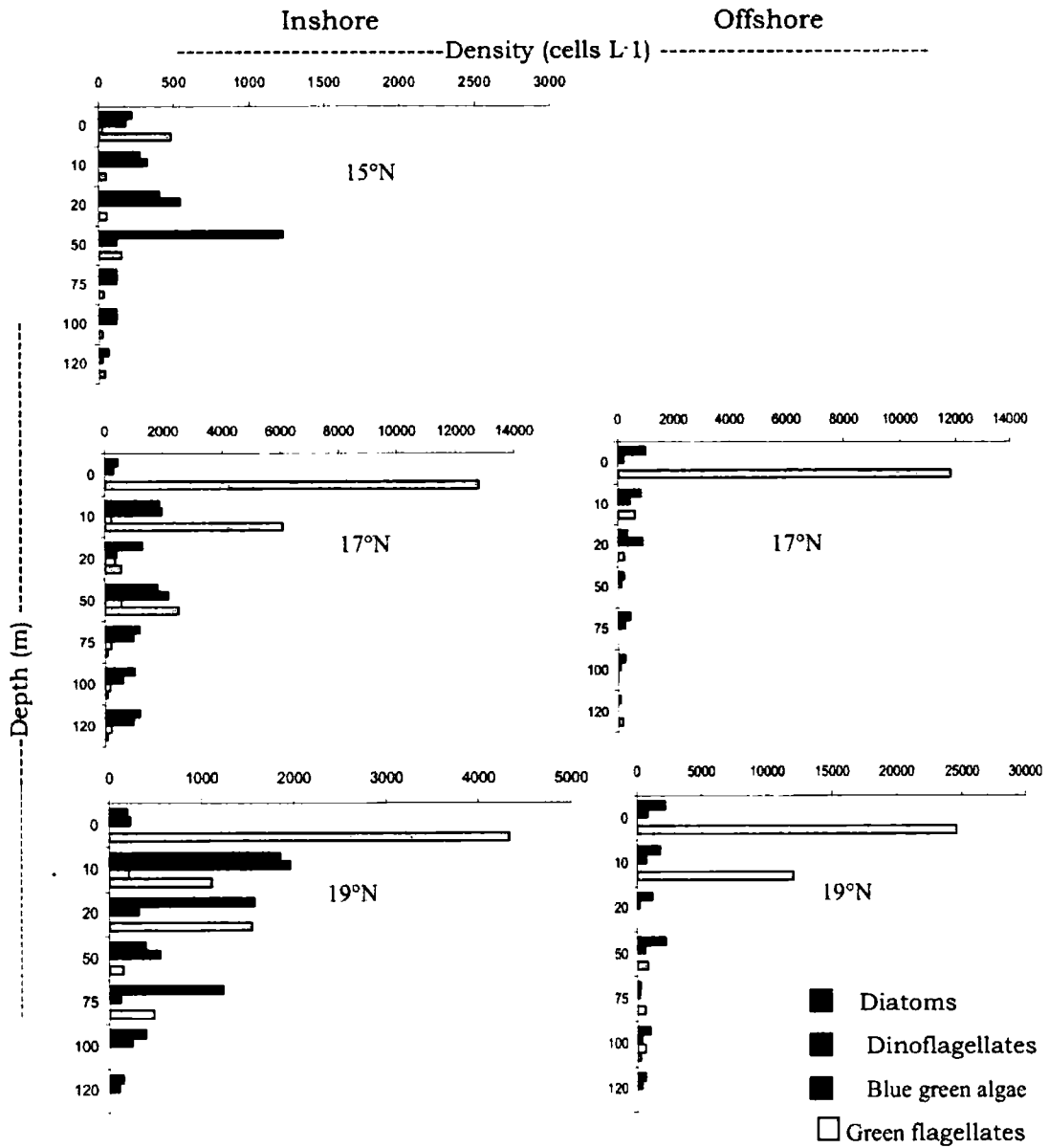


Fig. 5.4b. Vertical distribution of phytoplankton density in the inshore and offshore waters of EAS during OSM

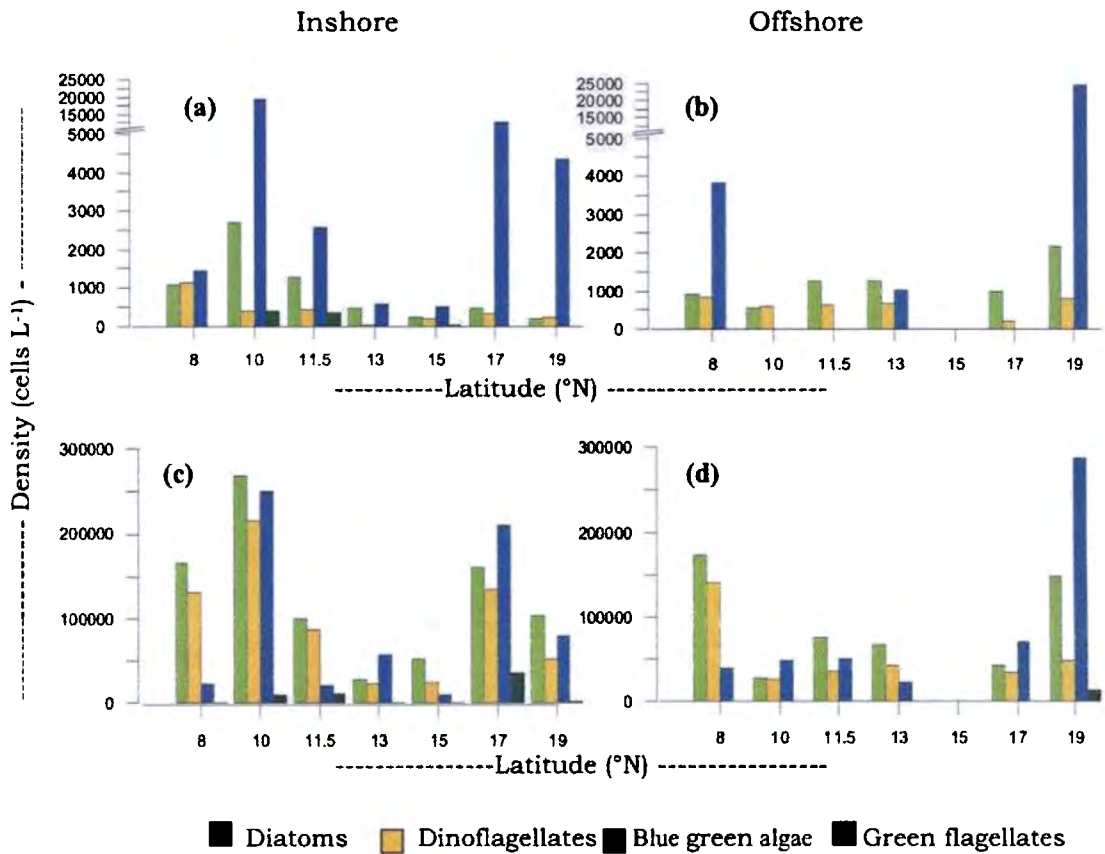


Fig.5.5. Distribution of phytoplankton density in the (a &b) surface and (c & d) 120 water column in the inshore and offshore waters of EAS during OSM

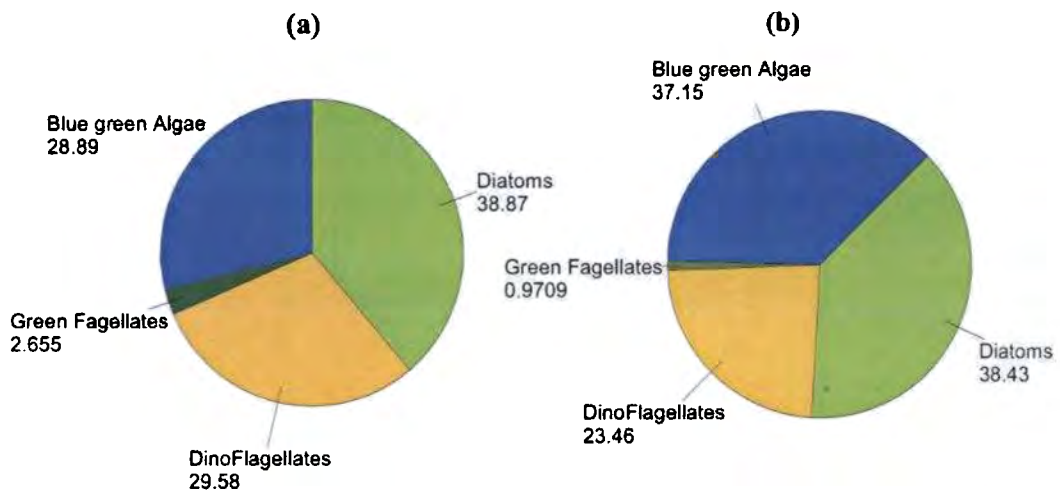


Fig. 5.6. Percentage (%) composition of total phytoplankton density in the (a) inshore and (b) offshore waters of EAS during OSM

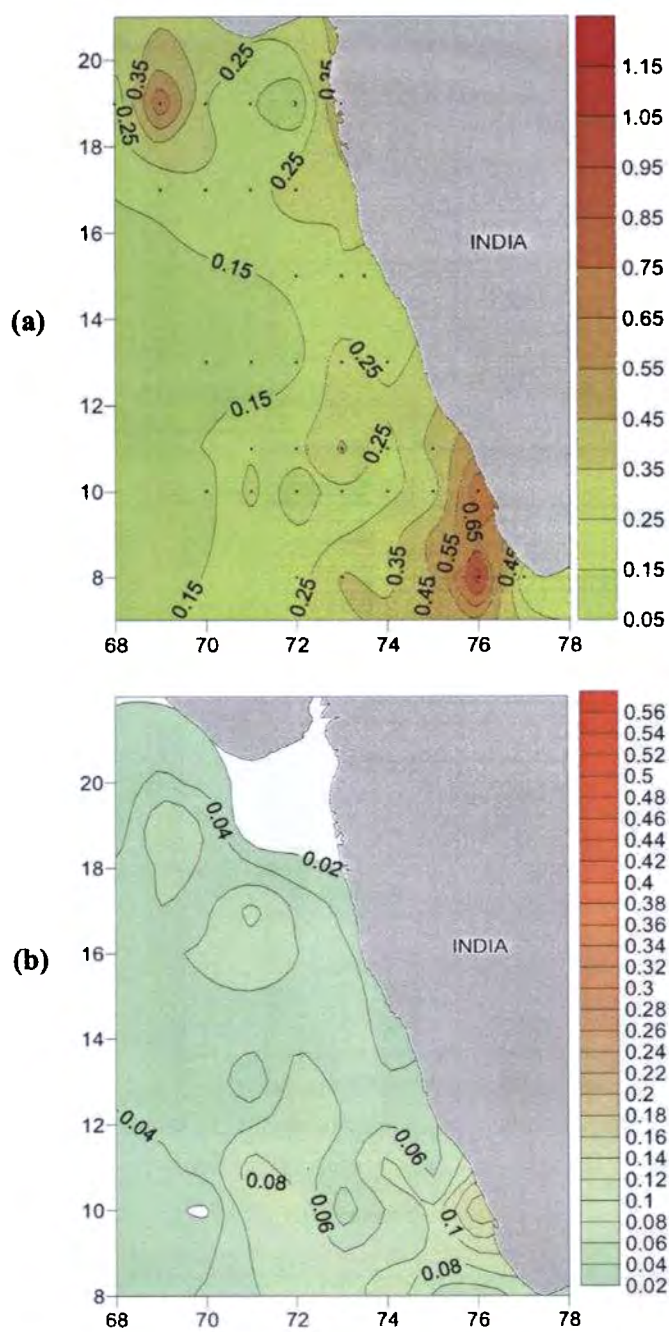


Fig. 5.7. Distribution of mesozooplankton biomass ( $\text{ml m}^{-3}$ ) in the (a) mixed layer and (b) thermocline layer of EAS during OSM

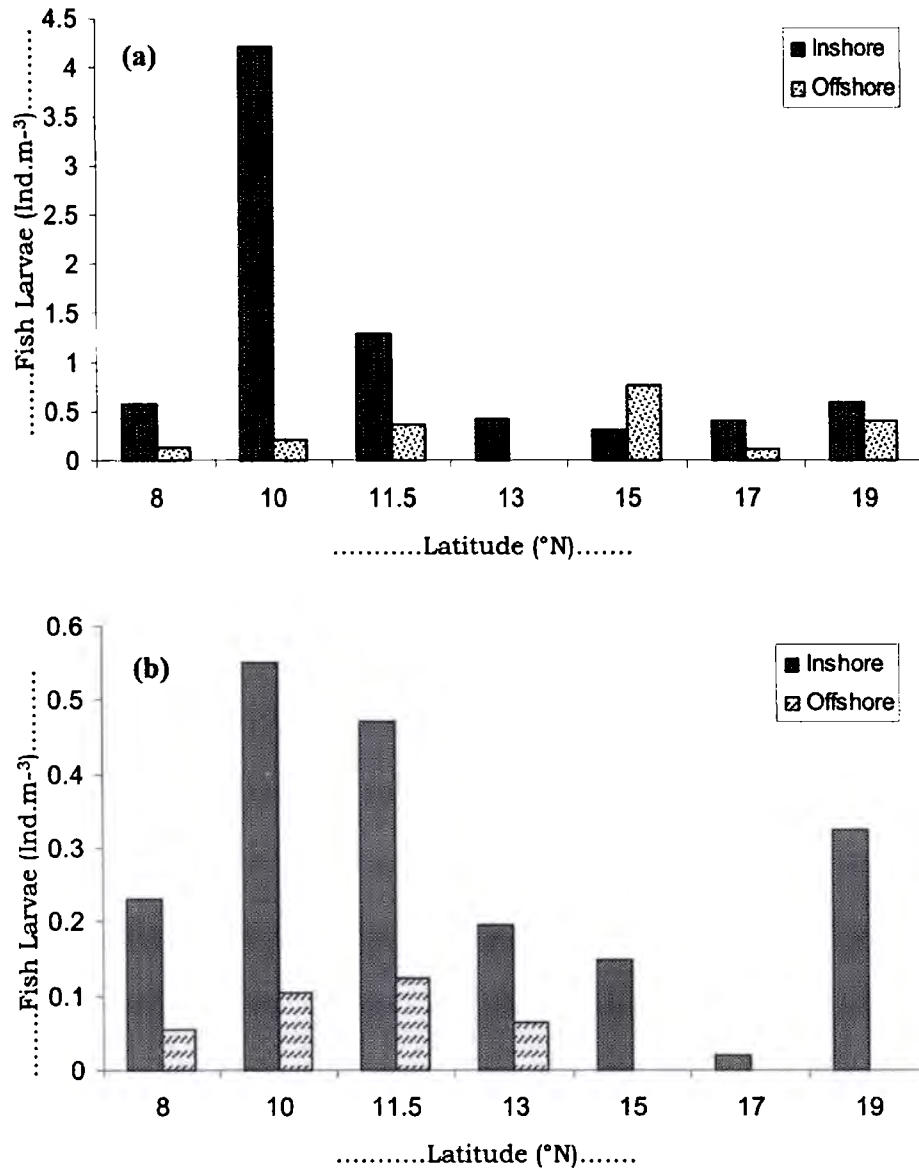


Fig. 5.8. Distribution of fish larvae (ind. m<sup>-3</sup>) in the (a) mixed layer and (b) thermocline layer of EAS during OSM

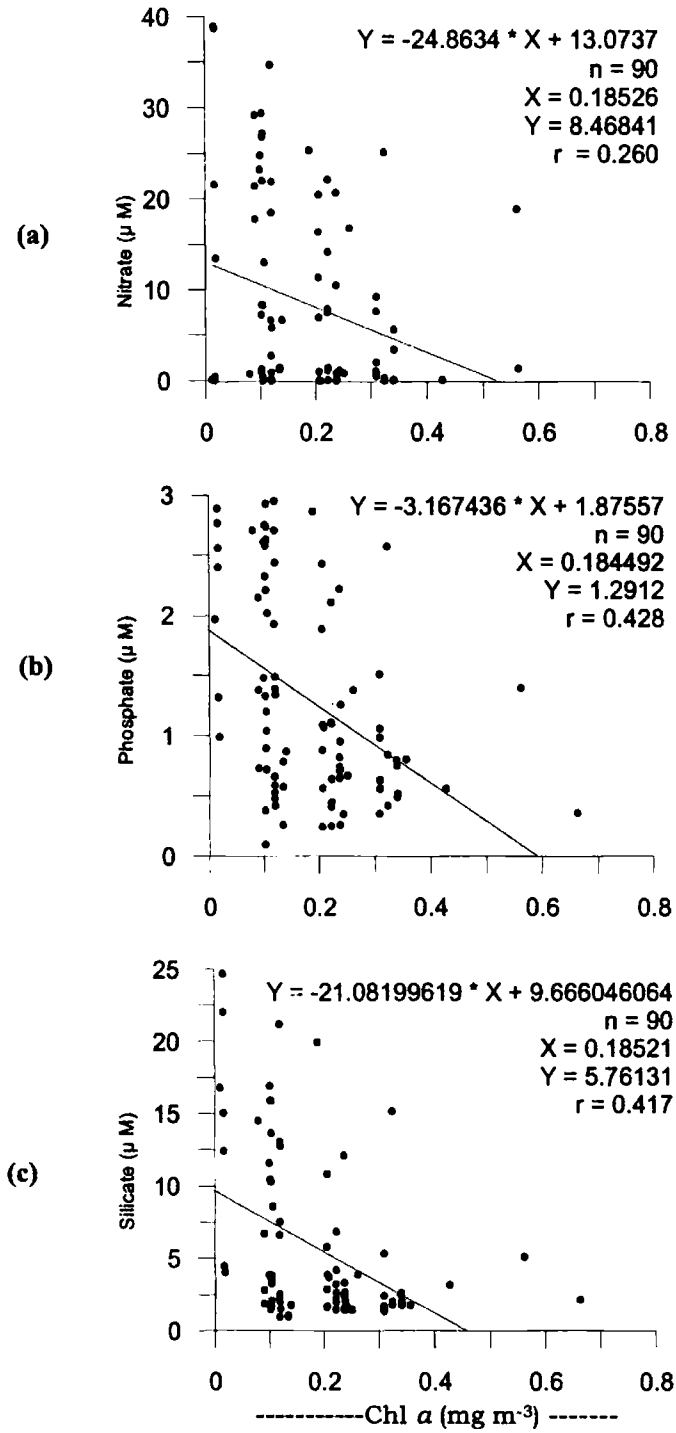


Fig. 5.9. Linear correlation Chl a between (a) nitrate (b) phosphate and (c) silicate during OSM

*Biological responses to upwelling events in the different phases of summer monsoon*

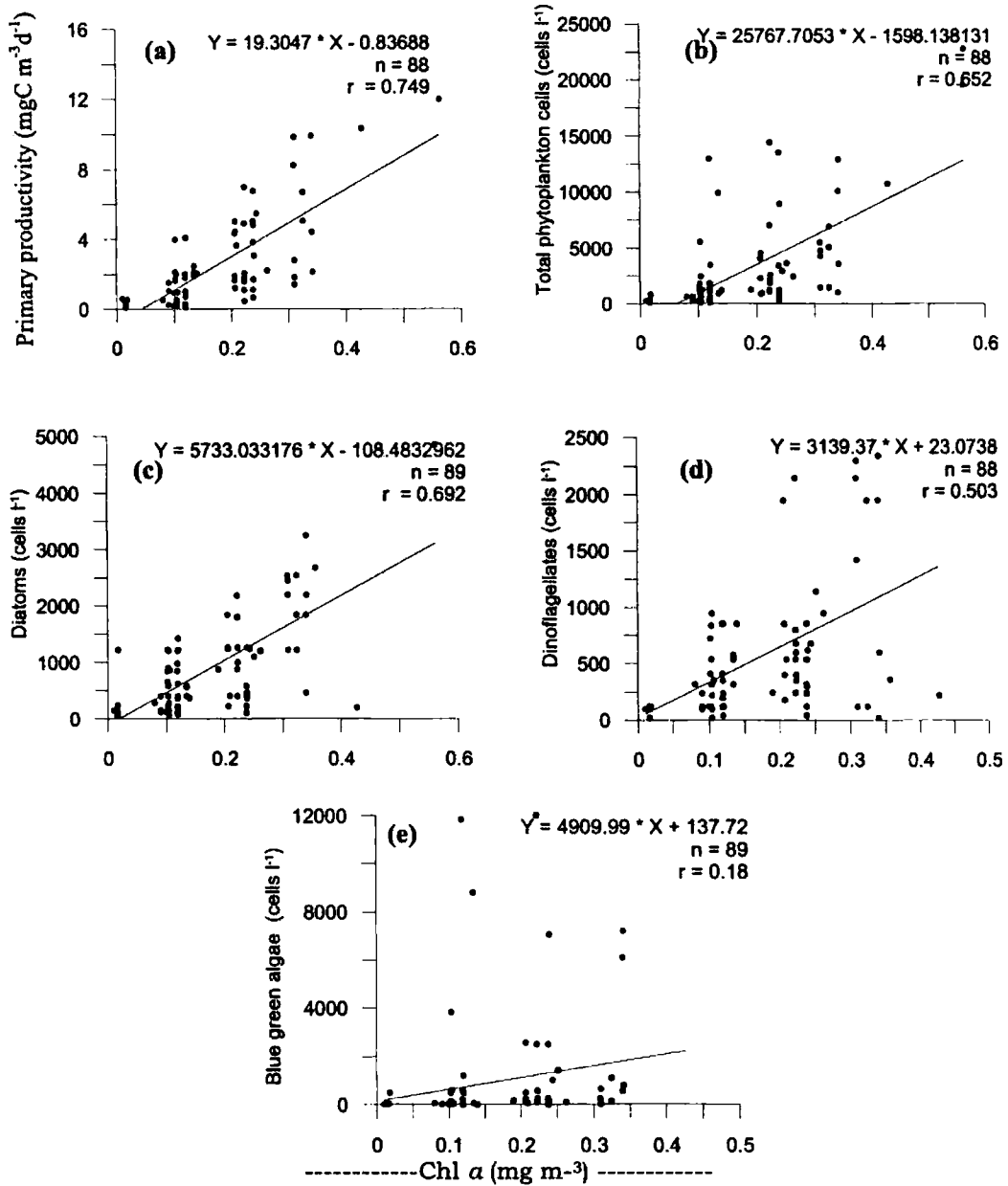


Fig. 5.10. Linear correlation of Chl *a* between (a) primary productivity (b) total phytoplankton density (c) diatom abundance (d) dinoflagellates abundance and (e) blue green algae abundance in the EAS during OSM

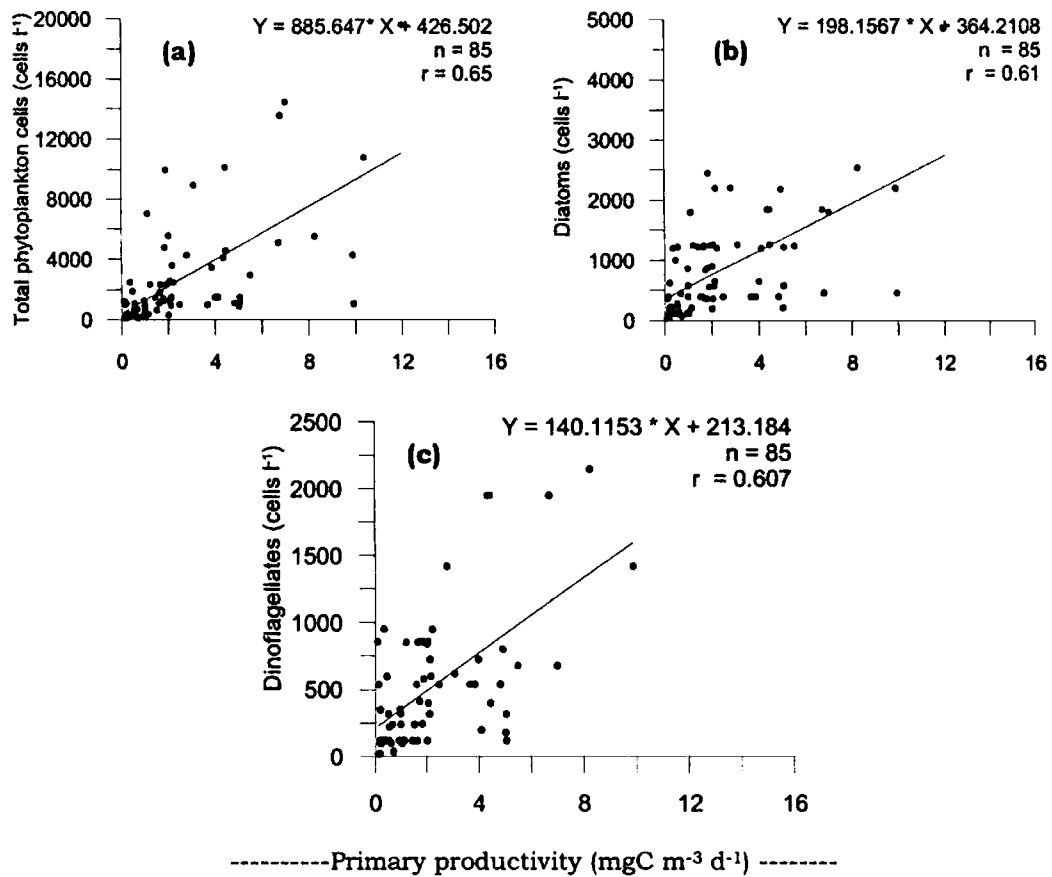


Fig. 5.11. Linear correlation of primary productivity between (a) total phytoplankton density (b) diatom abundance and (c) dinoflagellates abundance during OSM

Table 5.1. Primary productivity in the inshore and offshore waters of EAS during OSM

Latitude (°N)	Surface (mgC m <sup>-3</sup> d <sup>-1</sup> )		Column (mgC m <sup>-3</sup> d <sup>-1</sup> )	
	Inshore	Offshore	Inshore	Offshore
8	11.7	2.0	360	190
10	13.4	1.9	452	143
11.5	4.4	3.1	229	218
13	9.9	5.5	205	242
15	5.0	-	258	-
17	6.8	6.0	218	209
19	10.4	4.9	386	268
<b>Average</b>	<b>8.8</b>	<b>3.9</b>	<b>301</b>	<b>212</b>

Table 5.2. Chlorophyll *a* in the inshore and offshore waters of EAS during OSM

Latitude (°N)	Surface (mg m <sup>-3</sup> )		Column (mg m <sup>-2</sup> )	
	Inshore	Offshore	Inshore	Offshore
8	0.25	0.10	22.68	24.93
10	0.36	0.13	33.27	16.35
11.5	0.21	0.24	15.95	15.09
13	0.34	0.24	12.97	21.26
15	0.21	-	20.51	-
17	0.24	0.12	27.75	16.07
19	0.43	0.22	27.97	23.89
<b>Average</b>	<b>0.29</b>	<b>0.18</b>	<b>23.01</b>	<b>19.60</b>

Table 5.3. Phytoplankton density in the inshore and offshore waters of EAS OSM

Latitude (°N)	surface (cells L <sup>-1</sup> )		Column (x 10 <sup>6</sup> cells m <sup>-2</sup> )	
	Inshore	Offshore	Inshore	Offshore
8	3660	5560	320.81	354.07
10	22800	9940	744.83	103.65
11.5	4560	8940	219.80	162.88
13	1040	2940	110.05	134.63
15	900	-	85.70	-
17	13560	13020	541.84	148.97
19	4760	27520	236.85	498.52
<b>Average</b>	<b>7326</b>	<b>11320</b>	<b>322.84</b>	<b>233.78</b>

*Biological responses to upwelling events in the different phases of summer monsoon*

Table.5.4. Abundance of diatoms, dinoflagellates and blue green algae in the surface of inshore and offshore waters of EAS during OSM

Latitude (°N)	Inshore (cells L <sup>-1</sup> )			Offshore (cells L <sup>-1</sup> )		
	Diatoms	Dino	Blue green algae	Diatoms	Dino	Blue green algae
8	1100	1140	1420	900	840	3820
10	2680	360	19400	560	580	8800
11.5	1260	400	2560	1260	620	7060
13	460	20	560	1240	680	1020
15	220	180	480	0	0	0
17	460	300	12800	980	200	11840
19	200	220	4340	2180	800	24540
<b>Average</b>	<b>911</b>	<b>374</b>	<b>5937</b>	<b>1017</b>	<b>531</b>	<b>8154</b>

Table.5.5. Abundance of diatoms, dinoflagellates and blue green algae in the upper 120m water column of inshore and offshore waters of EAS during OSM

Latitude (°N)	Inshore (cells m <sup>-2</sup> )			Offshore (x 10 <sup>6</sup> cells m <sup>-2</sup> )		
	Diatoms	Dino	Blue green algae	Diatoms	Dino	Blue green algae
8	166.64	131.06	22.71	174.32	140.81	3.82
10	269.10	216.37	250.04	28.97	26.17	8.80
11.5	99.51	87.47	21.08	75.52	36.19	7.06
13	28.47	23.37	58.20	67.91	43.49	1.02
15	51.77	24.17	9.65	0	0	0
17	159.96	134.80	210.71	43.76	34.21	11.84
19	103.05	51.25	80.45	148.55	48.17	24.54
<b>Average</b>	<b>125.50</b>	<b>95.50</b>	<b>93.26</b>	<b>77.00</b>	<b>47.00</b>	<b>8.15</b>

Table.5.6 Mesozooplankton biomass in the mixed layer and thermocline layer of inshore and offshore waters of EAS during OSM

Latitude (°N)	Mixed layer (No m <sup>-3</sup> )		Thermocline layer (No m <sup>-3</sup> )	
	Inshore	Offshore	Inshore	Offshore
8	0.16	0.21	0.07	0.07
10	0.74	0.11	0.16	0.02
11.5	0.38	0.23	0.05	0.09
13	0.22	0.14	0.04	0.06
15	0.12	0.17	0.02	0.06
17	0.30	0.17	0.06	0.06
19	0.50	0.17	0.00	0.03
<b>Average</b>	<b>0.35</b>	<b>0.17</b>	<b>0.06</b>	<b>0.05</b>

Table 5.7. Percentage (%) composition of mesozooplankton biomass during OSM

Mesozooplankton (%)	Depth	
	Mixed Layer	Thermocline layer
Foraminifera	0.11	0.46
Medusa	0.05	0.11
Siphonophore	0.64	0.45
Polychaeta	0.27	0.56
Pteropoda	0.31	0.57
Heteropoda	0.04	0.02
Gastropoda	0.08	0.03
Ostracoda	7.96	7.57
Copepoda	83.83	81.24
Amphipoda	0.26	0.24
Euphausid	0.31	1.24
Decapoda	0.59	0.56
Chaetognatha	4.61	3.77
Copelata	0.01	0.00
Salpa	0.89	2.51
Doliolida	0.06	0.10
Fish eggs	0.09	0.09
Fish larva	0.08	0.20
Mysids	0.02	0.05
Other organisms	0.03	0.03

### 5.2.2. Peak Summer Monsoon (PSM)

#### (a) Primary productivity

During PSM, the surface primary productivity varied from 1.4 to 121.9 mgC m<sup>-3</sup>d<sup>-1</sup> (av. 28.8 ± 40.3 mgC m<sup>-3</sup>d<sup>-1</sup>) along the inshore waters, and 1.3 to 15.4 mgC m<sup>-3</sup>d<sup>-1</sup> (av. 4.9±50 mgC m<sup>-3</sup>d<sup>-1</sup>) along the offshore waters (Table 5.8). The inshore stations off Kanyakumari (8°N), off Kochi (10°N) and off Calicut (11.5°N) showed relatively higher production (>1000 mgC m<sup>-2</sup>d<sup>-1</sup>). Profound inshore-offshore and north-south variation in PP was observed in EAS (Fig. 5.12 a & b). The maximum surface primary production (122 mgC m<sup>-3</sup>d<sup>-1</sup>) was recorded in the inshore station off 10°N latitude where mature stage of

Biological responses to upwelling events in the different phases of summer monsoon

upwelling was observed during this season. The vertical distribution of primary productivity along the inshore and offshore stations is depicted in Fig. 5.13. In most of the stations productivity maxima were observed in the subsurface layers of the euphotic column

**(b) Chlorophyll *a***

The surface Chl *a* was (Fig. 5.12c) in the range of 0.12  $\text{mgm}^{-3}$  to 1.98  $\text{mgm}^{-3}$  (av.  $0.77 \pm 0.68 \text{ mgm}^{-3}$ ) in the inshore stations, while in the offshore region it ranged between 0.12 and 0.45 (av.  $0.24 \pm 0.10 \text{ mgm}^{-3}$ ). The corresponding column Chl *a* (Fig. 5.12d) varied from 11.5 to 68.9  $\text{mgm}^{-2}$  (av.  $32.2 \pm 21.5 \text{ mgm}^{-2}$ ) in and 8.9 to 32.7 ( $21.2 \pm 8.5 \text{ mgm}^{-2}$ ) respectively, in the inshore and offshore stations (Table 5.9). Southern inshore waters ( $8^{\circ}\text{N} - 11.5^{\circ}\text{N}$ ) exhibited high Chl *a* both in surface ( $> 1 \text{ mgm}^{-3}$ ) and column ( $> 46 \text{ mgm}^{-2}$ ). Maximum surface Chl *a* ( $1.98 \text{ mgm}^{-3}$ ) was observed in inshore waters off  $10^{\circ}\text{N}$ , while column Chl *a* was maximum along the inshore waters off  $11.5^{\circ}\text{N}$ . Surface and column distribution of primary productivity showed that southern latitudes are more productive during summer monsoon. The vertical distribution of Chl *a* in showed that, SCM was not consistently distributed through out the study area (Fig. 5.14). At the inshore stations off  $8^{\circ}\text{N}$  and  $11.5^{\circ}\text{N}$  transects, SCM was observed at 10-20m depth ( $8^{\circ}\text{N} - 1.4 \text{ mgm}^{-3}$ ,  $11.5^{\circ}\text{N} - 1.6 \text{ mgm}^{-3}$ ).

**(c) Phytoplankton abundance**

The phytoplankton density, the abundance of diatoms, dinoflagellates, blue green algae and green flagellates are given in

Biological responses to upwelling events in the different phases of summer monsoon

Tables 5.10 to 5.12. The total phytoplankton density in the surface waters were in the range of 800-15140 cells L<sup>-1</sup> (av. 10060 cells L<sup>-1</sup>) along the inshore and 1460 -10380 cells L<sup>-1</sup> (av. 3965 cells L<sup>-1</sup>) in the offshore waters. The integrated total phytoplankton density in the upper 120m water column varied between 73.41 x 10<sup>6</sup> to 1037.42 x 10<sup>6</sup> cells m<sup>-2</sup> (av. 440.34 x 10<sup>6</sup> cells m<sup>-2</sup>) along the inshore and 205.50 x 10<sup>6</sup> to 346.10 x 10<sup>6</sup> cells m<sup>-2</sup> in the offshore waters. Vertical distribution of phytoplankton cells is represented in Fig. 5.15 a & b. Abundance of green flagellates is note worthy in the subsurface layers along the inshore stations off 8°-11.5°N transects. Green flagellates were almost absent in the other northern inshore - offshore waters. Similar to the distribution PP and Chl *a*, high phytoplankton density showed higher values in the inshore waters SEAS (8-11.5°N) (Fig. 5.16).

In the upper 120m water column of the inshore waters diatoms formed the dominant fraction (52.3%) in the total phytoplankton followed by dinoflagellates (29.7%), green flagellates (11.6%) and blue green algae (6.2%). In the offshore waters the percentage composition (Fig. 5.17) of diatoms was 61.21% followed by dinoflagellates (30.35%), blue green algae (8.08%) and green flagellates (0.31%).

**(d) Mesozooplankton biomass**

The average mesozooplankton biomass in the mixed layer was 1.68 m<sup>3</sup>. The highest biomass (8.6m<sup>3</sup>) was recorded in the mixed layer along the inshore waters off Kochi. In the thermocline layer, the maximum biomass (0.91 m<sup>3</sup>) was observed along 17°N and 10°N.

Biological responses to upwelling events in the different phases of summer monsoon

The average mesozooplankton biomass in the in the inshore and off region of thermocline layer was  $0.37 \text{ m}^3$  and  $0.14 \text{ m}^3$ , respectively (Table 5.13). The mesozooplankton biomass decreased from the southern coastal region to northern coastal region (Fig. 5.18). Swarms of siphonophores and euphausiids were observed in the mixed layer and thermocline layer off Kochi ( $10^\circ\text{N}$ ). However the open ocean stations in the northern regions recorded high biomass due to the ostracod swarms. Distribution of fish larvae in the mixed layer and thermocline layer are shown in Fig. 5.19. Maximum abundance of fish larvae ( $9.2 \text{ ind.}^3$ ) was observed along the inshore waters off Kochi. In the thermocline layer also, abundance of fish larvae was observed in the inshore stations off  $10^\circ\text{N}$ ,  $15^\circ\text{N}$  and  $17^\circ\text{N}$ .

Copepods formed the dominant mesozooplankton community, in the mixed layer (59%) and in the thermocline region (69 %). The other groups prominent during this season are ostracods (12.14% in the MLD and 17 % in the thermocline layer), euphausiids (3.72% in the thermocline layer) and chaetognaths (about 3.5% in both depth strata). Highest abundance of fish eggs and fish larvae (0.70% and 0.18%) was recorded during this season (Table 5.14).

Linear correlation of Chl *a* between nitrate ( $r = 0.40$ ), phosphate ( $r = 0.36$ ) and silicate ( $r = 0.39$ ) are given in the Fig. 5.20. Significant correlation was obtained (Fig. 5. 21) between Chl *a* and primary productivity ( $r = 0.83$ ), Chl *a* and total phytoplankton cells ( $r = 0.92$ ), Chl *a* and diatoms ( $r = 0.84$ ), Chl *a* and dinoflagellates ( $r = 0.84$ ), and Chl *a* green flagellates ( $r = 0.85$ ). Similarly primary productivity also

*Biological responses to upwelling events in the different phases of summer monsoon*

showed significant linear correlation (Fig. 5.22) between and total phytoplankton cell density ( $r = 0.80$ ), diatoms ( $r = 0.73$ ), dinoflagellates ( $r = 0.69$ ), green flagellates ( $r = 0.65$ ).

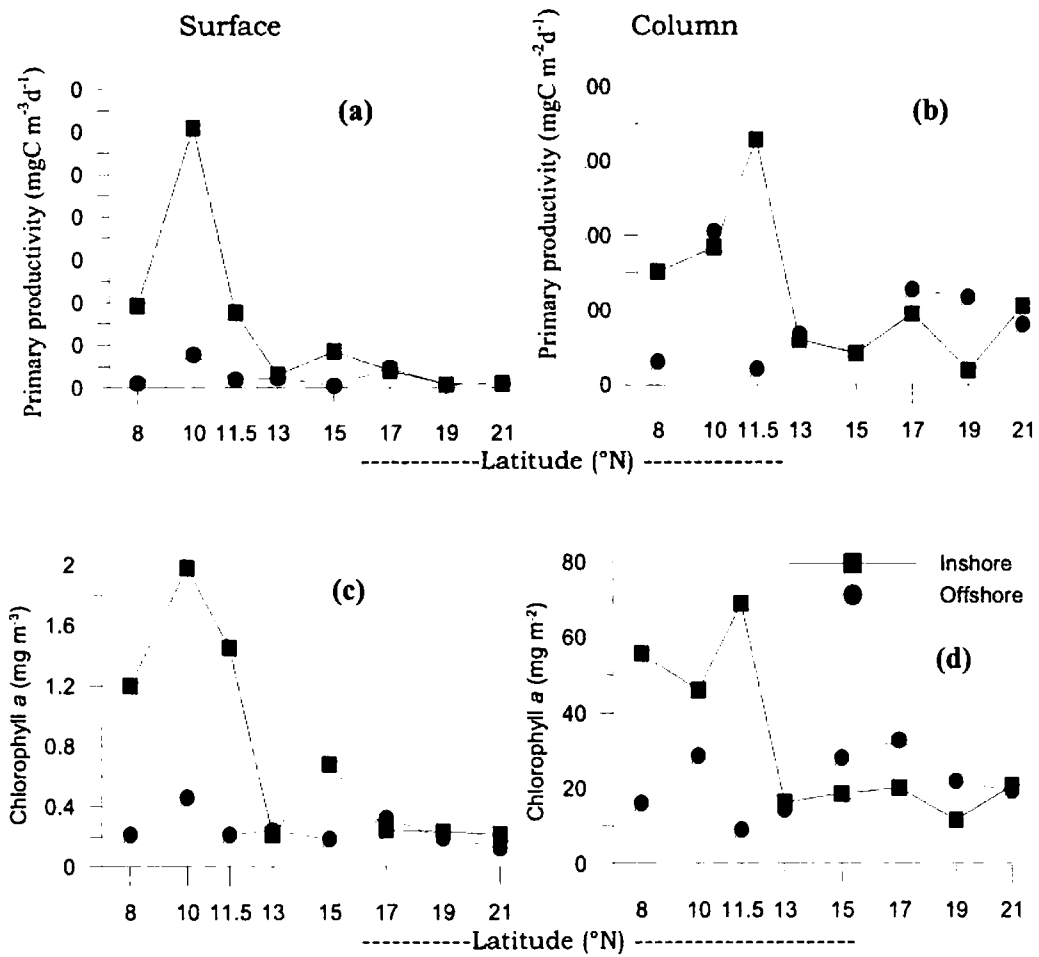


Fig.5.12. Distribution of (a & b) primary productivity and (c & d) chlorophyll *a* in the inshore and offshore waters of EAS during PSM

*Biological responses to upwelling events in the different phases of summer monsoon*

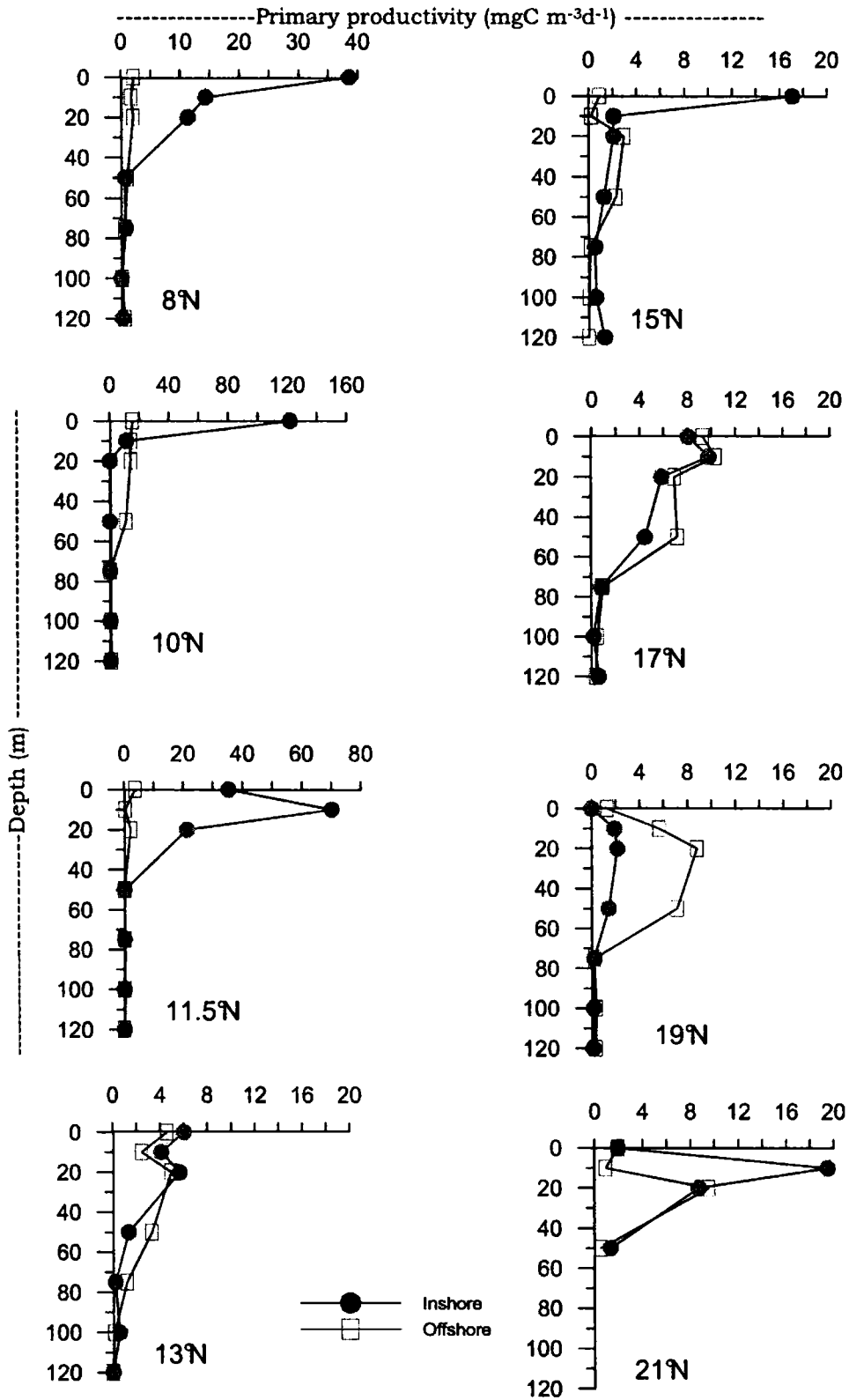


Fig. 5.13. Vertical distribution of primary productivity ( $\text{mgC m}^{-3}\text{d}^{-1}$ ) in the inshore and offshore waters of EAS during PSM





*Biological responses to upwelling events in the different phases of summer monsoon*

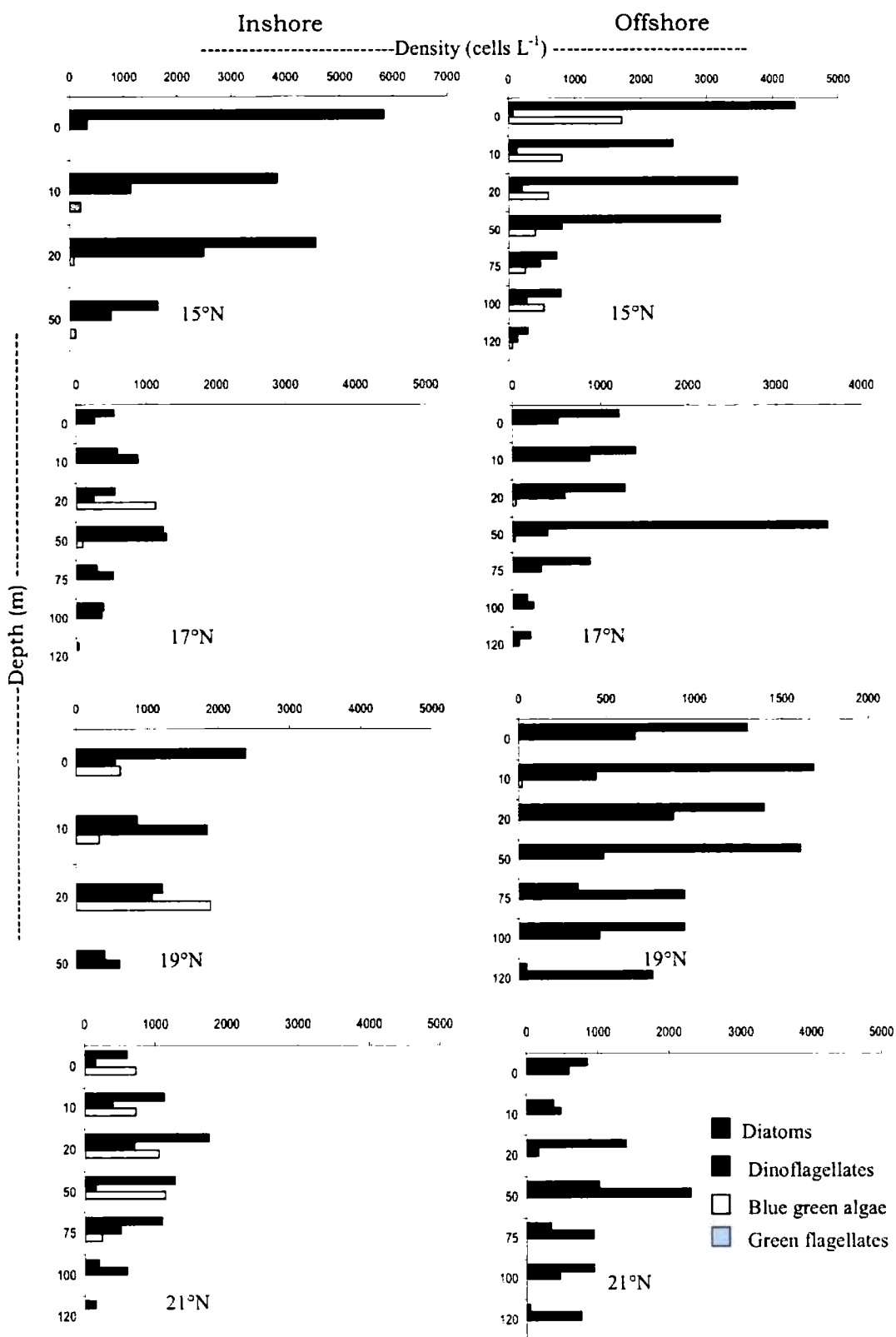


Fig.5.15 b. Vertical distribution of phytoplankton density in the inshore and offshore waters of EAS during PSM

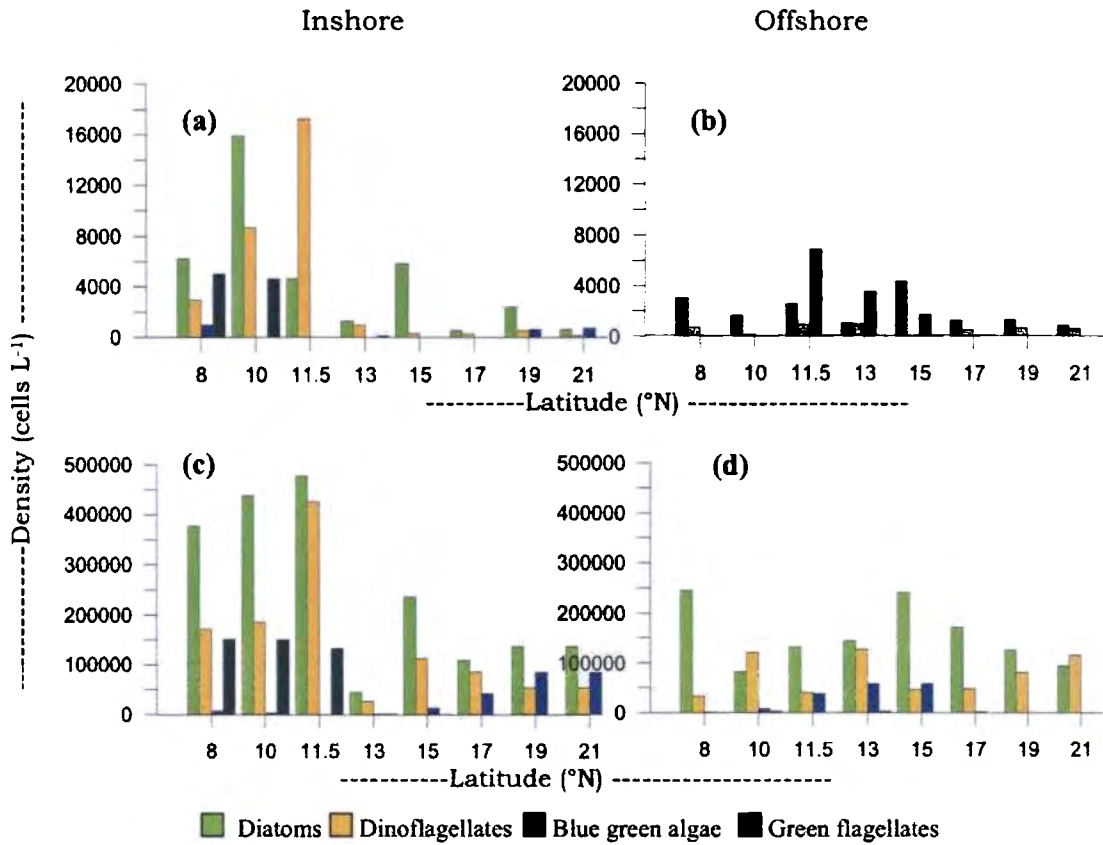


Fig. 5.16. Distribution of phytoplankton in the (a & b) surface and (c & d) 120 water column in the inshore and offshore waters of EAS during PSM

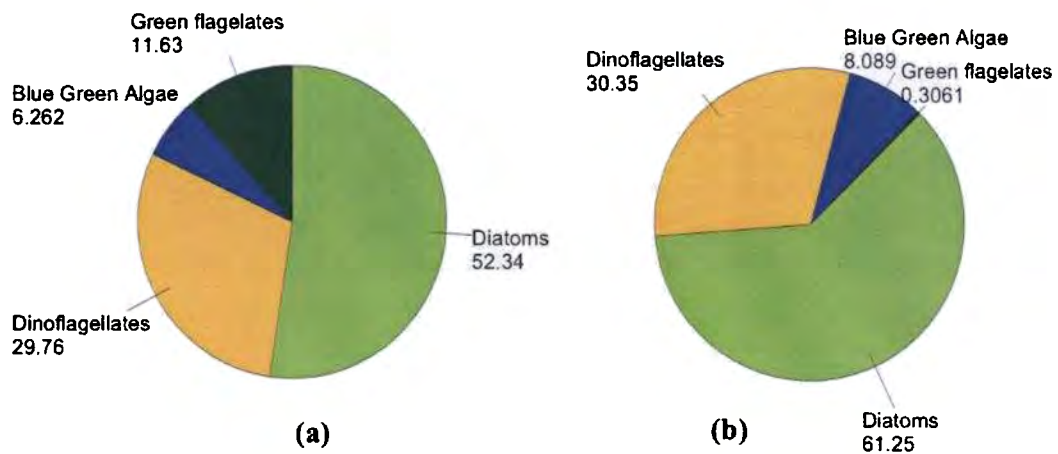


Fig. 5.17. Percentage (%) composition of total phytoplankton density in the (a) inshore and (b) offshore waters of EAS during PSM

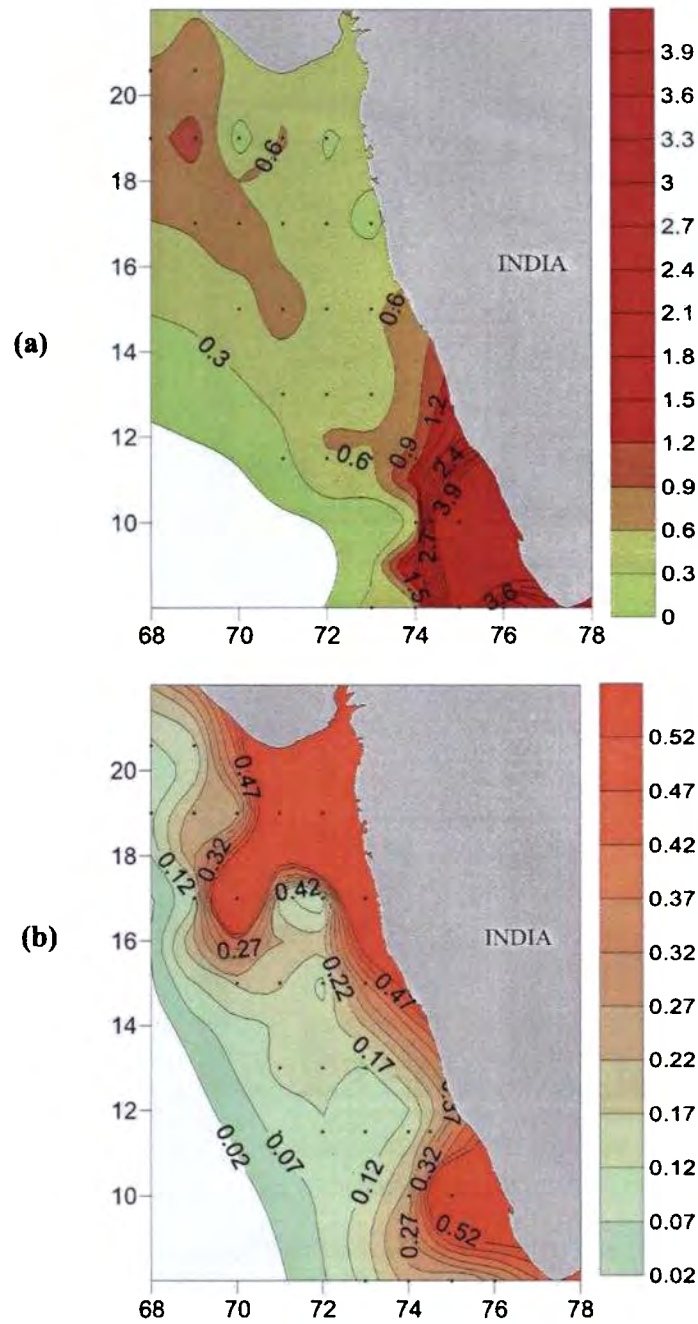


Fig. 5.18. Distribution of mesozooplankton biomass ( $\text{ml m}^{-3}$ ) in the (a) mixed layer and (b) thermocline layer of EAS during PSM

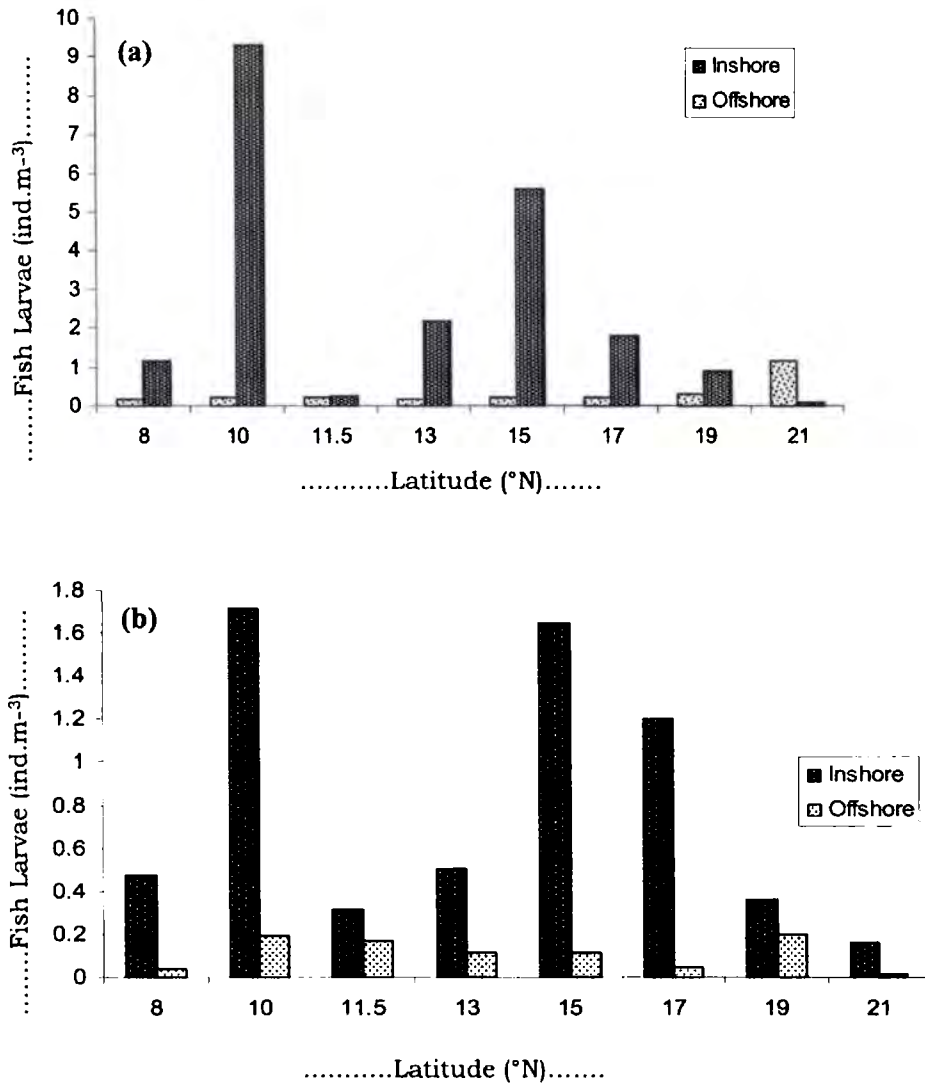


Fig. 5. 19 Distribution of fish larvae (ind. m<sup>-3</sup>) in the (a) mixed layer and (b) thermocline layer of EAS during PSM

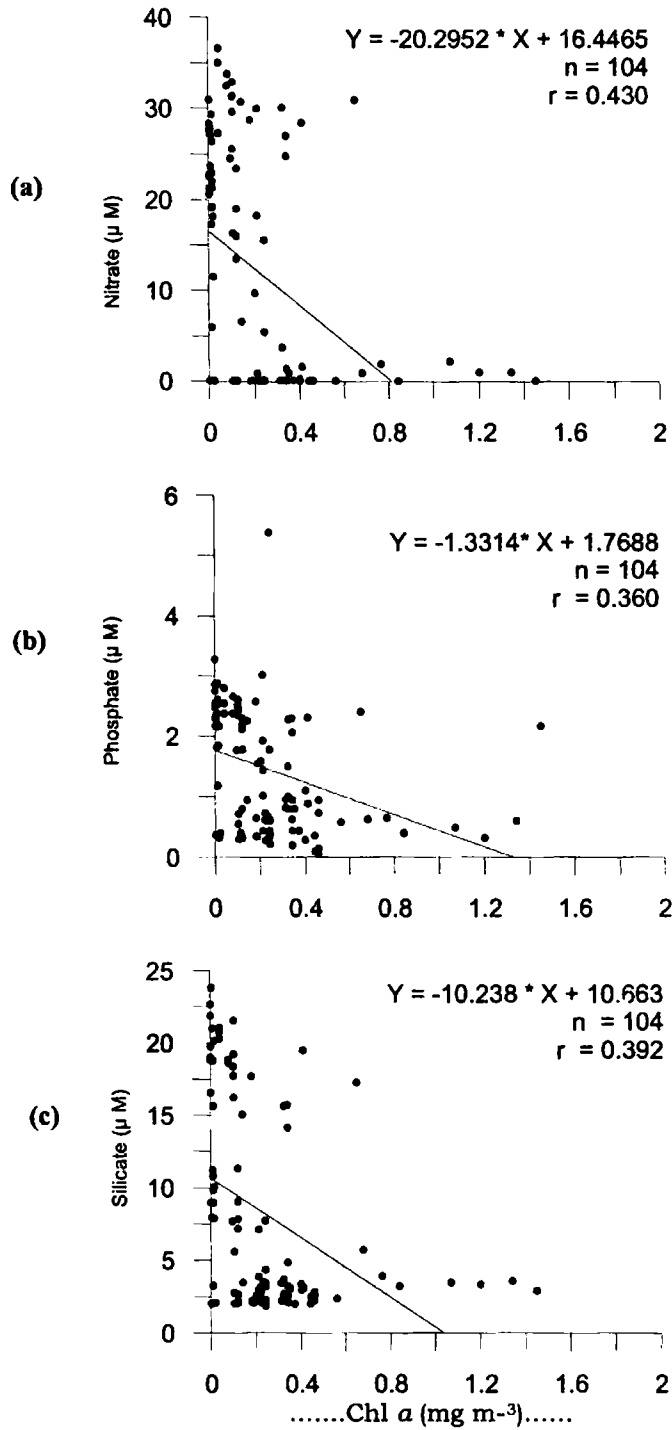


Fig. 5.20. Linear correlation of Chl *a* between (a) nitrate, (b) phosphate (c) silicate in the EAS during PSM

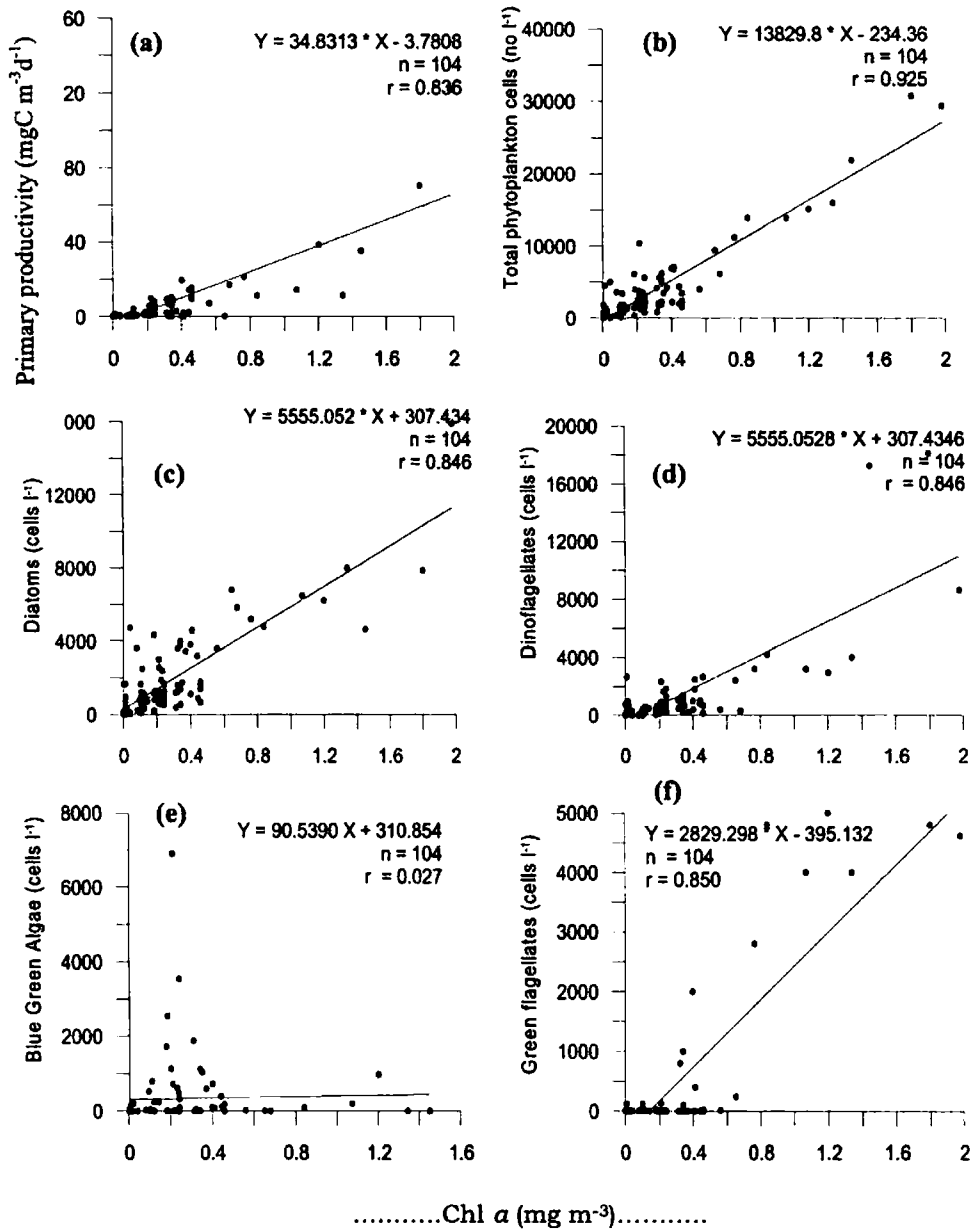


Fig. 5.21. Linear correlation of Chl a between (a) primary productivity, (b) total phytoplankton density (c) diatom abundance and (d) dinoflagellates abundance (e) blue green algae (f) green flagellates abundance in the EAS during PSM

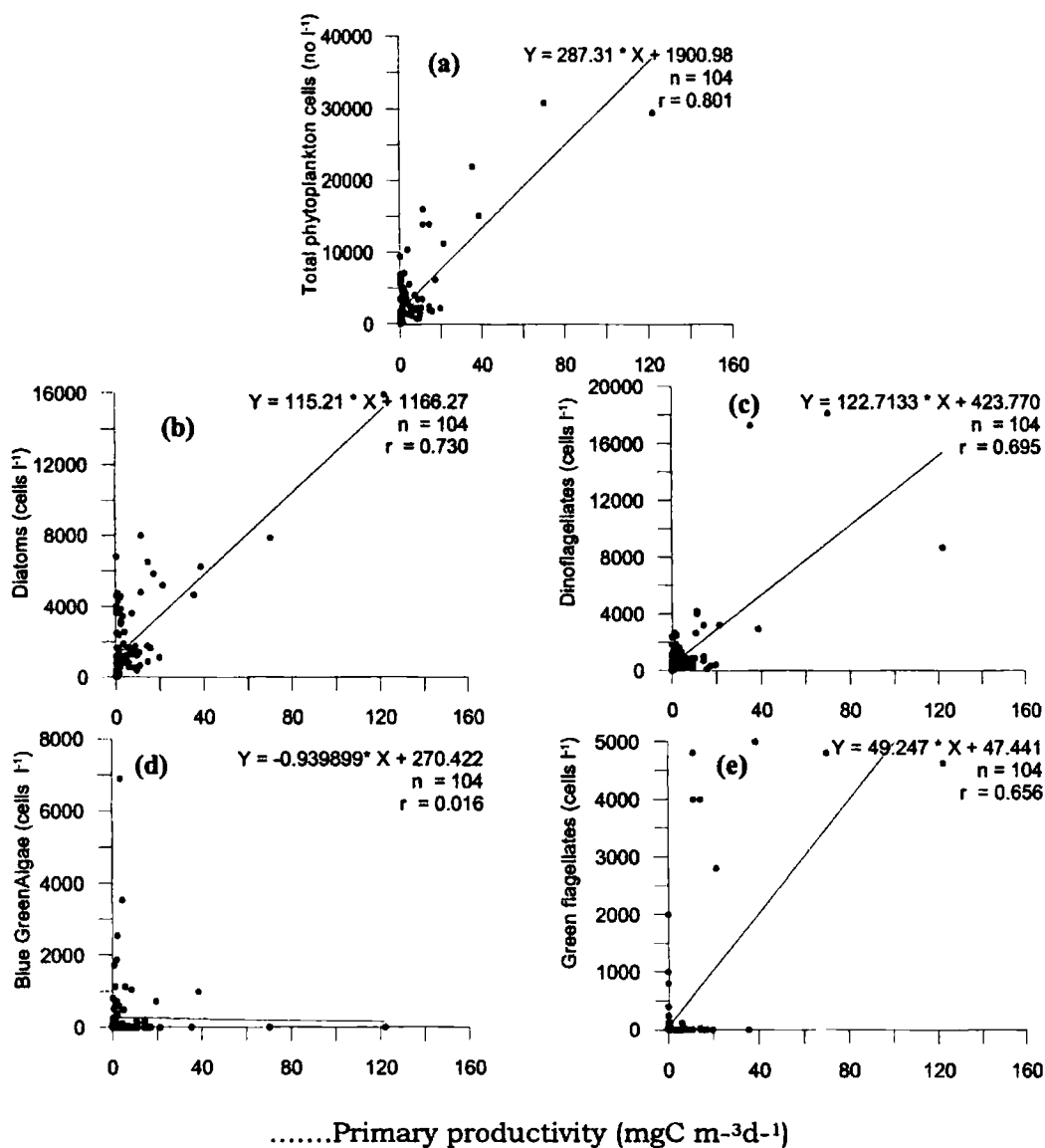


Fig. 5.22. Linear correlation between (a) primary productivity and total phytoplankton density (b) diatoms and (c) dinoflagellates, (d) blue green algae and (e) green flagellates during PSM

Table 5.8. Primary productivity in the inshore and offshore waters of EAS during PSM

Latitude (°N)	Surface (mgC m <sup>-3</sup> d <sup>-1</sup> )		Column (mgC m <sup>-3</sup> d <sup>-1</sup> )	
	Inshore	Offshore	Inshore	Offshore
8	38.6	2.1	607	123
10	122.0	15.5	736	821
11.5	35.4	3.8	1314	84
13	6.0	4.6	242	271
15	17.1	0.9	167	168
17	8.1	9.3	381	511
19	1.4	1.3	75	470
21	2.0	1.9	424	323
<b>Average</b>	<b>28.8</b>	<b>4.9</b>	<b>493</b>	<b>347</b>

Table 5.9. Chl *a* in the inshore and offshore waters of EAS during PSM

Latitude (°N)	Surface (mg m <sup>-3</sup> )		Column (mg m <sup>-2</sup> )	
	Inshore	Offshore	Inshore	Offshore
8	1.20	0.21	55.75	16.08
10	1.98	0.46	46.09	28.65
11.5	1.45	0.21	68.96	8.95
13	0.21	0.24	16.28	14.29
15	0.68	0.18	18.58	28.13
17	0.24	0.32	20.07	32.74
19	0.23	0.19	11.53	21.84
21	0.21	0.12	20.74	19.22
<b>Average</b>	<b>0.77</b>	<b>0.24</b>	<b>32.25</b>	<b>21.24</b>

Table 5.10. Phytoplankton density in the inshore and offshore waters of EAS during PSM

Latitude (°N)	Surface (cells x10 <sup>6</sup> m <sup>-3</sup> )		Column (cells x10 <sup>6</sup> m <sup>-2</sup> )	
	Inshore	Offshore	Inshore	Offshore
8	15140	1742	705.2	279.0
10	29200	2760	776.2	209.2
11.5	21920	10380	1037.4	210.2
13	2240	5560	73.4	328.8
15	6160	6120	360.4	346.1
17	800	1740	23.5	222.6
19	3540	1960	273.2	205.5
21	1480	1460	273.2	209.9
<b>Average</b>	<b>10060</b>	<b>3965</b>	<b>440.3</b>	<b>244.0</b>

*Biological responses to upwelling events in the different phases of summer monsoon*

Table 5.11. Abundance of diatoms, dinoflagellates blue green algae and green flagellates in the surface of inshore and offshore waters of EAS during PSM

Latitude (°N)	Inshore (cells l <sup>-1</sup> )				Offshore (cells l <sup>-1</sup> )			
	Diatoms	Dino	Blue green algae	Green flagllates	Diatoms	Dino	Blue green algae	Green flagllates
8	6220	2940	980	5000	3000	720	0	-
10	15900	8680	-	4620	1640	120	0	-
11.5	4640	17280	-	-	2560	920	6900	-
13	1300	940	-	-	1040	980	3540	-
15	5840	320	-	-	4340	60	1720	-
17	540	260	-	-	1220	520	0	-
19	2380	540	620	-	1300	660	0	-
21	600	160	720	-	860	600	0	-
<b>Average</b>	<b>4678</b>	<b>3890</b>	<b>773</b>	<b>4810</b>	<b>1995</b>	<b>573</b>	<b>1520</b>	<b>0</b>

Table 5.12. Abundance of diatoms, dinoflagellates blue green algae and green flagellates in the upper 120m water column of inshore and offshore waters of EAS during PSM

Latitude (°N)	Inshore (x10 <sup>6</sup> cells m <sup>-2</sup> )				Offshore (x10 <sup>6</sup> cells m <sup>-2</sup> )			
	Diatoms	Dino	Blue green algae	Green flagllates	Diatoms	Dino	Blue green algae	Green flagllates
8	376.9	170.5	6.9	151.0	24.5	32.5	1.1	0.0
10	437.6	185.7	3.0	148.9	81.7	120.2	7.4	3.2
11.5	477.8	426.1	0.5	133.1	131.1	41.2	3.8	0.0
13	45.2	26.0	0.9	1.4	143.9	127.7	57.2	2.7
15	235.5	112.1	12.8	0.0	241.9	46.6	57.7	0.0
17	108.3	84.6	42.0	0.0	172.3	48.6	1.7	0.3
19	136.3	53.1	83.9	0.0	125.4	80.0	0.2	0.0
21	136.3	53.1	83.9	0.0	94.2	115.7	0.0	0.0
<b>Average</b>	<b>244</b>	<b>139</b>	<b>29</b>	<b>127</b>	<b>127</b>	<b>77</b>	<b>16</b>	<b>1</b>

Table.5.13 Mesozooplankton biomass in the mixed layer and thermocline layer of inshore and offshore waters of EAS during PSM

Latitude (°N)	Mixed layer (ml m <sup>-3</sup> )		Thermocline layer (ml m <sup>-3</sup> )	
	Inshore	Offshore	Inshore	Offshore
8	1.80	0.40	0.46	0.14
10	8.66	0.39	0.91	0.24
11.5	0.91	0.15	0.09	0.08
13	0.38	0.39	0.11	0.13
15	0.53	0.39	0.47	0.18
17	0.24	0.64	0.02	0.11
19	0.27	0.80	0.80	0.11
21	0.68	0.59	0.09	0.11
<b>Average</b>	<b>1.68</b>	<b>0.47</b>	<b>0.37</b>	<b>0.14</b>

Table 5.14. Percentage composition of mesozooplankton biomass during PSM

Mesozooplankton (%)	Depth	
	Mixed Layer	Thermocline layer
Foraminifera	0.04	0.48
Medusa	0.14	0.18
Siphonophore	2.84	0.58
Polychaeta	0.11	1.79
Pteropoda	0.18	0.11
Heteropoda	0.01	0.05
Gastropoda	0.04	0.06
Ostracoda	12.14	17.4
Copepoda	59.75	69.04
Amphipoda	0.15	0.27
Euphausiid	0.84	3.72
Decapoda	0.86	0.95
Chaetognatha	3.49	4.08
Salpa	0.14	0.02
Doliolida	0.07	0.17
Fish eggs	0.70	0.22
Fish larva	0.08	0.17
Mysids	0.01	0.01
Other organisms	0.03	0.03

### **5.2.3. Late Summer Monsoon (LSM)**

#### ***(a) Primary productivity***

Distribution of primary productivity revealed that southern latitudes are more productive than northern latitudes (Fig. 5.23 a & b). The highest rate of primary productivity in the surface ( $37.4 \text{ mgC m}^{-3} \text{ d}^{-1}$ ) and column ( $1630 \text{ mgC m}^{-2} \text{ d}^{-1}$ ) were observed in the inshore stations off  $10^\circ\text{N}$ .

The Arabian Sea showed a wide range in primary production rates, at the surface and column. The surface primary productivity varied from  $4.2$  to  $37.4 \text{ mgC m}^{-3} \text{ d}^{-1}$  (av.  $11.8 \pm 11.5 \text{ mgC m}^{-3} \text{ d}^{-1}$ ) in the inshore waters and from  $2.0$  to  $10.67 \text{ mgC m}^{-3} \text{ d}^{-1}$  (av.  $6.3 \pm 2.9 \text{ mgC m}^{-3} \text{ d}^{-1}$ ) in the offshore waters. Integrated column primary production

Biological responses to upwelling events in the different phases of summer monsoon

for the euphotic zone varied from 179 to 1630 mgC m<sup>-2</sup>d<sup>-1</sup> (av. 495 ± 515 mgC m<sup>-2</sup>d<sup>-1</sup>) in the inshore waters and from 173 to 571 mgC m<sup>-2</sup>d<sup>-1</sup> (av. 306 ± mgC m<sup>-2</sup>d<sup>-1</sup>) in the offshore waters (Table 5.15). The vertical distribution of primary productivity along the inshore and offshore waters are represented in the Fig. 5.24. Subsurface productivity maxima (20 m) were observed along EAS during this season. At the inshore waters of 10°N primary productivity was maximum at 10m depth.

**(b) Chlorophyll a**

The surface waters of the south west coast showed higher concentration of Chl *a* during LSM. Surface Chl *a* was in the range of 0.12 to 0.75 mgm<sup>-3</sup> (av. 0.42 ± 0.25 mgm<sup>-3</sup>) in the inshore waters and 0.10 to 0.39 mgm<sup>-3</sup> (av. 0.24 ± 0.10 mgm<sup>-3</sup>) in the offshore waters. The variation in the integrated value of chl *a* in the euphotic column was between 14.96 to 60.7 mgm<sup>-2</sup> (av. 28.0 mgm<sup>-2</sup>) in the inshore stations, and 13.7 - 41.54 mg m<sup>-2</sup> (av. 21.96 mgm<sup>-2</sup>) in the open waters. (Table 5.16).

Distribution of Chl *a* in the surface and column along the inshore-offshore waters (8-21°N transects), showed higher concentration of Chl *a* in the southern transects (Fig. 5.23c & d). Latitudinal variations in the primary productivity and Chl *a* distribution showed that SEAS (8°N-15°N) is more productive than the northeastern Arabian Sea (15°N-21°N) and it was in good agreement with the hydrographic characteristics and upwelling intensity as well.

Biological responses to upwelling events in the different phases of summer monsoon

The vertical distribution of Chl *a* in the inshore-offshore waters of each transects is represented in the Fig. 5.25. SCM was observed at a depth of 10m in most of the stations, while in the offshore waters SCM was at 50m depth.

**(c) Phytoplankton abundance**

Phytoplankton density was found to be high along the south west coast during this season. The vertical distribution of phytoplankton abundance is represented in the Fig. 5.26 a & b. Density of total phytoplankton is given in the Table 5.17. Surface phytoplankton density was in the range of 1120 to 17060 cells L<sup>-1</sup> (av. 4851 cells L<sup>-1</sup>) along the inshore waters and 820 to 9760 cells L<sup>-1</sup> (av. 3377 cells L<sup>-1</sup>) along the offshore region. The integrated phytoplankton abundance in the 120m water column of inshore and offshore waters were in the range of 162.2 x 10<sup>6</sup> to 477.5 x 10<sup>6</sup> cells m<sup>-2</sup> (av. 289 x 10<sup>6</sup> cells m<sup>-2</sup>) and 183.75 x 10<sup>6</sup> to 353 x 10<sup>6</sup> cells m<sup>-2</sup> (av. 226 x 10<sup>6</sup> cells m<sup>-2</sup>) respectively. During this season 10°N is found to have the maximum phytoplankton abundance in surface (4851 cells l<sup>-1</sup>) and column (477.5 x 10<sup>6</sup> cells m<sup>-2</sup>) (Fig. 5.27). The population density of diatoms, dinoflagellates, blue green algae and green flagellates (surface and column) of inshore and offshore waters are given in Tables 5.18 & 5.19. Green flagellates were abundant in the surface waters off Kochi (8700 cells l<sup>-1</sup>).

In the 120m water column (Fig. 28) diatoms formed major constituent (31.2%) of the total phytoplankton community along the

Biological responses to upwelling events in the different phases of summer monsoon

inshore waters followed by dinoflagellates (27.1%), green flagellates (26.1%), and blue green algae (15.6%). In the offshore waters diatoms contributed 67.7% of the phytoplankton density, followed by dinoflagellates (15.9%) blue green algae (15.9%) and green flagellates (0.35%).

**(d) Mesozooplankton biomass**

Mesozooplankton biomass distribution in the mixed layer and thermocline layer is shown in the Fig. 5.29. During the season, the average mesozooplankton biomass in the mixed layer was  $0.57 \text{ ml m}^{-3}$ . Comparatively higher biomass ( $>0.7 \text{ ml m}^{-3}$ ) was observed in the mixed layer along the inshore waters off  $10^\circ\text{N}$  and offshore waters off  $15^\circ\text{N}$  and  $13^\circ\text{N}$  transects. Where as in the thermocline layer average zooplankton biomass observed was  $0.19 \text{ ml m}^{-3}$  and the maximum biomass ( $0.55 \text{ ml m}^{-3}$ ) was observed in the inshore off  $8^\circ\text{N}$  (Table 5.20).

In the mixed layer and the thermocline layer, copepods formed the highest component of mesozooplankton with a contribution of 83.3% and 81.5% respectively (Table 5.21) followed by ostracods (9.9% and 13.8%) and chaetognaths (3.2% and 1.9%). Distribution of fish larvae were 0.8% and 0.10% in the mixed layer and thermocline respectively during PSM. High abundance of fish larvae was observed ( $5.2 \text{ ind. m}^{-3}$ ) in the inshore waters off  $10^\circ\text{N}$  transect (Fig. 5.30).

Linear correlation of Chl *a* and nitrate ( $r = 0.43$ ), phosphate ( $r = 0.36$ ) and silicate ( $r = 0.36$ ) are given in Fig. 5.31. Chl *a* showed significant linear correlation (Fig. 5.32) to primary productivity ( $r =$

Biological responses to upwelling events in the different phases of summer monsoon

0.86), total phytoplankton cells ( $r = 0.73$ ), diatoms ( $r = 0.66$ ), dinoflagellates ( $r = 0.50$ ), and blue green algae ( $r = 0.7$ ). Similarly primary productivity also showed significant linear correlation with total phytoplankton density ( $r = 0.63$ ), diatoms ( $r = 0.84$ ) and dinoflagellates ( $r = 0.80$ ) Fig. 5.33).

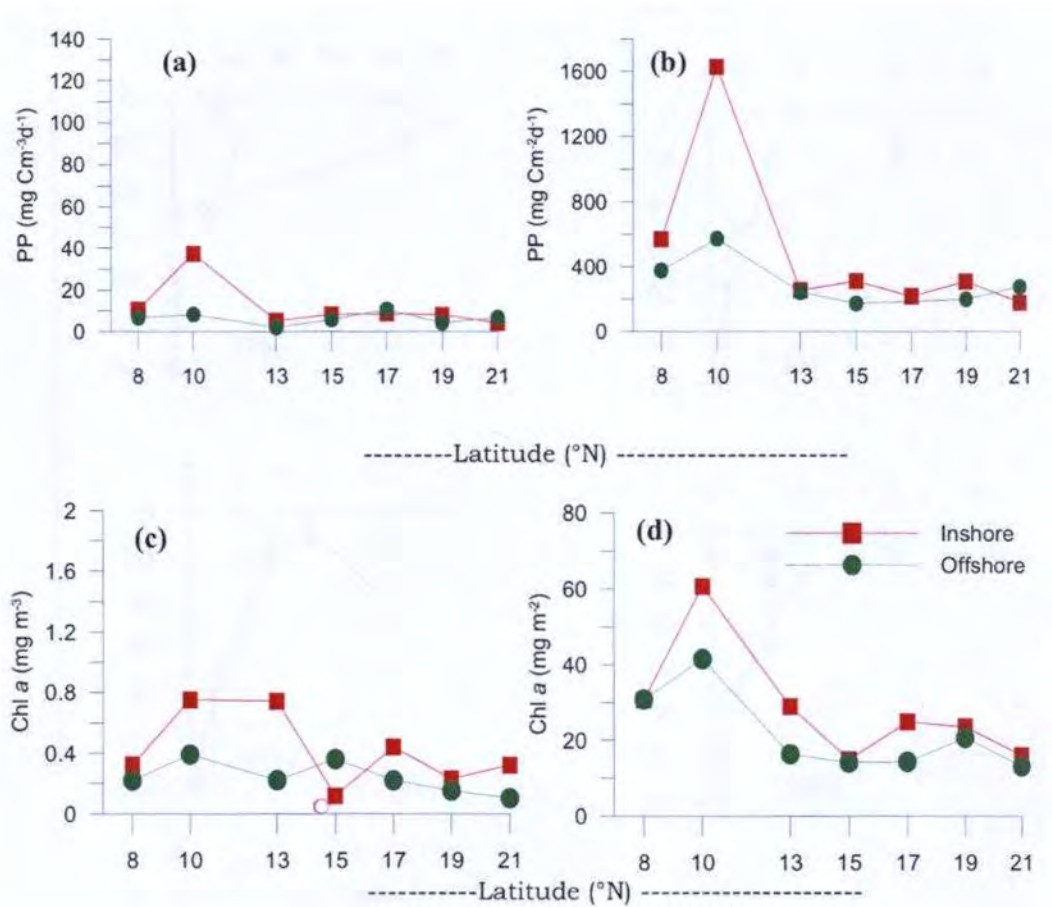


Fig.5.23. Distribution of primary productivity (a & b) and Chl *a* (c & d) along the inshore and offshore waters of EAS during LSM

*Biological responses to upwelling events in the different phases of summer monsoon*

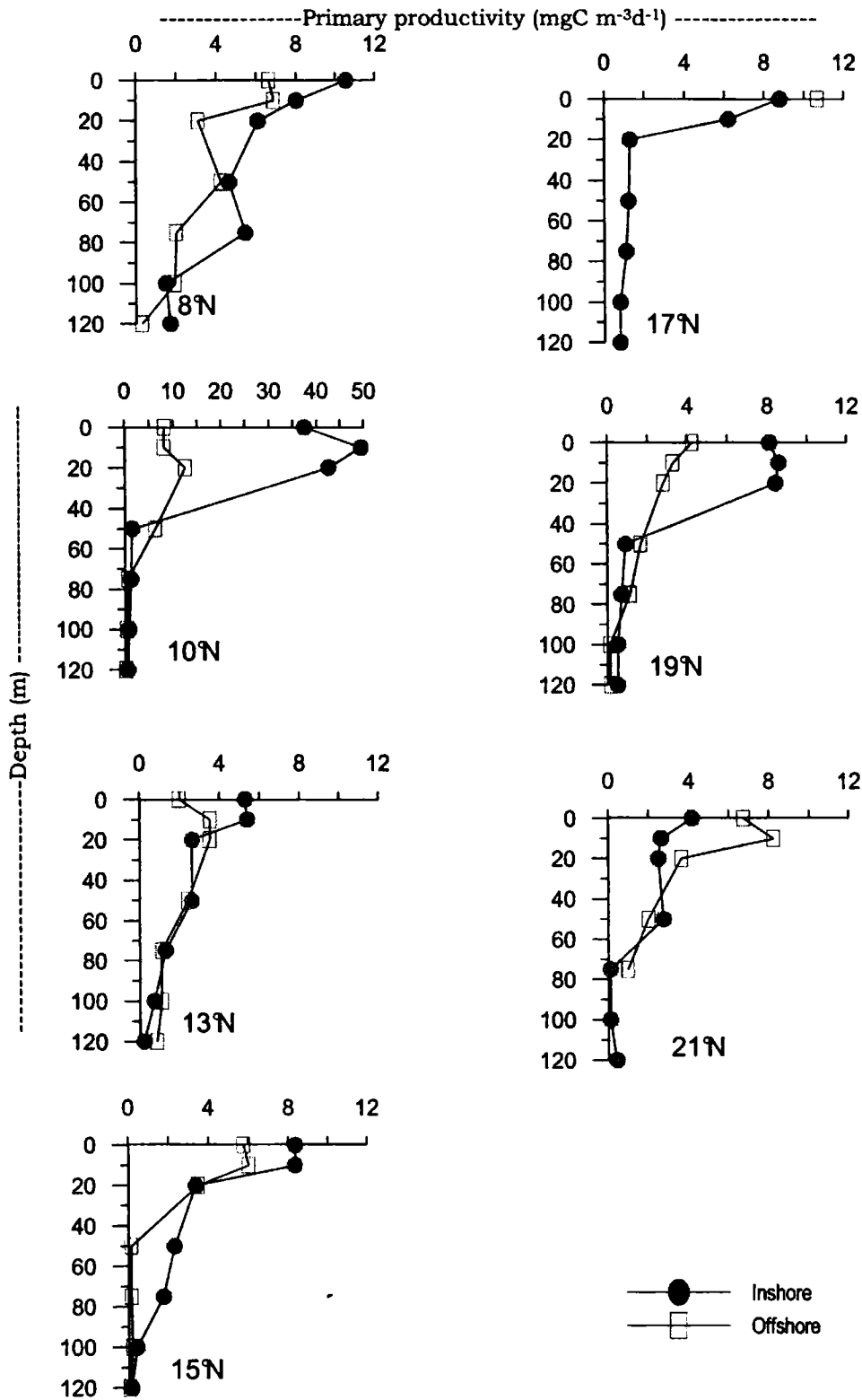


Fig.. 5.24. Vertical distribution of primary productivity ( $\text{mgC m}^{-3}\text{d}^{-1}$ ) in the inshore and offshore waters of EAS during LSM

*Biological responses to upwelling events in the different phases of summer monsoon*

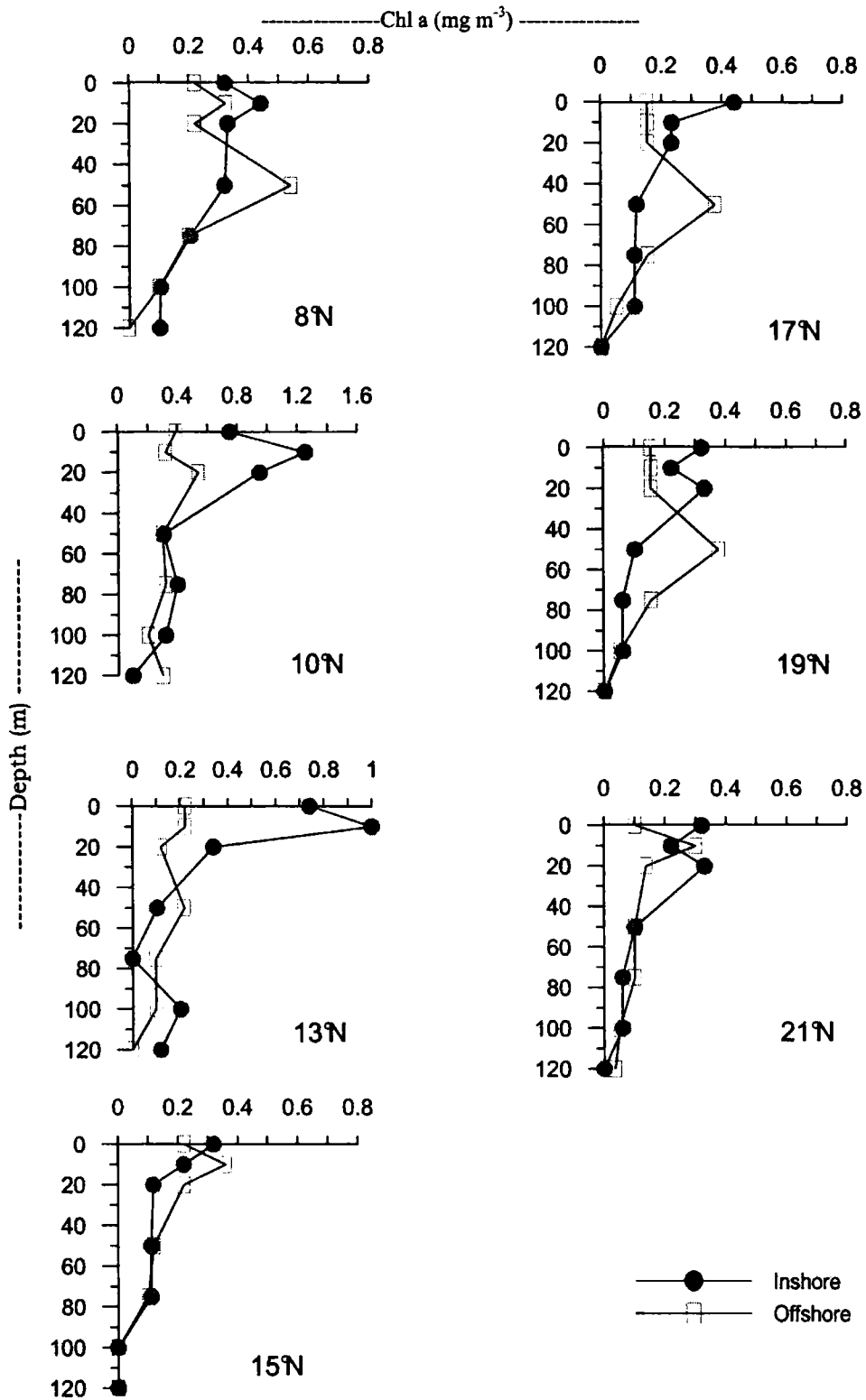


Fig. 5.25. Vertical distribution of chlorophyll  $\alpha$  ( $\text{mg m}^{-3}$ ) in the inshore and offshore waters of EAS during LSM

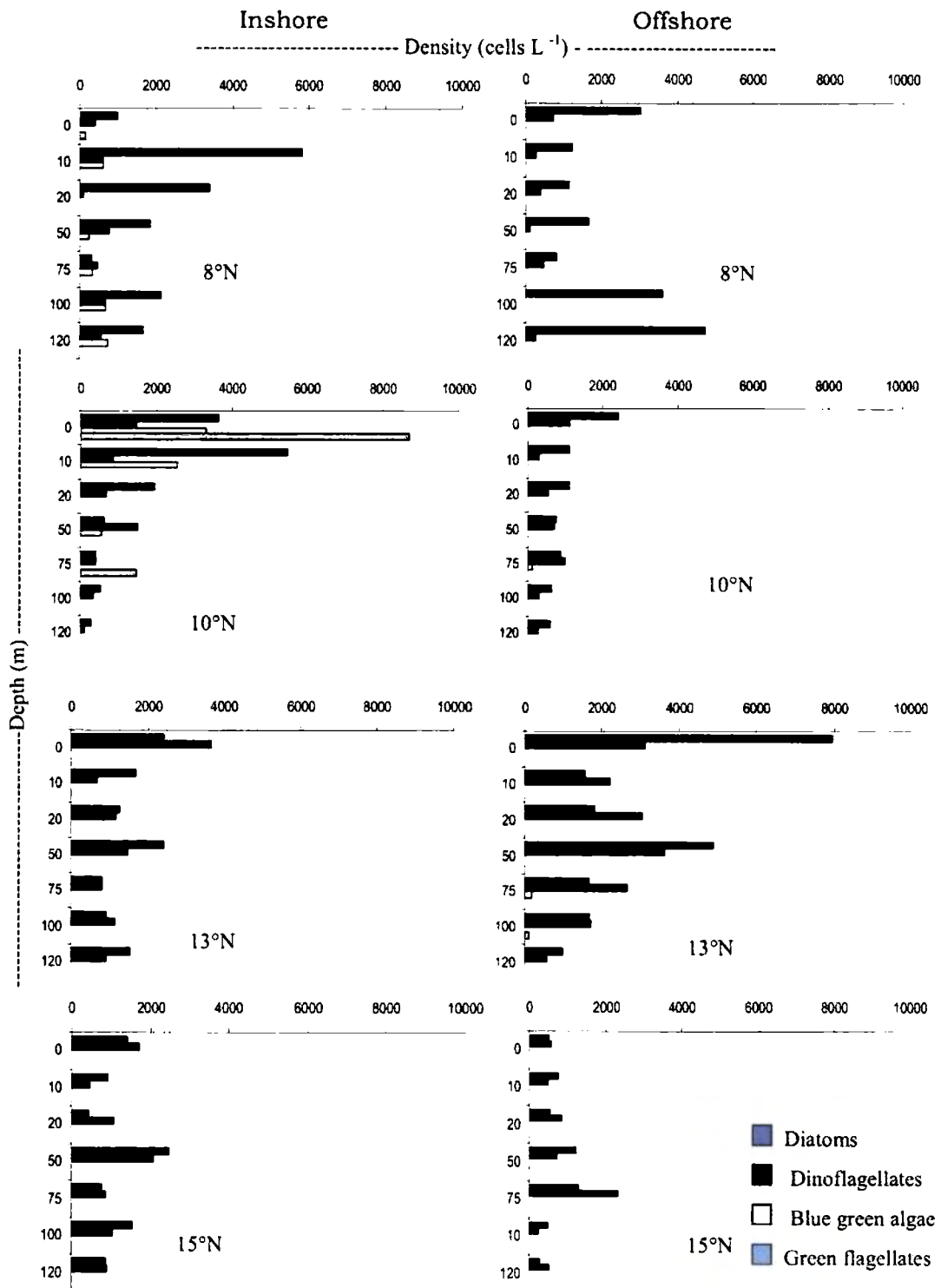


Fig.5.26a. Vertical distribution of phytoplankton density in the inshore and offshore waters of EAS during LSM

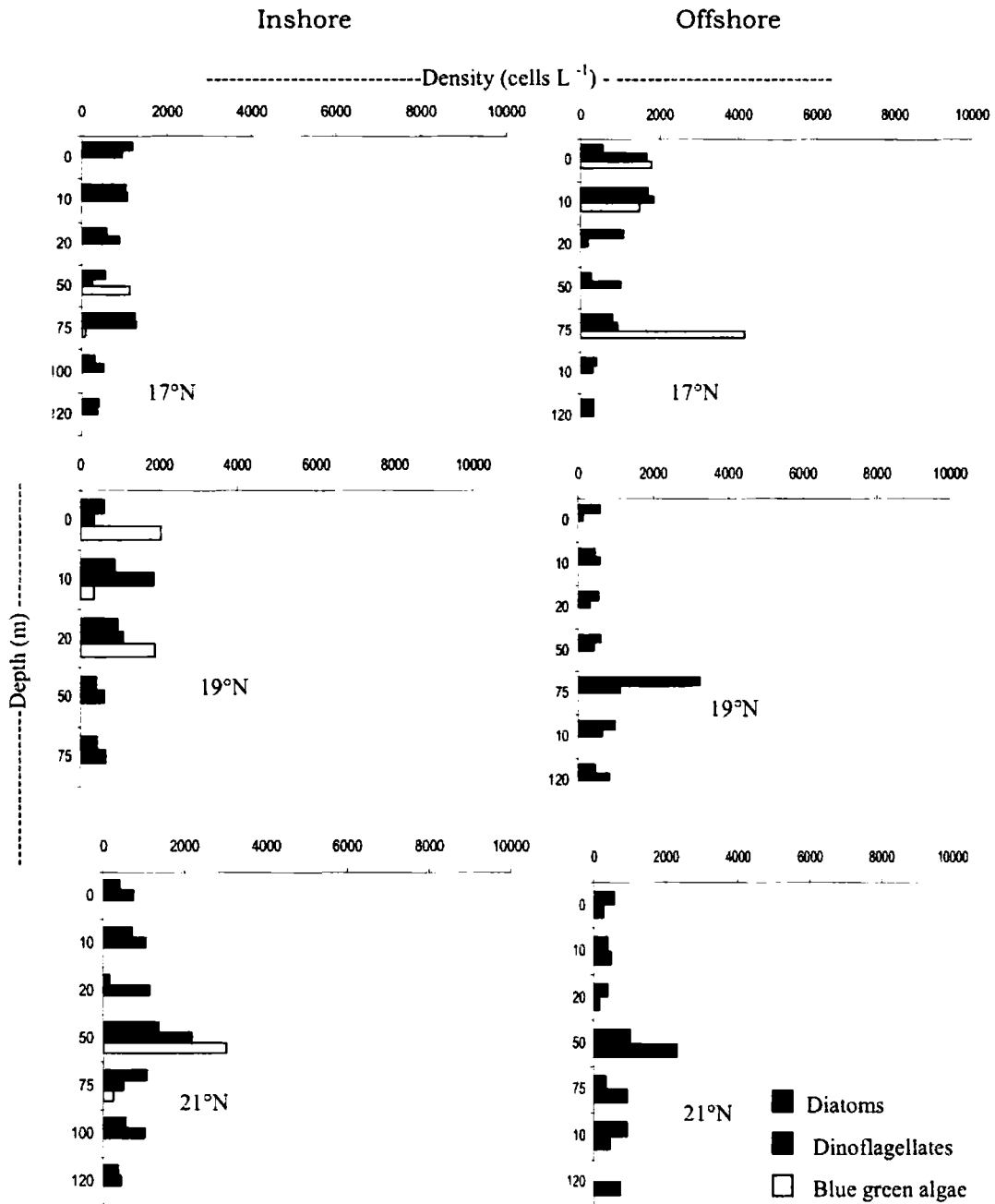


Fig.5.26b. Vertical distribution of phytoplankton density (cells L<sup>-1</sup>) in the inshore and offshore waters of EAS during LSM

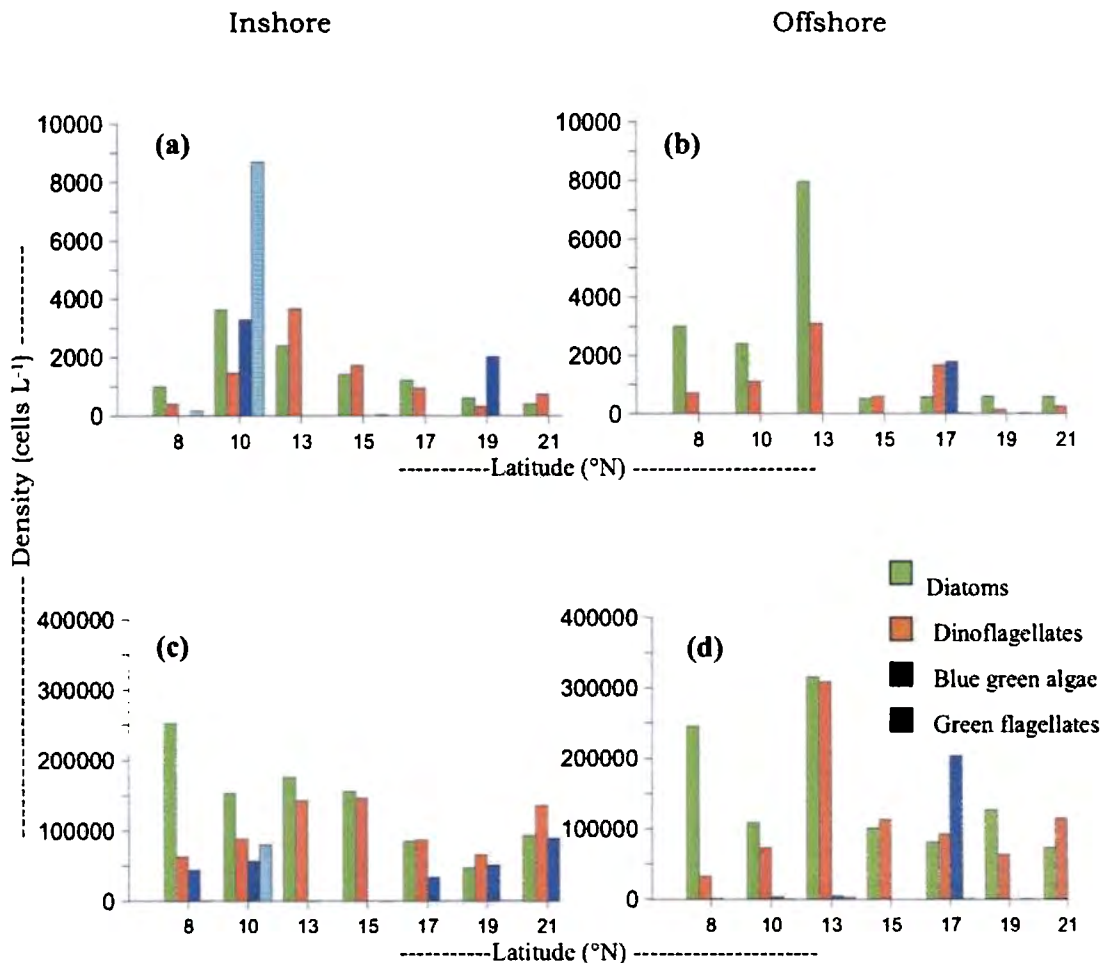


Fig.5.27. Distribution of phytoplankton density in the surface (cells L<sup>-1</sup>) (a & b) and 120 water column (c & d) in the inshore and offshore waters during LSM

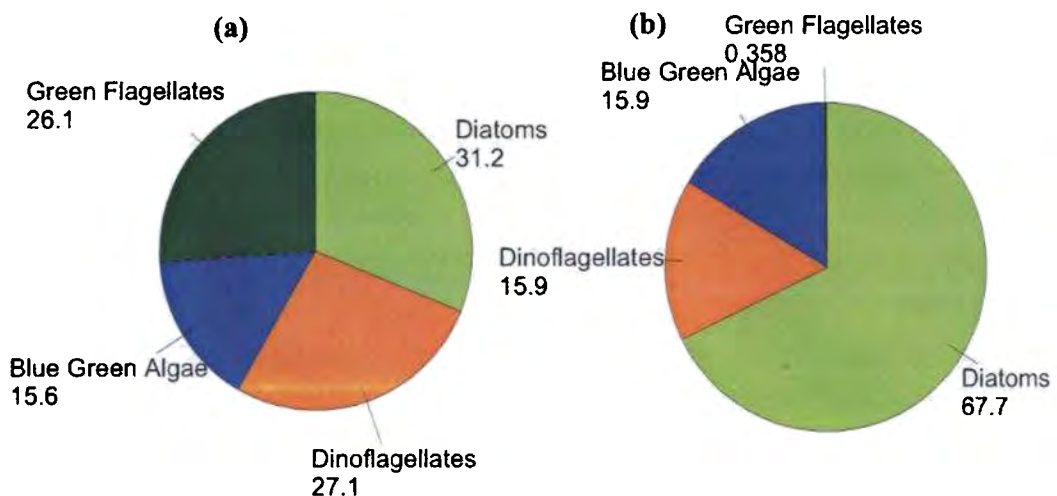


Fig. 5.28. Percentage composition of total phytoplankton density in the (a) inshore and (b) offshore waters of EAS during LSM

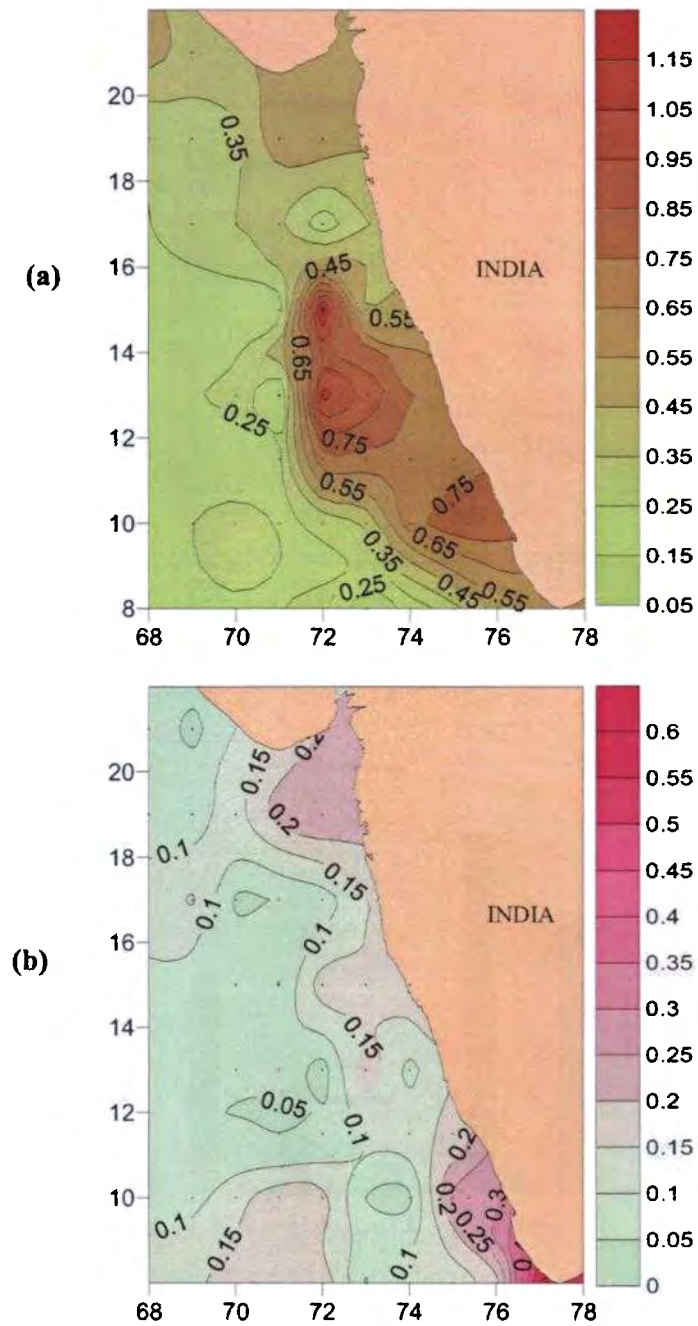


Fig. 5.29. Mesozooplankton distribution ( $\text{ml m}^{-3}$ ) in the (a) mixed layer and (b) thermocline layer in the EAS during LSM

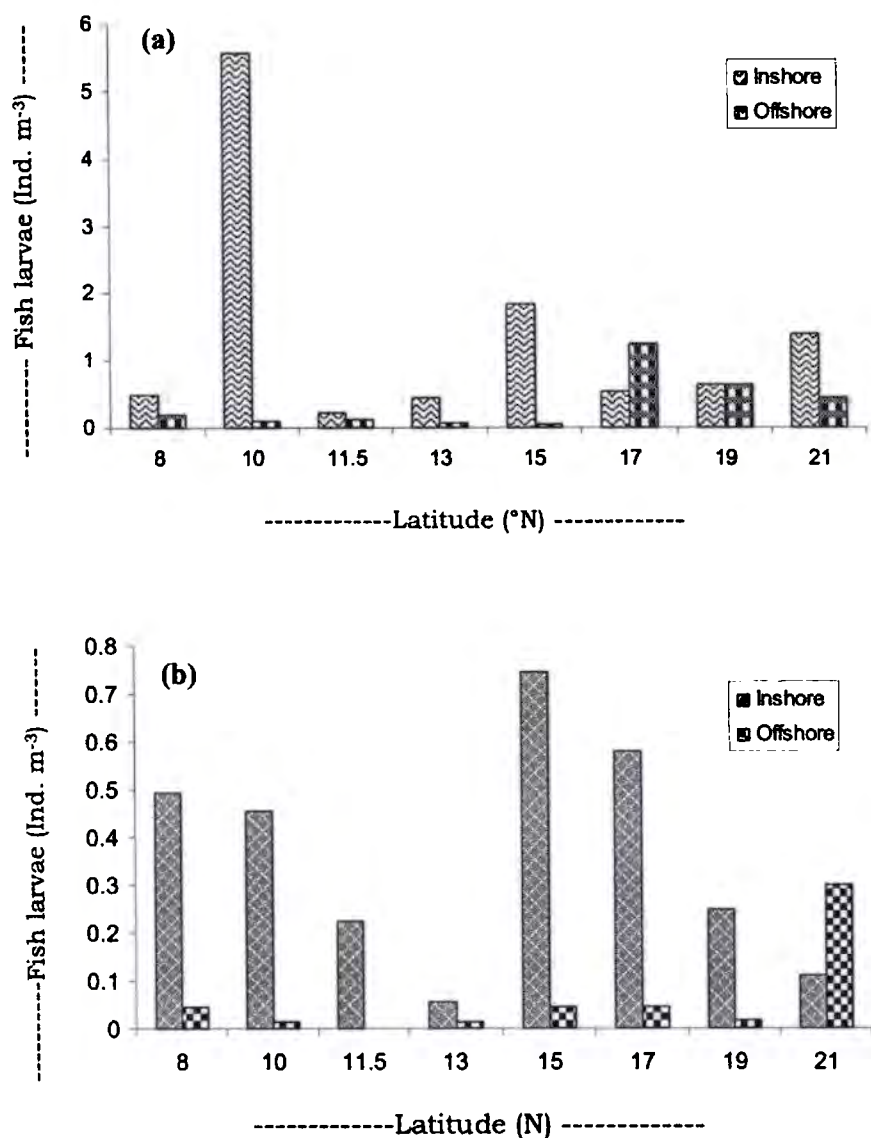


Fig. 5.30. Distribution of fish larvae (ind. m<sup>-3</sup>) in the (a) mixed layer and (b) thermocline layer during LSM

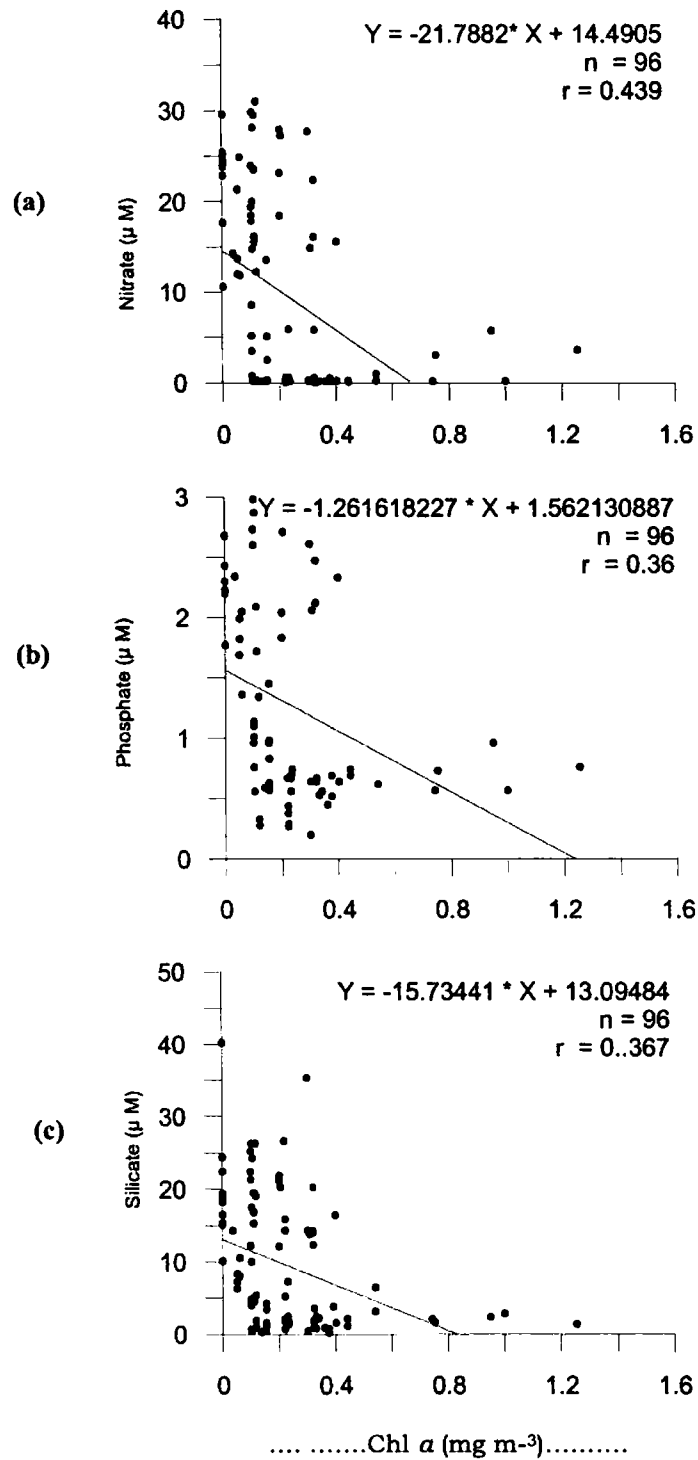


Fig. 5.31. Linear correlation of Chl  $a$  between (a) nitrate, (b) phosphate and (c) silicate during LSM

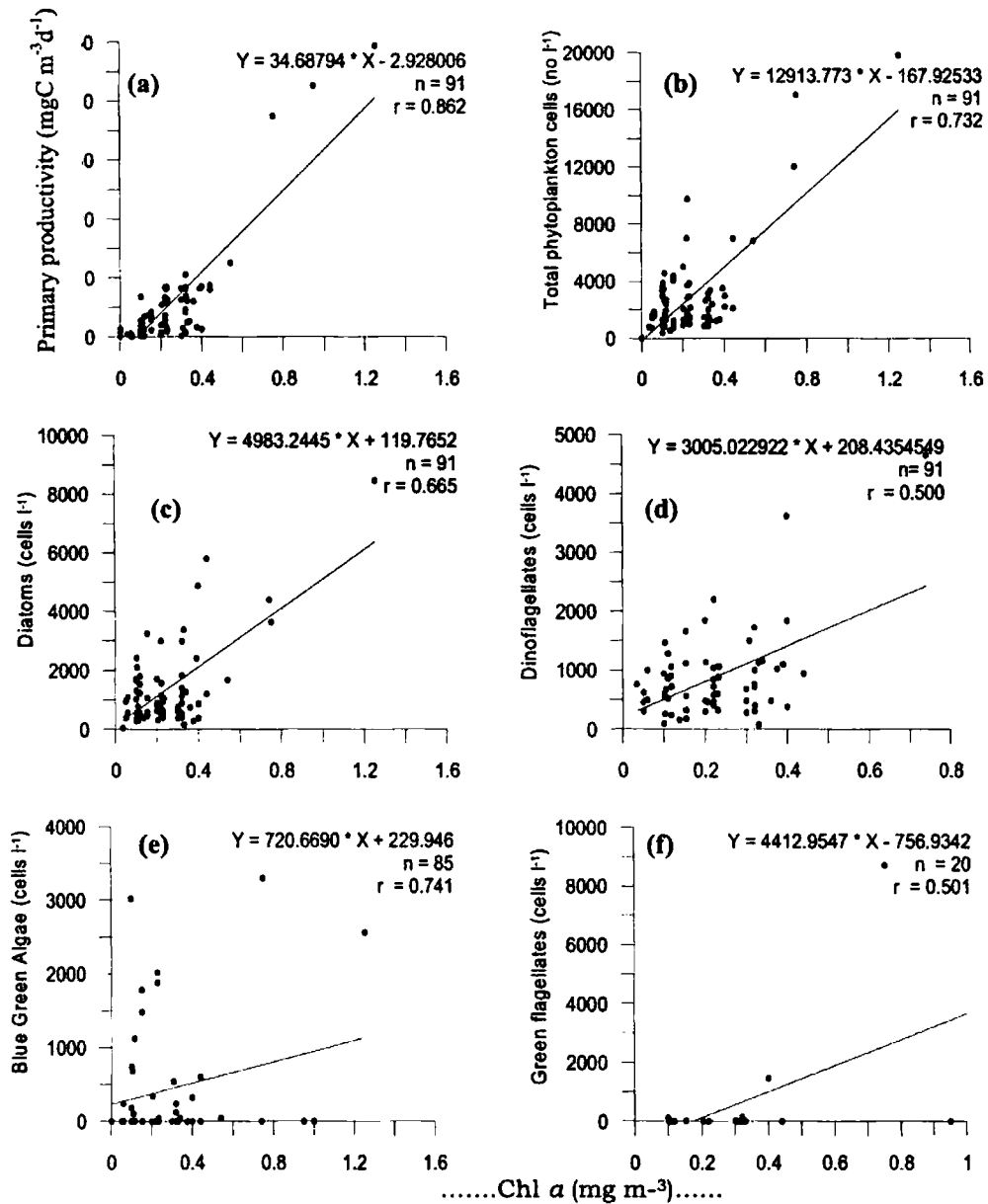


Fig. 5.32. Linear correlation of Chl a between (a) primary productivity (b) total phytoplankton density (c) diatoms (d) dinoflagellates (e) blue green algae and (f) green flagellates in the EAS during LSM

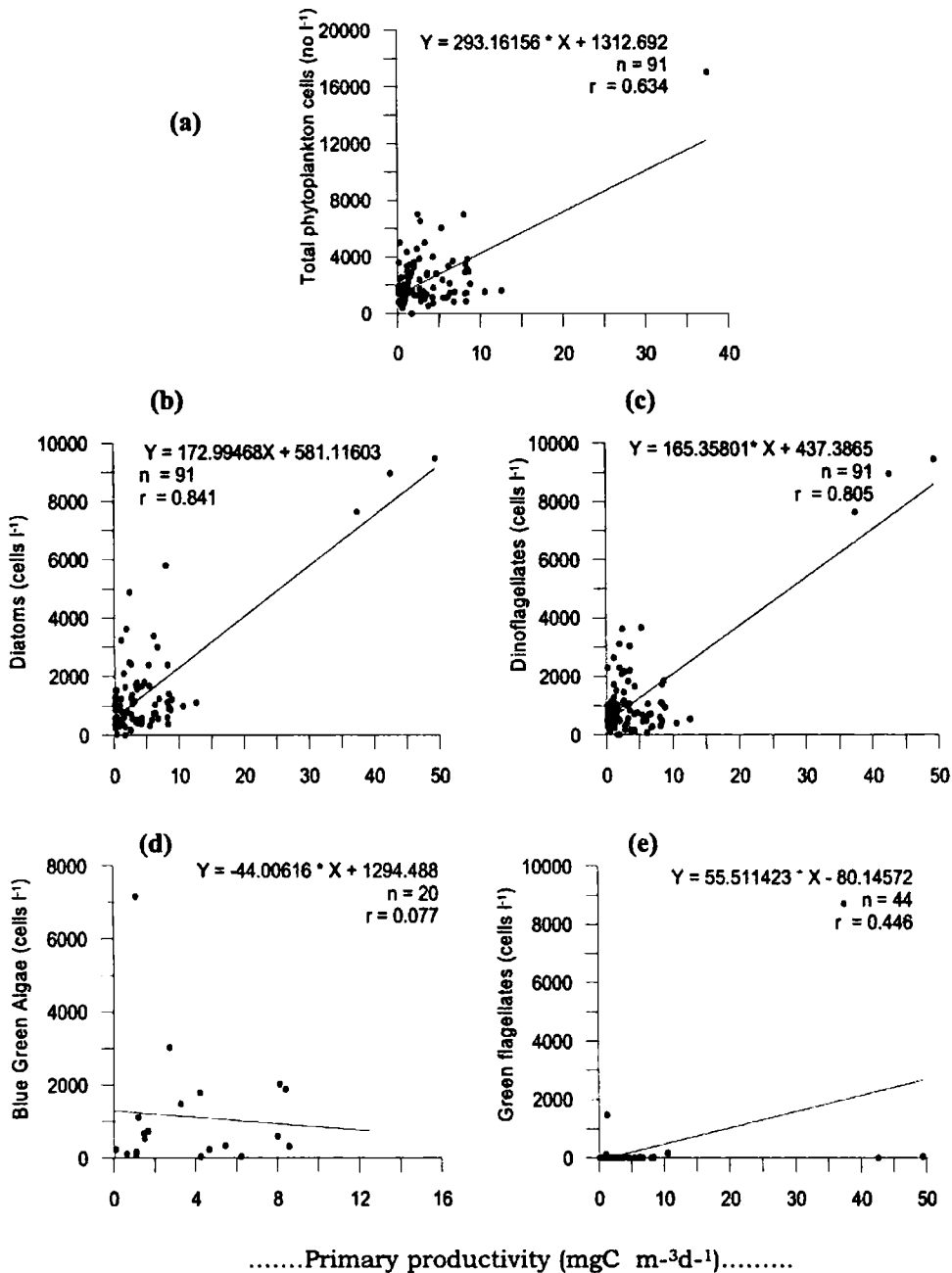


Fig. 5.33. Linear correlation of primary productivity between (a) total phytoplankton density (b) diatoms and (c) dinoflagellates (d) blue green algae and (e) green flagellates during LSM

Table 5.15. Primary productivity in the inshore and offshore waters of EAS during LSM

Latitude (°N)	Surface (mgC m <sup>-3</sup> d <sup>-1</sup> )		Column (mgC m <sup>-3</sup> d <sup>-1</sup> )	
	Inshore	Offshore	Inshore	Offshore
8	10.5	6.6	568	376
10	37.4	8.2	1630	572
13	5.3	2.0	255	243
15	8.4	5.8	311	173
17	8.8	10.7	218	-
19	8.1	4.2	308	199
21	4.2	6.7	179	275
<b>Average</b>	<b>11.8</b>	<b>6.3</b>	<b>496</b>	<b>306</b>

Table 5.16. Chl *a* in the inshore and offshore waters of EAS during LSM

Latitude (°N)	Surface (mg m <sup>-3</sup> )		Column (mgm <sup>-2</sup> )	
	Inshore	Offshore	Inshore	Offshore
8	0.32	0.22	30.70	30.83
10	0.75	0.39	60.70	41.54
13	0.74	0.22	29.03	16.37
15	0.12	0.36	14.96	14.15
17	0.44	0.22	24.89	14.37
19	0.23	0.15	23.60	20.67
21	0.32	0.10	16.00	13.17
<b>Average</b>	<b>0.42</b>	<b>0.24</b>	<b>28.55</b>	<b>21.59</b>

Table 5.17. Phytoplankton density in the inshore and offshore waters of EAS during LSM

Latitude (°N)	Surface (cells L <sup>-1</sup> )		Column (x10 <sup>6</sup> cells m <sup>-2</sup> )	
	Inshore	Offshore	Inshore	Offshore
8	1540	3720	357.5	278.8
10	17060	3500	477.5	183.75
13	6060	9760	317.3	353.1
15	3140	1100	297.2	212.65
17	2100	4020	204.85	175.0
19	2940	720	162.2	189.0
21	1120	820	206.65	186.3
<b>Average</b>	<b>4851</b>	<b>3377</b>	<b>289.0</b>	<b>226.0</b>

*Biological responses to upwelling events in the different phases of summer monsoon*

Table 5.18. Abundance of diatoms, dinoflagellates and blue green algae in the surface of inshore and offshore waters of EAS during LSM

Latitude (°N)	Inshore (cells L <sup>-1</sup> )				Offshore (cells (cells L <sup>-1</sup> ))			
	Diatoms	Dino	Blue green algae	Green flagellates	Diatoms	Dino	Blue green algae	Green flagellates
8	980	400	0	160	3000	720	0	.
10	3640	1460	3300	8700	2400	1100	0	-
13	2400	3660	0	-	7960	3100	0	-
15	1400	1720	0	20	520	580	-	.
17	1200	940	0	-	560	1660	1780	20
19	600	320	2020	-	580	140	-	20
21	400	720	0	-	560	260	-	-
<b>Average</b>	<b>1517</b>	<b>1317</b>	<b>760</b>	<b>2960</b>	<b>2226</b>	<b>1080</b>	<b>445</b>	<b>8</b>

Table 5.19. Abundance of diatoms, dinoflagellates and blue green algae in the upper 120m water column of inshore and offshore waters of EAS during LSM

Latitude (°N)	Inshore (x10 <sup>6</sup> cells m <sup>-2</sup> )				Offshore (x10 <sup>6</sup> cells m <sup>-2</sup> )			
	Diatoms	Dino	Blue green algae	Green flagellates	Diatoms	Dino	Blue green algae	Green flagellates
8	252.2	62.7	43.8	0.16	245.20	32.50	1.1	.
10	152.5	88.3	57.0	8.7	108.05	72.55	3	0.55
13	175.5	142.6	0.8	-	315.35	308.15	4.5	2.7
15	154.8	145.3	-	20	100.25	112.40	.	.
17	85.0	86.8	33.7	-	81.10	91.50	202.7	0.1
19	46.7	65.5	50.9	-	125.95	63.05	.	0.1
21	92.8	135.2	89.1	-	72.7	114.0	.	1.0
<b>Average</b>	<b>137</b>	<b>104</b>	<b>46</b>	<b>10</b>	<b>150</b>	<b>113</b>	<b>53</b>	<b>1</b>

Table 5.20 Mesozooplankton biomass in the mixed layer and thermocline layer of inshore and offshore waters of EAS during LSM

Latitude (°N)	Mixed layer (ind. m <sup>-3</sup> )		Thermocline layer (ind. m <sup>-3</sup> )	
	Inshore	Offshore	Inshore	Offshore
8	0.5	0.27	0.55	0.19
10	0.89	0.25	0.24	0.08
11.5	0.67	0.11	0.17	0.02
13	0.91	0.31	0.09	0.06
15	0.45	0.20	0.10	0.08
17	0.19	0.31	0.08	0.16
19	0.52	0.27	0.25	0.07
21	0.40	0.23	0.03	0.03
<b>Average</b>	<b>0.57</b>	<b>0.24</b>	<b>0.19</b>	<b>0.08</b>

Table. 5.21. Percentage (%) composition of mesozooplankton biomass during LSM

Mesozooplankton (%)	MLD	Thermocline
Foraminifera	0.18	0.22
Medusa	0.04	0.04
Siphonophore	0.79	0.58
Polychaeta	0.38	0.44
Pteropoda	0.25	0.24
Heteropoda	0.02	0.00
Gatropoda	0.08	0.11
Ostracoda	9.89	13.86
Copepoda	83.27	81.54
Amphipoda	0.35	0.07
Euphausiid	0.37	0.32
Decapoda	0.76	0.39
Stomatopoda	0.01	0.01
Chaetognatha	3.24	1.92
Salpa	0.14	0.04
Doliolida	0.09	0.09
Fisheggs	0.04	0.01
Fish larva	0.08	0.10

#### 5.2.4. Satellite chlorophyll imagery

Monthly averages of *SeaWiFS* chlorophyll concentration from May to October is presented in the Fig. 5.34. The present sensors used in *SeaWiFS* give abnormal values when cloud cover or some other abnormal interference such as land, etc. are present. So it was not possible to get enough data of daily and weekly Chl *a* concentration from satellite, so the monthly averages of the Chl *a* images are presented here. Spatial and temporal variations in Chl *a* concentration from OSM to LSM is very prominent in these images and these are in good agreement with the Chl *a* pattern observed in the *in situ* observations for the same period. During May Chl *a* concentration remain low compared to other months. However Chl *a*

Biological responses to upwelling events in the different phases of summer monsoon

concentration increased from June September and it is highest in September in the SEAS.

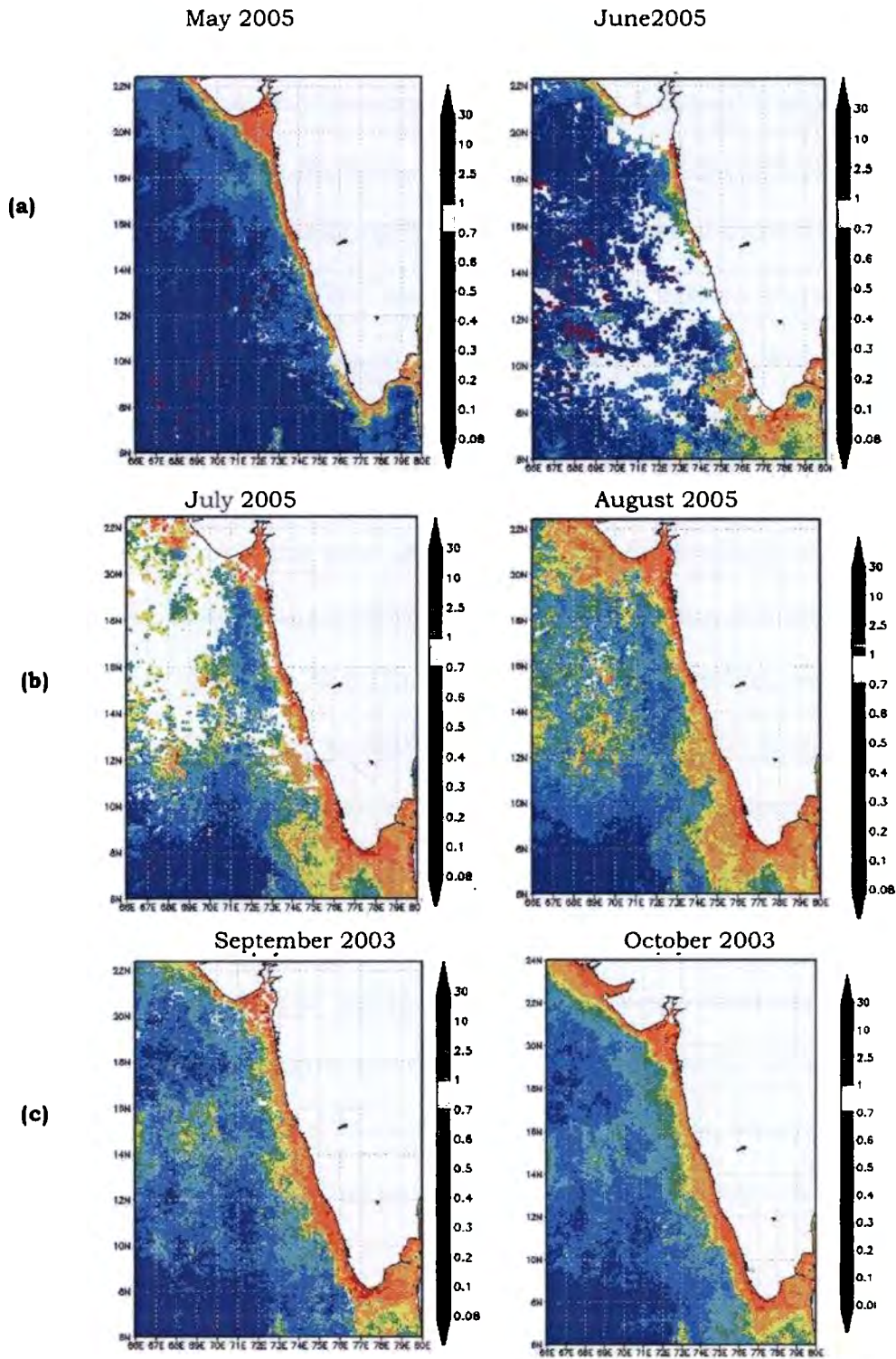


Fig. 5.34. Satellite derived chlorophyll concentration (Monthly average *SeaWiFS*) during (a) OSM (b) PSM and (c) LSM

#### **5.2.5. Pelagic fish landings**

The total fish landing along the west coast of India were analysed for the years 2003–2005. The source of data is the published data of marine fish landings in India by Central Marine Fisheries Research Institute (Srinath, *et al.*, 2006). The total fish landings and pelagic fish landings along the south west coast of India are presented in the Table 5.22. The state wise landings record showed clearest south - north variations in the pelagic fish landings (Fig. 5.35). Total and pelagic fish landing in Kerala was higher than other northern states. In Kerala pelagic fish landing contributed ~70% of the total fish landings during the year 2003-2005. Annual landings of oil sardine from the Kerala (southwest) coast of India during the year 2003 and 2004 are shown in the Fig. 5.36. Oil sardine landing was maximum ( $26.43 \times 10^4$  tonnes) in 2003 and 2004 ( $22.47 \times 10^4$  tonnes). In these years ~55% of the total pelagic fish landings were contributed by oil sardine. Oil sardine landing was found to be decreasing towards the northern states. Quarter wise landing records of oil sardine showed maximum landing in the last quarter (October–December) followed by first quarter (January–March) of the year. It would be interesting to analyze the landings on monthly basis (Fig. 5.37), which showed that total pelagic fish landing peaks in the months of July - October.

Table. 5.22. Annual total fish landing and pelagic fish landing along the west coast of India during the year 2003-'05

State	2003			2004			2005		
	Total Landings	Pelagic	% of pelagic fishery	Total Landings	Pelagic	% of pelagic fishery	Total Landings	Pelagic	% of pelagic fishery
Kerala	623293	443869	71%	616839	414723	67%	536245	384835	71%
Karnataka	184075	93244	50%	198216	114111	59%	224041	132527	59%
Goa	95890	69962	72%	83147	61508	73%	81601	65515	80%
Maharashtra	415094	146007	35%	350712	123618	35%	282375	87479	30%
Gujarat	444105	190726	42%	408982	17228	42%	421873	184395	43%

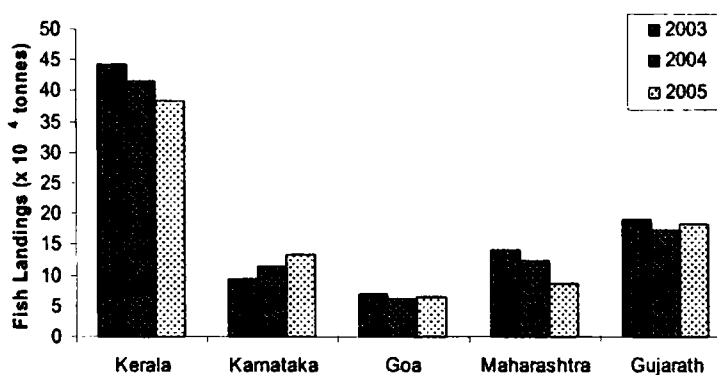


Fig. 5.35. Annual total pelagic fish landings in the west coast of India during the year 2003-'05

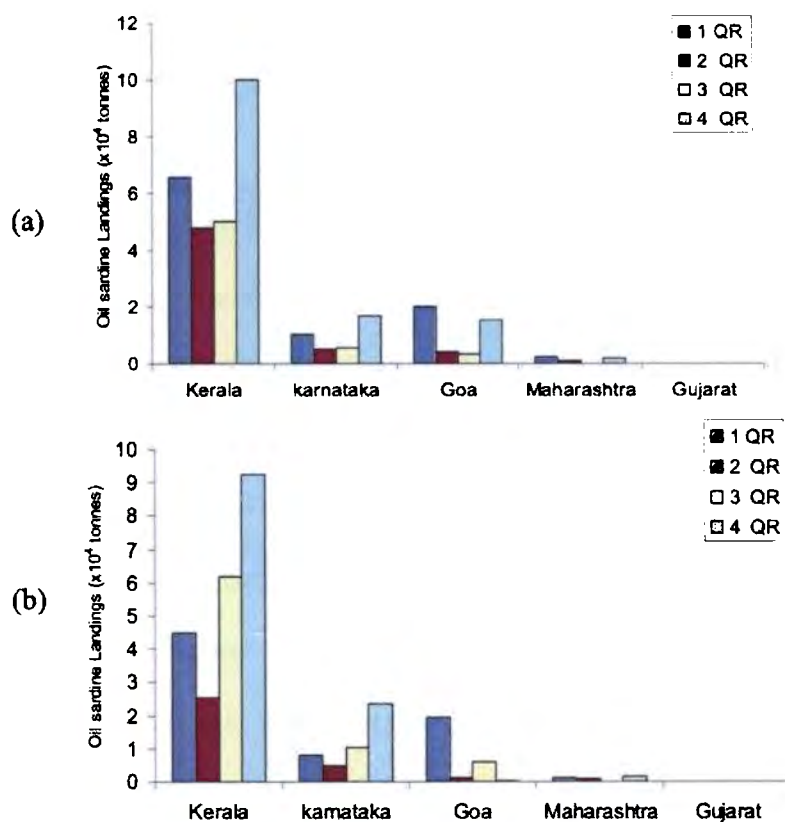


Fig. 5.36. Quarter wise oil sardine landings in the west coast of India during the year (a) 2003 and (b) 2004

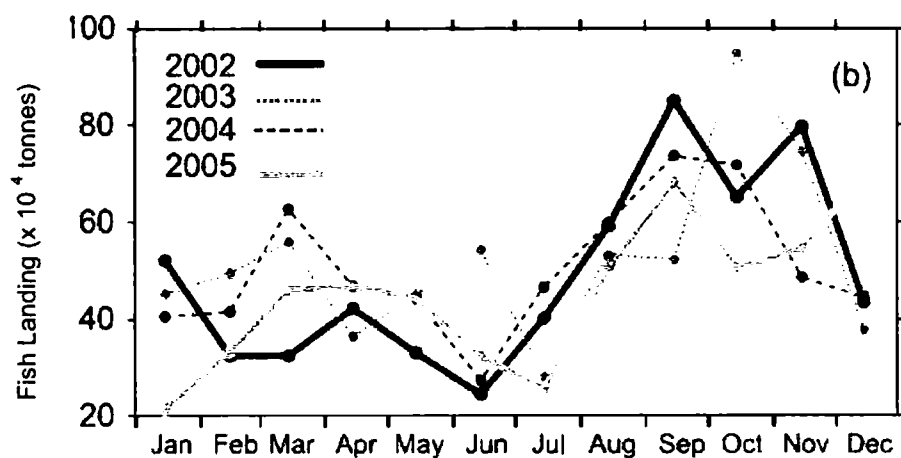


Fig. 5.37. Monthly total pelagic fish landings (tonnes) along the south west coast of India for the years 2002-'05 (Courtesy: Gopalakrishna, et al., 2008)

### **5.3. Discussion**

Arabian Sea is an oceanic basin, where the annual monsoons represent one of the most dynamic interactions between the ocean, atmosphere and continents (Clemens, *et al.*, 1991), propelling one of the most energetic current systems in the world (Elliot and Savidge, 1990). The seasonally varying surface currents, which respond to shifts in the monsoonal winds, drive variations in upwelling intensity and mixed layer distributions of temperature, nutrient concentration and primary production (Wyrtki, 1973). By May, the strong southwest monsoon, i.e., onset of summer monsoon (OSM) and associated anticyclonic currents have begun to develop. The summer monsoon reaches its peak, (PSM) in July/August. The resultant circulation persists until the collapse of the south west monsoon in September/October, i.e., late summer monsoon (LSM). The comparative study of different upwelling phases of the summer monsoon revealed spatial heterogeneity in productivity patterns. The asymmetry of the monsoon leads to spatial variability in biological responses in the basin.

In this chapter, relevant data are presented to illustrate the changes in physico-chemical properties and its biological responses to upwelling during summer monsoon. The study also emphasizes the influence of upwelling intensities on the biological productivity patterns with the existence of 3 types of upwelled waters *viz.*, newly upwelled water (Type I), mature upwelled water (Type II) and aged upwelled water (Type III).

With the onset of the summer monsoon, the winds begin to blow from the southwest over most of the northern Indian Ocean. The *Ekman* drift reverses to flow eastward over most of the Arabian Sea; it is south eastward in the eastern Arabian Sea, where the winds blow more from the west (Shankar, *et al.*, 2002). The wind blowing parallel to the coast generates offshore transport, which causes coastal upwelling between May and September. Sub-surface contours of temperature, salinity, and nutrients across the shelf exhibited a marked upwards deflection close to the coast which is consistent with upwelling. Within the upwelled area, the uplift of deep water results in colder temperatures, a shallow thermocline and enhanced nutrients in surface waters, which in turn gives rise to spectacularly high rates of primary and new production during the summer monsoon. This makes the basin one of the most productive regions of the world oceans (Nair, *et al.*, 1989).

Consistent with the progression of the southwest monsoon, the vertical structure of the surface layer changed markedly between June and September. The onset of summer monsoon (May-June) marks the beginning of upwelling along the SW coast of India (Sharma, 1966). It was clearly indicated that the northward propagation of upwelling events during the summer monsoon (Unnikrishnan and Antony, 1992) persists till October. The time of commencement of upwelling differs from depth to depth along the west coast of India. Off Kochi, the water at and below 100 m moves upright from February onwards while at 30 m depth upwelling starts in April. The upwelled water reaches the

*Biological responses to upwelling events in the different phases of summer monsoon*

surface in late May and persists up to July/August. The downward movement sets in by the end of August at all depths and earlier in deeper layers (Sharma, 1966). From the present study also it is clear that intensity of upwelling shows northward propagation and it varies because of the variability in wind stress.

***Upwelling intensities and biological responses***

The influence of wind blowing from the north to south and the Ekman transport from the inshore surface layers to offshore, replaces the deeper nutrient rich water to surface layers. This creates a density gradient, which is offset by the coriolis force and hence a geostrophic current is created (Yenstsch and Phinney, 1992). Maintenance of geostrophic transport requires the Ekman transport to continue to move offshore. By this process dense nutrient rich water enters the euphotic zone and consequently enhances the productivity (Prasanna Kumar, *et al.*, 2001). A relaxation in wind field will reduce the Ekman pumping of deep water to the surface of coastal waters, resulting in lesser supply of nutrients afterwards. In short, wind speed and direction along with the coastal orientation constitute a combination of physical factors ideal for upwelling and resultant biological responses during summer monsoon.

In upwelling regions, the distribution of phytoplankton biomass and production are strongly influenced by the combined effect of physico-chemical processes and are related to the strength of upwelling events and the subsequent ageing of the upwelled water.

The relation between the distribution of Chl *a* and seasonal changes in wind pattern have been recognized by Nair, *et al.*, (1989); Banse (1987), Smith (1984) and Smith and Codispoti (1980). Mc Issac, *et al.*, (1985) suggested that temporal changes in nitrate uptake rates were due to the physiological adjustments of phytoplankton to their environment and also described a productivity cycle along the upwelling plume. In upwelling system, there exist a lag period between the onset of favourable wind condition and the onset of upwelling, during summer monsoon. Servian, *et al.*, (1982) have estimated a lag time of one month for the upwelling in the equatorial Atlantic Ocean. Vertical mixing regulates the supply of irradiance and nutrients, but it is never deep enough to limit phytoplankton productivity, and nitrogen does not appear to be a factor limiting phytoplankton growth. Vertical mixing, however, also affects grazing by diluting micro-grazers along with phytoplankton. It is argued that mixed layer deepening acts as a natural 'dilution experiment' that allows phytoplankton to escape grazing losses and grow (Marra and Barber, 2005), and thereby create the observed variability in phytoplankton biomass. The existence of a lag period prior to the development of maximum uptake rates is presumably a time during which phytoplankton adapt to increased irradiance.

During the entire upwelling events, surface Chl *a* values ranged from 0.10 to 1.98 mg m<sup>-3</sup> and surface primary productivity from 1.88 to 121.9 mgC m<sup>-3</sup>d<sup>-1</sup>. During September (LSM), the primary productivity and Chl *a* in the coastal AS was reported to vary from 235

Biological responses to upwelling events in the different phases of summer monsoon

to 511 mgC m<sup>-2</sup>d<sup>-1</sup> and 12 to 46mg m<sup>-2</sup> (Owens, *et al.*, 1993). Nair, *et al.*, (1973) reported high primary productivity of 2090 mgC m<sup>-2</sup>d<sup>-1</sup> from the Wedge Bank waters of southern tip of India during summer monsoon. Sumitra-Vijayaraghavan and Kumari (1989) also reported very high concentration of Chl *a* (3.2mgm<sup>-3</sup>) and primary productivity (232 mgC m<sup>-3</sup>d<sup>-1</sup>) from southern coastal peninsular India in June (OSM). Madhu (2004) reported high rate of primary productivity (1629 mgC m<sup>-2</sup>d<sup>-1</sup>) and Chl *a* (45.7 mgm<sup>-2</sup>) in the inshore stations of 8°N during summer monsoon. In the present observations also, highest rates of Chl *a* and primary productivity were obtained from off Kanyakumari, Kochi and Calicut transects during summer monsoon. During summer monsoon as a part of Indian JGOFS programme, Bhattathiri, *et al.*, (1996) reported increased primary productivity as a result of upwelling. According to this report, primary productivity was 1760 mgC m<sup>-2</sup>d<sup>-1</sup> off Mangalore, 660 mgC m<sup>-2</sup>d<sup>-1</sup> off Kochi and 440 mgC m<sup>-2</sup>d<sup>-1</sup> off Bombay. The northern transects showed lower rates of production and biomass values, suggesting that upwelling was not active to bring nutrients to the surface. The average primary productivity during the entire summer monsoon was 430 mgC m<sup>-2</sup>d<sup>-1</sup> with the highest values off Kochi (1630 mgC m<sup>-2</sup>d<sup>-1</sup>) and Calicut (1314 mgC m<sup>-2</sup>d<sup>-1</sup>) was recorded during the present study. In the Type I stage, the rate of primary production was low because of the low biomass of phytoplankton in the upwelled waters, although the high concentrations of nutrients provide a conducive environment for active growth of phytoplankton. This mismatch is due to the fact that there

Biological responses to upwelling events in the different phases of summer monsoon

is normally a lag between strong upwelling and high phytoplankton biomass, because the population needs time to take up the nutrients and grow (Barber, *et al.*, 1971). A lag period of one week in biological production was observed by Duarthe (1990). According to him the lag period is due to the physical adjustments of phytoplankton to the changed environment and the external factors such as turbulence, grazing, etc. In other upwelling areas (Barber and Smith, 1981; Brown and Field, 1986), it was shown that the delay between upwelling and the onset of phytoplankton growth is affected by the low initial biomass. This fact is well established at 8°N transect, during onset of summer monsoon, where the surface waters were enriched with nutrients but with low phytoplankton biomass. Fast rates of production were found in Type II stage where the relaxed wind stress allows the water column to get stabilized.

In the upwelling conditions, phytoplankton growth rate varied with groups. Diatoms were found to be important, although they were patchily distributed (Burkill, 1999). They always had higher growth rate (Garrison *et al.*, 2000) than dinoflagellates and silicoflagellates. Among diatoms, pennales like *Nitzschia* grew faster than centric diatoms as observed during the late summer monsoon. Smith and Codispoti (1980) reported phytoplankton population in the upwelling region off Somalia dominated by *Nitzschia delicatissima*, *Rhizosolenia styliformis* (pennate diatoms) and other diatoms characteristic of other upwelling regions reaching  $5.6 \times 10^5$  cells  $L^{-1}$ . In the present study *N. seriata* and *R. alata* were dominant. Malone (1980) reported that

larger diatoms often predominate in highly productive areas such as upwelling systems. Initial dominance of flagellates (nannoplankton) were completely taken over by diatoms during Type III stage at 8°N, where stable water column prevailed after upwelling and the nannoplankton population still persisted at 10°N during the late phase, where the upwelling was at a relaxed phase. Similar conditions were observed by Ishizaka, *et al.*, (1986) in the coastal waters of Japan, which was also experimentally substantiated by Takahashi, *et al.*, (1982). The dominance of diatoms has also been reported in other upwelled waters. For instance, Tont (1976) observed diatom abundance in continuously occurring large-scale upwelling over a long period of time. It can be concluded that diatoms became dominant when significant quantity of nutrients was supplied to the surface layers of inshore waters. However, at some locations phytoplankton, other than diatoms (green flagellates) were dominant, that could be due to the differences in the rate of nitrate assimilation. This was accompanied by a concomitant shift in the vertical distribution of the chlorophyll maximum, which moved from the surface to deep chlorophyll maximum (DCM) situated at 40-80 m.

Spatial changes in zooplankton biomass during different phases are related to the changes in phytoplankton community and standing stock. In the upwelling waters, the zooplankton stocks were high in response to high phytoplankton production. The zooplankton community responded to the changes in the phytoplankton community and showed spatial heterogeneity according to the

physical forcings during summer monsoon. Results from the JGOFS India cruises in the eastern and central Arabian Sea showed that the average standing stock and mixed layer abundance of mesozooplankton did not vary much among seasons i.e., SIM, SM and NEM (Nair, *et al*, 1999; Smith and Madhuprathap, 2005). Normally phytoplankton populations are able to respond rapidly to favourable conditions provided by upwelling waters, whereas the zooplankton response may be rather slow. But the consensus between high phytoplankton and zooplankton standing stock in the upwelling zone seems to be that phytoplankton production normally exceeds the consumption by the zooplankton. The present results suggest that zooplankton often does respond with the increased algal growth.

It is also noted that increased algal growth cannot be an immediate result of enhanced nutrient supply. In some cases, the uplifted, nutrient rich water lies under a shallow, sharp thermocline as observed at 13°N, during PSM. The mixed layer acts to store much of the solar heat input, and the depth of the mixed layer relative to the light input strongly influences the rate of primary production. Therefore, the relationship between mixed layer depth and Chl *a* should be obscure at any station. Denman and Marra (1986) demonstrated that large variations in the depth to which phytoplankton are mixed have a significant impact on their subsequent growth because of changes in the light field to which they are exposed. During the summer monsoon, wind mixing was vigorous and heating was not sufficient to stratify the water, so the MLD

remained consistently deep and nutrients were plentiful in the surface waters. The physical processes responsible for this deepening are convective mixing and wind stirring during the coastal upwelling and offshore *Ekman* pumping during the summer monsoon (Brock, *et al.*, 1994). It was clear that a combination of upward *Ekman* pumping and coastal upwelling combine to supply nutrients to the euphotic zone (Swallow, 1984). Oceanward of this axis, downward *Ekman* pumping, which acts to deepen the mixed layer and negatively impacts euphotic zone nutrient availability, was considered the dominant forcing mechanism (Bauer, *et al.*, 1992). During the later phase of summer monsoon, deep mixing and the influence of upwelled water advected from the coast were the likely causes of an enhanced contribution of diatoms. In the Arabian Sea, productivity seems to be regulated mainly by nutrient inputs from below the euphotic zone via upwelling and mixed layer deepening. In systems with short-duration mixing events (few days), such as upwelling zones, the phytoplankton community becomes structured with cells like chain-forming diatoms which have a fast and explosive growth, whereas more stable-stratified conditions with weak upwelling may favour primary production based on small sized fractions of phytoplankton or solitary diatoms (Brink, *et al.*, 1995; Wollast, 1998). In this study, the chain forming *Chaetoceros* spp. were abundant in most of the stations. However, chain-forming diatoms are replaced by small size phytoplankton with lower nutrients requirements and lower sinking rates when water column stratification conditions prevail.

Correlation between primary production and Chl *a* was significant during all the phases, with the highest correlation during the peak phase of upwelling ( $r = 0.83$ ,  $n=106$ ). As biomass level increase, the correlation also becomes stronger, indicating that upwelled nutrients have induced the phytoplankton growth. The correlation between Chl *a* and productivity were comparatively weak during the onset period ( $r = 0.63$ ,  $n = 91$ ), suggesting that upwelled waters either reached the subsurface layers or the phytoplankton community have not utilized the replenished nutrients in the surface layers. It is evident that the hydrography and the nutrients as well as its biological responses are well correlated and varied sequentially with the different phases or intensities of upwelling. The phytoplankton and zooplankton community may respond to a large number of biological, physical and chemical factors that may vary in time and space. The analysis of species composition showed that changes in the structure of the autotrophic community are expressed in both abundance and differences in species assemblages. The present study is an example of such environmental variability in a system characterized by prevailing upwelling conditions. These changes occur not only over the seasonal scale but also over the spatial pattern of distribution. It is relevant to note that these changes correlate well to temporal variability of upwelling and spatial variation of upwelling conditions over the cross shelf axis. It was found that such temporal and spatial variation is mostly explained by changes in upwelling conditions occurring seasonally and also over the cross-

shelf gradient. Remotely sensed monthly composite of Chl *a* concentration from the eastern Arabian Sea suggests that the increase of Chl *a* from June to September and August -September are the most productive months during summer monsoon when the mature stages of upwelled water can be observed in SEAS.

### ***Upwelling and oil sardine fishery***

The variability of oil sardine fishery mostly *Sardinella longiceps*, along the upwelling coast of south-western India was noted as early as 1865 when Day suggested that the stocks were so uncertain in their availability that a planned industrial expansion of the fishery would probably fail. Later, Thurston (1900) discussed the periodic decrease in oil sardine fishery. Since then many have tried to predict the availability of oil sardine in this region (Longhurst and Pauly, 1987; Longhurst and Wooster, 1990). Information on the relative abundance and recruitment variability of tropical pelagic fishery over long periods is rare. From the available data source, a base line figure was made as state wise landing pattern. Monthly landings are also represented in the Fig. 5.33 as reported by Gopalakrishna, *et al.*, (2008). As the upwelling process and the pelagic fishery production are strongly coupled (Madhupratap, *et al.*, 1994; Srinath, *et al.*, 2006), the reported pelagic fish landings along the southwest coast of India were examined for the years 2003 to 2005. Of the total marine fish landings, 73% of the catch originates from the west coast of India. Oil sardine forms the dominant group among the pelagic groups. It is a

planktivore and forms one of the few clupeoids in which diatoms form a significant part of the adult diet. Annual landings of oil sardine from the Kerala (southwest) coast of India during the year 2003 and 2004 are shown in the Figs. 5.35 & 5.36. Oil sardine landing was maximum ( $26.43 \times 10^4$  tonnes) in 2003 and 2004 ( $22.47 \times 10^4$  tonnes). In these years ~55% of the total pelagic fishery was contributed by oil sardine. Higher productivity ( $<1300 \text{ mgCm}^{-2}\text{d}^{-1}$ ) was noticed during these years corresponding with intense upwelling. Oil sardine landing was found to be decreasing towards the northern states and the upwelling intensities also diminish after  $15^\circ\text{N}$ .

Hornell (1910) noted that the first arrival of sardine at the coast coincides with a diatom bloom and has been suggested that the migrations are timed to coincide with the blooms of *Nitzschia oceanica*. In the present observations, the diatoms form the abundant group during the upwelling season, with the abundance of *Nitzschia* in most of the stations. This is an example of match – mismatch hypothesis in the plankton and fish production as in the case of cod and *Calanus* production in the European water. Synchrony between the peak in phytoplankton abundance and arrival fish larvae, the so called ‘match - mismatch hypothesis’ has been put forwarded for Cod – *Calanus finamarichus* and diatom in north Atlantic and for anchovies along Peruvian coast (Hays, *et al.*, 2005). The initial abundance of diatoms at the start of the monsoon season is in correlation with the arrival of pre-spawning adults and in the mid-summer monsoon coincides with the main fishery for juveniles (Nair, 1960) along with dinoflagellates.

Biological responses to upwelling events in the different phases of summer monsoon

But since, there exists no time series index of diatom abundance; it has never been possible to associate diatom abundance statistically with heavy landings. In fact, some have interpreted their observations of the fishery to suggest that diatom abundance may merely act as a local attractant for sardine shoals (Raja, 1969). There are some important resemblances between pelagic community of other upwelling coasts that include sardine, anchovy and mackerel (Longhurst, 1971; Bakun and Parrish, 1982). Integration between the different consequences of variable upwelling strength has been achieved by Cury and Roy (1989) for the cases of the Peruvian (*Sardinops sagax*, *Engraulis ringens*) and West African clupeoids (*Sardina pilchardus*, *Sardinella aurita* and *S. madrasensis*). Madhupratap, *et al.*, (2001), related the Arabian Sea productivity and potential fisheries and showed that the poor catch during April to June due to low primary productivity and the same condition was noticed in the south-eastern Arabian Sea during 2003-2005. But fairly high catches of clupeids during summer monsoon along the southwest coast show that they indeed flourish during this season and it should be noted that landings may not be truly representative since fishing is either prohibited or comparatively less during peak summer monsoon. The total fish landing of records and the abundance of oil sardine in the south west coast is in good agreement with the hydrographic conditions and plankton productivity pattern of the west coast of India. It could be pointed out that better landings pelagic fishes after the summer monsoon along the south west coast is

mainly due to the upwelling and plankton productivity (Madhupratap, *et al.*, 1994). Thus it could be noted that the better landings during late phase and after (September-October) is mainly due to fair weather plus the oceanographic conditions with the advantages of different intensities of upwelling.

## References

- Bakun, A. and Parrish, R.H., 1982. Turbulence, transport and pelagic fish in the California and Peru Current systems. *Rep. Cal. Co-op. Ocean. Fish. Invest.*, 23: 99-112.
- Banse, K., 1968. Hydrography of the Arabian Sea shelf of India and Pakistan and effects on demersal fishes. *Deep Sea Res.*, 15: 45-79.
- Banse, K., 1987. Seasonality of phytoplankton chlorophyll in the central and northern Arabian Sea. *Deep Sea Res.*, 34: 713-723.
- Barber, R. T. and Smith, R. L., 1981. Coastal upwelling ecosystems. In: Longhurst, A.R. (Ed). *Analysis of Marine Ecosystems*. Academic Press, London, U. K. pp: 31-68.
- Barber, R.T., Dugdale, R.C., Mc Issac, J.J. and Smith, R.G., 1971. Variation in phytoplankton growth associated with source conditioning of upwelled water *Invest. Pesq.* 35 (1): 171-173.
- Barlow, R.G, 1982. Phytoplankton ecology to the Southern Benguela Current I, Biochemical composition. *J. Exp. Mar. Biol. Ecol.*, 63: 209-227.
- Barton, E.D., Huyer, A. and Smith, R.L, 1977. Temporal Variation observed in the hydrographic regimes near Carbo Cobeiro in the north west African upwelling region, February to April 1974. *Deep Sea Res.*, 24: 7-24.
- Bauer, S., Hitchcock, G.L. and Olson, D.B., 1992. Response of the Arabian Sea surface layer to monsoon forcing. In: Desai, B.N. (Ed.), *Oceanography of the Indian Ocean*. Oxford & IBH, New Delhi, pp: 659-672.
- Bhattathiri, P.M.A., Pant, A., Sawant, S., Gauns, M., Matondkar, S.G.P. and Mohanraju, R., 1996. Phytoplankton production and chlorophyll distribution in the eastern and central Arabian Sea. *Curr. Sci.*, 71(11): 857-862.
- Brink, K., Abrante, F., Bernal, P., Estrada, M., Hutchings, L., Jahnke, R., Müller, P. and Smith, R., 1995. Group report: how do coastal upwelling systems operate as integrated physical, chemical, and

- biological systems and influence the geological record? The role of physical processes in defining the spatial structures of biological and chemical variables. In: Summerhayes, C., Emeis, K., Angel, M., Smith, R., Zeitzschel, B., (Eds.), *Upwelling in the Oceans: Modern Processes and Ancient Records*. John Wiley & Sons, pp: 103–125.
- Brock, J., Sathyendranath, S. and Platt, T., 1994. A model study of seasonal mixed layer primary production in the Arabian Sea. *Proc.Indian Acad. Sci., (Earth Planet. Sci.)*,103:163–176.
- Brown, P.C. and Field, J.J., 1986. Factors limiting phytoplankton production in a near shore upwelling area. *J. Plankton Res.* 8(1): 558.
- Burkill, P.H., 1999. ARABESQUE: an overview. *Deep Sea Res. II* 46 (3–4): 529–547.
- Clemens, S.C., Prell, W., Murray, D., Shimmield, G., Weedon, G., 1991. Forcing mechanisms of the Indian Ocean monsoon. *Nature*,353: 720–725.
- Cury, P. and Roy, C., 1989. Optimal environmental window and pelagic fish recruitment success in upwelling areas. *Can. J. Fish. Aquat. Sci.*, 46: 670–680.
- Day, F., 1865. *The Fishes of Malabar*, B. Quaritch, London, 293p.
- Denman, K.L. and Marra, J., 1986. Modelling the time dependent photoadaptation to fluctuating light. In: Nihoul J.C.J. (Ed.) *Marine interface eco-hydrodynamics*. Elsevier, Amsterdam, pp: 341–359.
- Duarthe, C.M., 1990. Time lag in algal growth: Generality, causes and consequences. *J. Plankton Res.*, 120: 873–883.
- Elliot, A. J. and Savidge, G., 1990. Some features of upwelling off Oman. *J. Mar. Res.*, 48: 319–333.
- Gardner, W.D., Gundersen, J.S., Richardson, M.J. and Walsh, I.D., 1999. The role of seasonal and diel changes in mixed-layer depth on carbon and chlorophyll distributions in the Arabian Sea. *Deep Sea Res. II*, 46: 1833–1858.
- Garrison, D.L., Gowing, M.M., Hughes, M.P., Campbell, L., Caron, D.A., Dennett, M.R., Shalapyonok, A., Olson, R.J., Landry, M.R., Brown, S.L., Liu, H.B., Azam, F., Steward, G.F., Ducklow, H.W., and Smith, D.C., 2000. Microbial food web structure in the Arabian Sea: a US JGOFS study. *Deep Sea Res. II* 47: 1387–1422.
- Gopalakrishna, V.V., Rao, R.R., Nisha, K., Girishkumar, M.S., Pankajakshan, T., Ravichandran, M., Johnson, Z., Girish, K., Anishkumar, N., Srinath, M., Rajesh, S. and Rajan, C.K., 2008. Observed anomalous upwelling in the Lakshadweep Sea during the summer monsoon season of 2005. *J. Geophys. Res.*, 113C05001, doi: 10.1029/2007JC004240, 2008.

Biological responses to upwelling events in the different phases of summer monsoon

- Halpern, D., 1976. Structure of coastal upwelling event observed off Goa during July 1973. *Deep Sea Res. II*, 23: 495-508.
- Hays, G.C., Richardson, A.J. and Robinson, C., 2005. Climate change and marine plankton. *Trends in Ecology and Evolution*, 20(6): 337-344.
- Hornell, J., 1910. Report of the results of a fishery cruise along the Malabar Coast and to Laccadive islands. *Madras Fish. Bull.*, 4: 71-126.
- Ishizaka, J., M. Takahashi and Idimeira, 1986. Changes in the growth rate of phytoplankton in local upwelling around the Izu Peninsula, Japan. *J. Plankton. Res.*, 8(1): 169-181.
- Longhurst, A.R. and Pauly, D., 1987. *Ecology of tropical oceans*. Academic Press, San Diego, pp: 1-407.
- Longhurst, A.R. and Wooster, W.S., 1990. Abundance of oil sardine (*Sardinella longiceps*) and upwelling on the southwest coast of India. *Can. J. Fish. Aquat. Sci.*, 47: 2407-2419.
- Longhurst, A.R., 1971. The clupeid resources of tropical seas. *Oceanogr. Mar. Biol.*, 9: 349-385.
- Madhu, N.V., 2004. Seasonal studies on primary production and associated environmental parameters in the Indian EEZ. *PhD. Thesis, Cochin University of Science and Technology*, 234p.
- Madhupratap, M., Nair, K.N.V., Venugopal, P., Gauns, M., Haridas, P., Gopalakrishnan, T.C. and K.K.C. Nair, 2001. Arabian Sea Oceanography and Fisheries. *Curr. Sci.*, 81(4): 355-361.
- Madhupratap, M., Shetye, S.R., Nair, K.N.V. and Sreekumaran Nair, 1994. Oil Sardine and Indian Mackerel: their fishery, problems and coastal oceanography. *Curr. Sci.*, 66: 340-348.
- Malone, T.C., 1980. Size-fractionated primary productivity of marine phytoplankton. In: Falkowski, P.G. (Ed.), *Primary productivity in the sea*. Plenum Press, New York, pp: 301-319.
- Mantora, R.F.C., Law, C.S., Owens, N.J.P., Burkil, P.H., Woodward, E.M.S., Howland, R.J.M. and Llewellyn, C.A., 1993. Nitrogen biochemical cycling in the northwestern Indian Ocean. *Deep Sea Res. II*, 40: 651-671.
- Marra, J., Barber, R.T., 2005. Primary productivity in the Arabian Sea: a synthesis of JGOFS data. *Prog. Oceanogr.*, 65(2-4): 159-175.
- Mc Issac, J.J, Dugdale, R.C, Barber, R.T, Blasco and Packard, T.T 1985. Primary production in the upwelling center, *Deep Sea Res. II*, 32: 503-529.
- Nair, K.K.C., Madhuprathap, M., Gopalakrishnan, T.C. and Haridas, P., 1999. The Arabian Sea: Physical Environment, Zooplankton and Myctophid abundance. *Indian J. Mar. Sci.*, 28: 138-145.
- Nair, P.V.R., Samuel, S., Joseph, K.J. and Balachandran, V.K., 1973. Primary production and potential fishery resources in the seas around India. In: *Proc. Symp. Living Resources of the Sea around India, 1968. Spl. Publ. Cent. Mar. Fish. Res. Inst., Kochi*, pp: 184-198.

Biological responses to upwelling events in the different phases of summer monsoon

- Nair, R.R., Ittekkot, V., Manganini, S.J., Ramaswamy, V., Haake, B., Degens, E.T., Desai, B.N. and Hanjo, S., 1989. Increased particle flux to the deep ocean related to monsoon. *Nature*, 338: 749-751.
- Nair, R.V., 1960. Synopsis of the biology and fishery of the Indian sardine (Species synopsis # 11). *Proc. FAO World Sci. Meeting on the Biology of Sardine*, 2: 329-414.
- Owens, N.J.P., Burkill, P.H., Mantoura, R.F.C., Woodward, E.M.S., Bellan, I.E., Aiken, J., Howland, R.J.M. and Llewellyn, C.A., 1993. Size fractionated primary production and nitrogen assimilation in the western Indian Ocean. *Deep Sea Res.*, II, 40: 697-709.
- Prasanna Kumar, S., Madhupratap, M., Dileepkumar, M., Gauns, M., Muraleedharan, P.M., Sarma, V.V.S.S. and D' Souza, S., 2000. Physical control of primary productivity on a seasonal scale in central and eastern Arabian Sea. *Proc. Indian Acad. Sci. (Earth and Planet. Sci)*, 109(4): 433-441.
- Prasanna Kumar, S., Madhupratap, M., Kumar, M.D., Muraleedharan, P.M., D' Souza, S.N., Gauns, M. and Sarma, V.V.S.S., 2001. High biological productivity in the central Arabian Sea during the summer monsoon driven by Ekman pumping and lateral advection. *Curr. Sci.*, 81: 1633-1638.
- Qasim, S.Z., 1977. Biological productivity of the Indian Ocean. *Indian J. Mar. Sci.*, 6: 122-137.
- Qasim, S.Z., 1982. Oceanography of the northern Arabian Sea. *Deep Sea Res.*, II, 29: 1041-1068.
- Radhakrishna, K., Devassy, V.P., Bhargava, R.M.S. and Bhattathiri, P.M.A., 1978. Primary production in the Northern Arabian Sea. *Indian J. Mar. Sci.*, 7: 271-275.
- Raja, B.T.A., 1969. The Indian Oil Sardine. *Bull. Cent. Mar. Fish. Res. Inst.*, 16: 1-28.
- Rodriguez, E.G, Valentine, J.L., Andre, D.L. and Jacob, S.A., 1992. Upwelling and down welling at Cabo Frio (Brazil). Comparison of biomass and production responses. *J. Plankton. Res.*, 14(2): 289-306.
- Roy, R., Pratihary, A., Mangesh, G. and Naqvi, S.W.A., 2006. Spatial variation of phytoplankton pigments along the southwest coast of India. *Estuar. Coast. Shelf Sci.*, 69: 189-195.
- Ryther, J.H., 1969. Photosynthesis and fish production in the sea. *Science*, 166: 72-80.
- Sankaranarayanan, V.N., Rao, D.P. and Antony, M.K., 1978. Studies on some hydrographic characteristics of estuarine and inshore waters of Goa during the southwest monsoon 1972. *Mahasagar- Bull. Natl. Inst. Oceanogr.*, 11: 125-136.
- Sastry, J.S. and D'Souza, R.S., 1972. Upwelling and upward mixing in the Arabian Sea. *Indian J. Mar. Sci.*, 1: 17-27.
- Servain, S.J, Picaut and J. Merle, 1982. Evidence of remote sensing in the equatorial Atlantic Ocean. *Journal of Physic. Oceanogr.*, 12: 457-463.

Biological responses to upwelling events in the different phases of summer monsoon

- Shankar, D., Vinayachandran, P.N. and Unnikrishnan, A.S., 2002. The monsoon currents in the north Indian Ocean. *Prog. Oceanogr.*, 52: 63-120.
- Sharma, G.S., 1966. Seasonal variations of some hydrographic properties of the shelf waters off the west coast of India. *Proc. Symp. Indian Ocean., Bull. Natl. Inst. Sci., India*, pp: 38.
- Smith, S.L., 1984. Biological indications of active upwelling in the northwestern Indian Ocean, in 1964 and 1979 and a comparison with Peru and northwest Africa. *Deep Sea Res.*, 31: 951-961.
- Smith, S.L., and Codispoti, L.A., 1980. Southwest monsoon of 1979: Chemical and biological response of Somali coastal waters. *Science*, 209: 597-600.
- Smith, S.L., Madhuprathap, M., 2005. Mesozooplankton in the Arabian Sea: pattern influenced by season, upwelling and oxygen concentration. *Prog. Oceanogr.*, 65: 214-231.
- Srinath, M., Somy Kuriakose, P.L. Ammini, C.J. Prasad, K. Ramani and Beena, M.R., 2006. Marine Fish Landings in India, 1985-2004. Estimates and Trends. *CMFRI Spl. Publ.*, No. 89, 161pp.
- Sumitra-Vijayaraghavan and Kumari, L.K., 1989. Primary productivity in the south-eastern Arabian Sea during southwest monsoon. *Indian J. Mar. Sci.*, 18: 30-32.
- Swallow, J.C., 1984. Some aspects of the physical oceanography of the Indian Ocean. *Deep Sea Res. I*, 31: 639-650.
- Takahashi, M., Kerke, I., Isaki, K., Branfang, P.K. and Hatton, A., 1982. Phytoplankton species responses to nutrient changes in experimental enclosures and coastal waters. In: Grice, G.D. and Reeve, M.R. (Eds.). *Marine Mesocosms*. Springer Verlag, NY, pp: 33-340.
- Thurston, E., 1900. The sea fisheries of Malabar and South Kanara. *Madras Govt. Mus. Bull.*, 3: 93-183.
- Tont, S.A., 1976. Short period climate fluctuation effects on diatom biomass. *Science*, 194: 942-944.
- Unnikrishnan, A.S. and Antony, M.K., 1992. On an upwelling front along the west coast of India during later part of southwest monsoon. In: Physical process in the Indian seas. *Proc. First. Convention, ISPO 1990*. pp: 131-135.
- Wiggert, J.D., Hood, R.R. and Banse, K., 2005. Kindle Monsoon-driven biogeochemical processes in the Arabian Sea. *Prog. Oceanogr.*, 65: 176-213.
- Wollast, R., 1998. Evaluation and comparison of the global carbon cycle in the coastal zone and in the open ocean. In: Brink, K., Robinson, A. (Eds.), *The Sea*, vol. 10. Johns Wiley & Sons, pp: 213-251.

Biological responses to upwelling events in the different phases of summer monsoon

- Wyrski, K., 1973. Physical oceanography of the Indian Ocean. In: Zeitzschel, B. (Ed.). *The Biology of the Indian Ocean*. Chapman and Hall. pp: 18-36.
- Yenstsch, C.S. and Phinney, D.A., 1992. The effect of wind direction and velocity on the distribution of phytoplankton chlorophyll in the western Arabian Sea. In: *Oceanography of Indian Ocean*, B.N. Desai (Ed), pp: 57-66.

## Chapter VI

# Phytoplankton community structure

---

- 6.1. Introduction
- 6.2. Results
  - 6.2.1. Community structure
    - i) Species composition
    - ii) Diversity indices
    - iii) Similarity indices
  - 6.2.2. Phytoplankton pigment characteristics
- 6.3. Discussion
- References

---

### 6.1. Introduction

Phytoplankton communities play a crucial role in marine ecosystems, affecting nutrient cycling, the structure and efficiency of the food web, and the flux of particles to deep waters (Smith and Sakshaug, 1990). Accounting for approximately one-fourth of all plants in the world (Jeffrey and Hallegraeff, 1990), marine phytoplankton are important contributors to global carbon fluxes (Falkowski, *et al.*, 1998).

The ocean climate determines the composition and size of the regional – scale phytoplankton system and modify the global chemical budgets by a number of mechanisms. Three areas of importance are the utilization of CO<sub>2</sub> through photosynthesis thus affecting the global CO<sub>2</sub> budget (Williamson and Gribbin, 1991); a contribution to seasonal warming of the surface layers of the ocean (Sathyendranath, *et al.*, 1991) by absorbing and scattering light; and the production of quantities of volatile compounds which escape into the atmosphere and act as cloud seeding nuclei. The growth and reproduction of

phytoplankton in the ocean is determined by light and nutrients. The nutrients reach the euphotic zone from the deeper layers by turbulence or upwelling processes. This process, in turn determines the species composition and abundance of phytoplankton in the sea.

Phytoplankton are taxonomically diverse group of mostly, single celled, photosynthetic aquatic organisms that drift with currents. This group consists of approximately 20,000 species distributed among at least eight taxonomic divisions or phyla (Falkowski, *et al.*, 1998). Their diversity is immense and representatives of most algal divisions may be found in the ocean. The best known are the siliceous diatoms (Bacillariophyta), which account for up to 10,000 living species (Margulis, *et al.*, 1990). The dinoflagellates (Dinophyta) encompass about 1200 species, only half of which are photosynthetic (Jeffrey and Hallegraeff, 1990). The golden brown flagellates of the Haptophyta and Chrysophyta are very diverse, and may dominate the phytoplankton in particular regions and at certain times of the year. Picoplanktonic blue green algae (Cyanophyta) and free-living prochlorophytes (Prochlorophyta) are ubiquitous in the world's oceans, often preferring the dimly lit regions at the base of the euphotic zone (Chishlom, *et al.*, 1988).

Although there is considerable information on the primary productivity in the eastern Arabian Sea (Qasim, 1982; Bhattathiri, *et al.*, 1996; Prasanna Kumar, *et al.*, 2001, Madhu, 2004), not much is known about phytoplankton community structure, except from inshore waters of the west coast of India (Subrahmanyam, 1959;

Devassy, 1983). Sawant and Madhupratap, (1996) studied the seasonality and composition of phytoplankton in the Arabian Sea as part JGOFS (India) programme. Occurrence of *Phaeocystis globosa* in the waters off Kochi was reported by Madhupratap, *et al.*, (2000). Parab, *et al.*, (2006) studied the phytoplankton community structure in the northeastern Arabian Sea based on the microscopic and HPLC analysis methods. Upwelling induced changes in phytoplankton community and primary productivity was elucidated by Habeebrehman, *et al.*, (2008). In this chapter, the species composition, diversity and similarity patterns of phytoplankton community during inter-monsoon spring and different phases of summer monsoon were discussed. Phytoplankton pigment characteristics of SEAS (8°-15°N) during OSM and PSM were also studied using HPLC method.

## **6.2. Results**

### **6.2.1. Community structure**

#### **i) Species composition**

During the entire study period, a total of 177 species of phytoplankton were identified (Plates 6.1a, 6.1b and 6.2). A few unidentified green flagellates were also noticed during the study. They belong to 6 classes, namely Bacillariophyceae, Dinophyceae, Primensiophyceae, Dictyochophyceae, Prasinophyceae and Cyanophyceae. Among these, 104 species were diatoms (Bacillariophyceae), 67 species dinoflagellates (Dinophyceae), two species each of blue green algae (Cyanophyceae) and

Primnesiophyceae (Fig. 6.1). Prasinophyceae and Dictyochophyceae were represented by single species each (Table 6.1). Among diatoms at the genus level, *Rhizosolenia* presented the highest number of species (12 species), followed by *Coscinodiscus* (7 species) and *Nitzschia* (7 species). At the genus level, the best represented dinoflagellate was *Ceratium* (16 species), followed by *Protooperidinium* (10 species), *Goniaulax* (6 species) and *Prorocentrum* (6 species).

**(a) SIM:** In the inshore waters, 38 species of diatoms, 12 species of dinoflagellates and 2 species of blue green algae were found. Among diatoms, *Rhizosolenia alata* was the dominant species having a cell density of  $270 \pm 151.19$  cells  $L^{-1}$ , where as *Protooperidinium* sp. dominated ( $165 \pm 162.39$  cells  $L^{-1}$ ) in dinoflagellate community. *Trichodesmium erythraeum* constituted a cell density of  $2957.5 \pm 4661.19$  cells  $L^{-1}$ .

In the offshore waters, 32 species of diatoms, 12 species of dinoflagellates and 2 species of blue green algae were found. *Rhizosolenia alata* was the dominant diatom species having an average density of  $205 \pm 175$  cells  $L^{-1}$  and present in all transects. Among dinoflagellates, *Protooperidinium* sp. was dominant ( $193 \pm 174$  cells  $L^{-1}$ ). Abundance of *Trichodesmium erythraeum* observed in the offshore stations of northern transects.

**(b) OSM:** In the inshore waters, 55 species of diatoms, 17 species of dinoflagellates, one species of green algae and two species of blue green algae were recorded. Among diatoms *R. alata* was the dominant species having an average cell density of  $260 \pm 252.7$  cells  $L^{-1}$ . High cell

density of this species was found in 10°N transect (720 cells L<sup>-1</sup>) and lowest (40 cells L<sup>-1</sup>) at 15°N transect. Among dinoflagellates, *Protoperidinium* sp. was dominated (av. 277±311.9 cells L<sup>-1</sup>), having highest cell density of 960 cells L<sup>-1</sup> at 8°N. The cell density of *Trichodesmium erythraeum* was in the range of 480 at 15°N to 19400 cells L<sup>-1</sup> at 10°N.

In the offshore waters 26 species of diatoms, 10 species of dinoflagellates and 2 species of blue green algae were found. *R. alata* showed uniform distribution in all the stations with an average value of 697±247 cells L<sup>-1</sup>. *Protoperidinium* sp. was the dominant species among dinoflagellates (av. 543±243 cells L<sup>-1</sup>). *Trichodesmium erythraeum* was present in all transects and more abundant in northern transects with an average cell density of 9157±8445 cells L<sup>-1</sup>. Highest cell density (24540 cells L<sup>-1</sup>) was recorded in the 19°N transect.

**(c) PSM:** 60 species of diatoms, 41 species of dinoflagellates, one species each of blue green algae and green flagellates were observed in the inshore stations during PSM. Among diatoms, *R. alata* was the dominant species with an av. cell density of 642.5±294 cells L<sup>-1</sup>. *Goniaulax polyedra*, having the highest cell density of 6020 cells L<sup>-1</sup> (av. 752.5±218.4 cells L<sup>-1</sup>) at 11.5°N, was the dominant species among dinoflagellates. *T. erythraeum* was comparatively low and absent from 10°N, 11.5°N, 13°N, 15°N and 17°N. Green flagellates were abundant in 8°N and 10°N transects and the density was 5000 and 4620 cells L<sup>-1</sup> respectively.

In the offshore stations, 34 species of diatoms, 10 species of dinoflagellates and 2 species of blue green algae were observed. *Chaetoceros affinis* was the dominant species having an average cell density of  $1006 \pm 1325$  cells  $L^{-1}$  and highest cell density at  $15^{\circ}N$  (3640 cells  $L^{-1}$ ). *Protoperidinium* sp. was the dominant species among diatoms ( $449 \pm 378$  cells  $L^{-1}$ ). *Trichodesmium erythraeum* was present only in southern transects and showed highest cell density at  $11.5^{\circ}N$  (5120 cells  $L^{-1}$ ).

**(d) LSM:** During this season, 58 species of diatoms, 34 species of dinoflagellates, 3 species of green flagellates, 2 species of blue green algae and one species of silicoflagellate were present. Among diatoms, *Rhizosolenia* sp. was dominant; having the average cell density of  $285.7 \pm 392.5$  cells  $L^{-1}$  and maximum density (1140 cells  $L^{-1}$ ) was recorded at  $11.5^{\circ}N$ . *Protoperidinium* sp. was the dominant one among dinoflagellates (av.  $814.3 \pm 694.4$  cells  $L^{-1}$ ). *Phaeocystis globosa* (Primensiophyceae) was dominated at  $10^{\circ}N$  transect and the density was 8640 cells  $L^{-1}$ . *T. theibautii* showed dominance at  $10^{\circ}N$  (3240 cells  $L^{-1}$ ). *T. erythraeum* was comparatively less during this season.

In the offshore waters species of diatoms, 19 species of dinoflagellates 2 species of blue green algae and 2 species of silicoflagellates were found. *R. alata* was the dominant species among diatoms (av.  $514 \pm 733$  cells  $L^{-1}$ ) and *Protoperidinium* sp., among dinoflagellates ( $666 \pm 581$  cells  $L^{-1}$ ). Blue green algae and silicoflagellates were found only in  $17^{\circ}N$  transect.

Table 6.1. List of phytoplankton species in the eastern Arabian Sea during the study period

Speceis	SIM	OSM	PSM	LSM
<b>Bacillariophyceae</b>				
<i>Cyclotella meneghiniana</i>	-	-	-	+
<i>Cyclotella striata</i>	-	+	-	-
<i>Cyclotella</i> sp.	+	+	-	+
<i>Lauderia annulata</i>	-	+	-	+
<i>Planktoniella sol</i>	-	-	+	-
<i>Skeletonema costatum</i>	-	-	+	+
<i>Schroderella</i> sp.	-	-	-	+
<i>Thalassiosira gravida</i>	+	+	+	+
<i>Thalassiosira subtilis</i>	+	-	+	+
<i>Thalassiosira</i> sp.	+	+	+	+
<i>Asteromphalus</i> sp.	-	-	+	-
<i>Melosira sulcata</i>	-	+	-	-
<i>Leptocylindrus danicus</i>	+	+	+	-
<i>Leptocylindrus minimus</i>	+	+	+	+
<i>Leptocylindrus</i> sp.	+	+	+	+
<i>Coscinodiscus concinnus</i>	-	+	+	+
<i>Coscinodiscus excentricus</i>	+	+	+	-
<i>Coscinodiscus granii</i>	-	+	-	-
<i>Coscinodiscus marginatus</i>	+	+	+	-
<i>Coscinodiscus radiatus</i>	-	+	+	+
<i>Coscinodiscus</i> sp.	+	+	+	+
<i>Coscinodiscus sublineatus</i>	-	-	-	+
<i>Hemidiscus</i> sp.	+	+	+	-
<i>Actinotychus undulatus</i>	-	-	-	+
<i>Guinardia flaccida</i>	-	-	-	+
<i>Rhizosolenia alata</i>	+	+	+	+
<i>Rhizosolenia calcar</i>	+	-	-	-
<i>Rhizosolenia castracanei</i>	-	-	-	+
<i>Rhizosolenia crassispina</i>	-	+	-	-
<i>Rhizosolenia hebetata</i>	+	+	+	+
<i>Rhizosolenia imbricata</i>	-	-	-	+
<i>Rhizosolenia nitzschioides</i>	-	-	+	-
<i>Rhizosolenia robusta</i>	+	+	+	+
<i>Rhizosolenia setigera</i>	+	+	+	+
<i>Rhizosolenia stoltzenforthii</i>	+	+	+	+
<i>Rhizosolenia styliformis</i>	+	+	+	+
<i>Rhizosolenia</i> sp.	+	+	+	+
<i>Sirirella flummiensis</i>	-	+	-	-
<i>Climacodinium fraunfeldii</i>	-	+	+	+
<i>Climacodinium</i> sp.	+	+	+	+
<i>Eucampia cornuta</i>	-	-	-	+
<i>Eucampia zodiacus</i>	-	+	+	+
<i>Eucampia</i> sp.	+	+	+	+

*Phytoplankton community structure*

<i>Hemiaulus</i> sp.	-	-	-	+
<i>Biddulphia nobiliensis</i>	-	+	-	-
<i>Biddulphia sinensis</i>	-	-	-	+
<i>Biddulphia pulchellum</i>	+	+	+	+
<i>Biddulphia rhombus</i>	-	+	+	-
<i>Biddulphia</i> sp.	-	+	+	+
<i>Isthmia inervis</i>	-	-	+	-
<i>Bacteriastrum cosmosum</i>	-	+	-	-
<i>Chaetoceros affinis</i>	-	+	+	-
<i>Chaetoceros coarctatus</i>	+	+	+	-
<i>Chaetoceros debilis</i>	+	+	+	+
<i>Chaetoceros socialis</i>	+	-	-	+
<i>Chaetoceros</i> sp.	+	+	+	+
<i>Bellerochea malleus</i>	-	-	+	-
<i>Lithodesmium undulatum</i>	+	+	+	+
<i>Lithodesmium</i> sp.	+	-	-	-
<i>Triceratium dubium</i>	+	+	+	+
<i>Triceratium reticulatum</i>	+	+	-	+
<i>Triceratium rhombus</i>	-	-	-	+
<i>Triceratium robertsonianum</i>	-	+	-	-
<i>Triceratium</i> sp.	+	+	+	-
<i>Trachinies aspera</i>	-	-	+	-
<i>Streptotheca</i> sp.	-	-	-	+
<i>Asterionella japonica</i>	-	-	+	+
<i>Climacosphenia moniligera</i>	+	-	-	+
<i>Fragilaria oceanica</i>	-	+	-	+
<i>Grammatophora marina</i>	-	-	+	-
<i>Grammatophora undulata</i>	-	+	+	+
<i>Grammatophora</i> sp.	-	-	+	-
<i>Licmophora abbreviata</i>	-	-	-	+
<i>Licmophora</i> sp.	+	+	+	+
<i>Rhabdonema</i> sp.	-	+	-	-
<i>Rhaphoneis discoides</i>	-	-	-	+
<i>Thalassionema nitzschioides</i>	+	+	+	+
<i>Thalassionema</i> sp.	+	-	-	+
<i>Thalassiothrix delicatula</i>	-	-	+	-
<i>Thalassiothrix fraunfeldii</i>	+	+	+	+
<i>Thalassiothrix longissima</i>	+	+	+	-
<i>Thalassiothrix</i> sp.	+	+	+	+
<i>Amphora lineolata</i>	+	-	+	+
<i>Campylodiscus iyyengarai</i>	-	+	-	-
<i>Campylodiscus</i> sp.	+	-	+	-
<i>Diploneis</i> sp.	+	+	+	+
<i>Diploneis weisfloggii</i>	-	+	-	-
<i>Gyrosigma polygramma</i>	-	-	-	+
<i>Gyrosigma</i> sp.	+	-	+	-
<i>Navicula</i> sp.	+	-	+	+
<i>Pleurosigma carinatum</i>	-	-	-	+

<i>Pleurosigma directum</i>	-	+	+	-
<i>Pleurosigma</i> sp.	+	+	-	+
<i>Bacillaria paradoxa</i>	+	+	+	+
<i>Nitzschia delicatissima</i>	-	-	+	-
<i>Nitzschia longissima</i>	-	+	-	-
<i>Nitzschia panduriformis</i>	-	+	+	+
<i>Nitzschia pungens</i>	+	+	+	+
<i>Nitzschia seriata</i>	-	+	+	+
<i>Nitzschia sigma</i>	-	-	+	+
<i>Nitzschia</i> sp.	-	-	-	+
<i>Pseudonitzschia</i> sp.	-	-	-	+
<i>Synedra undulata</i>	-	-	+	-
<i>Synedra</i> sp.	+	+	+	+
<b>Dinophyceae</b>				
<i>Prorocentrum balticum</i>	-	-	+	-
<i>Prorocentrum dentatum</i>	-	-	-	+
<i>Prorocentrum micans</i>	-	+	+	+
<i>Prorocentrum rostratum</i>	-	-	+	+
<i>Prorocentrum scutellum</i>	-	-	-	+
<i>Prorocentrum</i> sp.	+	+	+	+
<i>Amphisolenia bidentata</i>	+	+	+	+
<i>Amphisolenia bifurcata</i>	+	-	+	+
<i>Amphisolenia thrinax</i>	-	-	-	+
<i>Amphisolenia</i> sp.	+	+	+	+
<i>Alexandrium</i> sp.	-	-	+	+
<i>Triposolenia bicornis</i>	-	-	+	-
<i>Dinophysis caudata</i>	-	-	+	+
<i>Dinophysis dense</i>	-	-	-	+
<i>Dinophysis miles</i>	-	-	+	+
<i>Dinophysis</i> sp.	-	-	-	+
<i>Ornithocercus</i> sp.	-	-	+	+
<i>Amphidinium</i> sp.	+	+	+	+
<i>Cochlodinium</i> sp.	-	-	-	+
<i>Gymnodinium breve</i>	-	-	+	-
<i>Gymnodinium catenatum</i>	+	+	-	-
<i>Gymnodinium splendens</i>	-	-	-	+
<i>Gymnodinium</i> sp.	+	+	+	+
<i>Gyrodinium</i> sp.	-	-	-	+
<i>Gyrodinium falcatum</i>	-	-	-	+
<i>Gyrodinium</i> sp.	+	-	-	-
<i>Polykrikos</i> sp.	-	+	-	+
<i>Noctiluca miliaris</i>	+	+	+	-
<i>Ceratium axiale</i>	-	+	-	-
<i>Ceratium carriens</i>	-	-	-	+
<i>Ceratium furca</i>	-	+	+	+
<i>Ceratium fusus</i>	+	+	+	+
<i>Ceratium gibbus</i>	-	-	+	-
<i>Ceratium gravida</i>	-	-	-	+

*Phytoplankton community structure*

<i>Ceratium inflatum</i>	-	-	+	+
<i>Ceratium limulus</i>	-	-	+	-
<i>Ceratium macroceros</i>	-	-	+	-
<i>Ceratium massiliens</i>	-	-	-	+
<i>Ceratium monoceros</i>	-	-	+	-
<i>Ceratium pulchellum</i>	-	-	+	+
<i>Ceratium ranipes</i>	-	-	-	+
<i>Ceratium trichoceros</i>	+	-	-	-
<i>Ceratium tripos</i>	-	-	+	+
<i>Ceratium</i> sp.	-	-	+	+
<i>Ceratocorys horrida</i>	+	-	+	-
<i>Ceratocorys</i> sp.	-	-	-	+
<i>Goniaulax birostris</i>	+	+	+	+
<i>Goniaulax polyedra</i>	-	-	+	-
<i>Goniaulax polygramma</i>	-	-	+	-
<i>Goniaulax spinifera</i>	+	-	+	-
<i>Goniaulax triacantha</i>	-	-	+	-
<i>Goniaulax</i> sp.	-	+	+	-
<i>Oxytoxum diploconius</i>	-	-	-	+
<i>Oxytoxum scolopax</i>	+	-	+	+
<i>Oxytoxum</i> sp.	-	-	+	+
<i>Pyrocystis</i> sp.	-	-	+	+
<i>Pyrophacus horologicum</i>	-	-	-	+
<i>Protoperidinium brevipes</i>	-	-	+	-
<i>Protoperidinium conicum</i>	+	+	+	-
<i>Protoperidinium depressum</i>	-	-	+	-
<i>Protoperidinium elegans</i>	-	-	+	-
<i>Protoperidinium oblongum</i>	-	-	+	-
<i>Protoperidinium oceanicum</i>	-	+	+	+
<i>Protoperidinium pallidum</i>	-	-	+	-
<i>Protoperidinium pedunculatum</i>	-	-	-	+
<i>Protoperidinium pentagonum</i>	-	-	+	+
<i>Protoperidinium</i> sp.	+	+	+	+
<b>Primnesiophyceae</b>				
<i>Phaeocystis globosa</i>	-	-	-	+
<i>Coccolithus</i> sp.	-	-	-	+
<b>Dictyochophyceae</b>				
<i>Dictyocha</i> sp.	-	-	-	+
<b>Prasinophyceae</b>				
<i>Pterosperma polygonum</i>	-	+	-	+
<b>Cyanophyceae</b>				
<i>Trichodesmium erythraeum</i>	+	+	+	+
<i>Trichodesmium theibautii</i>	+	+	+	+
<b>Unidentified Green flagellates</b>	+	+	+	+
<b>Total</b>	<b>67</b>	<b>83</b>	<b>112</b>	<b>117</b>

+ present

- absent

In order to find out the variations in seasonal and spatial scales a two way Analysis of Variance (ANOVA) is carried out with season and station (Tables 6.2 to 6.7) as the factors. Box-Cox Transformation was made to follow the normal distribution of variables. Significant factors at 0.05 level of significance were shown in bold letters.

**Table 6.2. Two way ANOVA for diatoms in the inshore stations**

Source	Sum of Squares	df	Mean Square	F	Sig.
Season	.030	3	.010	7.332	<b>.002</b>
Station	.022	7	.003	2.335	.067
Error	.026	19	.001		
Total	.074	29			

**Table 6.3. Two way ANOVA for Dinoflagellates in the inshore stations**

Source	Sum of Squares	df	Mean Square	F	Sig.
Season	27.340	3	9.113	6.572	<b>.003</b>
Station	17.530	7	2.504	1.806	.144
Error	26.345	19	1.387		
Total	67.002	29			

**Table 6.4. Two way ANOVA for Blue Green algae in the inshore stations**

Source	Sum of Squares	df	Mean Square	F	Sig.
Season	2.695	3	.898	3.748	.068
Station	21.408	7	3.058	12.758	<b>.002</b>
Error	1.678	7	.240		
Total	26.660	17			

**Table 6.5. Two way ANOVA for Diatoms in the offshore stations**

<b>Source</b>	<b>Sum of Squares</b>	<b>df</b>	<b>Mean Square</b>	<b>F</b>	<b>Sig.</b>
Season	10.849	3	3.616	5.465	<b>.008</b>
Station	2.452	7	.350	.529	.801
Error	11.912	18	.662		
Total	25.384	28			

**Table 6.6. Two way ANOVA for Dinoflagellates in the offshore stations**

<b>Source</b>	<b>Sum of Squares</b>	<b>df</b>	<b>Mean Square</b>	<b>F</b>	<b>Sig.</b>
Season	2297544.7	3	765848.23	2.634	.081
Station	2829711.4	7	404244.48	1.390	.269
Error	5234188.7	18	290788.26		
Total	10050013.8	28			

**Table 6.7. Two way ANOVA for Blue Green algae in the offshore stations**

<b>Source</b>	<b>Sum of Squares</b>	<b>df</b>	<b>Mean Square</b>	<b>F</b>	<b>Sig.</b>
Season	7.975	3	2.658	3.369	.136
Station	6.286	7	.898	1.138	.478
Error	3.156	4	.789		
Total	20.715	14			

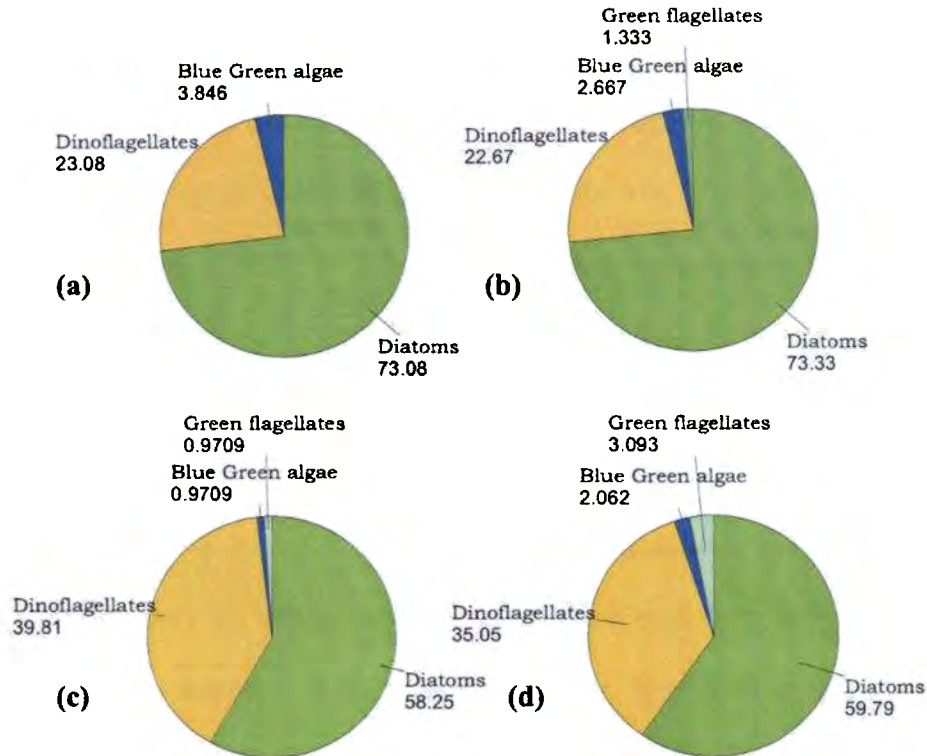


Fig. 6.1. Percentage composition of phytoplankton species during (a) SIM (b) OSM, (c) PSM and (d) LSM

## ii) Diversity indices

The diversity indices calculated were the Shannon-Weiner diversity index ( $H' \log_2$ ), Margalef Richness index ( $d$ ), Pielou's Evenness index ( $J'$ ) and Simpson's Dominance Index ( $D$ ). The seasonal average values were represented in the Fig. 6.2. The highest and lowest values of diversity indices were given in the Tables 6.8 and 6.9 respectively for inshore and offshore stations.

**(a) SIM:** The average dominance value in the inshore stations was  $0.58 \pm 0.31$  and  $0.67 \pm 0.18$  was in the offshore stations. The average richness index was  $1.76 \pm 1.07$  and  $1.41 \pm 0.64$  respectively for inshore and offshore stations. The average evenness value in the inshore stations was  $0.56 \pm 0.29$  and that for offshore stations, it was

0.68±0.18. The average Shannon diversity index in the inshore stations was 2.14±1.33 and in the offshore stations it was 2.26±0.70.

**(b) OSM:** The average dominance value in the inshore stations was 0.50±0.25 and 0.41±0.24 was in the offshore stations. The average richness index was 2.33± 1.18 and 1.16±0.35 respectively for inshore and offshore stations. The average evenness value in the inshore stations was 0.45±0.21 and that for offshore stations, it was 0.38±0.21. The average Shannon diversity index in the inshore station was 1.19±0.96 and in the offshore stations it was 1.32±0.68.

**(c) PSM:** The average dominance value in the inshore stations was 0.84±0.06 and 0.72±0.11 was in the offshore stations. The average richness index was 3.09±0.87 and 1.56±0.38 respectively for inshore and offshore stations. The average evenness value for the season in the inshore stations was 0.74±0.06 and that for offshore stations, it was 0.67±0.14. The average Shannon diversity index in the inshore station was 3.52±0.58 and in the offshore stations, it was 2.45±0.49.

**(d) LSM:** The average dominance value in the inshore stations was 0.75±0.12 and 0.79±0.06 in the offshore stations. The average richness index was 2.59±1.92 and 1.97±1.03 respectively for inshore and offshore stations. The average evenness value for the season in the inshore stations was 0.68±0.13 and that for offshore stations, it was 0.74±0.11. The average Shannon diversity index in the inshore stations was 2.84±0.63 and in the offshore stations it was 2.80±0.53.

Table 6.8. Diversity indices in the inshore stations during SIM, OSM, PSM and LSM

	Richness(d)		Evenness (J)		Diversity ( $H' \log_2$ )		Dominance (D)	
	High	Low	High	Low	High	Low	High	Low
<b>SIM</b>	3.73 (11.5°N)	0.67 (10°N)	0.87 (8°N)	0.14 (10°N)	3.75 (11.5°N)	0.39 (10°N)	0.88 (8°N)	0.10 (10°N)
<b>OSM</b>	4.04 (11.5°N)	0.94 (19°N)	0.67 (8°N)	0.20 (19°N)	2.88 (11.5°N)	0.62 (19°N)	0.68 (13°N)	0.17 (19°N)
<b>PSM</b>	4.83 (10°N)	2.09 (17°N)	0.83 (15°N)	0.67 (21°N)	<b>4.67</b> (10°N)	2.93 (21°N)	<b>0.93</b> (10°N)	0.73 (21°N)
<b>LSM</b>	<b>6.77</b> (10°N)	1.00 (21°N)	<b>0.90</b> (8°N)	0.49 (10°N)	3.68 (8°N)	1.90 (21°N)	0.91 (8°N)	0.60 (21°N)

Table 6.9. Diversity indices in the offshore stations during SIM, OSM, PSM and LSM

	Richness(d)		Evenness (J')		Diversity (H')		Dominance (D)	
	High	Low	High	Low	High	Low	High	Low
<b>SIM</b>	2.43 (17°N)	0.48 (21°N)	0.89 (8°N)	0.36 (10°N)	3.18 (8°N)	1.09 (10°N)	0.87 (8°N)	0.30 (10°N)
<b>OSM</b>	1.57 (19°N)	0.74 (17°N)	0.72 (13°N)	0.19 (19°N)	2.16 (13°N)	0.61 (17°N)	0.72 (13°N)	0.17 (17°N)
<b>PSM</b>	1.92 (21°N)	0.92 (15°N)	<b>0.90</b> (10°N)	0.51 (13°N)	3.35 (10°N)	1.87 (15°N)	<b>0.88</b> (10°N)	0.58 (13°N)
<b>LSM</b>	<b>3.48</b> (13°N)	0.75 (21°N)	0.88 (21°N)	0.59 (17°N)	<b>3.60</b> (8°N)	2.26 (21°N)	0.87 (8°N)	0.72 (13°N)

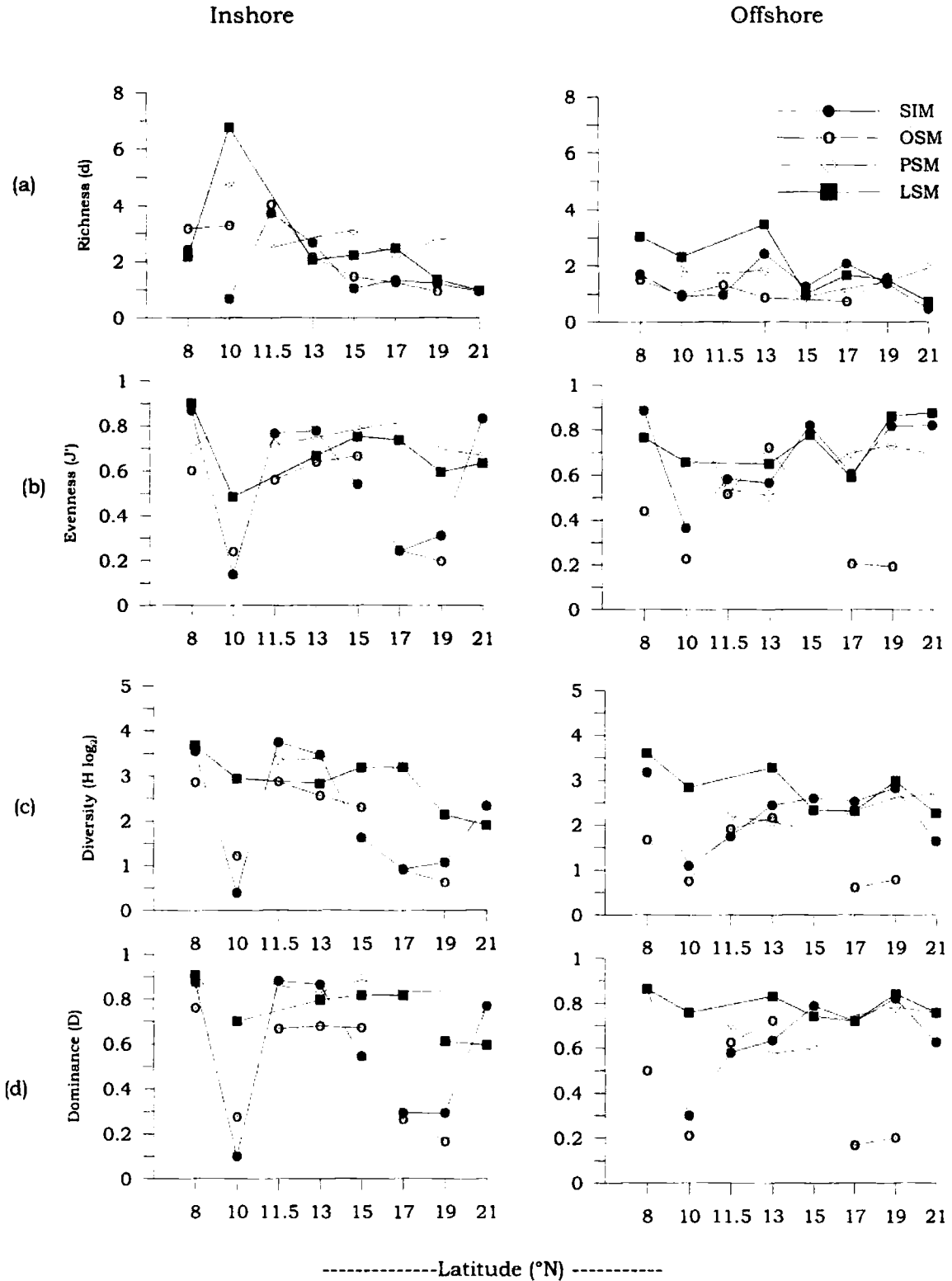


Fig. 6.2. Diversity indices (a) Margalef Richness (d) (b) Pielou's Evenness (J')(c) Shannon Diversity (H'log<sub>2</sub>) and (d) Dominance (D)

**iii) Similarity indices**

For finding out the similarities between seasonal and spatial aspects of phytoplankton abundance, Bray Curtis similarity dendrogram plots were made using numerical abundance data. From the dendrogram it was found that 6 clusters (Figs. 6.3) have more than 50% similarity in the inshore stations. Highest similarity of 75.9% was observed between SIM 17 and OSM 17 stations.

In the offshore stations, 12 clusters (Fig. 6.4) showed similarity more 50% and highest similarity of 70.46% was observed between the numerical abundance of phytoplankton at SIM 10 and OSM 19.

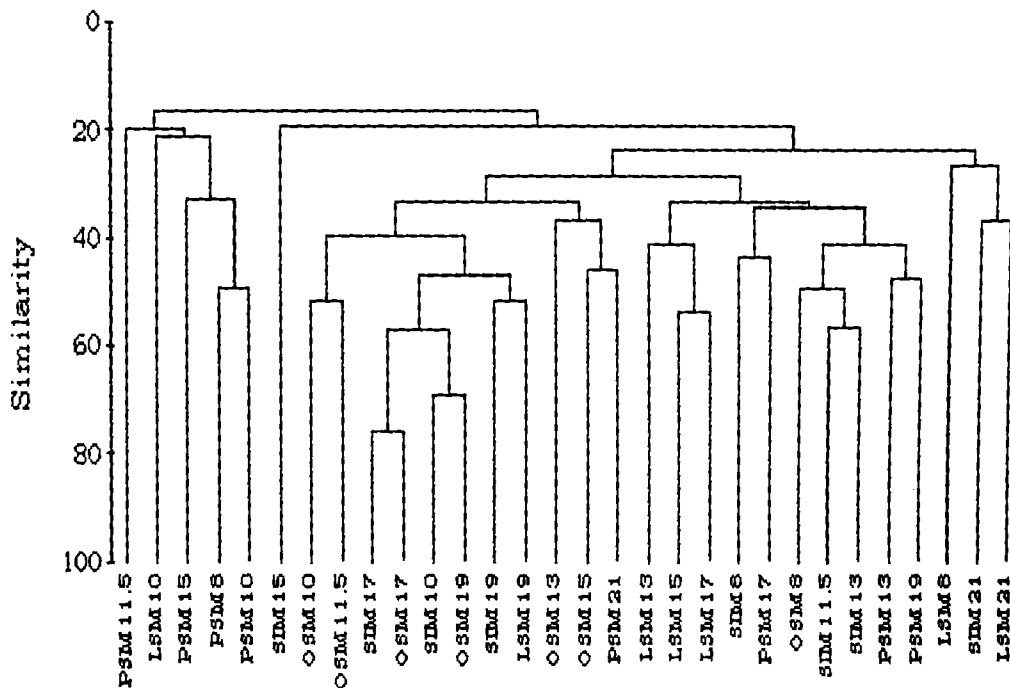


Fig. 6.3. Bray-Curtis similarity profile (Dendrogram) showing the similarity of phytoplankton density in the inshore stations

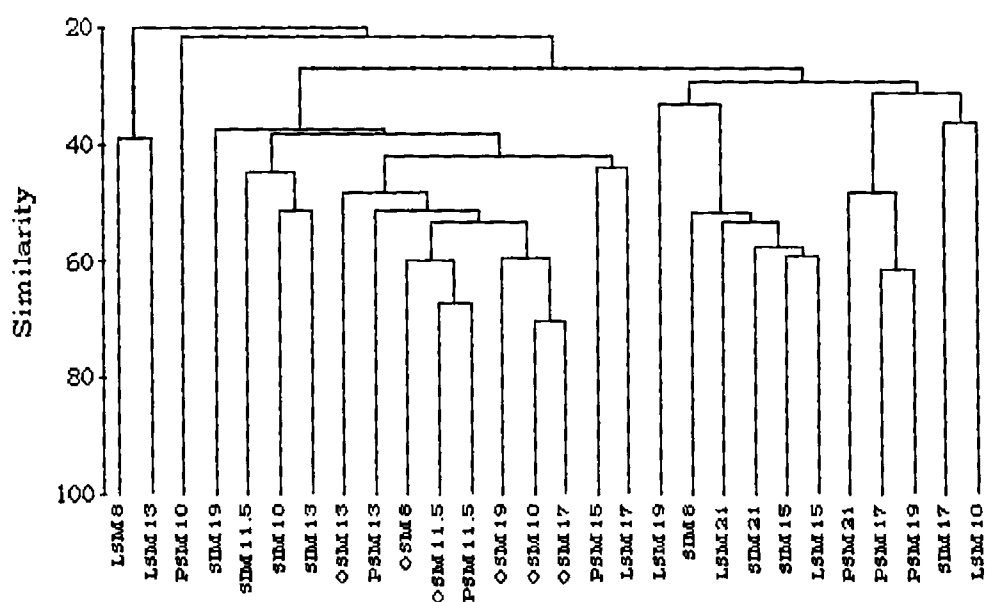


Fig. 6.4. Bray-Curtis similarity profile (Dendrogram) showing the similarity of phytoplankton density in the inshore stations

### 6.2.2. Phytoplankton pigment characteristics

HPLC derived phytoplankton characteristics were examined in the south eastern Arabian Sea (8-15°N) during OSM and PSM. Sampling was done from surface, 10m and 100m depth. The methodology used to analyse the samples were given in the chapter II. The objectives were comparing the pigment signatures with the microscopically revealed phytoplankton composition in relation to prevailing hydrographic conditions. An alternative and compliment to the microscopic examination, pigment distribution can be used to identify the presence of different algal groups (Wright, *et al.*, 1991; Jeffrey, *et al.*, 1997; Bidigare and Charles, 2002). HPLC provide

chemotaxonomic information on the range of phytoplankton groups that make up the community structure.

**a) Pigment characteristics during OSM**

The phytoplankton pigments identified during OSM were Chl *a*, fucoxanthin, zeaxanthin, peridinin, Chl *c1* and diadinoxanthin. Chl *b*,  $\beta$  carotene, MV Chl *a*, divinyl Chl *a*, *etc.* are also observed in trace concentration. Distributions of phytoplankton pigment concentration were shown in the Fig.6.5a. Relatively pigment concentration was low during OSM. The total Chl *a* (MV chl *a*+ DV Chl *a*+ divinyl Chl *a*) was in the range of 0.21 to 0.51  $\mu\text{g l}^{-1}$  (av. 0.4  $\mu\text{g l}^{-1}$ ). From the vertical distribution, it was revealed that pigment concentration was maximum was at the sub surface layers (Fig. 6.6).

Percentage composition of all major pigments were shown in the Fig. 6.7. Chl *a* was the dominant pigment in almost all transects, followed by zeaxanthin, fucoxanthin, peridinin, Chl *c1*,  $\beta$  carotene, *etc.*

**b) Pigment characteristics during PSM**

The phytoplankton pigment distribution showed elevated levels in the south west coast (8-15°N) during the PSM (Fig 6.5b). The bulk of the phytoplankton pigments were located in the subsurface (20m). The total Chl *a* was in the range of 0.4 to 1.2  $\mu\text{g l}^{-1}$  (av. 0.6  $\mu\text{g l}^{-1}$ ). Profiles of Chl *a* and accessory pigments for all stations are presented in Fig. 6.6 to illustrate their vertical variation in each transect. Percentage composition of all major pigments were shown in the Fig. 6.8. Chl *a* was the dominant pigment in almost all transects, followed by fucoxanthin, Chl *b*, peridinin, Chl *c1*  $\beta$  carotene, *etc.*

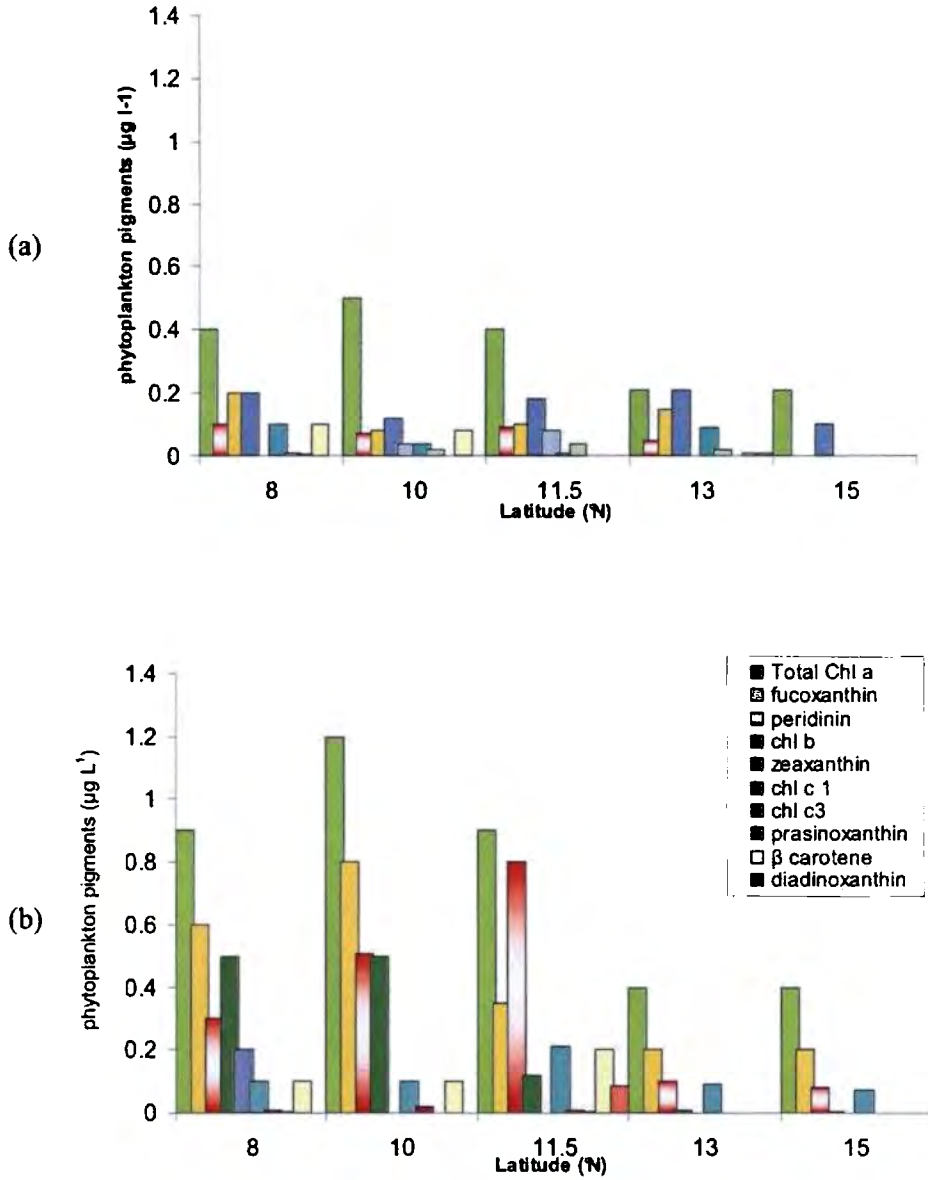


Fig. 6.5. Distribution of phytoplankton pigments during (a) OSM and (b) PSM

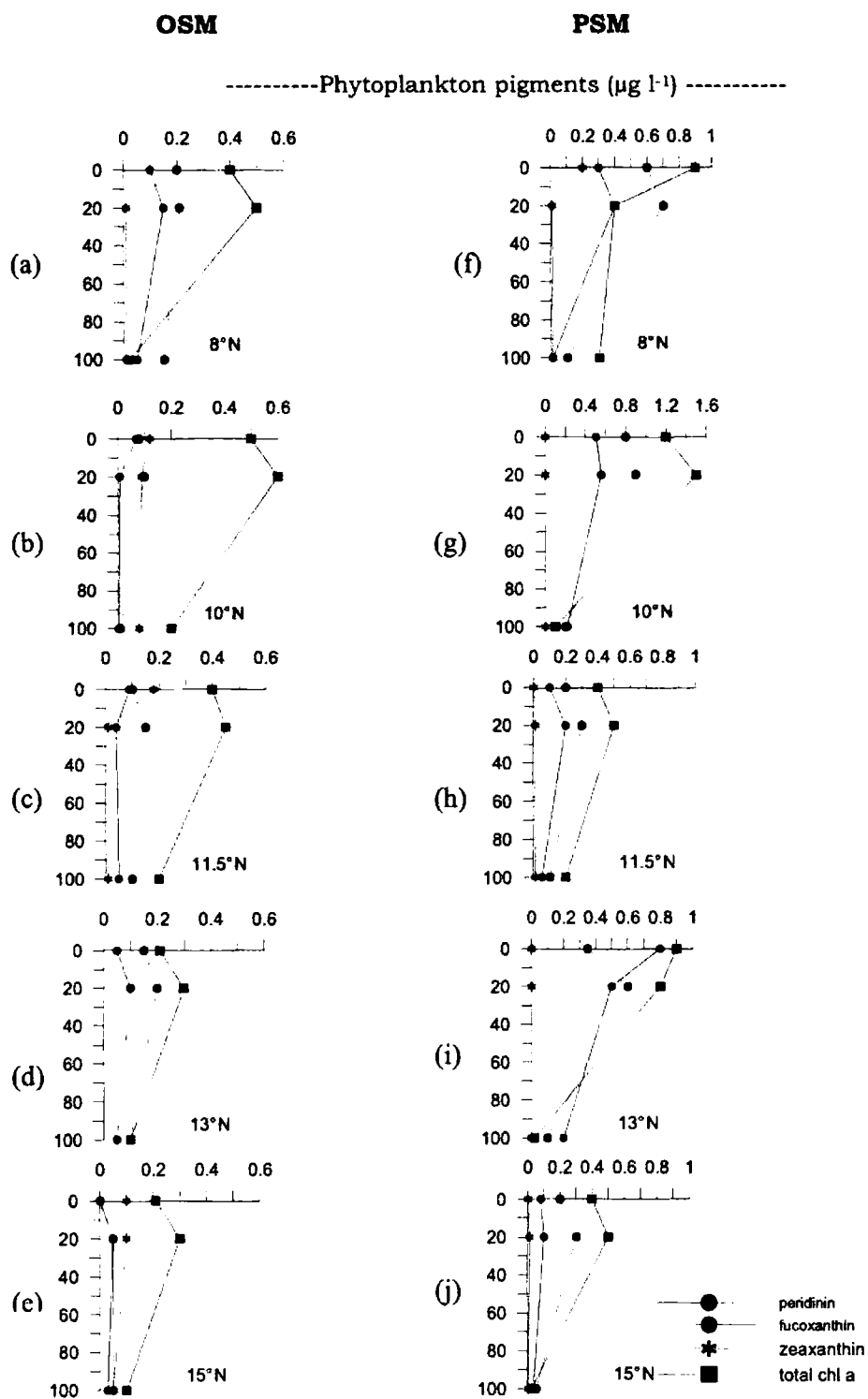


Fig. 6.6. Vertical distribution of phytoplankton marker pigments during (a, b, c, d, & e) OSM and (f, g, h, i, & j) PSM

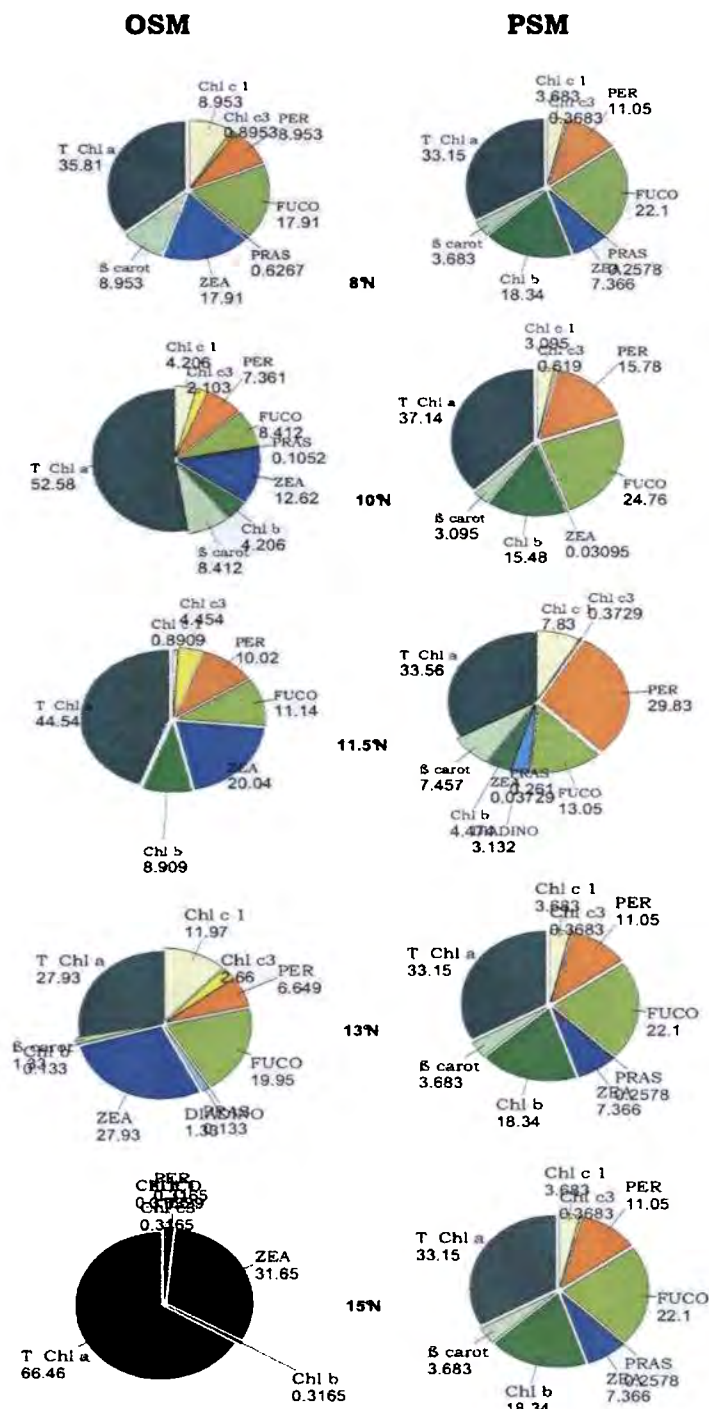


Fig. 6.7. Percentage composition of major phytoplankton pigments during OSM and PSM at 8°N, 10°N and 11.5°N

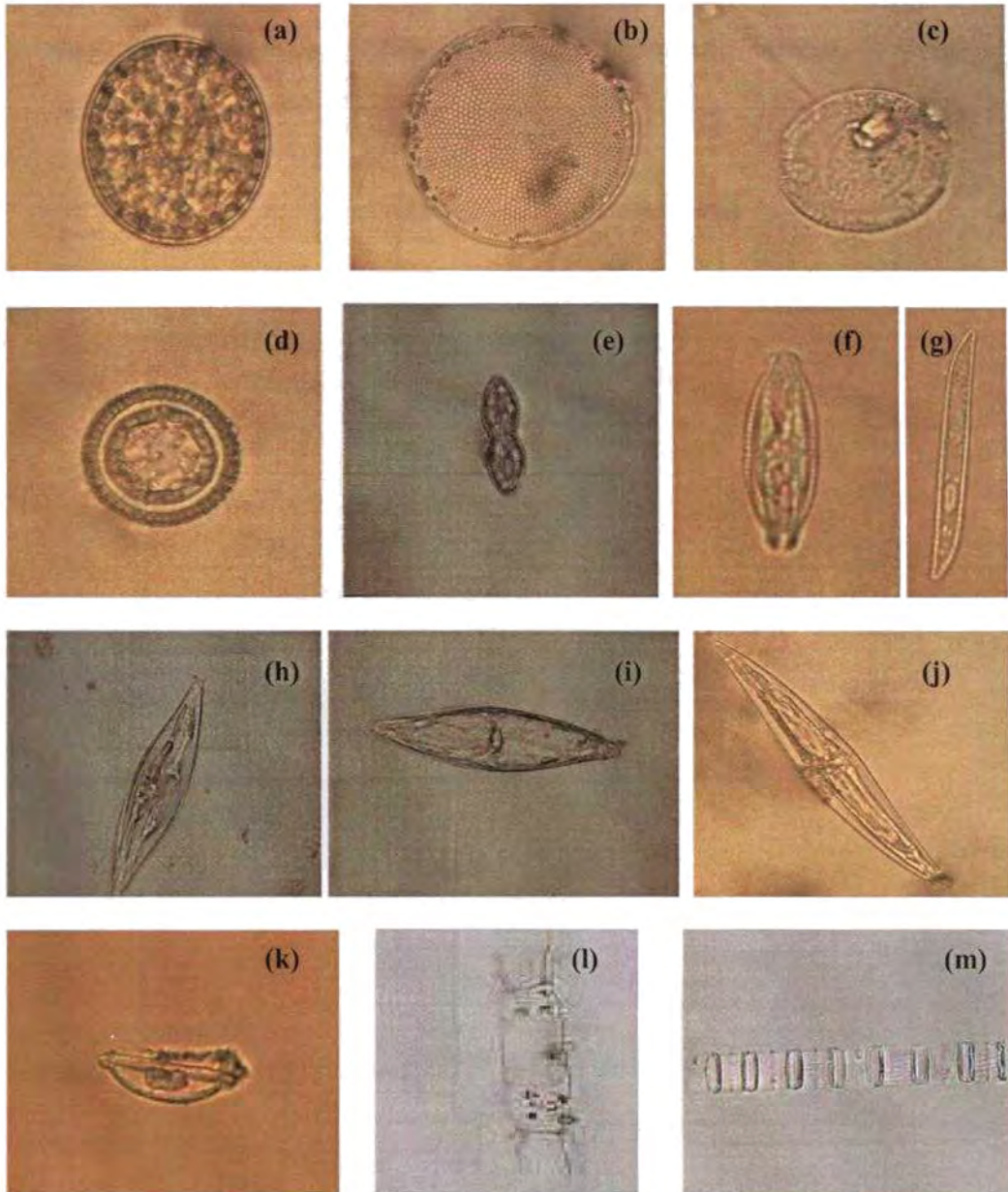


Plate 6.1a. Diatoms observed during the study period in the EAS

- (a) *Coscinodiscus marginatus* (b) *Coscinodiscus radiatus* (c) *Cyclotella* sp.  
(d) *Melosira sulcata* (e) *Diploneis weissflogii* (f) *Diploneis* sp. (g) *Navicula* sp.  
(h) *Pleurosigma cariantum*. (i) *Pleurosigma directum* (j) *Pleurosigma* sp. (k)  
*Amphora leniolata* (l) *Biddulphia sinensis* (m) *Skeletonema costatum*

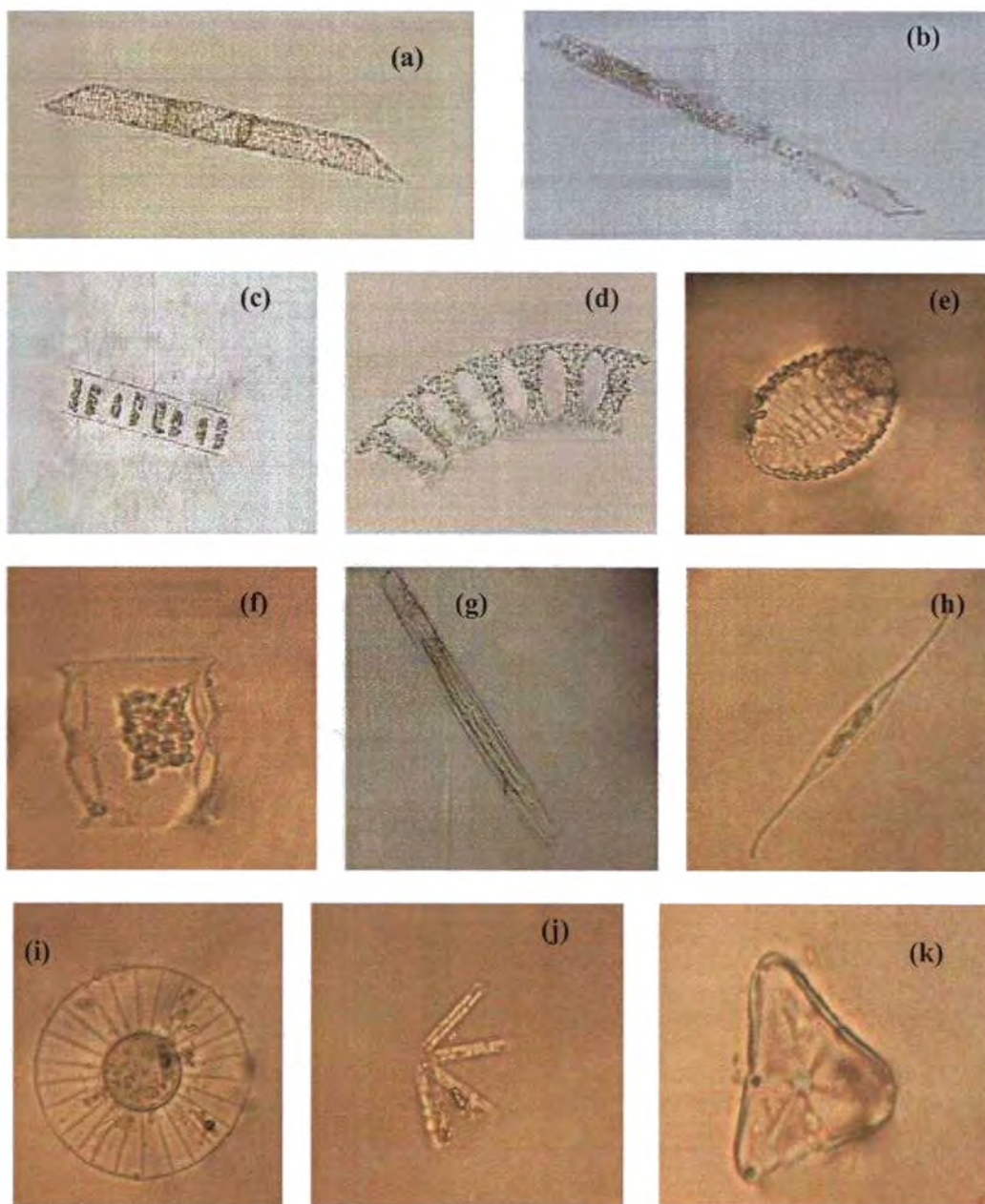


Plate 6.1b. Diatoms observed during the study period in the EAS

- a) *Rhizosolenia hebetata* (b) *Rhizosolenia alata* (c) *Chaetoceros* sp.  
(d) *Eucampia zodiacus* (e) *Campylodiscus* sp. (f) *Lithodesmium* sp. (g)  
*Nitzschia* (h) *Synedra* sp. (i) *Planktoniella sol* (j) *Thalassionema*  
*nitzschioides* (k) *Triceratium reticulatum*.

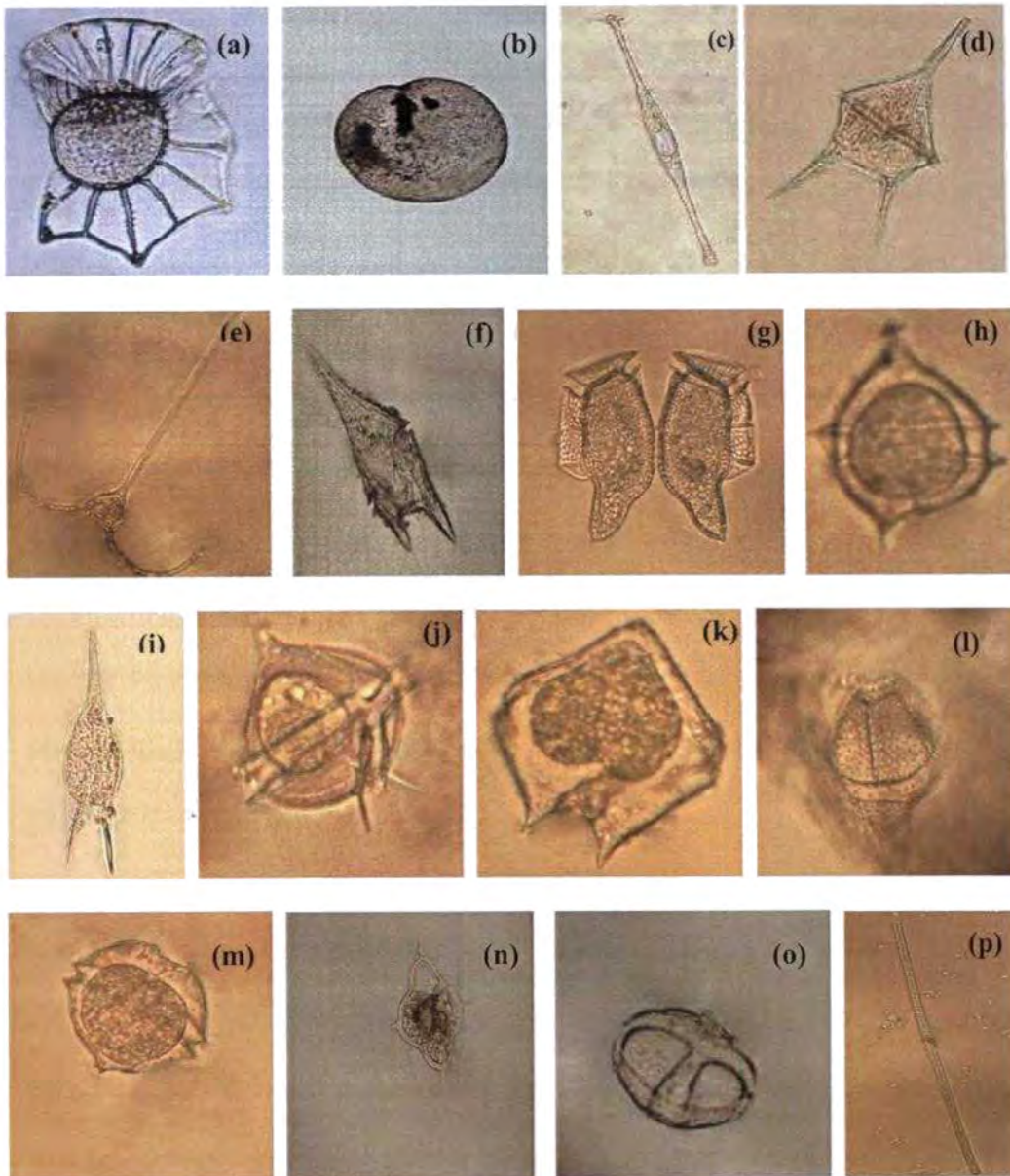


Plate 6.2. Dinoflagellates, silicoflagellates and blue green alga observed during the study period in the EAS

(a) *Ornithocercus* sp. (b) *Noctiluca miliaris* (c) *Amphisolonia* sp. (d) *Ceratium* sp. (e) *Ceratium trichoceros* (f) *Ceratium furca* (g) *Dinophysis caudata* (h) *Goniaulax spinifera* (i) *Goniaulax* sp. (j) *Protoperidinium pedunculatum* (k) *Protoperidinium* sp. (l) *Protoperidinium pentagonum* (m) *Protoperidinium conicum* (n) *Dictyocha* sp. (o) *Coccolithus* sp. (p) *Trichodesmium erythraeum*

### **6.3. Discussion**

Communities are recognized as recurrent organized systems of organisms responding in a related way to changes in the environment (Legendre and Legendre, 1978). Any changes in many growth variables of an individual, which ultimately leads the community to become, reorganized (Smayda, 1963). In the marine environment, phytoplankton forms communities which are highly complex and variable in terms of diversity and dynamics. As these communities can change within a short period, proper assessment by microscopic identification and quantification (Utermohl, 1958; Hillebrand, *et al.*, 1999); and by analyzing pigment composition by HPLC method (Millie, *et al.*, 1993) are necessary. Knowledge of the presence, absence and timing of abundance of phytoplankton is a prerequisite for successful planning of studies on primary productivity and its utilization at various levels of the ecosystem.

The marked seasonal changes of current direction and mixed layer depth that occur in the open ocean, modifies the nutrient supply and hence phytoplankton composition (Banse, 1987). Diatoms, dinoflagellates, blue green algae, green flagellates and silicoflagellates are the important groups of phytoplankton that compete for light and nutrients. They are often found to dominate in more turbulent environments (Lochte, *et al.*, 1993; Townsend and Thomas, 2002) and the transient blooms associated with upwelling events (Cushing, 1989; Brown, *et al.*, 1999; Tilstone, *et al.*, 2000; Sahayak, *et al.*, 2005). In the present observations, diatoms were dominated during all

the seasons and most of the stations, followed by dinoflagellates and some minor groups of algae such as blue green algae, silicoflagellates, *etc.* either together or separately. These minor groups do not contributed to the bulk of the plankton except the cyanophycean elements, species of *Trichodesmium* on some occasions during the warmer months, i.e., during SIM and OSM.

During the present study, a total of 177 species of phytoplankton were recorded. Subrahmanyam (1959) recorded 360 species of phytoplankton from the west coast of India. Sawant and Madhupratap (1996) reported 36 dominant species from the central and eastern Arabian Sea. Madhu (2004) recorded 90 species of dominant phytoplankton in the EAS. Highest number of species were found during LSM (117 species), followed by PSM (112 species). Lowest number of species (62 species) was recorded during SIM. These variations can be attributed to the shifts in nutrient regime influenced by the stratification during SIM and changing intensities of upwelling during from OSM to LSM through PSM.

During all the seasons, diatoms were dominated. They constituted 73% during SIM and OSM, 58% during PSM and 59% during LSM. Subrahmanyam and Sharma (1967) reported the abundance of diatoms during the summer monsoon and the dominance during pre monsoon and post monsoon (Devassy and Goes, 1988) and Sawant and Madhupratap (1996) recorded the dominance of diatoms up to 90% during the JGOFS (India) studies in the central and eastern Arabian Sea. Parab, *et al.*, (2006) by HPLC

method concluded the dominance of diatoms in the north eastern Arabian Sea during spring, summer and winter monsoon seasons. They made this inference on the basis of the high concentration of fucoxanthin, which is the dominant marker pigment for diatoms. Phytoplankton community showed the dominance of diatoms both inshore and offshore regions, eventhough their percentage occurrence were different in spatial and temporal patterns. Dinoflagellate, the second dominant group of phytoplankton also showed variations both seasonally and spatially. They constitute 23% during SIM, 22% during OSM, 39% during PSM and 35% during LSM. Maximum variety of diatom species occurred during summer monsoon. Important species in terms of abundance are *Rhizosolenia* sp., *R. alata*, *Nitzschia seriata*, *Chaetoceros socialis*, *Skeletonema coastatum*, *Thalassiosira* sp., *Thalassionema nitzschioides*, *Asterionella japonica*, *Biddulphia pulchellum*, etc. Most of the other species such as *Amphora* sp., *Cyclotella* sp., *Campylodiscus iyyengarii*, *Climacodinium* sp., *Melosira sulcata*, *Licmophora* sp., *Lithodesmium* sp., *Rhizosolenia* sp., *Synedra* sp., *Triceratium* sp., etc. were recorded in one or two stations during each season.

Relatively high percentage occurrence of dinoflagellate during PSM, which is characterized by the mature upwelling stage, is mainly due to the abundance of *Goniaulax polyedra* at 11.5°N. During PSM, which is characterized by intense upwelling signatures, the turbulent conditions favoured the growth of dinoflagellates. The pattern of flora keeps on changing at varying intervals as also the numbers of the

different species. The phytoplankton responded to the above physical environment with a typical upwelling community dominated by chain forming diatoms such as *Chaetoceros* and *Nitzschia* showed high numerical abundance and dinoflagellates formed second place in abundance. This pattern prevailed during the study, although with replacement of dominant species and changes in abundance. The dominance of green flagellates and silicoflagellates (Primnesiophyceae and Prasinophyceae) in the phytoplankton community was significant along southern transects (8°N to 13°N) during PSM and LSM. Their distribution in the euphotic zone appeared to be limited primarily by the nitrate concentrations  $>0.1\mu\text{mol}$  as discussed in the chapter III. Their distribution in the Indian waters was not clearly understood, because of the negligence during microscopic analysis. Madhupratap, *et al.*, (2000) first reported the occurrence of *Phaeocystis globosa* off Kochi region during the upwelling conditions. Their abundance was due to the high nutrient content and relaxed upwelling conditions. The high occurrence of green flagellates, silicoflagellates and small diatoms appears to be a feature of many upwelling systems (Cushing, 1989; Garrison, *et al.*, 1998; Brown, *et al.*, 1999).

Microscopic and HPLC analysis of surface phytoplankton population showed the dominance of blue green algae, particularly in southern and northern transects. This population was dominated by *Trichodesmium erythraeum*. At the surface, a combination of high light, high oxygen and the absence of nitrogenous nutrients appeared to favour a surface cyanobacterial population. Most cyanobacterial

strains are capable of: (1) fixing atmospheric nitrogen to meet their nitrogenous nutrient requirements and (2) tolerating high amounts of light (Burkill *et al.*, 1993). This is the reason for the high abundance of cyanobacteria in the Arabian Sea, mainly during the SIM period and partially during OSM. Following the onset of the upwelling season in June, *Trichodesmium* disappeared and in its place a diatom rich population comprising of species of *Rhizosolenia*, *Chaetoceros*, *Coscinodiscus* and *Nitzschia* was emerged. The oligotrophic water of northern transects were also characterized by the dominance of *Trichodesmium* during SIM and OSM. The results demonstrated that different phytoplankton taxa dominated spatially and temporally in the eastern Arabian Sea. This switching between taxa appeared to be the result of the ambient nutrient concentrations.

During the SIM period, species richness, evenness and diversity of phytoplankton were much lower compared to the summer monsoon. Locations along the 8°N transect had relatively high diversity indices, compared to the other locations. Relatively high diversity indices of phytoplankton were found at 10°N, compared to other locations.

The vertical mixing initiates phytoplankton growth in stratified waters, when limiting conditions of nutrients are overcome by mixing of water masses. These conditions were thought to be a key aspect of diatom survival, with the negatively-buoyant, non-motile cells being dependent on turbulence to transfer them into the photic zone (Ross, 2006). On the other hand dinoflagellates and coccolithophores are

found in regions with established stratification, either co-existing with or dominating diatoms (Holligan and Harbour, 1977; Pingree, *et al.*, 1982; Sharples, *et al.*, 2001). Such conditions can be established by the persistent stratification model (Lucas, *et al.*, 1998) and critical turbulence model (Huisman, *et al.*, 1999). Similar situations were found during the LSM periods of the present study. For instance, dinoflagellates are often thought to have significant physiological disadvantages compared to diatoms and yet the two are often seen to co-exist. Dinoflagellates are thought to have lower photosynthetic rates (Furnas, 1990; Tang, 1995) and higher metabolic costs (Smayda, 1997). Vertical migration, mixotrophy, chemically-regulated inter-specific competition, and anti-predation defences have all been suggested as possible adaptations that might allow dinoflagellates to offset these physiological disadvantages and enable them to compete successfully with diatoms.

Such changes are due to the differences in responses of each species to the changes in the surrounding environment. Each phytoplankton has its own niche, and abundance in the environment varies depending upon the limitation of that niche. This study demonstrated that there were significant seasonal and spatial changes in the distribution and composition of phytoplankton in the EAS. These differences may be attributed to the effects of the summer monsoon, which drives the upwelling process, leading to the abundant growth of phytoplankton during summer monsoon and the stratification during the spring inter-monsoon. Several studies have

reported that different levels of stratification can have the influence on species composition (Hutchings, *et al.*, 1994; Brink, *et al.*, 1995).

During the study period, considerable temporal and spatial variability in the abundance of different species of phytoplankton was observed. Inshore-offshore changes in phytoplankton assemblages are typical of dynamic oceanic ecosystems (Ondrusek, *et al.*, 1991; Barlow, *et al.*, 1999) and similar spatial variations in diatom-dinoflagellate communities have been observed in the EAS. When the dominant cells are in chains or colonies, the dominant cell size can be smaller than the dominant size fraction (Ciotti, *et al.*, 2002). With the onset of summer monsoon and upwelling during May-June and its intensities during July-August, lead to marked increase in phytoplankton growth in the EAS. Ishizaka, *et al.*, (1983) demonstrated phytoplankton growth competition in culture experiments by simulating upwelling conditions. The vertical motion produced by the upwelling and the associated introduction of nutrients into photic layers could explain the growth of different species of phytoplankton in a successive pattern. In nutrient rich turbulent environments, non-motile, fast growing diatoms could be favoured (Margaleff, 1978) as high nutrient concentrations allow fast division rates and turbulence reduces sedimentation losses out of photic zone (Kiorbe, 1993). The hydrological structure (as analysed in the chapter III) had an important effect on phytoplankton distribution and community composition. Upwelling conditions, which start in May, lead to the initiation of diatom dominated phytoplankton blooms

that persist until September. These phytoplankton blooms are apparent in field observations (Sahayak, *et al.*, 2005) and satellite data during the summer monsoon and spread well offshore of the initial upwelling regions. An interesting feature observed during summer monsoon was the decrease in cyanobacterial population drastically. This is probably because *Trichodesmium* requires stable, warm conditions for their growth (Devassy, 1983). The occurrence of *Fragilaria oceanica* has been noted to be common during different phases of summer monsoon.

Two way ANOVA results showed that in the inshore stations significant seasonal variations were existed ( $p < 0.005$ ) in diatom and dinoflagellate cell density, while blue green algae showed significant variations ( $p < 0.005$ ) in cell density spatially. In the offshore stations, only diatom cell density showed significant seasonal variations ( $p < 0.05$ ). Dinoflagellates and blue green algae showed no significant variations both seasonally or spatially.

Understanding the processes affecting the structure of the autotrophic phytoplankton community in marine ecosystem is relevant, as the species dependant characters may affect the productivity and carbon fluxes of the ocean. The shifts in physical processes induce the changes in species diversity and similarities in the phytoplankton community. In the present analysis, highest Shannon diversity index (4.67) and dominance (0.93) was recorded during PSM in the inshore stations. Similarly, highest Margalef species richness (6.77) and Pielou's Evenness index (0.90) were

observed during LSM. In the offshore stations, highest species diversity (3.6) was recorded during LSM at 8°N and lowest (0.61) during OSM at 17°N. Highest species richness was in the inshore station at 13°N during LSM. The relaxed upwelling conditions with enriched nutrient levels influenced the growth of different species of phytoplankton and resulted in high species diversity and richness. Evenness and dominance indices were high (0.90 and 0.88) at 10°N stations. The existence of different phases of upwelling conditions with corresponding nutrient regimes favoured the growth and distribution of phytoplankton evenly. This may be due to the variability in the occurrence of physical processes in the inshore and offshore regions. Generally it is observed that high species diversity and richness existed in southern transects.

Bray-Curtis similarity indices, calculated based on the species level numerical abundance of phytoplankton showed highest similarity of 75.9% between the stations at 17°N during SIM and OSM in the inshore stations. This similarity was mainly attributed to the abundance of *Trichodesmium erythraeum* and *T. theibautii* in the inshore waters. Relatively uniform hydrographic conditions prevailed there during both SIM and OSM. The offshore stations at 10°N during SIM and 19°N station during OSM showed highest similarity of 70.46% among offshore stations. The formation of more similarity clusters in the offshore stations indicates the low variability in the hydrographic conditions, which influences the growth of phytoplankton. No significant similarity clusters were formed with the

PSM and LSM. This condition may be due to the difference in the phytoplankton species and abundance during the summer monsoon and spring inter-monsoon. This condition can be attributed to the variability in the nutrient regime during each season influenced by the prevailing physical processes.

The present investigation on the community structure of phytoplankton revealed that diatoms dominated in all the seasons, eventhough their percentage varied during different seasons with highest during SIM. The principal result of this study is that physical seasonality in the eastern Arabian Sea leads to marked seasonality of phytoplankton community structure and diversity.

#### ***Phytoplankton pigment characteristics***

The alternative or complementary method for characterizing phytoplankton communities is to determine their pigment composition by High Performance Liquid Chromatography (HPLC) method (Millie, *et al.*, 1993). HPLC has frequently been used in natural phytoplankton communities world wide, but only a few studies have been conducted in the eastern Arabian Sea (Roy, *et al.*, 2006 and Parab, *et al.*, 2006). Piippola and Kononen (1995) studied the pigment composition of spring and late summer phytoplankton blooms in the Gulf of Finland. They found that even if no quantitative calibration of pigments was made, significant correlations of peridinin and diadinoxanthin with dinoflagellates, fucoxanthin with diatoms, alloxanthin with cryptophytes, zeaxanthin, and  $\beta$ - carotene with blue green algae and chlorophyll *b* with green flagellates. Ston, *et al.*, (2002) concluded that

carotenoids were useful for predicting the presence of certain phytoplankton groups off Polish coast, while Schluter, *et al.*, (2000) reported that phytoplankton composition based on pigment and microscopic analyses did show good agreement for some data. The present study does not reconstruct algal classes from pigment data, but focuses on the explanatory power of pigment diversity as compared to taxonomic diversity in reflecting environmental changes. It has been shown that spatial and seasonal variations were reflected by pigment composition and cell density. Eventhough zeaxanthin, the bio-marker for blue green algae was present in all transects (0.2 – 0.5  $\mu\text{g L}^{-1}$ ), it was widely detected along 8-15°N transects during OSM particularly in the surface layers. The abundance of this pigment was largely due to the abundance of blue green algae (*Trichodesmium erythraeum*) as revealed in microscopic analysis. Presence of fucoxanthin and peridinin were observed along the 8 to 11.5°N transects during PSM, where diatoms and dinoflagellate was abundant. From the results of hydrographic studies as mentioned in the Chapter III, it was revealed that upwelling signatures were very intense in these transects and hence the density of diatoms dinoflagellates and green flagellates was high in these transects. Pigment concentration to a great extent reflected the trends of phytoplankton density. Microscopic cell counts and as well as the elevated concentration of fucoxanthin, peridinin, Chl *b*, observed in the 8-11.5° N transects were matching.

Presence of Chl *b* was prominent along 8-11.5° where, abundance of green flagellates was observed during PSM. In addition to these pigments, Chl *c*<sub>1</sub> + *c*<sub>2</sub> and diadinoxanthin concentrations were also quantified. The concentration of fucoxanthin, which is the marker of diatoms (Wright and Jeffrey, 1997), was observed to be high at 8-11.5°N transects during PSM. Some discrepancies may occur in the comparative studies related to pigments and cell density. The possible reasons are the negligence of small phytoplankton cells during microscopic analysis and the physiological conditions the phytoplankton. The pigment analyses summarises the physiological condition of the phytoplankton (Wanstrand and Snoeijs, 2006), while counts consider the organisms as either dead or alive.

Given that phytoplankton pigments vary in chemotaxonomic specificity, their relative abundance can reveal phytoplankton community structure at the level of algal class (Millie, *et al.*, 1993; Mackey, *et al.*, 1996). Abundance of peridinin and fucoxanthin pigment was high at southern upwelling transects (8°N, 10°N and 11.5°N) during PSM. High resemblance was found between the abundance of peridinin with dinoflagellates, fucoxanthin with diatoms and Chl-*b* with green flagellates. Zeaxanthin generally followed the variations in cyanobacterial abundance. Other pigments such as Chl *c*<sub>1</sub>, Chl *c*<sub>3</sub>, diadinoxanthin, prasinoxanthin, *etc.* showed dissimilarities with taxonomic data sets. Concentration of pigments was high during PSM when compared to OSM. This indicates the abundance of algal cells due to upwelling events. High prevalence of zeaxanthin pigment

during OSM was due to the abundance of *Trichodesmium* sps. in the oligotrophic conditions, before the onset of upwelling in the surface waters. It was less pronounced during PSM as the *Trichodesmium* cells were less.

The pigment concentrations adequately described the general pattern of phytoplankton production and community composition. The pattern obtained in this study was that lower pigment concentrations were obtained during OSM and higher during PSM which is in correlation with the phytoplankton cell density and diversity. Better understanding of the roles of dinoflagellate characteristics within the physical environment, particularly in coastal waters, may lead to a better predictive capability of these harmful blooms. Understanding the interplay between the different characteristics of phytoplankton species and the physical environment is a key requirement in developing our insight into the structure and variability of plankton ecosystems. It is advocated that available resources of long term studies such as environmental monitoring, can be used more efficiently by utilising the high ecological resolution of pigment composition in combination with high frequent ships-of-opportunity sampling.

In view of the present analysis, it is assessed that the changing upwelling and stratified conditions in terms of physico-chemical variables may have roles in structuring the phytoplankton community and productivity. Therefore, the distribution of, and variations in, the

phytoplankton community, including in the chlorophyll contents, is critical in the study of marine carbon cycles.

## References

- Banse, K., 1987. Seasonality of phytoplankton chlorophyll in the central and northern Arabian Sea. *Deep Sea Res.*, 34: 713-723.
- Barlow, R.G., Mantoura, R.F.C. and Cummings, D.G., 1999. Monsoonal influence on the distribution of phytoplankton pigments in the Arabian Sea. *Deep Sea Res.*, II 46: 677-699.
- Bhattathiri, P.M.A., Pant, A., Sawant, S., Gauns, M., Matondkar, S.G.P. and Mohanraju, R., 1996. Phytoplankton production and chlorophyll distribution in the eastern and central Arabian Sea in 1994-95. *Curr. Sci.*, 71: 857-862.
- Bidigare, R.G. and Charles, C.T., 2002. HPLC phytoplankton pigments: sampling, laboratory methods and quality assurance procedures. In: Fargion, G.S., Mueller, J.L., (Eds.), *Protocols for Satellite Ocean Colour Validation Revision 2*. NASA, Goddard Space Flight Centre, Greenbelt, M.D., pp: 154-160.
- Brink, K., Abrante, F., Bernal, P., Estrada, M., Hutchings, L., Jahnke, R., Müller, P. and Smith, R., 1995. Group report: how do coastal upwelling systems operate as integrated physical, chemical, and biological systems and influence the geological record? The role of physical processes in defining the spatial structures of biological and chemical variables. In: Summerhayes, C., Emeis, K., Angel, M., Smith, R., Zeitzschel, B., (Eds.), *Upwelling in the Oceans: Modern Processes and Ancient Records*. John Wiley & Sons, pp: 103-125.
- Brown, S.L., Landry, M.R., Barber, R.T., Campbell, L., Garrison, D., Gowing, M.M., 1999. Picoplankton dynamics and production in the Arabian Sea during the 1995 southwest monsoon. *Deep Sea Res. II*, 46: 1745-1768.
- Burkill, P.H., Mantoura, R.F.C. and Owens, N.J.P., 1993. Biogeochemical cycling in the north western Indian Ocean: a brief overview. *Deep Sea Res. II*, 40: 643-649.
- Chishlom, S.W., Olson, R.J., Zettler, E.R., Goericke, R.J., Waterbury, B. and Welschmeyer, N.A., 1988. A novel free living prochlorophyte abundant in the oceanic euphotic zone. *Nature*, 334: 340-343.
- Ciotti, A.M., Lewis, M.R. and Cullen, J., 2002. Assessment of the relationships between dominant cell size in natural phytoplankton communities and the spectral shape of the absorption coefficient. *Limnol. Oceanogr.*, 47(2): 404-417.

- Cushing, D.H., 1989. A difference in structure between ecosystems in strongly stratified waters and in those that are only weakly stratified. *J. Plank. Res.* 11, 1-13.
- Devassy, V.P. and Goes, J.I., 1988. Phytoplankton community structure and succession in a tropical estuarine complex (Central west coast of India). *Estuar. Coast. Shelf Sci.*, 27: 671-685.
- Devassy, V.P., 1983. Plankton ecology of some estuarine and marine regions of the west coast of India. *Ph.D. Thesis*, University of Kerala.
- Falkowski, P.G., Barber, R.T. and Smetacek, V., 1998. Biogeochemical controls and feed backs on ocean primary production. *Science*, 281: 200-206.
- Furnas, M., 1990. In situ growth rates of marine phytoplankton: Approaches to measurement, community and species growth rates. *J. Plankt. Res.*, 12(6):1117-1151.
- Garrison, D.L., Gowing, M.M., Hughes and M.P., 1998. Nano and microplankton in the northern Arabian Sea during the southwest monsoon, August-September 1995. A US-JGOFS Study. *Deep Sea Res. II*, 45: 2269-2299.
- Habeebrehman, H., Prabhakaran, M.P., Jacob, J., Sabu, P., Jayalakshmi, K.J., Achuthankutty, C.T. and Revichandran, C., 2008. Variability in biological responses influenced by upwelling events in the eastern Arabian Sea. *J. Mar. Syst.*, 74: 545-560.
- Hillebrand, H., Durselen, C.D., Kirschtel, D., Pollinger, U. and Zohary, T., 1999. Biovolume calculation of pelagic and benthic microalgae. *J. Phycol.*, 35: 403-424.
- Holligan, P.M. and Harbour, D.S., 1977. The vertical distribution and succession of phytoplankton in the western English Channel in 1975 and 1976. *J. Mar. Biol. Assn., UK*, 57: 1075-1093.
- Huisman, J., van Oostveen, P. and Weissing, F.J., 1999. Critical depth and critical turbulence two different mechanisms for the development of phytoplankton blooms. *Limnol. Oceanogr.*, 44: 1781-1787.
- Hutchings, L., Pitcher, G., Probyn, T. and Bailey, G., 1994. The chemical and biological consequences of coastal upwelling. In: Summer-hayes, C.P., Emers, K.C., Angel, M.V., Smith, R.L. and Zeitzchell, B. (Eds.), *Upwelling in the oceans: Modern process and ocean records*. John Wiley and Sons, pp: 65-81.
- Ishizaka, J., Takahashi, M. and Ichimura, S., 1983. Evaluation of coastal upwelling effects on phytoplankton growth by simulated culture experiments. *Mar. Biol.*, 76: 271-278.
- Jeffrey, S.W. and Hallegraff, G.M., 1990. Phytoplankton ecology in Australian waters. In: Clayton, M.N. and King, R.J. (Eds.). *Biology of Marine Plants*, Longman - Cheshire, Melbourne, pp: 310-348.

- Jeffrey, S.W., Mantoura, R.F.C. and Wright, S.W., 1997. *Phytoplankton pigments in oceanography: Guidelines to modern methods*. Paris: UNESCO Publishing, 661p.
- Kiorbe, T., 1993. Turbulence, phytoplankton cell size, and the structure of pelagic food webs. *Adv. Mar. Biol.*, 29: 1-72.
- Legendre, L. and Legendre, P., 1978. Associations. In: *Phytoplankton Manual* (Sournia, A., ed.). UNESCO, Paris. pp: 261-273.
- Lochte, K., Ducklow, H.W., Fasham, M.J.R. and Stienen, C., 1993. Plankton succession and carbon cycling at 47°N-20°W during the JGOFS North-Atlantic Bloom Experiment. *Deep Sea Res. II*, 40(1-2): 91-114.
- Lucas, L.V., Cloern, J.E., Koseff, J.R., Monismith, S.G. and Thompson, J.K., 1998. Does Svedrup critical depth model explain bloom dynamics in estuaries ? *J. Mar. Res.* 56: 375-415.
- Mackey, M.D., Mackey, D.J., Higgins, H.W. and Wright, S.W., 1996. CHEMTAX-a programme for estimating class abundances from chemical markers: application to HPLC measurements of phytoplankton. *Mar. Ecol. Prog. Ser.*, 144: 265-283.
- Madhu, N.V., 2004. Seasonal studies on primary production and associated environmental parameters in the Indian EEZ. *PhD. Thesis, Cochin University of Science and Technology*, 234p.
- Madhupratap, M., Sawant, S. and Gauns, M., 2000. A first report on a bloom of the marine prymnesiophycean, *Phaeocystis globosa* from the Arabian Sea. *Oceanol. Acta.*, 23: 83-89.
- Margaleff, R., 1978. Life forms of phytoplankton as survival alternatives in an unstable environment. *Oceanol. Acta*, 1: 493-510.
- Margulis, L., Corliss, J.O., Melkonoan, M. and Chapman, D.J., 1990 *Handbook of Protoctista*. Jones and Barlett, Boston, 914p.
- Millie, D.F., Pearl, H.W. and Hurley, J.P., 1993. Micro-algal pigment assessments using high-performance liquid chromatography: a synopsis of organismal and ecological applications. *Canadian J. Fish. Aqua. Sci.*, 50: 2513-2527.
- Ondrusek, M.E., Bidigare, R.R., Sweet, S.T., Defreitas, D.A. and Brooks, J.M., 1991. Distribution of phytoplankton pigments in the North Pacific Ocean in relation to physical and optical variability. *Deep Sea Res. II*, 38: 243-266.
- Parab, S.G., Matondkar, S.G.P., Gomes, H.R. and Goes, J.J., 2006. Monsoon driven changes in phytoplankton populations in the eastern Arabian Sea as revealed by microscopy and HPLC pigment analysis. *Conti. Shelf Res.*, 26: 2538-2558.
- Piipola, S. and Kononen, K., 1995. Pigment composition of phytoplankton in the Gulf of Finland. *Aqua Fennica*, 25: 39-48.

- Pingree, R.D., Holligan, P.M., Mardell, G.T. and Harris, R.P., 1982. Vertical distribution of plankton in the Skagerrak in relation to doming of the seasonal thermocline. *Conti. Shelf Res.*, 1(2): 209-219.
- Prasanna Kumar, S., Madhupratap, M., Kumar, M.D., Muraleedharan, P.M., D'Souza, S.N., Gauns, M. and Sarma, V.V.S.S., 2001. High biological productivity in the central Arabian Sea during the summer monsoon driven by Ekman pumping and lateral advection. *Curr. Sci.*, 81: 1633-1638.
- Qasim, S.Z., 1982. Oceanography of the northern Arabian Sea. *Deep Sea Res.*, 29: 1041-1068.
- Ross, O.N., 2006. Particles in motion: How turbulence affects plankton sedimentation from an oceanic mixed layer. *Geophys. Res. Lett.* 33(10): L10609, doi: 10.1029/2006GL026352.
- Roy, R., Pratihary, A., Mangesh, G., Naqvi, S.W.A., 2006. Spatial variation of phytoplankton pigments along the southwest coast of India. *Estuar. Coast. Shelf Sci.*, 69: 189-195.
- Sahayak, S., Jyothibabu, R., Jayalakshmi, K.J., Habeebrehman, H., Sabu, P., Prabhakaran, M.P., Jasmine, P., Shaiju, P., Rejomon, G., Thresiamma, J. and Nair, K.K.C., 2005. Red tide of *Noctiluca miliaris* off south of Thiruvananthapuram subsequent to the 'stench event' at the southern Kerala Coast. *Curr. Sci.*, 89: 1472-1473.
- Sathyendranath, S., Gouveia, A.D., Shetye, S.R., Ravindram, P. and Platt, T., 1991. Biological control of surface temperature in the Arabian Sea. *Nature*, 349: 54-56.
- Sawant, S. and Madhupratap, M., 1996. Seasonality and composition of phytoplankton in the Arabian Sea. *Curr. Sci.*, 71(11): 869-873.
- Schluter, L.M., Ohlenberg, F., Havskum, H. and Larsen, S., 2000. The use of phytoplankton pigments for identifying and quantifying phytoplankton groups in coastal areas: testing the influence of light and nutrients on pigment/chlorophyll *a* ratios. *Mar. Ecol. Prog. Ser.*, 19: 49-63.
- Sharples, J., Moore, C.M., Rippeth, T.R., Holligan, P.M., Hydes, D.J., Fisher, N.R. and Simpson, J., 2001. Phytoplankton distribution and survival in the thermocline. *Limnol. Oceanogr.*, 46(3): 486-496.
- Smayda, T.J., 1963. Succession of phytoplankton and the ocean as an holocentric environment. In: *Symposium on Marine Microbiology* (Oppenheimer, C.H., ed.). Springfield, Illinois, pp: 260-274.
- Smayda, T.J., 1997. Harmful algal blooms: Their ecophysiology and general relevance to phytoplankton blooms in the sea. *Limnol. Oceanogr.* 42(5):1137-1153.

- Smith, W.O. and Sakshaug, E., 1990. Polar phytoplankton. In: Smith, W.O., (Ed.), *Polar Oceanography, Part, B: Chemistry, Biology and Geology*. Academic Press, San Diego. pp: 477-525.
- Ston, J., Kosakowska, A., Lotocka, M. and Lysiak-Pastuszak, E., 2002. Pigment composition in relation to phytoplankton community structure and nutrient content in the Baltic Sea. *Oceanologia*, 44: 419-437.
- Subrahmanyam, R., 1959. Studies on the phytoplankton of the west coast of India. Parts I and II *Proc. Indian Acad. Sci.*, 24B: 85-197.
- Subrahmanyam, R. and Sarma, A.H.V., 1967. Studies on the phytoplankton of the west coast of India. Part IV, magnitude of the standing crop for 1955-1962, with observations on nanoplankton and its significance to fisheries. *J. Mar. Biol. Asso. Ind.* 7: 406-419.
- Tang, Y., 1995. The allometry of algal growth rates. *J. Plank. Res.*, 17(6): 1325-1335.
- Tilstone, G.H., Miguez, B.M., Figueiras, F.G. and Fermin, E.G., 2000. Diatom dynamics in a coastal ecosystem affected by upwelling: coupling between species succession, circulation and biogeochemical processes. *Mar. Ecol. Prog. Ser.*, 205: 23-41.
- Townsend, D.W. and Thomas, M., 2002. Spring time nutrient and phytoplankton dynamics on Georges Bank. *Mar. Ecol. Prog. Ser.*, 228: 57-74.
- Utermohl, H., 1958. Zur Vervollkommnung der quantitativen phytoplankton methodik. *Mitteilungen der Internationale Vereinigung für Theoretische und Angewandte. Limnologie*, 9:1-38.
- Wanstrand, I. and Snoeijs, P., 2006. Phytoplankton community dynamics assessed by ships-of-opportunity sampling in the northern Baltic Sea: A comparison of HPLC pigment analysis and cell counts. *Estuar. Coast. Shelf Sci.*, 66: 135-146.
- Williamson, P. and Gribbin, J., 1991. How plankton changes the climate. *New Scientist*, 129: 44-48.
- Wright, S.W. and Jeffrey, S.W., 1997. High resolution HPLC system for chlorophylls and carotenoids of marine phytoplankton. In: Jeffrey, S.W., Mantoura, R.F.C. and Wright, S.W., (Eds.). *Phytoplankton Pigments in Oceanography: Guidelines to Modern Methods*. UNESCO, Paris. pp: 327-341.
- Wright, S.W., Jeffrey, S.W., Mantoura, R.G.C., Llewellyn, C.A., Bjornland, D.R. and Welschmeyer, N., 1991. Improved HPLC method for the analysis of chlorophylls and carotenoids from marine phytoplankton. *Mar. Ecol. Prog. Ser.*, 77: 183-196.

## Chapter VII

### Summary and conclusion

---

The thesis presents comparative biological features in the Eastern Arabian Sea (EAS) during the stratified period (spring intermonsoon) and different phases of coastal upwelling (onset, peak and late summer monsoon). Earlier studies on biological responses in the EAS were restricted to single seasonal observations with poor sampling resolution. Therefore, the present study forms baseline information on how biological features in the EAS transforms from stratified period to different phases of coastal upwelling.

Field observations were carried out in the EAS during the spring intermonsoon (March-April), onset of summer monsoon (May-June), peak summer monsoon (August-September) and late summer monsoon (September-October) to understand the biological responses to various physical processes. In order to accomplish this, the following hydrographical parameters were measured in the EAS. The physico-chemical parameters considered were temperature salinity, density, dissolved oxygen, nitrate, phosphate and silicate. Biological parameters studied includes Chlorophyll *a* (Chl *a*), primary productivity, phytoplankton community structure, phytoplankton pigment characteristics, mesozooplankton biomass and composition. All measurements were carried out onboard *FORV Sagar Sampada* under Marine Research on Living Resource (MR-LR) programme (2002-'07), funded by Centre for Marine Living Resources and Ecology (CMLRE), Ministry of Earth Sciences (MoES), Govt. of India.

During SIM the EAS was characterized by weak winds ( $\sim 3$  m/s), warm SST ( $>29.6$ ) and low SSS ( $<34.2$ ), vertically stratified (MLD av. 30m) well oxygenated ( $> 205\mu\text{M}$ ) nutrient depleted ( $\text{NO}_3 < 0.1\mu\text{M}$ ,  $\text{PO}_4 < 0.6$ ) surface waters. Intense surface layer stratification and nutrient depletion resulted in low Chl *a* at the surface (av.  $0.24 \text{ mg m}^{-3}$ ) and water column (av.  $18.8 \text{ mgm}^{-2}$ ). Average primary production was also less in both surface ( $<3.2 \text{ mgC m}^{-3}\text{d}^{-1}$ ) and water column ( $<190 \text{ mgC m}^{-2}\text{d}^{-1}$ ). Nutrient depletion in the surface waters also caused deep subsurface chlorophyll maximum (av. 50-75m). The phytoplankton density was low, with a major contribution from *Trichodesmium erythraeum* (av.  $2795 \text{ cells L}^{-1}$ ). High abundance of *Trichodesmium erythraeum* ( $14440 \text{ cells L}^{-1}$ ) generally considered as a biological response of strongly stratified tropical waters. Percentage composition phytoplankton density showed the dominance (64%) of blue green algae. The total mesozooplankton biomass exhibited a significant north-south gradient. It was high both in mixed layer (av.  $0.95 \text{ ml m}^{-3}$  and thermocline layer (av.  $0.52 \text{ ml m}^{-3}$ ) in northern region as compared to the southern region ( $0.45 \text{ mlm}^{-3}$  and  $0.12 \text{ ml m}^{-3}$ ).

With the onset of summer monsoon (May-June), coastal upwelling began in the southern part of study area. A three fold increase in wind speed was noticed ( $\sim 15 \text{ m s}^{-1}$ ) along the coast of  $8^\circ\text{N}$  and  $10^\circ\text{N}$ . Shoaling of isotherms to the coastal waters (signatures of upwelling) was prevalent in the southern transects whereas northern transects ( $13^\circ\text{-}21^\circ\text{N}$ ) remained vertically stratified.

Intense upwelling was prevalent in the southern part (8-15°N) of the study area during the peak summer monsoon (August) with maximum intensity along 10°N transects. Due to intense upwelling, nutrients level in the surface layer was noticeably high ( $> 2\mu\text{M}$  nitrate,  $> 4\mu\text{M}$  silicate,  $> 2\mu\text{M}$  phosphate). As a result of high estuarine influx, low saline plumes were also evident along 10- 11.5°N. The vertical thermal structure in the upper layer showed a clear frontal structure towards the coast, especially along 8-11.5°N transects. During the late summer monsoon (September) upwelling signatures receded from 8°N transect but was still prevalent in the inshore waters north of 10°N indicating the northward shift of upwelling during late summer monsoon period.

The biological responses during different phases of upwelling showed fair correspondence with the physico-chemical changes in the study area. During the OSM, primary productivity was low in the study area ( $259 \text{ mgC m}^{-2}\text{d}^{-1}$ ). Relatively low phytoplankton biomass and production observed during the OSM could be due to the possible lag in nutrient injection and efficient absorption by the phytoplankton cells. Since OSM follows stratified low productive SIM period, the observed low phytoplankton biomass and production observed during the former period are explainable. High primary productivity (av.  $420 \text{ mgCm}^{-2}\text{d}^{-1}$ ), Chl *a* ( $26.7 \text{ mgm}^{-3}$ ) and mesozoopklankton biomass ( $8.6 \text{ mlm}^{-3}$ ) were the characteristic features during the peak phase of summer monsoon. These features were evidently due to a direct coupling between enriched nutrient levels, high phytoplankton

biomass and zooplankton. In nutrient enriched waters, pennate diatoms dominate over the dinoflagellates and silicoflagellates, as observed in the present study possibly due to its higher nutrient uptake rate.

A total of 177 species of phytoplankton were identified during the present study. A total of 67 species of phytoplankton were recorded during SIM, where as it was 83 species during OSM, 112 species during PSM and 117 species during LSM. Bacillariophyceae (Diatoms) formed the dominant class of phytoplankton community having 108 species. *Rhizosolenia* was the dominant form (12 species) in the EAS. Abundance of green flagellates (41010 cells m<sup>-2</sup>) was also observed along the inshore waters of 10°N and 11.5°N transects during PSM and LSM. *Fragilaria oceanica* was also noted in the phytoplankton samples through out the summer monsoon.

The result of phytoplankton pigment analysis using High Performance Liquid Chromatography (HPLC) showed higher concentration of fucoxanthin, peridinin, and zeaxanthin. These accessory pigments represent diatoms, dinoflagellates and bluegreen algae respectively. The presence of chlorophyll *b* in the pigment composition was associated with green flagellates.

High primary productivity (1630 mgC m<sup>-2</sup>d<sup>-1</sup>) Chl *a* (1.98 mgm<sup>-2</sup>), phytoplankton abundance (29200 cellsL<sup>-1</sup>) and mesozooplankton biomass (8.6 m<sup>3</sup>) were observed in the inshore waters off Kochi (10°N) during all the three phases of summer monsoon. Abundance of fish larvae also was relatively high in this region, compared to other

transects. High estuarine influx (Cochin estuary) in the region may probably play a major role in enriching the nutrients causing enriched biological production.

The marked difference in the distribution of Chl *a* and phytoplankton density observed during the different period of the present study (SIM, OSM, PSM and LSM) was also evident in the satellite derived chlorophyll *a* imagery. This similarity between *in situ* and satellite chlorophyll *a* strongly supports the contention that interseasonal (between SIM and SM) and intraseasonal (OSM, PSM, and LSM) variability are significant in the EAS.

Analysis of the pelagic fish landing data in relation to the productivity pattern observed during the present study showed a close correspondence. Peak fish landing coincided with the peaks in primary and secondary productivity during the summer monsoon period of the present study. This directly point towards the close coupling between upwelling phenomenon, plankton productivity and the pelagic fishery resources along the south west coast of India.

To conclude, the thesis provides baseline information on how biological features in EAS transform from spring intermonsoon period to different phases of summer monsoon. The results showed significant intraseasonal variability in plankton productivity in the EAS during summer monsoon. This variability in biological responses was basically linked to the difference in intensity and spatial variations of upwelling.

## ***Papers published***

1. **Habeebrehman, H.**, Prabhakaran, M.P., Josia Jacob, Sabu, P., Jayalakshmi, K.J., Achuthankutty, C.T. and Revichandran, C., 2008. Variability in biological responses influenced by upwelling events in the Eastern Arabian Sea. ***Journal of Marine Systems*, 74: 545-560.**
2. Vimal Kumar, K.G., Dinesh Kumar, P.K., Smitha, B.R., **Habeebrehman, H.**, Josia Jacob, Muraleedharan, K.R., Sanjeevan, V.N. and Achuthankutty, C.T., 2008. Hydrographic characterization of southeast Arabian Sea during the wane of southwest monsoon and spring intermonsoon. ***Environment Monitoring Assessment*, 140: 231-247.**
3. Jyothibabu, R., Asha Devi, C.R., Madhu, N.V., Sabu, P., Jayalakshmy, K.V., Josia Jacob, **Habeebrehman, H.**, Prabhakaran, M.P., Balasubramanian, T. and Nair, K.K.C., 2008. The response of micro-zooplankton (20-200  $\mu\text{m}$ ) to coastal upwelling and summer stratification in the southeastern Arabian Sea. ***Continental Shelf Research*, 28: 653-671.**
4. Satish Sahayak, Jyothibabu, R., Jayalakshmi, K.J., **Habeebrehman, H.**, Sabu, P., Prabhakaran, M.P., Jasmine, P., Shaiju, P., Rejomon, G., Thresiamma, J. and Nair K.K.C., 2005. Red tide of *Noctiluca miliaris* off south of Thiruvananthapuram subsequent to the 'stench event' at the southern Kerala coast. ***Current Science* 89 (9): 1471-1472.**
5. Rosamma Stephen, Jayalakshmi, K.J., **Habeebrehman, H.**, Karuppuswamy, P.K. and Nair, K.K.C., 2006. Tsunami 2004 and the biological oceanography of Bay of Bengal. ***Proceedings of Commemorative conference on Tsunami, Madurai, 2006***
6. Josia J., Jayaraj, K.A., **Habeebrehman, H.**, Chandramohankumar, N., Balaichandran, K.K., Raveendran, T.V., Nair, M. and Achuthankutty, C.T., 2009. Seasonal and spatial variations in biogeochemistry of surface sediments along the western continental shelf of India  
**(Accepted: Chemistry and Ecology)**

## ***Papers under review***

7. **Habeebrehman, H.**, Prabhakaran, M.P., Sabu, P., Josia Jacob, Revichandran, C. and Nair, K.K.C. Effects of monsoon and upwelling on the biological productivity in the Eastern Arabian Sea **(Under Review: Journal of Hydro Environmental Research).**
8. Prabhakaran, M.P., **Habeebrehman, H.**, Anilkumar, K., Priyaja, P., Biju, A., Martin, G.D., Karuppusamy, P.K., Arun, A.U. and K.K.C. Nair. Bio-physical and chemical interactions in the Andaman Sea - A Winter Monsoon Scenario. **(Under Review: Journal of Hydro Environmental Research)**
9. Jyothibabu, R., Madhu, N.V., **Habeebrehman, H.**, Jayalakshmy, K.V. and Nair, K.K.C. Re- evaluation of Arabian sea Paradox. **(Under Review: Progress in Oceanography).**